QUARTERLY JOURNAL
OF THE
ROYAL METEOROLOGICAL SOCIETY

Editor: G. D. ROBINSON

Vol. 83 APRIL 1957 No. 356

CONTENTS

PAGE

W. L. GATES—A dynamical model for large-scale tropospheric and stratospheric motions 141

N. D. CLARENCE and D. J. MALAN—Preliminary discharge processes in lightning flashes to ground (Plates I-II) 161

G. F. WALTON—The relation between an *umkehr* curve and the vertical distribution of atmospheric ozone 173

N. E. RIDER—Water losses from various land surfaces 181

C. G. JOHNSON—The vertical distribution of aphids in the air and the temperature lapse rate 194

I. F. LONG—Instruments for micro-meteorology (Plate III) 202

H. RIEHL and D. FULTZ—Jet streams and long waves in a steady rotating-dishpan experiment: structure of the circulation (Plate IV) 215

F. H. BUSHBY and VERA HUCKLE—Objective analysis in numerical forecasting .. 232

R. C. SMITH—Air motion over a heated land mass: II 248

Shorter Contributions—

N. C. HELLIWELL, J. K. MACKENZIE and M. J. KERLEY—Some further observations from aircraft of frost point and temperature up to 50,000 ft 257

H. F. LIDDELL and N. W. WOOTTEN—The detection and measurement of water droplets (Plate V) 263

A. W. BREWER—Ozone concentration measurements from an aircraft in N. Norway .. 266

Correspondence—

G. SPURR and C. H. B. PRIESTLEY—The bent-over plume of hot gas 269

P. PETERSON and J. R. SCOTT—The zonal wind in the upper troposphere and weather at Singapore 270

R. S. SCORER—Airflow over mountains 271

Discussions—

G. N. PLASS—The influence of the 9·6 μ ozone band on the atmospheric infra-red cooling rate. The influence of the 15 μ carbon-dioxide band on the atmospheric infra-red cooling rate (*Q.J.*, **82**, p. 30 and p. 310) 272

P. HUGHES—A determination of the relation between wind and sea-surface drift (*Q.J.*, **82**, p. 494). 276

Proceedings at meetings of the Society 278

Reviews—

Physics in meteorology, A. C. Best (B.J.M.); *Mathematics in action*, O. G. Sutton (T.G.C.); *Flugmeteorologie*, W. Georgii (S.E.V.); *Lehrbuch der Klimatologie*, B. P. Alissov, O. A. Drosdov and E. S. Rubinstein (C.E.P.B.); *Fortschritte in der meteorologischen Forschung seit 1900*, B. Neis (C.E.P.B.) 281

Obituary Notices 283

PUBLISHED AND SOLD BY THE
ROYAL METEOROLOGICAL SOCIETY
49 CROMWELL ROAD, LONDON, S.W.7
PRICE TWENTY-FIVE SHILLINGS
ANNUAL SUBSCRIPTION £4 - 3 - 0, POST FREE

ROYAL METEOROLOGICAL SOCIETY

Founded on 3 April 1850, for the advancement of meteorological science. The Society was incorporated by Royal Charter in 1866.

Membership

Membership is open to all persons genuinely interested in meteorology. The annual subscription is as follows :

Fellows	£3-3-0 (Entrance fee, 1 guinea)	
Foreign Members ..	£3-3-0	„ „
Associates	£2-0-0	„ „
Students	£1-10-0	

All Members receive free the regular publications of the Society, including the monthly publication *Weather* (annual subscription to non-members 24s.).

The Descriptive Account of the Society and an application form will be sent on request to the Assistant Secretary.

Quarterly Journal

Editing committee

G. D. Robinson — *Editor and Chairman*

G. A. Bull R. M. Goody R. F. Jones G. Manley F. Pasquill
H. L. Penman J. S. Sawyer R. C. Sutcliffe T. W. Wormell

The primary purpose of the *Quarterly Journal* is to publish results of original research and reports of the Society's scientific meetings. Papers intended for the *Journal* **should be submitted in accordance with standards laid down by the Council in the Society's memorandum** ' Preparation of Papers for the *Quarterly Journal*' which is available on request. Failure to conform with these standards involves the Society's officers and staff in much needless work and the Society in unnecessary expense. **Manuscripts will therefore not be considered for publication unless they conform reasonably closely with the procedure laid down.** The attention of authors is drawn particularly to the requirements in regard to mathematics and diagrams and the Assistant Secretary will be pleased to advise authors on their special problems of illustration before papers are formally submitted. Diagrams should, if possible, be submitted flat, not rolled, and a duplicate rough set for refereeing purposes should be included. Where rulings on a diagram are desirable the closest acceptable spacing is approximately 1 cm and this may de done on **blue-lined** graph paper by thickening the centimetre rulings. Manuscripts may be submitted in duplicate to expedite refereeing, but authors must retain complete copies in their possession.

Price to non-members is £4-3-0 (post free) per annum and £1-5-0 for single issues (postage extra).

Publications

Copies of the publications *Centenary Proceedings of the Royal Meteorological Society, 1950* (£1. 1s.) and *Proceedings Toronto Meteorological Conference 1953* (£1. 10s.) are still available.

Reprints of papers recently published in the *Quarterly Journal* are generally available, the prices being as follows (postage extra) : 8 pp., 1s. 2d. ; 16 pp., 1s. 10d. ; 20 pp., 2s. 2d.

Articles in the series ' Reviews of Modern Meteorology ' commenced in Jan. 1951 include : 1. Meteorological measurements ; 2. Radiation in the troposphere and lower stratosphere ; 3. Dynamics of flow patterns in extra-tropical regions (2s. 6d.) ; 4. The evolution of 20th-century forecasting in the British Isles ; 5. Tropical meteorology ; 6. Principles of synoptic weather forecasting (3s. 2d.) ; 7. Turbulence and transfer processes in the atmosphere ; 8. Atmospheric electricity, some recent trends and problems ; 9. Climatic variation ; 10. Convection in the atmosphere ; 11. The physical state of the upper atmosphere (1s. 10d.) ; 12. The problem of tropical hurricanes (3s. 6d.) ; 13. Cloud physics. (Reprints of only Nos. 3, 6, 11 and 12 are now available).

The Society's offices

Assistant Secretary — M. E. Shoenberg, B.A.
49 Cromwell Road, London, S.W.7
(*Telephone :* KENsington 0730)

The offices and library of the Society are open daily (Monday to Friday) from 10 a.m. to 5 p.m. All enquiries and correspondence concerning the Society and its publications should be addressed to the Assistant Secretary.

This Journal is printed in Horley Series

SHORT & MASON

Manufacturers

of the finest

Scientific

Instruments

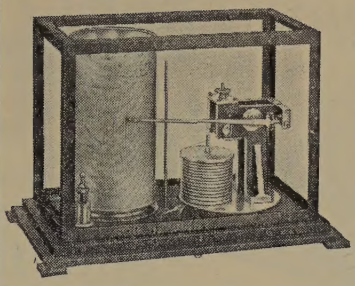

MICRO-BAROGRAPH

This recorder has a very open scale in which 2½ linear inches equal 1" barometric pressure. Essential for weather forecasting, barometric pressure studies and survey work. Supplied with 24-hour or 7-day revolution clock and charts in inches, millimetres and millibars. Prompt delivery.

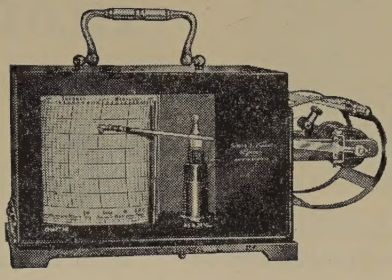

THERMOGRAPH

This is a highly sensitive bimetallic coil instrument having a low-drum weekly clock, exposed element and "gate" suspension pen arm. Supplied complete with 6" setting Thermometer, a year's supply of charts and ink. Prompt delivery.

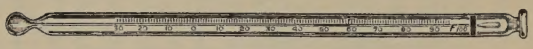

METEOROLOGICAL THERMOMETERS

Standard Maximum, Minimum, Ordinary and 'Solar Radiation' Thermometers can be supplied either sheathed or mounted. These thermometers can be supplied with N.P.L. Certificates if required. Prompt delivery.

ALSO BRASS CASE BAROMETERS • SURVEYING ANEROID BAROMETERS • MERCURIAL BAROMETERS • HYGROMETERS HYGROGRAPHS • STANDARD THERMOMETERS • WIND SPEED AND DIRECTION INDICATORS • ANEMOMETERS RAIN GAUGES • GAS MEASURING INSTRUMENTS, etc., etc

Catalogue and Price List sent on request

SHORT & MASON LTD ANEROID WORKS, HALE END ROAD WALTHAMSTOW. LONDON, E.17. TELEPHONE: LARKSWOOD 3371-6

Distribution in the U.S.A and Canada through THE TAYLOR INSTRUMENT COMPANIES of Rochester, N.Y., U.S.A., and Toronto, Canada.

Why you should specify

Beritex REGD SEAMLESS

SOUNDING AND PILOT BALLOONS

Made by **THE GUIDE BRIDGE RUBBER CO. LTD**

They're the finest available for meteorological work because:—

Beritex Balloons have years of research and development behind them.
Every balloon is guaranteed and has been rigorously tested and individually inspected.
Made from the finest Rubber Latex they require no special pre-flight treatment.

* * *

Les ballons 'Beritex' ont des années de recherches et de mise au point derrière eux.
Chaque ballon est garanti et a fait l'objet d'un essai rigoureux et d'une vérification individuelle.
Fabriqués en latex de caoutchouc de la meilleure qualité ils n'ont besoin d'aucun traitement spécial avant l'envol.

* * *

Los globos Beritex están respaldados por muchos años de investigación y fabricación.
Todos los globos están garantizados y han sido rigurosamente probados e individualmente verificados.
Los globos, fabricados con inmejorable caucho látex, no requieren ningún tratamiento especial antes del vuelo.

OVERSEAS SALES
Phillips Patents Limited · 250 Western Avenue · Acton · London · W3

HOME SALES
Guide Bridge Rubber Co. Ltd · Vulcan Mill · Butcher Lane · Bury · Lancs.

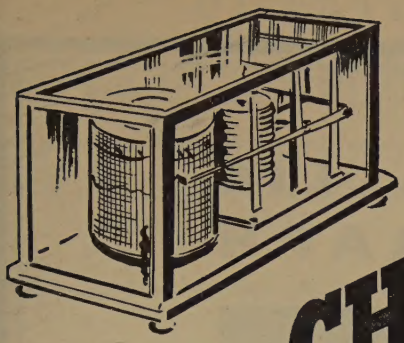

HORSTMANN CHART CLOCK

NEWBRIDGE WORKS BATH
REGISTERED TRADE MARK

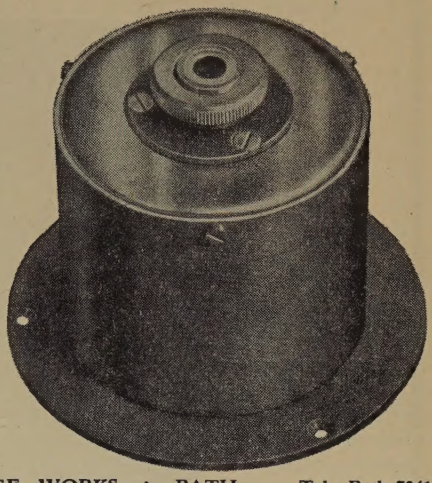

Horstmann Chart Clocks are used extensively by the Air Ministry Meteorological Office. Two types are available, one to drive chart drums revolving once in every 24 hours and the other for 7 day rotation. The clockwork movements of both types have a centre spindle drive.

The movements are of robust construction and incorporate very high quality jewelled platform escapements, which ensure extreme accuracy in time keeping.

Chart Clocks having speeds other than those mentioned above can also be supplied to special order.

THE HORSTMANN GEAR CO. LTD. · NEWBRIDGE WORKS · BATH Tel.: Bath 7241

T. A. REYNOLDS SON & WARDALE LTD.

40-42 PERCIVAL STREET, LONDON, E.C.1

Telephone : CLErkenwell 6127 Telegrams : Therbarome, London

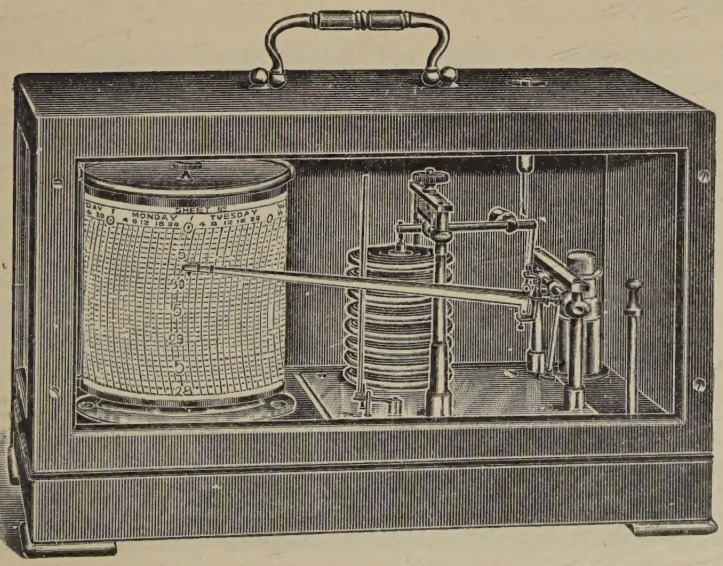

AUSTRALIAN REPRESENTATIVE :
W. A. AARON
Box 339, G.P.O., Sydney

NEW ZEALAND REPRESENTATIVE :
H. T. JOHNSON & Son, Ltd.
48 High Street,
Auckland, C.1

Manufacturers of

SCIENTIFIC INSTRUMENTS

ANEROID BAROMETERS

THERMOMETERS

BAROGRAPHS, etc.

CASELLA
LONDON

Established 1810

A BIMETALLIC ACTINOGRAPH

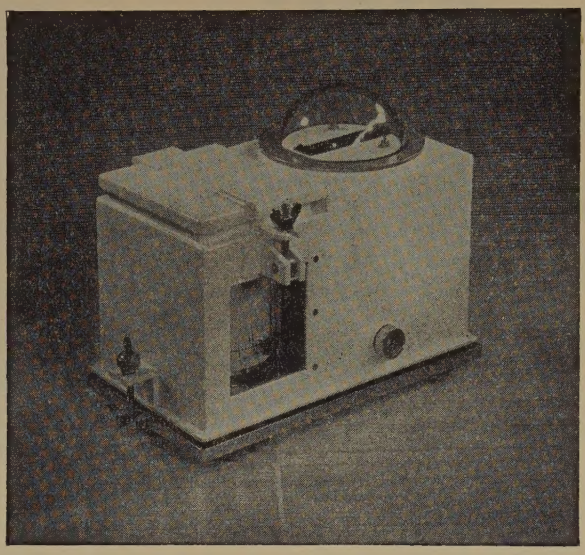

This is a new instrument designed by the British Meteorological Office to record the shortwave radiation received from the sun and sky on a horizontal surface.

The sensitive element consists of a blackened bimetallic strip mounted at one end on two shaded strips. The free end of the blackened strip records deflections proportional to the incident radiation. This recording is made on a standard daily rotation clock drum.

The combination of black and shaded strips provides compensation for ambient temperature changes. Further bimetallic strips provide compensation for changes of temperature.

The element is exposed to the radiation through a hemispherical glass dome mounted in the top of a white painted metal cover. The whole is made watertight by rubber gaskets and the inside is kept dry by a removable tube containing silica gel.

C. F. CASELLA & CO. LTD.

REGENT HOUSE, FITZROY SQUARE, LONDON, W.1

Telephone : ★ EUSton 3944

Member Scientific Instrument Manufacturers' Association of Great Britain

QUARTERLY JOURNAL
OF THE
ROYAL METEOROLOGICAL SOCIETY

Vol. 83 APRIL 1957 No. 356

551.509.313 : 551.515

A dynamical model for large-scale tropospheric and stratospheric motions

By W. LAWRENCE GATES
Air Force Cambridge Research Center, Cambridge, U.S.A.

(Manuscript received 22 May 1956, in revised form 22 November 1956)

SUMMARY

A physical model of the atmosphere is postulated in which both the troposphere and stratosphere are characterized by a uniform thermal wind and a constant static stability, and are separated by a tropopause across which these quantities are discontinuous. Assuming the tropopause to be quasi-isobaric, a simplified model for the mean velocity, temperature and vertical motion fields of both the troposphere and stratosphere, the velocity near the earth's surface, and both the horizontal and vertical motion at the tropopause is constructed. The model may be regarded alternatively as a four-parameter or four-level model, but it is felt to avoid the primary disadvantages of the exclusive use of either the parameterized or layered formulation. Analysis of the special case of an equivalent-barotropic stratosphere indicates the existence of systematic tropopause variations, with the vertical motion at this level generally in phase with that of the mid-troposphere, and with a system of opposing vertical motion higher in the stratosphere. These features are in general agreement with the results of observational and synoptic research, although the details of the role of the tropopause must await further calculations. The analysis of the stability of tropospheric perturbations in a baroclinic zonal current shows a stabilizing influence of the stratosphere on the initial amplification of the disturbances. The minimum vertical shears required for instability with a basic jet current of 40 m sec^{-1} are more than twice those required without a stratosphere, and are shown to lie between the mean summer and winter shears in the zone of maximum westerlies.

1. INTRODUCTION AND GENERAL REMARKS

In the construction of simple baroclinic models for the study of quasi-geostrophic flow, such as those presented by Sawyer and Bushby (1953), Eady (1952) and Thompson (1953), attention has been focused upon the baroclinic troposphere and its role in the development of large-scale disturbances. The extensive tests of these models reported by Bushby and Hinds (1954), Gates, Pocinki and Jenkins (1955), and Thompson and Gates (1956), have shown the need for further refinement of the numerical procedures employed on the one hand, and for the introduction of new physical features of the atmosphere into the models on the other. Research on the reduction of numerical and mathematical error is under way in a number of quarters, and significant advances are being made in the art of computation in problems of numerical weather prediction. (See Thompson (1955), Blackburn and Gates (1956), and Shuman (1955)). At the same time, the extension of the physical basis of the models has by and large been in the direction of providing a more detailed description of the lower regions of the atmosphere. The vertically-differenced (or multiple-level) models, whose character is determined by the number (and location) of levels selected, may be generalized by the addition of new levels, as in the three-level models of Charney and Phillips (1953) or the five-level models of Charney, Gilchrist and Shuman (1955). Similarly, the vertically-integrated (or multiple-parameter) models, in which the vertical structure of the atmosphere is described by a modelling approximation, may be generalized by the introduction of new parameters, as in the models of Árnason (1952, 1953) and Berkofsky (1956).

In the development of generalized models, however, one of the most striking and persistent features of the observed gross structure of the atmosphere has generally been neglected, namely, the presence of the stratosphere and the associated tropopause. For this reason, as well as because of the increasing practical importance of the stratosphere for aircraft operation, it would clearly be desirable to develop a baroclinic model to incorporate this feature. Such a model, however, should retain the merits but avoid the primary disadvantages of the more general multiple-parameter models discussed above. In the vertically-differenced models, the simplicity of the governing equations at each level is offset by the difficulty of tracing a specific physical effect in the solutions and by the relatively large amount of data required. Serious truncation errors may also be made in the vertical resolution. In the vertically-integrated models, the diagnostic character of the model's equations and the representativeness of vertical means are to be balanced by the confinement of the solutions to levels in the middle and lower troposphere and the great increase in the complexity of the governing equations as new parameters are added.

In the present paper, a model for large-scale tropospheric and stratospheric motions is developed by vertical integration over the troposphere and stratosphere *separately*; static stability and thermal wind are assumed constant in each. For quasi-geostrophic motions, this structure implies a discontinuity of vertical wind shear and horizontal temperature gradient across the tropopause, with a sharp jet or wind maximum there. No vertical differences are taken across the tropopause, however, and application of the appropriate boundary conditions at this surface allows the model to determine not only the mean horizontal and vertical motions of the troposphere and stratosphere (including sea-level motions), but those at the tropopause as well. In this manner, the model provides a basis for the systematic extension of numerical prediction techniques into the stratosphere, and may therefore be regarded as a four-level model. The point to be emphasized, however, is that these levels result naturally from the gross physical description of the atmosphere, while the model's governing equations retain the character of those for a simple multiple-parameter model.

2. The physical model and the governing equations

As the starting point in the analysis, we consider the familiar quasi-geostrophic equations

$$\frac{\partial \nabla^2 \psi}{\partial t} + J(\psi, \nabla^2 \psi + f) - f\frac{\partial \omega}{\partial p} = 0 \quad . \quad . \quad . \quad (1)$$

$$\frac{\partial \phi}{\partial t} + J(\psi, \phi) + \sigma\omega = 0 \quad . \quad . \quad . \quad . \quad (2)$$

$$\frac{\partial \psi}{\partial p} + \frac{\phi}{p} = 0 \quad . \quad . \quad . \quad . \quad . \quad (3)$$

Eq. (1) is the vorticity equation for frictionless flow with the terms representing the vertical advection of vorticity ($\omega\, \partial \nabla^2 \psi / \partial p$) and the reorientation of the axes of vortex tubes ($-\nabla\phi \cdot \nabla\omega/p$) omitted. The relative vorticity $\nabla^2 \psi$ has also been neglected in comparison to the Coriolis parameter f in the coefficient of the last (divergence) term of Eq. (1). Eq. (2) is the thermodynamical energy equation (first law of thermodynamics) for adiabatic flow, and Eq. (3) is the hydrostatic relationship. The equation of continuity has been used in Eq. (1) in the form

$$\frac{\partial \omega}{\partial p} + \nabla \cdot \mathbf{v} = 0$$

in order to avoid the explicit appearance of the divergence $\nabla \cdot \mathbf{v}$, where $\mathbf{v}$ is the geostrophic velocity. In these equations, $\psi = gz/f$ is the geostrophic stream function, with g the

gravitational acceleration, z the height of an isobaric surface, and f the Coriolis parameter; $\phi = RT/f$ is a stream function for the thermal wind, with R the gas constant and T the absolute temperature; $\omega = dp/dt$ is the material or individual rate of change of pressure p; $\sigma = \partial\phi/\partial p - \kappa\phi/p$ is a measure of the static stability, with $\kappa = R/c_p$ where c_p is the specific heat of air at constant pressure. The x, y, p, t coordinate system is used, with the x-axis directed toward the east (unit vector **i**), the y-axis directed toward the north (unit vector **j**), and the negative p-axis directed vertically upward (unit vector **k**), and with t the time. The differentiations with respect to x, y and t are to be carried out at constant pressure, and are written $J(a, b) = (\partial a/\partial x)(\partial b/\partial y) - (\partial a/\partial y)(\partial b/\partial x)$ for the Jacobian operator, $\nabla^2 a = \partial^2 a/\partial x^2 + \partial^2 a/\partial y^2$ for the Laplace operator, and $\nabla a = \mathbf{i}\,\partial a/\partial x + \mathbf{j}\,\partial a/\partial y$ for the gradient operator.

Properly belonging with Eqs. (1)-(3) is a statement of the boundary conditions, ensuring no net mass transport across the top and bottom of the atmosphere. These conditions are most easily written in the form

$$\left.\begin{aligned} \omega &= 0, & p &= 0 \\ \omega &= -g\rho_0 J(\psi_0, h), & p &= p_0 \end{aligned}\right\} \quad . \quad . \quad . \quad (4)$$

where ρ is density, h is the height of the earth's terrain above sea-level, and the subscript zero denotes evaluation near the earth's surface. For convenience in the present development, we shall neglect the effects of the earth's topography upon the motion; this effect is not an essential ingredient of the present formulation and may be introduced when desired with little additional effort.* We will consequently use the boundary condition

$$\omega = 0 \quad . \quad . \quad . \quad . \quad . \quad (5)$$

at both the upper and lower limits of the atmosphere.

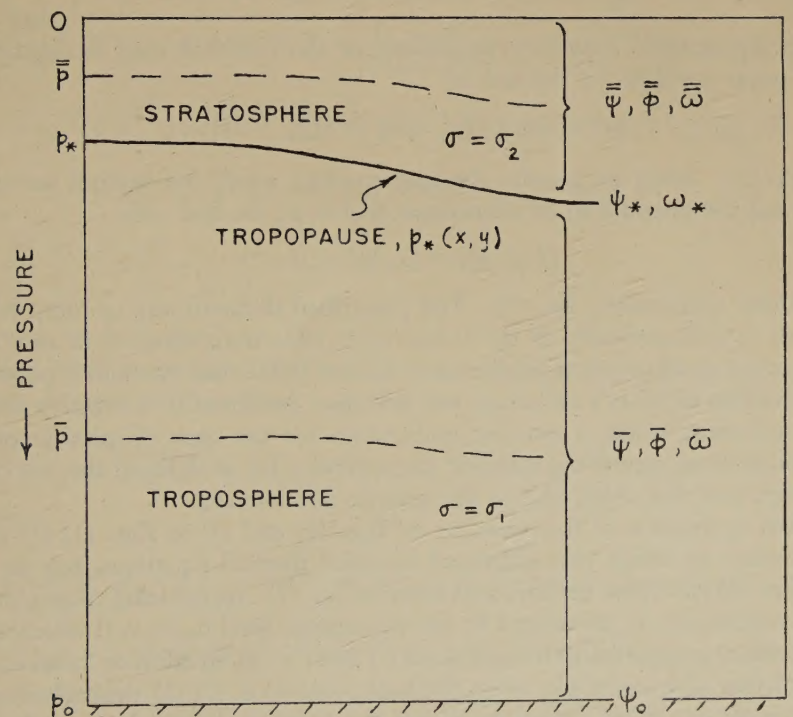

Figure 1. The physical model and primary variables of the baroclinic model with a tropopause.

* In the practical application of a numerical prediction model to forecasting, however, the neglect of the effects of irregular terrain may lead to an appreciable systematic error; see Thompson and Gates (1956) and Gates, Pocinki and Jenkins (1955).

The basic physical characterization of the atmosphere will be its division into two simply baroclinic layers, each of a uniform stability and separated by an interface at which the stability is discontinuous as shown schematically in Fig. 1. Over the troposphere and stratosphere we shall perform a vertical integration with respect to pressure, defined by the operators

$$\overline{(\ )} = (p_0 - p_*)^{-1} \int_{p_*}^{p_0} (\ )\, dp \quad . \quad . \quad . \quad . \quad (6)$$

$$\overline{\overline{(\ )}} = (p_*)^{-1} \int_{0}^{p_*} (\ )\, dp \quad . \quad . \quad . \quad . \quad (7)$$

where the subscript * denotes evaluation at the interface. The modelling approximations may be written

$$\nabla\phi = (p/\bar{p})\, \overline{\nabla\phi}, \qquad p_0 \geqslant p > p_* \quad . \quad . \quad . \quad (8)$$

$$\nabla\phi = (p/\bar{p})\, \overline{\overline{\nabla\phi}}, \qquad p_* > p \geqslant 0 \quad . \quad . \quad . \quad (9)$$

and state that the vertical (geostrophic) wind shear is proportional to the mean temperature gradient.

At the interface or tropopause itself, the internal boundary conditions are given by the requirements of continuous pressure and continuous velocity. The dynamical boundary condition for the material interface may be written at $p = p_*$ as

$$\frac{\partial p}{\partial t} + \mathbf{v}_3 \cdot \nabla_3 p = 0 \quad . \quad . \quad . \quad . \quad (10)$$

where the subscript 3 denotes the three-dimensional vector. Assuming hydrostatic equilibrium and writing $\alpha = p_*/p_0$ with p_0 constant, we may write this condition in the form

$$\frac{\partial \alpha}{\partial t} = -\mathbf{k} \times (\nabla\psi)_* \cdot \nabla\alpha + p_0^{-1}\, \omega_* \quad . \quad . \quad . \quad (11)$$

The necessary kinematical boundary conditions at the interface may be obtained by applying the jump operator [ ] defined as

$$[f] = \lim_{\epsilon \to 0} \{f(p_* + \epsilon) - f(p_* - \epsilon)\} \quad . \quad . \quad . \quad (12)$$

to the Eqs. (1)-(3). Since we require the (geostrophic) wind, the vertical motion, the temperature, and the pressure to be continuous at $p = p_*$ we find only

$$[J(\psi, \phi)] + \omega_* [\sigma] = 0 \quad . \quad . \quad . \quad . \quad (13)$$

from the adiabatic relationship, Eq. (2). The prescribed discontinuity or jump $[\sigma]$ must then be related to a discontinuity in the temperature advection, which is in turn related to the discontinuity in the vertical wind shear. Lowell (1951) has previously pointed out that the specification of $[\sigma]$ is a necessary and sufficient condition to determine the jump in vertical wind shear across a material tropopause for the case of quasi-geostrophic flow. One might then regard the stability discontinuity $[\sigma]$ as *defining* the tropopause, and this concept will play a key role in the present development.

The formal application of the operators of Eqs. (6) and (7) to Eqs. (1)-(3) yields a set of six equations to which two additional so-called thermal equations may be added by applying Eqs. (6) and (7) to the first p-moment of Eq. (1). In reducing these equations, considerable complication is introduced by the tropopause level $p_*(x, y, t)$ which appears as a variable limit of integration in the operators $\overline{(\ )}$ and $\overline{\overline{(\ )}}$. In an effort to avoid excessive involvement of this sort, especially since the basic equations (1)-(3) themselves contain several approximations, it will be assumed that the tropopause may be regarded as an isobaric surface *for the purposes of developing the model's governing equations*. This approximation will be most seriously in error in cases of a steeply inclined tropopause, and the

present model should be regarded as describing only the bulk or gross troposphere – stratosphere interaction. Although the height amplitude of the tropopause variations is characteristically several times that of the adjacent isobaric surfaces, synoptic evidence indicates the two are generally in phase (Sawyer 1954). Even with the present simplification it turns out that the behaviour of the tropopause itself can still be described approximately and will be considered in § 5.

Proceeding on the basis of a quasi-isobaric tropopause and focusing our attention first on the troposphere, we may write the hydrostatic relation Eq. (3) in the form

$$\overline{\psi} - \overline{\phi} = (1-\alpha)^{-1}(\psi_0 - \alpha\,\psi_*) \quad . \quad . \quad . \quad (14)$$

From the application of the $\overline{(\,)}$-operator to Eq. (1) we next consider

$$\begin{aligned}\overline{J(\psi, \nabla^2\psi + f)} &= \overline{\frac{\partial}{\partial p} J(p\psi, \nabla^2\psi)} + \beta\frac{\partial\overline{\psi}}{\partial x} + \overline{J(\psi, \nabla^2\phi)} + \overline{J(\phi, \nabla^2\psi)} \\ &= (p_0 - p_*)^{-1}(p_0 J(\psi_0, \nabla^2\psi_0) - p_* J(\psi_*, \nabla^2\psi_*)) \\ &\quad + \beta\frac{\partial\overline{\psi}}{\partial x} + \frac{1}{\overline{p}} J(\overline{p\psi}, \nabla^2\overline{\phi}) + \frac{1}{\overline{p}} J(\overline{\phi}, \nabla^2\overline{p\psi}) \quad . \quad . \quad (15)\end{aligned}$$

where $\beta = \partial f/\partial y$, following an analysis similar to that of Thompson and Gates (1956). Here ψ_* is now to be identified with the isobaric surface p_* in the vicinity of the tropopause, and the operator $\overline{(\,)}$ has been freely commuted with the various differential operators.

Collecting these results from Eq. (15) and expanding the expression $\nabla\overline{p\psi}$ we obtain for Eq. (1) in the troposphere

$$\begin{aligned}&\frac{\partial\nabla^2\overline{\psi}}{\partial t} + (1-\alpha) J(\overline{\psi}, \nabla^2\overline{\psi}) + \frac{(1-\alpha)^2}{3(1+\alpha)^2}\left\{1 + 3\alpha\left(\frac{1+\alpha}{1-\alpha}\right)\right\} J(\overline{\phi}, \nabla^2\overline{\phi}) \\ &\quad + \frac{\alpha^2}{1+\alpha}\{J(\overline{\psi}, \nabla^2\overline{\phi}) + J(\overline{\phi}, \nabla^2\overline{\psi}) - J(\overline{\phi}, \nabla^2\psi_*) - J(\psi_*, \nabla^2\overline{\phi})\} \\ &\quad + \alpha\{J(\overline{\psi}, \nabla^2\psi_*) + J(\psi_*, \nabla^2\overline{\psi}) - J(\psi_*, \nabla^2\psi_*)\} \\ &\quad + \beta\frac{\partial\overline{\psi}}{\partial x} + \frac{f\omega_*}{p_0(1-\alpha)} = 0 \quad . \quad . \quad . \quad . \quad . \quad . \quad (16)\end{aligned}$$

where $\alpha = p_*/p_0$ as before.

Seeking now the so-called thermal vorticity equation for the troposphere, we may write the p-moment of Eq. (1) as

$$\frac{\partial\nabla^2(\overline{p\psi})}{\partial t} + \overline{J(p\psi, \nabla^2\psi)} + \beta\frac{\partial\overline{p\psi}}{\partial x} - f\overline{\left(p\frac{\partial\omega}{\partial p}\right)} = 0 \quad . \quad . \quad (17)$$

Upon writing

$$\begin{aligned}\overline{J(p\psi, \nabla^2\psi)} &= \tfrac{1}{2}\left\{\overline{\frac{\partial}{\partial p} J(p^2\psi, \nabla^2\psi)} + \overline{J(\phi, \nabla^2 p\psi)} + \overline{J(p\psi, \nabla^2\phi)}\right\} \\ &= \{p_0^2 J(\psi_0, \nabla^2\psi_0) - p_*^2 J(\psi_*, \nabla^2\psi_*)\}\{2(p_0 - p_*)\}^{-1} \\ &\quad + \{J(\overline{\phi}, \nabla^2\overline{p^2\psi}) + J(\overline{p^2\psi}, \nabla^2\overline{\phi})\}\{p_0 + p_*\}^{-1}\end{aligned}$$

and expanding the expression $\nabla\overline{p^2\psi}$ we find that after some rearrangement Eq. (17) takes the form

$$\tfrac{1}{2}\frac{\partial \nabla^2 \bar{\psi}}{\partial t} + \left(\frac{1-\alpha^3}{3(1-\alpha^2)} - \tfrac{1}{2}\right)\frac{\partial \nabla^2 \bar{\phi}}{\partial t} + \frac{\alpha}{2}\frac{\partial \nabla^2 \psi_*}{\partial t} + \left(\frac{1-\alpha}{2}\right) J(\bar{\psi}, \nabla^2 \bar{\psi})$$
$$+ \left(\frac{1-\alpha}{6}\right) J(\bar{\phi}, \nabla^2 \bar{\phi}) + \left\{\frac{3\alpha^2-1}{6(1+\alpha)}\right\}\left\{J(\bar{\psi}, \nabla^2 \bar{\phi}) + J(\bar{\phi}, \nabla^2 \bar{\psi})\right\}$$
$$+ \left\{\frac{\alpha}{2}\right\}\left\{J(\bar{\psi}, \nabla^2 \psi_*) + J(\psi_*, \nabla^2 \bar{\psi})\right\}$$
$$- \left\{\frac{\alpha}{6}\right\}\left\{J(\bar{\phi}, \nabla^2 \psi_*) + J(\psi_*, \nabla^2 \bar{\phi})\right\} + \frac{\beta}{2}\frac{\partial \bar{\psi}}{\partial x}$$
$$+ \frac{\beta\alpha}{2}\frac{\partial \psi^*}{\partial x} + \left\{\frac{1-\alpha^3}{3(1-\alpha^2)} - \tfrac{1}{2}\right\}\left\{\beta\frac{\partial \bar{\phi}}{\partial x}\right\} - \frac{f\alpha\omega_*}{p_0(1-\alpha)} + \frac{f\bar{\omega}}{p_0} = 0 \quad . \quad (18)$$

Before further reducing Eqs. (16) and (18), it is convenient to consider the stratospheric equations. By a procedure analogous to that outlined above, the hydrostatic equation (3) may be written for the stratosphere as

$$\bar{\bar{\psi}} - \bar{\bar{\phi}} = \psi_* \quad . \quad . \quad . \quad . \quad . \quad (19)$$

and the application of the $\overline{\overline{(\ )}}$-operator to Eq. (1) yields

$$\frac{\partial \nabla^2 \bar{\bar{\psi}}}{\partial t} + J(\psi_*, \nabla^2 \psi_*) + J(\bar{\bar{\psi}}, \nabla^2 \bar{\bar{\phi}}) + J(\bar{\bar{\phi}}, \nabla^2 \bar{\bar{\psi}})$$
$$- \tfrac{2}{3} J(\bar{\bar{\phi}}, \nabla^2 \bar{\bar{\phi}}) + \beta\frac{\partial \bar{\bar{\psi}}}{\partial x} - \frac{f\omega_*}{\alpha p_0} = 0 \quad . \quad . \quad . \quad (20)$$

The thermal vorticity equation for the stratosphere may be written

$$\frac{\partial \nabla^2 \overline{\overline{p\psi}}}{\partial t} + \frac{p_*}{2} J(\psi_*, \nabla^2 \psi_*) + \frac{1}{p_*}\{J(\bar{\bar{\phi}}, \nabla^2 \overline{\overline{p^2\psi}})$$
$$+ J(\overline{\overline{p^2\psi}}, \nabla^2 \bar{\bar{\phi}})\} + \beta\frac{\partial \overline{\overline{p\psi}}}{\partial x} + f\bar{\bar{\omega}} - f\omega_* = 0 \quad . \quad . \quad (21)$$

or, using Eq. (20) and the relation $\nabla \overline{\overline{p^2\psi}} = \nabla\psi_*\left(\frac{p_*^2}{3}\right) + \nabla\bar{\bar{\phi}}\left(\frac{p_*^2}{6}\right)$, we may write

$$\frac{\partial \nabla^2 \bar{\bar{\phi}}}{\partial t} + J(\bar{\bar{\psi}}, \nabla^2 \bar{\bar{\phi}}) + J(\bar{\bar{\phi}}, \nabla^2 \bar{\bar{\psi}}) + \beta\frac{\partial \bar{\bar{\phi}}}{\partial x} - \frac{6f\bar{\bar{\omega}}}{\alpha p_0} + \frac{3f\omega_*}{\alpha p_0} = 0 \quad . \quad (22)$$

Eqs. (16), (18), (20) and (22) may be regarded as containing the four unknown tendencies in $\bar{\psi}$, $\bar{\phi}$, $\bar{\bar{\psi}}$, and $\bar{\bar{\phi}}$, since ψ_* may be eliminated by Eq. (19). We note, however, that they also contain the as yet unknown vertical motions $\bar{\omega}$, $\bar{\bar{\omega}}$ and ω_*. Application of Eqs. (6) and (7) to the adiabatic equation (2) provides two equations in $\bar{\omega}$ and $\bar{\bar{\omega}}$, which may be written in the form

$$\bar{\omega} = -\sigma_1^{-1}\left\{\frac{\partial \bar{\phi}}{\partial t} + (1+\alpha)^{-1} J(\bar{\psi} + \alpha\psi_*, \bar{\phi})\right\} \quad . \quad . \quad (23)$$

$$\bar{\bar{\omega}} = -\sigma_2^{-1}\left\{\frac{\partial \bar{\bar{\phi}}}{\partial t} + J(\bar{\bar{\psi}}, \bar{\bar{\phi}})\right\} \quad . \quad . \quad . \quad . \quad (24)$$

Finally, for the required additional equation in ω_*, the vertical motion at the tropopause, we turn to Eq. (13) which may now be written as

$$\omega_* = [\sigma]^{-1}\{\mathbf{k} \cdot \nabla\psi_* \times [\nabla\phi]\}$$
$$= -2[\sigma]^{-1}\{\alpha(1+\alpha)^{-1} J(\psi_*, \bar{\phi}) - J(\psi_*, \bar{\bar{\phi}})\} \quad . \quad . \quad (25)$$

We may now collect and restate the governing equations of the model as follows :

$$\frac{\partial \nabla^2 \bar{\psi}}{\partial t} + J(\bar{\psi}, \nabla^2 \bar{\psi}) + \frac{(1-\alpha)^2}{3(1+\alpha)^2}\left\{1 + 3\alpha\left(\frac{1+\alpha}{1-\alpha}\right)\right\} J(\bar{\phi}, \nabla^2 \bar{\phi})$$
$$- \frac{\alpha^2}{1+\alpha}\{J(\psi_* - \bar{\psi}, \nabla^2 \bar{\phi}) + J(\bar{\phi}, \nabla^2(\psi_* - \bar{\psi}))\}$$
$$- \alpha J(\psi_* - \bar{\psi}, \nabla^2(\psi_* - \bar{\psi})) + \beta \frac{\partial \bar{\psi}}{\partial x}$$
$$- \mu_1^2 \left(\frac{2A}{1-\alpha}\right) \frac{\sigma_1}{[\sigma]} \{\alpha(1+\alpha)^{-1} J(\psi_*, \bar{\phi}) - J(\psi_*, \bar{\phi})\} = 0 \quad . \quad (26)$$

$$(\nabla^2 - \mu_1^2) \frac{\partial \bar{\phi}}{\partial t} - \mu_2^2 \left(\frac{\alpha}{2A}\right) \frac{\partial \bar{\phi}}{\partial t} - \frac{\alpha^2}{3A}\left(\frac{1-\alpha}{(1+\alpha)^2}\right) J(\bar{\phi}, \nabla^2 \bar{\phi})$$
$$- \{6A(1+\alpha)\}^{-1} \{J(\bar{\psi}, \nabla^2 \bar{\phi}) + J(\bar{\phi}, \nabla^2 \bar{\psi})\} + \beta \frac{\partial \bar{\phi}}{\partial x}$$
$$+ \left\{\frac{\alpha(2\alpha-1)}{6A(1+\alpha)}\right\} \left\{J(\bar{\phi}, \nabla^2 \psi_*) + J(\psi_*, \nabla^2 \bar{\phi})\right\}$$
$$+ \frac{\alpha}{3A} J(\bar{\phi}, \nabla^2 \bar{\phi}) - \mu_1^2 \{J(\bar{\psi}, \bar{\phi}) + \alpha J(\psi_*, \bar{\phi})\}$$
$$- \mu_2^2 \frac{\alpha}{2A} J(\bar{\psi}. \bar{\phi}) + \mu_1^2 \left(\frac{2\alpha-1}{1-\alpha}\right) \left(\frac{3\sigma_1}{[\sigma]}\right) \{\alpha(1+\alpha)^{-1} J(\psi_*, \bar{\phi})$$
$$- J(\psi_*, \bar{\phi})\} = 0 \quad . \quad . \quad . \quad . \quad . \quad . \quad (27)$$

$$\frac{\partial \nabla^2 \bar{\psi}}{\partial t} + J(\bar{\psi}, \nabla^2 \bar{\psi}) + \tfrac{1}{3} J(\bar{\phi}, \nabla^2 \bar{\phi}) + \beta \frac{\partial \bar{\psi}}{\partial x}$$
$$- \mu_2^2 \left(\frac{\sigma_2}{3[\sigma]}\right) \{\alpha(1+\alpha)^{-1} J(\psi_*, \bar{\phi}) - J(\psi_*, \bar{\phi})\} = 0 \quad . \quad . \quad (28)$$

$$(\nabla^2 - \mu_2^2) \frac{\partial \bar{\phi}}{\partial t} + J(\bar{\psi}, \nabla^2 \bar{\phi}) + J(\bar{\phi}, \nabla^2 \bar{\psi}) + \beta \frac{\partial \bar{\phi}}{\partial x} - \mu_2^2 J(\bar{\psi}, \bar{\phi})$$
$$+ \mu_2^2 \left(\frac{\sigma_2}{[\sigma]}\right) \{\alpha(1+\alpha)^{-1} J(\psi_*, \bar{\phi}) - J(\psi_*, \bar{\phi})\} = 0 \quad . \quad . \quad (29)$$

In these equations we have introduced the notations

$$A = \frac{1-\alpha^3}{3(1-\alpha^2)} - \tfrac{1}{2} \quad . \quad . \quad . \quad . \quad (30)$$

$$\mu_1^2 = f(A\, p_0\, \sigma_1)^{-1} \quad . \quad . \quad . \quad . \quad (31)$$

$$\mu_2^2 = -6f(\alpha\, p_0\, \sigma_2)^{-1} \quad . \quad . \quad . \quad . \quad (32)$$

There remains the question of the specification of the tropospheric and stratospheric stabilities σ_1 and σ_2, respectively. The stability jump $[\sigma]$ provides one relationship,

$$[\sigma] = \sigma_1 - \sigma_2 \quad . \quad . \quad . \quad . \quad . \quad (33)$$

To obtain a second relationship we may write,

$$\sigma = \frac{\partial \phi}{\partial p} + \kappa \frac{\partial \psi}{\partial p}$$

which upon integration yields

$$\int \sigma \, dp = \phi + \kappa \psi + f(x, y, t)$$

where $f(x, y, t)$ is an arbitrary function. Noting that σ is assumed constant over the ranges of integration defined by the operators $\overline{(\ )}$ and $\overline{\overline{(\ )}}$, we may write

$$\sigma_1 \bar{p} = \bar{\phi} + \kappa \bar{\psi} + f(x, y, t)$$

$$\sigma_2 \bar{\bar{p}} = \bar{\bar{\phi}} + \kappa \bar{\bar{\psi}} + f(x, y, t)$$

upon identifying the levels $\bar{p}$ and $\bar{\bar{p}}$ with the variables $\bar{\psi}$, $\bar{\phi}$ and $\bar{\bar{\psi}}$, $\bar{\bar{\phi}}$ respectively. Combining these equations to eliminate $f(x, y, t)$, we find

$$\alpha [\sigma] + \sigma_1 + 2p_0^{-1} (\bar{\bar{\phi}} + \kappa \bar{\bar{\psi}} - \bar{\phi} - \kappa \bar{\psi}) = 0 \quad . \quad . \quad (34)$$

This equation, together with Eq. (33), serves to determine the values of σ_1 and $[\sigma]$ in terms of $\bar{\psi}$, $\bar{\phi}$, $\bar{\bar{\psi}}$, $\bar{\bar{\phi}}$ and σ_2. The stability σ_2 is therefore a parameter which may be adjusted to the study of physical systems of different stratospheric intensity.*

Eqs. (26)-(29), together with Eqs. (23)-(25) for the vertical motions and the hydrostatic relations Eqs. (14) and (19), constitute the complete mathematical formulation of the model in terms of the variables $\bar{\psi}$, $\bar{\phi}$, $\bar{\omega}$, $\bar{\bar{\psi}}$, $\bar{\bar{\phi}}$, $\bar{\bar{\omega}}$, ψ_0, ψ_* and ω_*. These equations therefore provide a basis for studying the behaviour of large-scale tropospheric and stratospheric disturbances, and suggest the general nature of the coupling between the troposphere and stratosphere. Eqs. (26, (27) for the troposphere reflect the presence and structure of the stratosphere through both the parameter α and new baroclinic terms, several of which may contribute significantly to the behaviour of tropospheric disturbances. Eqs. (28) and (29) for the stratosphere on the other hand, are linked to the troposphere only by means of the vertical motion at the tropopause.

The case of no stratosphere or $\alpha = 0$ reduces the system of Eqs. (26)-(29) to those of the thermotropic model with a linear wind shear (Thompson and Gates 1956; Thompson 1953),

$$\frac{\partial \nabla^2 \bar{\psi}}{\partial t} + J(\bar{\psi}, \nabla^2 \bar{\psi}) + \tfrac{1}{3} J(\bar{\phi}, \nabla^2 \bar{\phi}) + \beta \frac{\partial \bar{\psi}}{\partial x} = 0 \quad . \quad . \quad (35)$$

$$(\nabla^2 - \mu^2) \frac{\partial \bar{\phi}}{\partial t} + J(\bar{\psi}, \nabla^2 \bar{\phi}) + J(\bar{\phi}, \nabla^2 \bar{\psi}) + \beta \frac{\partial \bar{\phi}}{\partial x} - \mu^2 J(\bar{\psi}, \bar{\phi}) = 0 \quad . \quad . \quad . \quad . \quad (36)$$

where the variables are now integrated over the entire depth of the atmosphere and $\mu^2 = -6 f p_0^{-1} \sigma^{-1}$. Here, of course, no direct information on the behaviour of the stratosphere or tropopause is obtained. We note that it is the stratospheric equations (28) and (29) which assume the form of those of the thermotropic model, but are now supplemented by a term depending upon the vertical motion at the tropopause, ω_*. Through this term, both the stability jump $[\sigma]$ and the troposphere's thermal structure $\bar{\phi}$ are introduced into the stratosphere's dynamics, which otherwise has no dependence upon the troposphere.

In several earlier models the presence of the stratosphere has been indirectly recognized in one way or another. In the barotropic model, for example, Bolin (1956) has simulated the effect of a non-vanishing vertical motion at the tropopause by the introduction of a homogeneous stratosphere whose density is approximately 7/8 that of the assumed homogeneous troposphere, and has thereby increased the mean tropospheric divergence.

* If one employs vertical finite-differences on ψ within the troposphere, and up to, but not crossing, the tropopause, the value of σ_1 may be determined approximately by writing

$$\sigma_1 \simeq -p\, \partial^2 \psi / \partial p^2 - (1 - \kappa)\, \partial \psi / \partial p$$

This approximation, together with Eqs. (33) and (34), serves to determine each of σ_1, σ_2 and $[\sigma]$. Identifying ψ_0, $\bar{\psi}$ and ψ_* with the 1,000, 600 and 200-mb surfaces, respectively, this approximation tailors $[\sigma]$ to the observed atmosphere; for the standard atmosphere heights of these surfaces, we find $\sigma_2 \simeq 7\sigma_1$ and $[\sigma] \simeq -6\sigma_1$.

In the actual atmosphere, however, the stability is much more nearly discontinuous at the tropopause than the density (or temperature) itself, and in the present model this effect of high-level divergence is represented in Eqs. (26)-(29) by the terms in ω_* and is proportional to $[\sigma]^{-1}$. In the vertically-integrated two-paramater models, such as those of Sawyer and Bushby (1953) and Eliassen (1952), the stratosphere is recognized by extending the vertical integration only over the troposphere or by extending the tropospheric modelling parameters into the stratosphere with the aid of a normal or climatological variation. These procedures have the effect of altering some of the coefficients in the models, but no new baroclinic effects are thereby introduced and the behaviour of the tropopause and stratosphere is not determined. Finally, in the multiple-parameter model of Árnason (1952, 1953) the height of an isothermal stratosphere is introduced by means of a parametric representation, using a variable tropospheric stability. Here also the behaviour of the stratosphere is not determined and its effects upon the troposphere are not brought out in the analysis.

3. The case of equivalent-barotropic flow

(i) *An equivalent-barotropic stratosphere*

Synoptic studies of the lower stratosphere, such as those reported by Palmén and Nagler (1949), Kochanski (1954), and Austin (1951, 1952) have suggested that there is little vertical tilt to the large-scale pressure systems in this region. This conclusion may, in part, be due to the general paucity of observations in the lower stratosphere, but an equivalent-barotropic characterization is probably more applicable here than in the troposphere. On the basis of this simplification, it is of interest to examine the reduction of the more general equations.

Writing $\nabla\overline{\phi} = -\nabla\overline{\psi}$ as the condition for equivalent-barotropic flow in the stratosphere, with the wind decreasing uniformly toward zero with decreasing pressure above the tropopause wind maximum,* we find only a slight change in Eq. (23) for the mean vertical motion in the troposphere

$$\overline{\omega} = -\sigma_1^{-1}\left\{\frac{\partial\overline{\phi}}{\partial t} + (1+\alpha)^{-1} J(\overline{\psi} + 2\alpha\overline{\psi}, \overline{\phi})\right\} \quad . \quad . \quad (37)$$

since the above condition of equivalent-barotropy also implies $\nabla\psi_* = 2\nabla\overline{\psi}$ by virtue of Eq. (19). The mean stratospheric vertical motion, Eq. (24), now reduces, however, to

$$\overline{\overline{\omega}} = -\sigma_2^{-1}\frac{\partial\overline{\phi}}{\partial t} = \sigma_2^{-1}\frac{\partial\overline{\psi}}{\partial t} \quad . \quad . \quad . \quad . \quad . \quad (38)$$

since $J(\overline{\psi}, \overline{\phi}) = 0$ in the present case. From Eq. (25) we find that the vertical motion at the tropopause ω_* is now given by

$$\omega_* = -4\alpha[\sigma]^{-1}(1+\alpha)^{-1} J(\overline{\psi}, \overline{\phi}) \quad . \quad . \quad . \quad . \quad (39)$$

and is dependent upon the relative configuration of the mean tropospheric thermal field and the mean stratospheric flow. For the troposphere, Eqs. (26) and (27) are also modified through the simplification of certain terms by the assumption of an equivalent-barotropic stratosphere, although their essential character is unchanged. For the stratosphere, however, Eqs. (28) and (29) reduce to a single equation for the mean stratospheric flow

$$\frac{\partial\nabla^2\overline{\psi}}{\partial t} + \tfrac{4}{3}J(\overline{\psi}, \nabla^2\overline{\psi}) + \beta\frac{\partial\overline{\psi}}{\partial x} - \mu_2^2\left(\frac{2\sigma_2}{3[\sigma]}\right)\alpha(1+\alpha)^{-1} J(\overline{\psi}, \overline{\phi}) = 0 \quad . \quad (40)$$

* A variety of wind profiles for an equivalent-barotropic stratosphere may be considered by writing $\nabla\overline{\phi} = c\,\nabla\overline{\psi}$ with $c \leqslant 0$; the case of high-level easterlies corresponds to $c < -1$.

These reductions represent a weakening of the coupling between the troposphere and stratosphere; the vertical motion at the tropopause (Eq. (39)), upon which the last term of Eq. (40) depends, is the primary mechanism linking the two. This action is such that for a typical middle-latitude disturbance (with an equivalent-barotropic stratosphere), the characteristic downward mean vertical motion behind the westward-tilting, low-level trough will be shared by the tropopause and opposed by rising mean vertical motion in the stratosphere. Such a distribution is shown schematically in Fig. 2, and may be compared with the vertical motion patterns deduced synoptically by Fleagle (1947), Austin (1951), Sawyer (1954), and Kochanski (1954).

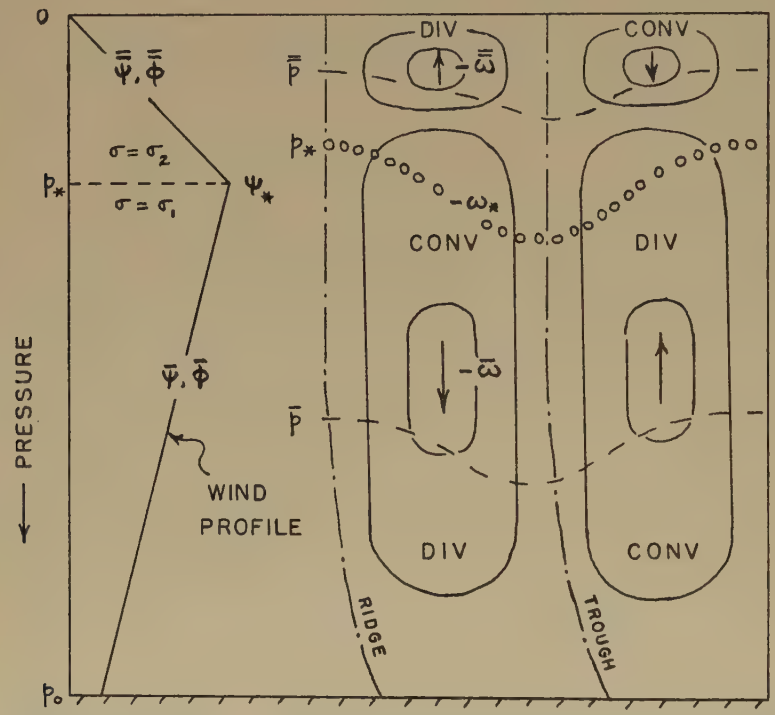

Figure 2. Schematic wind profile and vertical motion distribution for the case of an equivalent-barotropic stratosphere. The observed tropopause, levels of non-divergence, and ridge and trough axes are indicated by the open circles, dashed lines and dash-dotted lines, respectively.

(ii) *Equivalent-barotropic stratosphere and troposphere*

Having just considered the case in which the stratosphere is equivalent-barotropic, it is of interest to consider briefly at this point the further specialized case in which *both* the troposphere and stratosphere are equivalent-barotropic, i.e., possess parallel isotherms and contours at all levels. The thermal wind above and below the tropopause would then have the same orientation but would be oppositely directed, with the wind maximum at the tropopause. The discontinuity of stability is retained and is reflected in the complete reversal of mean temperature gradient across the tropopause.

For simplicity, we may assume no geostrophic wind at the surface p_0, i.e., $\nabla\psi_0 = 0$, and write

$$\nabla\bar{\phi} = c_1 \nabla\bar{\psi}, \qquad \nabla\bar{\bar{\phi}} = c_2 \nabla\bar{\bar{\psi}}$$

where c_1 and c_2 are constants representing the shear in the equivalent-barotropic layers.

From Eqs. (14) and (19) we then find

$$\nabla\bar{\psi}\,(1 - c_1) = -\,\alpha\,(1 + \alpha)^{-1}\,(1 - c_2)\,\nabla\bar{\bar{\psi}}$$

and upon setting $c_2 = -1$ as before, we obtain $c_1 = (1 + \alpha)\,(1 - \alpha)^{-1}$. In this case the governing dynamical equations are

$$\frac{\partial \nabla^2 \bar{\psi}}{\partial t} + \tfrac{4}{3} J\,(\bar{\psi}, \nabla^2 \bar{\psi}) + \beta \frac{\partial \bar{\psi}}{\partial x} = 0 \qquad . \qquad . \qquad . \qquad (41)$$

$$\frac{\partial \nabla^2 \bar{\bar{\psi}}}{\partial t} + \tfrac{4}{3} J\,(\bar{\bar{\psi}}, \nabla^2 \bar{\bar{\psi}}) + \beta \frac{\partial \bar{\bar{\psi}}}{\partial x} = 0 \qquad . \qquad . \qquad . \qquad (42)$$

with the vertical motions given by

$$\bar{\omega} = -\,\sigma_1^{-1}\,(1 + \alpha)\,(1 - \alpha)^{-1}\,\frac{\partial \bar{\psi}}{\partial t} \qquad . \qquad . \qquad . \qquad (43)$$

$$\bar{\bar{\omega}} = \sigma_2^{-1}\,\frac{\partial \bar{\bar{\psi}}}{\partial t} \qquad . \qquad . \qquad . \qquad . \qquad . \qquad . \qquad (44)$$

$$\omega_* = 0 \qquad . \qquad . \qquad . \qquad . \qquad . \qquad . \qquad (45)$$

In such an atmosphere the motions of the troposphere and stratosphere proceed independently, with the flow in each layer governed by the familiar equivalent-barotropic equation. Although the thermodynamics do not appear in this formulation, the stability discontinuity [σ] is required for the basic model, with opposite wind shears in the troposphere and stratosphere and a wind maximum at the tropopause. It is interesting to note that in this case the mean vertical motion in both the troposphere and stratosphere is determined, although the mean flow in each layer is not influenced by the presence of the tropopause. Moreover, Eqs. (43) and (44) lead to a two-cell picture of mean vertical motions, similar to that shown in Fig. 2 for the case of an equivalent-barotropic stratosphere only, with rising tropospheric and sinking stratospheric vertical motion ahead of the typical middle-latitude disturbance. In the present case, however, the troughs and ridges are everywhere vertical and the tropopause is a surface of zero vertical motion.

On the basis of this simplified model one may thus identify the presence of vertical motions ω_* at the tropopause level, and the degree to which the patterns of mean vertical motion $\bar{\omega}$ and $\bar{\bar{\omega}}$ are not coincident with the patterns of $\partial\bar{\psi}/\partial t$ and $\partial\bar{\bar{\psi}}/\partial t$, respectively, as measures of the atmosphere's baroclinity. The more complete models may then be visualized as providing modifications to a picture essentially determined by the equivalent-barotropic atmosphere.

4. The stability of large-scale tropospheric disturbances

In order to assess further the role of the stratosphere in the present model, we consider the problem of determining the conditions under which a baroclinic disturbance will grow. This problem has been examined in rather general terms by Charney (1947), Eady (1949), Fjörtoft (1950), and Kuo (1952), and in more simplified versions by a number of other workers. In general, these studies have indicated the presence of both stable (damped or neutral) and unstable (amplified) waves among the spectrum of atmospheric disturbances, although the approaches taken to the problem are somewhat different. In particular, Eady (1949) has shown the existence of a *most* unstable wavelength, whose amplification is a function of both the vertical wind shear and the static stability. Eady's analysis is particularly relevant to the present problem since he has explicitly considered a two-layer regime with a stratosphere, whose static stability is larger than that of the

troposphere and which may contain a reversed horizontal temperature gradient. For this case he finds a slow decay of the tropospheric disturbance into the stratosphere, and indicates that the vertical motion at the interface is generally in the same sense as that in the troposphere, while the stratospheric troughs and ridges have little vertical slope. On the basis of this analysis, we might, therefore, expect the general character of the tropospheric stability properties for the present model to resemble those for the analysis of the more general three-dimensional problem, but with a general stabilization due to the introduction of the relatively stable stratosphere.

In a complete stability analysis, the phase speeds and amplification rates of both tropospheric and stratospheric disturbances would be obtained, but even for a simplified model this represents a formidable task. For the present, we shall consider the atmosphere with an equivalent-barotropic stratosphere as examined in § 3, and seek the effects of such a stratosphere upon the stability of the large-scale *tropospheric* disturbances. We shall also neglect the effects of the tropopause vertical motion since its contribution is relatively small at any given time, although it is, of course, an important cumulative effect over the life-cycle of the disturbance. Such a stability analysis will therefore not correspond precisely to the model as presented above, but may be sufficient to display the basic stability properties of the general formulation.

For the stability analysis we may assume that the three variables $\bar{\psi}$, $\bar{\phi}$ and $\bar{\bar{\psi}}$ can be decomposed into a basic or undisturbed portion, which is a function of the north-south coordinate y only, and into a perturbation which is a function of the east-west coordinate x and of the time t. Considering harmonic perturbations of the form $\exp\{im(x-ct)\}$, where m is the wave number and c the wave speed, we obtain the following approximate perturbation equations for the simplified case of an equivalent-barotropic stratosphere :

$$W_1\{m^2 c-(1-\alpha)v_1 m^2+\beta-2\alpha v_2 m^2\}$$
$$+V_1\left\{-\frac{(1-\alpha)^2}{3(1+\alpha)^2}\left(1+3\alpha\left(\frac{1+\alpha}{1-\alpha}\right)\right)v_1^* m^2-2\alpha m^2(v_1-2v_2)v_2 v_1^{*-1}\right\}=0 \quad . \quad (46)$$

$$W_1\left\{\frac{v_1^* m^2}{6A(1+\alpha)}+\mu_1^2 v_1^*\right\}$$
$$+V_1\left\{c(m^2+\mu_1^2)+\frac{v_1 m^2}{6A(1+\alpha)}+\beta-\frac{2\alpha(2\alpha-1)v_2 m^2}{3A(1+\alpha)}-\mu_1^2 v_1\right.$$
$$\left.-\frac{c_s v_2 \alpha \mu_2^2}{2A v_1^*}-\frac{v_2^2 \alpha m^2}{3A v_1^*}\right\}=0 \quad . \quad . \quad . \quad . \quad . \quad (47)$$

Here W_1 and V_1 are the amplitudes of the $\bar{\psi}$ and $\bar{\phi}$ perturbations, respectively. The third perturbation equation for the stratospheric disturbance reduces in the present case to

$$c_s=\tfrac{4}{3}v_2-\frac{\beta}{m^2} \quad . \quad . \quad . \quad . \quad (48)$$

which has been used with the condition $W_2=V_1(v_2/v_1^*)$ to eliminate W_2, the amplitude of the $\bar{\bar{\psi}}$ disturbance, from Eqs. (46) and (47); Eq. (48) is the phase speed for an equivalent-barotropic stratosphere. In these equations we have written v_1, v_2 and v_1^* for the undisturbed zonal geostrophic wind in the troposphere and stratosphere, and for the mean zonal tropospheric thermal wind, respectively.

The stability problem has thus been reduced to essentially that of a two-parameter model, and in this form cannot be expected to display the complete effects of the present

model. With these simplifications, the condition that non-trivial solutions to the above system exist results in the frequency equation

$$c = \tfrac{1}{2}\left\{\frac{v_1(n^2+\mu_1^2)-\beta-r(\alpha)+q(\alpha)}{m^2+\mu_1^2} - \frac{\beta}{m^2} + (1-\alpha)v_1 + 2\alpha v_2\right\} \pm \Delta^{\frac{1}{2}} \quad . \quad (49)$$

where the discriminant Δ is given by

$$\Delta = \tfrac{1}{4}\left\{\frac{v_1(n^2+\mu_1^2)-\beta-r(\alpha)+q(\alpha)}{m^2+\mu_1^2} + \frac{\beta}{m^2} - (1-\alpha)v_1 - 2\alpha v_2\right\}^2 - \{(v_1^*)^2 K(\alpha) + s(\alpha)\}\frac{\mu_1^2-m^2}{\mu_1^2+m^2} \quad . \quad (50)$$

Here we have introduced the notations

$$n^2 = -m^2/6A(1+\alpha) \quad . \quad (51)$$

$$q(\alpha) = \frac{\alpha\mu_2^2 v_2 c_s}{2A v_1^*} = \frac{\alpha\mu_2^2 v_2}{2A v_1^*}\left(\tfrac{4}{3}v_2 - \frac{\beta}{m^2}\right) \quad . \quad (52)$$

$$r(\alpha) = \frac{2\alpha m^2 v_2}{6A v_1^*(1+\alpha)}\{2v_1^*(1-2\alpha) - v_2(1+\alpha)\} \quad . \quad (53)$$

$$s(\alpha) = -2\alpha v_1^* v_2\left(\frac{1-\alpha}{1+\alpha}\right) \quad . \quad (54)$$

$$K(\alpha) = \frac{(1-\alpha)^2}{3(1+\alpha)^2}\left\{1+3\alpha\left(\frac{1+\alpha}{1-\alpha}\right)\right\} \quad . \quad (55)$$

where A, μ_1^2, and μ_2^2 are given by Eqs. (30)-(32).

The phase speed is seen to depend in a rather involved way upon the mean zonal velocities v_1 and v_2, upon the tropopause level α, and upon the stratospheric stability σ_2, as well as upon the usual parameters of tropospheric wind shear v_1^* and stability σ_1. Since the basic wind profiles are linear and in the stratosphere the zonal current v_2 (at $\bar{p}$) has been set equal to one-half the jet or maximum speed v_m (at p_*), this dependence may be reduced to that on σ_1, α, v_1^* and v_2, when Eqs. (33) and (34) are used to relate σ_2 to σ_1. The most interesting dependence for the present study is that of the phase speed c upon the tropospheric shear v_1^* and tropopause level α; we shall accordingly assign the constant although representative values $\sigma_1 = -0{\cdot}195 \times 10^{10}$ cm^2 sec^{-1} mb^{-1} and $v_2 = 20$ m sec^{-1}.

TABLE 1. STABILITY CHARACTERISTICS OF TROPOSPHERE with basic jet speed $v_m = 40$ m sec^{-1}. The minimum tropospheric wind shear for instability is denoted by $v_{1,c}'$ and the corresponding (most unstable) wavelength for 45°N by L_c. The thermal wind corresponding to $v_{1,c}'$ and α is given by $v_{1,c}^* = v_{1,c}' p_0(1+\alpha)/2$. The stability jump $[\sigma]$ was computed from Eq. (34) using the standard atmosphere's pressure heights.

α	$R\sigma_1 f^{-1}$ (deg cb^{-1})	$R[\sigma]f^{-1}$ (deg cb^{-1})	$v_{1,c}'$ (m sec^{-1} cb^{-1})	$v_{1,c}^*$ (m sec^{-1})	L_c (km)
0	−6·8	—	1·67	8·3	4,220
0·1	−6·8	57·2	3·50	19·2	4,170
0·2	−6·8	34·3	3·73	22·4	4,020
0·3	−6·8	28·9	3·87	25·2	3,850
0·4	−6·8	28·8	4·00	28·0	3,750

The conditions for critical phase speeds, i.e., the conditions separating neutral and damped waves from amplified waves, are given by setting $\Delta = 0$ in Eq. (50), and are summarized in Fig. 3 and Table 1. It may be seen that the bulk presence of a stratosphere has produced a stabilization of the flow with respect to tropospheric disturbances, in the sense that their initial amplification requires greater shear than is the case without a stratosphere. Once the amplification of the disturbance has begun, however, the development might be either more or less intense than in an atmosphere without a tropopause, depending upon the particular initial conditions as described by the more complete differential equations of § 2. As the level of the tropopause lowers, the critical shear for instability increases, while the minimum unstable wavelength or 'cut-off' L_c decreases according to

$$L_c = 2\pi \left(\frac{-p_0 \sigma_1}{6f(1+\alpha)} \right)^{\frac{1}{2}} \quad . \quad . \quad . \quad . \quad (56)$$

where $\sigma_1 < 0$ is the tropospheric stability. The most unstable wavelength appears to decrease less slowly with increasing α than L_c, and there is a general flattening of the critical instability curves for larger α. With the tropopause between 100 and 400 mb, we note that the tropospheric shears required for instability are about *twice* those required in an atmosphere without a stratosphere. The relative insensitivity of the analysis to the precise level of the tropopause is probably caused by the extensive simplifications made with respect to the stratosphere, and should be interpreted with appropriate caution.

The dashed curves in Fig. 3 are the critical curve for instability obtained by Fjörtoft (1950) from an analysis of three-dimensional disturbances, and the critical curve for the

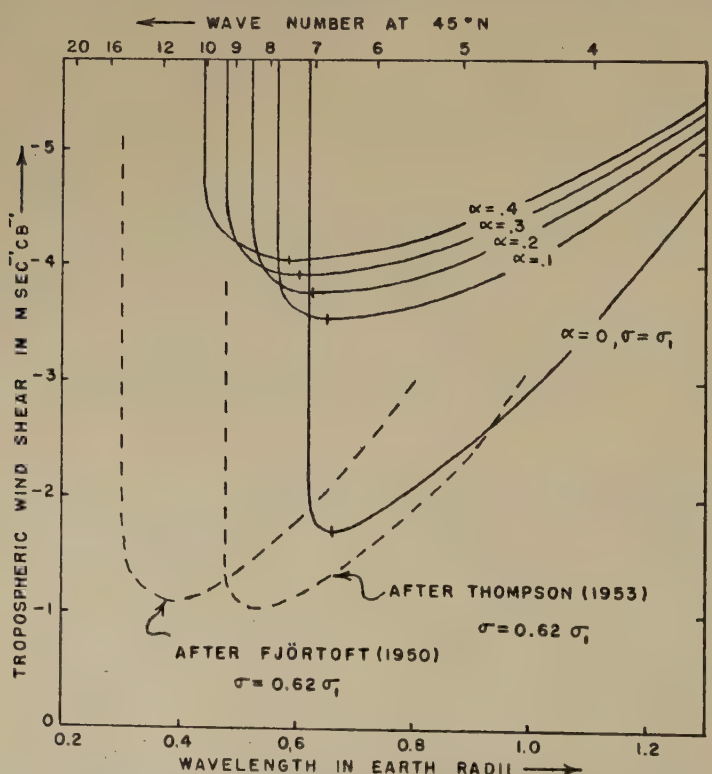

Figure 3. Stability characteristics of tropospheric flow with a stratosphere at $p_* = \alpha p_0$, for $\sigma_1 = -0{\cdot}195 \times 10^{10}$ cm^2 sec^{-1} mb^{-1} (corresponding to $R\sigma_1 f^{-1} = (T/\theta)\,\partial\theta/\partial p = -6{\cdot}8$ deg cb^{-1} at 45°N) and a stratospheric current $v_2 = 20$ m sec^{-1}.

equivalent-baroclinic model of Thompson (1953).* The latter curve may be compared with that for $\alpha = 0$ in the figure as an indication of the effect of the tropospheric stability σ_1 upon the growth of the disturbances. The dependence of the stability characteristics upon the mean stratospheric wind speed v_2, or equivalently, upon the maximum or jet speed, is such that for greater jet speeds greater tropospheric shear is required for instability, all other factors remaining unchanged. For the present case of a constant jet speed $v_m = 40$ m sec^{-1}, representative of average wintertime conditions, the critical wind profiles for the disturbances of maximum instability are shown in Fig. 4. By comparison with the critical profiles without a tropopause, the stabilizing effect of the stratosphere can be clearly seen.

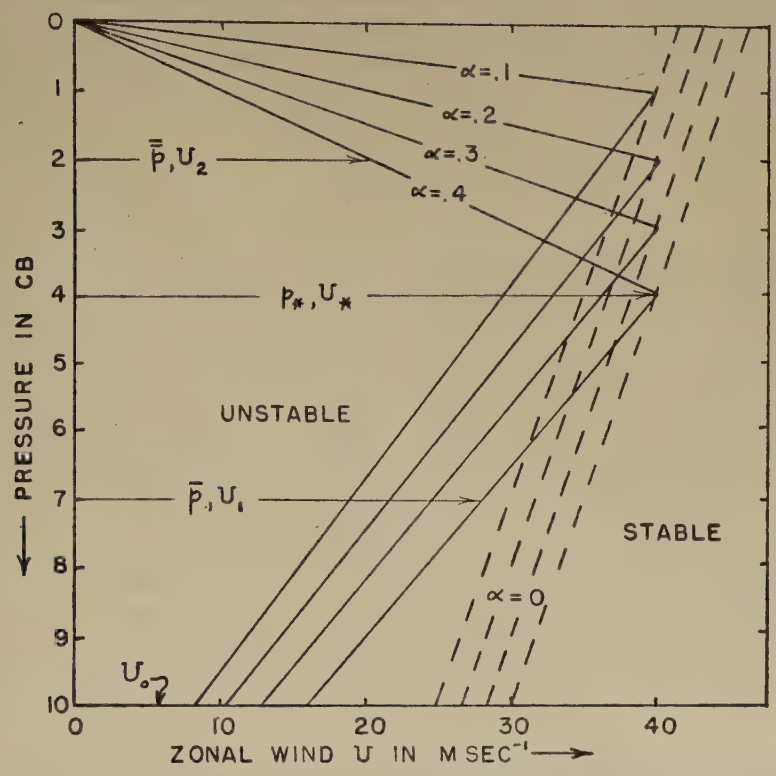

Figure 4. Critical wind profiles for instability with respect to tropospheric perturbations of the most unstable wavelength (see Fig. 3 and Table 1), for various tropopause levels $\alpha = p_*/p_0$ and a jet speed of 40 m sec^{-1}. The critical profiles without a tropopause are shown by the dashed lines for the corresponding jet speeds. The velocities v_0, v_1, v_m, and v_2 are identified for the case $\alpha = 0{\cdot}4$.

For the case of no stratosphere, $\alpha = 0$, we find $q(\alpha) = r(\alpha) = s(\alpha) = 0$, $K(\alpha) = 1/3$, $A = -1/6$ and $n^2 = m^2$, giving the frequency equation

$$c_T = v_1 - \frac{\beta}{2}\left(\frac{1}{m^2} + \frac{1}{\mu_1^2 + m^2}\right) \pm \Delta_T^{\frac{1}{2}} \quad . \quad . \quad . \quad (57)$$

with the discriminant Δ_T given by

$$\Delta_T = \frac{\beta^2}{4}\left(\frac{1}{m^2} - \frac{1}{\mu_1^2 + m^2}\right)^2 - \frac{(v_1^*)^2}{3}\left(\frac{\mu_1^2 - m^2}{\mu_1^2 + m^2}\right) \quad . \quad . \quad (58)$$

* This curve differs from that presented by Thompson (1953) to the extent that the β-term in the thermal vorticity equation has been retained in the present analysis.

These equations are those of the two-parameter thermotropic model, Eqs. (35) and (36). Here the essential mechanism of instability is the presence of the thermal wind v_1^* and has been described by Thompson (1953). These equations reduce to the familiar barotropic or Rossby frequency equation upon setting $v_1^* = 0$.

5. The behaviour of the tropopause and some comparisons with the atmosphere

Although in the derivation of the present model the tropopause has been assumed to be an isobaric surface, this formulation nevertheless permits the determination of the vertical and horizontal motions at this level. By identifying these motions with those of the actual, locally-determined tropopause and using the dynamical boundary condition, Eq. (11), it is possible to trace the motion and deformation of the tropopause surface itself. To the present approximation, however, we note that Eq. (11) is an auxilliary relationship only, and is not used to determine the behaviour of the model. With this viewpoint, we may combine Eqs. (11) and (25) and write

$$\frac{\partial \alpha}{\partial t} = -2p_0^{-1}[\sigma]^{-1}\{\alpha(1+\alpha)^{-1}J(\psi_*, \bar{\phi}) - J(\psi_*, \bar{\phi})\} - J(\psi_*, \alpha) \quad . \quad (59)$$

Here the first and second terms on the right-hand side represent the effects of vertical motions on variations of the tropopause level, while the last term represents the horizontal 'advection' of the tropopause. In the case of an equivalent-barotropic stratosphere, the second term in Eq. (59) vanishes and we may more easily estimate the relative contributions of vertical motion and advection to variations of the tropopause. Selecting $\alpha = 0{\cdot}2$ and using an average value of $[\sigma]$, we find that a change of 1°C in the mean tropospheric temperature ($\bar{\phi}$) along the tropopause wind direction ($\mathbf{k} \times \nabla\psi_*$) makes approximately the same contribution to $\partial\alpha/\partial t$ through the accompanying vertical motion as does a change of 1 mb in the tropopause pressure in the same direction through advection.

The various synoptic studies of the structure and variations of the tropopause and the associated jet stream, such as those reported by Palmén and Nagler (1949), Austin (1952), Kochanski (1954, 1955), Endlich, Solot and Thur (1955), and Sawyer (1951, 1954), of which the last is the most comprehensive, lend some support to the present approximations with respect to the tropopause. These studies have indicated the existence of organized large-scale vertical motions in the lower stratosphere, often in an opposite sense to those characteristic of the troposphere. They also show that in general the variations of the tropopause follow closely the changes of the high-tropospheric flow pattern, with a characteristic amplitude of the order of 100 mb. The apparent vertical motions of the material tropopause responsible for such changes are about 2 cm sec^{-1} (approximately 60 mb day^{-1}), and those given by the present model are of this order.*

In the initial stages of the life-cycle of the typical cyclonic disturbance, it appears that the tropopause variation is mainly determined by the vertical motion effect, and is such that there is a lowering of the tropopause by downward vertical motion in the vicinity of the upper trough, to the rear of the low-level disturbance. As the disturbance grows, the effects of vertical motion and advection upon tropopause variations become more nearly equal, with the changes in the occlusion stage being mainly determined by advection. In this connection it is interesting to note that Sawyer (1954) has found the effects of vertical motion and advection to be of approximately equal importance for variations of the tropopause during the growing stages of middle-latitude disturbances. The lowering tropopause accompanying the developing cyclone discussed above may provide a dynamical

* We are in no way explaining the existence of the tropopause, but are only considering its dynamical effects on the assumption that it is a characteristic of the atmosphere. For a discussion of the basic processes in the formation and long-term maintenance of the tropopause, see Goody (1954).

mechanism for the observed increases in atmospheric ozone content in relation to cyclones, as described by Dobson, Brewer and Cwilong (1946) and studied by Reed (1950) and others. The present model may also be used to study the transformations of potential and kinetic energy in the atmosphere, and may illuminate the role of the stratosphere in the general circulation.

In lieu of actual numerical solutions of the governing equations, which will be presented in a later paper, it is of interest to compare the basic features of the model with the observed mean atmosphere. In Fig. 5 (a), the average northern hemisphere zonal wind profiles after Mintz (1954) are shown for both summer and winter at the latitude of the seasonal mean jet (30°N in winter, 45°N in summer). These data suggest that the mean atmosphere at least is reasonably well portrayed by a p-linear wind profile in both the troposphere and lower stratosphere with a jet at about 200 mb. Fig. 5 (b) shows the corresponding vertical wind shears, together with those for $\alpha = 0$ and for the most unstable disturbance under these average wintertime conditions (see Fig. 4). It may be noted that the mean winter and summer shears in the upper troposphere lie respectively above and below the critical shear for the model.

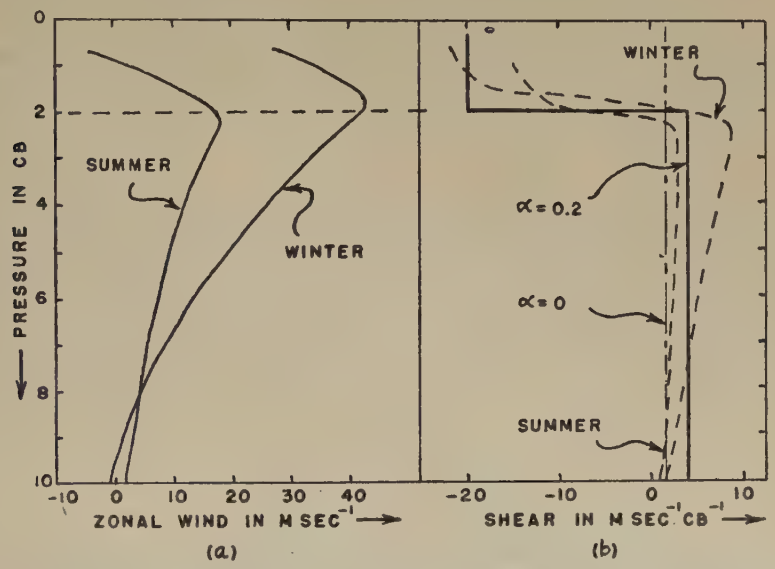

Figure 5 (a). The observed average zonal wind profiles for the northern hemisphere at the latitude of the winter and summer jets from the data of Mintz (1954). (b) The observed average vertical wind shears (dashed lines) corresponding to the profiles in (a), with the critical shears for the most unstable wavelength found from the stability analysis ($\alpha = 0{\cdot}2$, solid line; $\alpha = 0$, dash-dotted line). See also Figure 4.

As a further comparison with the atmosphere, the vertical variation of the static stability, as calculated from the mean hemispheric cross sections presented by Wexler (1950), as shown in Fig. 6 (a), together with the values used in the stability analysis. The corresponding temperature profiles are shown in Fig. 6 (b), with that for the model calculated for the same mean (600 mb) temperature as observed. These comparisons serve to illustrate the near constancy of the tropospheric stability, and show the general nature of temperature soundings given by the model. The near discontinuity of stability and the abrupt change of lapse rate across the tropopause may also be seen in individual wintertime cross-sections, such as those presented by Palmén (1951). Since $[\sigma]$ may be varied to some extent (see § 3), the stratospheric stability and lapse rate may be adjusted to representative synoptic conditions.

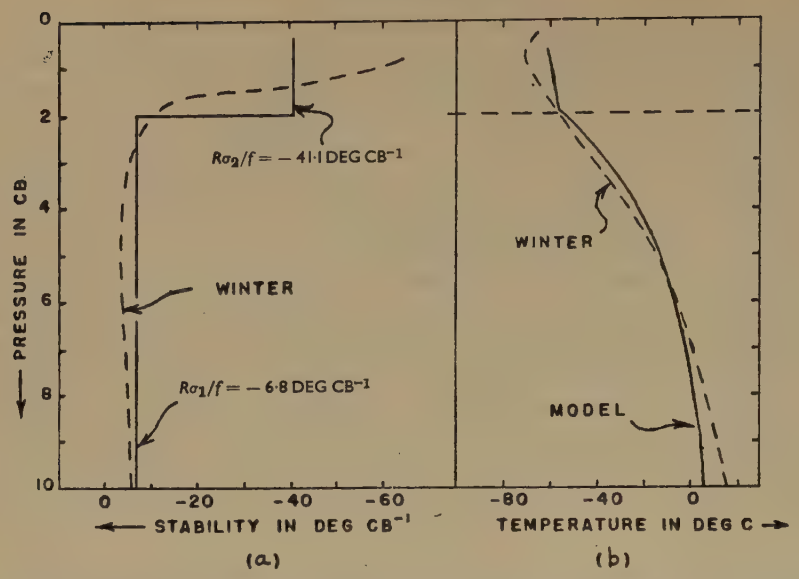

Figure 6. (a) The observed mean stability profile for the northern hemisphere at 30°N (latitude of mean winter jet) from the data of Wexler (1950), compared with the model. (b) The corresponding observed mean temperature profile and that calculated from the model for the same mean temperature.

On the basis of these comparisons, we might select $\alpha = 0{\cdot}2$ as representative of average wintertime conditions for use with Eqs. (23)-(29) in numerical calculations, while using Eq. (59) to follow the actual tropopause. This would present the practical convenience of identifying ψ_* with the 200-mb surface, and upon selecting $p_0 = 1{,}000$ mb, $\overline{\psi}$ and $\overline{\overline{\psi}}$ might then be asosciated with the 600- and 100-mb surfaces, respectively. (This approximation implies that the levels $\overline{p} = (p_0 + p_*)/2$ and $\overline{\overline{p}} = p_*/2$ are equivalence levels in the baroclinic model, and depending upon the magnitude of the tropopause vertical motion, they will more or less resemble the levels of non-divergence (see § 3)).

6. Summary and conclusions

In this paper, the governing equations for vertically-integrated tropospheric and stratospheric large-scale disturbances have been formulated (Eqs. (23)-(29)), on the basis of a simple model characterized by a uniform thermal wind and constant static stability in both troposphere and stratosphere. These regions are separated by an interface or tropopause across which the stability and thermal wind are discontinuous. To avoid undue complication in the equations and at the same time to retain a significant troposphere-stratosphere interaction, the theory is developed by treating the tropopause as a quasi-isobaric surface. This model allows the prediction of the mean velocity and temperature in both the troposphere and (lower) stratosphere, as well as the mean tropospheric and stratospheric vertical motion. As a consequence of the hydrostatic equations, the horizontal (geostrophic) velocity both near the earth's surface and near the tropopause is also obtained. Finally, the vertical motion at the tropopause itself is determined from the internal boundary conditions, and allows the deformation of the tropopause to be studied, although in cases of a steeply inclined or so-called multiple tropopause, we should perhaps expect some systematic error. The stratosphere is seen to introduce new baroclinity into the tropospheric equations while the stratosphere itself is governed by equations which resemble those for an equivalent-baroclinic or thermotropic fluid.

From an analysis of the stability of the large-scale disturbances with an equivalent-barotropic stratosphere, a marked stabilization of the initial amplification of the tropospheric disturbances is seen to be introduced by the presence of the stratosphere. For a constant basic zonal current of 20 m sec^{-1} in the stratosphere, the minimum vertical shears for instability are more than twice those found in the absence of a tropopause, and are seen to lie between the mean winter and summer shears in the zone of maximum westerlies. The most unstable wavelength shifts slightly toward shorter waves as the tropopause lowers, with a value of approximately 4,000 km for a tropopause at 200 mb, characteristic of average wintertime conditions in the middle latitudes.

For this case of an equivalent-barotropic stratosphere, the governing equations are simplified but still retain the essential physical features of the model. The existence of a tropopause vertical motion generally similar to that characteristic of the troposphere is indicated (rising motion from trough to ridge, sinking motion from ridge to trough), with the field of high-level convergence or divergence extending across the tropopause into the lower stratosphere. This behaviour may account for the systematic tropopause variations in relation to cyclones and anticyclones, and may offer a dynamical mechanism for the observed ozone variations. The presence of a high-level system of vertical motion in the stratosphere generally opposing that in the troposphere is also indicated. In the further special case when both troposphere and stratosphere are equivalent-barotropic, each layer behaves independently of the other, with a mean vertical motion of opposite signs and proportional to the mean height tendency. The tropopause vertical motion is in this case zero.

Although the present formulation may be viewed as a four-level model, it is felt to avoid both the seemingly undue complication characteristic of the higher-parameter models, and the truncation errors made in crossing the tropopause in the usual multi-level models. Supported by synoptic and observational studies of the large-scale disturbances in relation to the tropopause, the model is believed to furnish the basis for a method of numerical prediction for both tropospheric and stratospheric large-scale motions.

References

Árnason, G.	1952	*Tellus*, **4**, p. 356.
	1953	*Ibid.*, **5**, p. 386.
Austin, J. M.	1951	*Compendium of Meteorology*, Amer. Met. Soc., p. 630.
	1952	*Tech. Rep. MIT*, No. 11, Cambridge, U.S.A.
Berkofsky, L.	1956	*J. Met.*, **13**, p. 102.
Blackburn, J. F. and Gates, W. L.	1956	*Ibid.*, **13**, p. 59.
Bolin, B.	1956	*Tellus*, **8**, p. 61.
Bushby, F. H. and Hinds, M. K.	1954	*Quart. J. R. Met. Soc.*, **80**, p. 165.
Charney, J. G.	1947	*Tellus*, **4**, p. 135.
Charney, J. G. and Phillips, N. A.	1953	*J. Met.*, **10**, p. 71.
Charney, J. G., Gilchrist, B. and Shuman, F.	1956	*Ibid.*, **13**, p. 489.
Dobson, G. M. B., Brewer, A. W. and Cwilong, B. M.	1946	*Proc. Roy. Soc.* A, **185**, p. 144.
Eady, E. T.	1949	*Tellus*, **1**, p. 33.
	1952	*Ibid.*, **4**, p. 157.
Eliassen, A.	1952	*Ibid.*, **4**, p. 145.
Endlich, R. M., Solot, S. B. and Thur, H. A.	1955	*Tellus*, **7**, p. 308.
Fjörtoft, R.	1950	*Geofys. Publ.*, **17**, No. 6.
Fleagle, R. G.	1947	*J. Met.*, **4**, p. 165.
Gates, W. L., Pocinki, L. S. and Jenkins, C. F.	1955	*Geophys. Res. Pap.*, No. 46, U.S.A.F. Geophys. Res. Dir., Cambridge, U.S.A.
Goody, R. M.	1954	*The physics of the stratosphere*, Cambridge University Press.

Kochanski, A.	1954	*A.W.S. Tech. Rep.* 105-129, Washington, D.C.
	1955	*J. Met.*, **12**, p. 95.
Kuo, H.-L.	1952	*Ibid.*, **9**, p. 260.
Lowell, S. C.	1951	*Tellus*, **3**, p. 78.
Mintz, Y.	1954	*Bull. Amer. Met. Soc.*, **35**, p. 208.
Palmén, E.	1951	*Compendium of Meteorology*, Amer. Met. Soc., p. 599.
Palmén, E. and Nagler, K. M.	1949	*J. Met.*, **6**, p. 227.
Reed, R. J.	1950	*Ibid.*, **7**, p. 263.
Sawyer, J. S.	1951	*Quart. J. R. Met. Soc.*, **77**, p. 480.
	1954	*Geophys. Mem. Met. Off.*, No. 92.
Sawyer, J. S. and Bushby, F. H.	1953	*J. Met.*, **10**, p. 54.
Shuman, F. G.	1955	*Tech. Mem.*, No. 7, JNWP Unit, Washington.
Thompson, P. D.	1953	*Quart. J. R. Met. Soc.*, **79**, p. 51.
	1955	*Tech. Mem.*, No. 1, JNWP Unit, Washington.
Thompson, P. D. and Gates, W. L.	1956	*J. Met.*, **13**, p. 127.
Wexler, H.	1950	*Tellus*, **2**, p. 262.

551.594.221

Preliminary discharge processes in lightning flashes to ground

By N. D. CLARENCE and D. J. MALAN

Physics Department, University of Natal, Durban

Bernard Price Institute of Geophysics, Witwatersrand University, Johannesburg

(Manuscript received 6 June 1956)

SUMMARY

By using different techniques of recording the electrical effects of lightning discharges occurring at varying distances, it has been possible to sort out the major components of pre-return stroke field changes. A comparison between these field changes has shown that the first return stroke of a lightning flash to ground is usually preceded by three successive and distinct discharge processes.

The first, or breakdown stage, is identified from the reversal of its field change with distance as a discharge between the main negative charge centre and the positive charge centre near the base of the cloud at heights of 3·6 and 1·4 km respectively, the discharge probably just as often starting from the positive as from the negative centre. This is followed by the second stage during which the highly conducting channel then existing in the cloud is being negatively charged. The charging continues until the field in front of the channel has become sufficiently strong to propagate a downward-moving stepped leader breakdown streamer.

Stepped leaders have been observed to precede more than 75 per cent of all flashes to ground, though the radiation fields of most stepped leaders are so small that they can only be detected by using very high amplification.

The probable mechanisms involved in the preliminary stages are discussed.

1. Introduction and terminology

The work described in this paper was carried out at Johannesburg to investigate the electrical breakdown processes which take place inside and below a thundercloud before the first return stroke of a flash to ground.

Wormell (1952, 1953) has pointed out the importance of the slow electrostatic field changes of exceptionally long duration which often precede flashes to ground in England. In the earlier work of Schonland, Hodges and Collens (1938), the time constants of the aerial circuits were too short to detect slow field changes. Later observations (Malan 1952), and those described in this paper, have established that in South Africa also electrostatic field changes, sometimes lasting for several hundred milliseconds, precede flashes to ground. The observed durations are in complete agreement with those published by Pierce (1955) for thunderstorms in England. Similar field changes of long duration have been observed in Japan (Kitagawa, Iizuka, Murai and Kobayashi 1954).

The intensity in esu of the electric field at an instant t and at a distance D from a thundercloud is given by the equation (Lejay 1926)

$$E = \frac{M}{D^3} + \frac{1}{cD^2}\frac{dM}{dt} + \frac{1}{c^2 D}\frac{d^2 M}{dt^2} \quad . \quad . \quad . \quad (1)$$

provided that D is large compared with the height and linear dimensions of charge distribution; c is the velocity of light and M the total electric moment of the cloud charges at the time $(t - D/c)$. The terms at the right of the equation are respectively the electrostatic, induction and radiation components of the field. The electrostatic component, which is inversely proportional to D^3, decreases more rapidly with distance than the induction component which is inversely proportional to D^2. The induction component in turn decreases more rapidly with distance than the radiation component which is inversely proportional to D.

By making observations at different ranges of distance and using techniques of recording suitable to each range, it has proved possible to separate the various phases of preliminary discharges.

At distances up to 20 km the electrostatic component of field change is predominant, whereas at distances exceeding 200 km the effect of the radiation field change by far outweighs the other two. Between 30 and 80 km both induction and radiation effects are appreciable.

It will be shown that pre-return stroke discharges usually take place in three successive stages.

The diagrams of Fig. 1 illustrate the general nature of the field changes associated with the first stroke of a lightning flash to ground when observations are made respectively at 5, 50 and 500 km. R is the return stroke field change and J the post-return stroke field change. The preliminary stages have been called by us the B or breakdown stage, the I or intermediate stage and the L or leader stage. By comparing the diagrams of Fig. 1 it can be seen that the B, I and L stages are clearly distinguished by the variations of the relative amplitudes of their field changes at different distances. It will be shown that the L stage can be attributed to the stepped leader and that the B and the I stages are preparatory discharges which take place inside the cloud before the launching of the stepped leader.

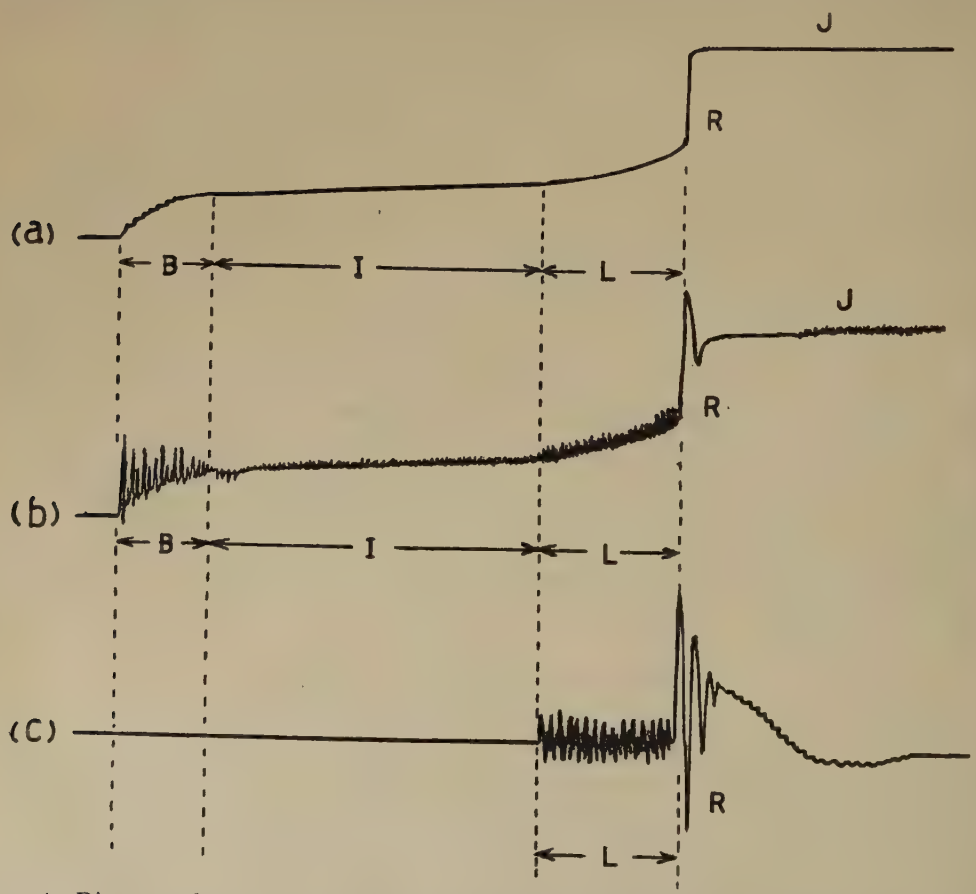

Figure 1. Diagrams of typical field changes of discharges to ground. (a) Electrostatic fields at 5 km. (b) Electrostatic, induction and radiation fields at 50 km. The relative amplitude of the R part has been reduced. (c) Radiation fields at 500 km.
Durations : B from 2 to 10 millisec; I from 0 to 400 millisec; L from 4 to 30 millisec.

For these reasons the term ' leader,' as used in this paper, is restricted to the stepped leader and does not refer to the preliminary breakdown process as a whole (Malan 1955).

The probable mechanisms of the B and I discharges are discussed in § 7.

2. Experimental procedure

Various methods of recording were used, the method depending on the type of field change to be examined. The field changes were displayed on a cathode-ray oscilloscope and photographed by revolving drum cameras, one of which had a fast- and a slow-moving drum.

The methods used are briefly outlined below.

(i) For slow variations of the electrostatic fields of storms up to 20 km the output from an electrostatic fluxmeter (Malan and Schonland 1950) was first recorded on magnetic tape (Clarence and Malan 1951).

(ii) A modification of the electrostatic fluxmeter which measures the charges induced on a well-insulated aerial (Malan 1954) was used to record electrostatic field changes from storms up to 150 km.

(iii) The oscillographic method of Appleton, Watson-Watt and Herd (1926) was used for measuring rapid field changes, the output from the aerial circuit being fed in parallel to the two channels of a double-beam oscilloscope used without time-base. The oscillograph spots were masked by small strips of red paper.

The amplifier of one channel of the oscilloscope was adjusted by trial so that the return-stroke deflections of flashes to ground just filled the screen. The sensitivity of the second channel was then made about 5 times as great as that of the first to accentuate the smaller field changes.

This method of recording is particularly useful at distance ranges up to 80 km as it obviates the necessity of beam triggering. The initial electrostatic field changes are appreciable enough at these distances to cause the electron beam of the high-gain channel to emerge from behind the mask at the outset of the preliminary discharge process (Fig. 3a, Plate II).

(iv) Field changes from distant storms were recorded on a magnetic tape machine which had two identical narrow gap heads and a tape speed of 75 cm/sec. The first head was used for recording and the second for reproducing. The combined recording and reproducing system had a linear response from 200 c/sec to 20 kc/sec.

The aerial system of (iii) above was connected to the Y amplifier of one (A) channel of a double-beam oscilloscope. The output from the reproducing head was fed through a pre-amplifier to the input of the other (B) channel of the oscilloscope. An input signal from the aerial was thus immediately displayed on the A channel and 140 millisec later on the B channel, this being the time taken by the tape to travel from the recording to the reproducing head.

The two spots in their stationary positions remained behind a mask which covered the lower portion of the oscilloscope screen. When a signal whose amplitude exceeded a pre-set level was picked up, it triggered a single cycle of a sawtooth time-base which caused both beams to emerge rapidly from behind the mask and to return slowly to their rest positions. During their emergence the beam excursions were photographed by a continuously revolving drum camera.

When channel A triggers the sweep and thus exposes both A and B spots, the B spot records events which had occurred 140 millisec before those shown by the A spot. Some double records obtained in this way are illustrated in Figs. 4 (a), (b) and (c) (Plate I) in which the A record is on the left and the corresponding B record on the right of each pair.

140 millisec is sufficient to establish with a fair degree of certainty whether the triggering pulse belonged to the first stroke of the flash. Both channels were photographed to check the fidelity of reproduction of the tape machine.

3. Electrostatic field changes

Six records illustrating the typical electrostatic field changes of long duration preceding the first return stroke R of flashes to ground are reproduced in Fig. 2 (Plate I), where (a) and (b) are electrostatic fluxmeter records (method (i), § 2), the arrows indicating which side of the envelope must be used for measurement. The start of the preliminary field change at B is thus negative on these two records, which were taken at distances of 1 and 2 km respectively.

Figs. 2 (c) and (d), show double records obtained simultaneously by the modified fluxmeter and by the method of Appleton, Watson-Watt and Herd ((ii) and (iii), § 2). The start of the preliminary field change is positive on these records, taken at 25 and at 40 km respectively. Pre-return stroke electrostatic field changes of long duration generally consist of the three successive B, I and L phases mentioned in § 1.

(*a*) *The electrostatic* B *field change : reversal of sign with distance*

The rate of change of field during the first 2 to 10 millisec, the time varying from flash to flash, is higher than the succeeding rate-of-change of field. This effect is very marked in Figs. 2 (b) and (c) and less so in Figs. 2 (a) and (d). An analysis of the effect of distance upon the sign of the B field change has revealed the following significant facts :

At distances up to 2 km the B field changes are negative, whereas at distances in excess of 5 km they are positive. In 43 records, obtained between 2 and 5 km, 21 of the B field changes were positive-starting and 22 were negative-starting, the distribution of sign being random throughout the range; the sign however usually changes during the course of the discharge.

It has been shown (Simpson 1927) that when the vertical height H of an electric charge varies, the field observed at the ground at a horizontal distance D passes through a maximum when $H = 2^{-\frac{1}{2}} D$. The respective heights of a charge to produce maximum fields at distances of 2 and 5 km are thus 1·4 and 3·6 km. It follows then that either a positive charge moving upwards from 1·4 km or a negative charge moving downwards from 3·6 km altitude will always give negative field changes at distances nearer than 2 km and positive field changes at distances greater than 5 km.

It is thus obvious that B field changes can be attributed either to positive charge moving upwards from a minimum height of 1·4 km, or to negative charge moving downwards from a maximum height of 3·6 km. Which of the two is the more likely can be determined from the sign of the B field changes occurring between 2 and 5 km.

In this intermediate range of distance, positive charge moving upwards from 1·4 km will give positive-starting field changes, whilst negative charge moving downwards from 3·6 km will give negative-starting field changes. Since positive and negative B field changes are evenly distributed in the distance range 2 to 5 km the two possibilities are apparently equally probable.

The fact that the calculated heights of 1·4 and 3·6 km are in close agreement with the respective heights of the base of the cloud (1·5 to 2 km) and the lower region of the negative-charge centre N (3 to 4 km), (Malan and Schonland 1951b), strongly suggests that the B field change is due to a discharge between N and the positive-charge centre p situated near the base of the cloud. The discharge probably starts just as often from p as from the N centre.

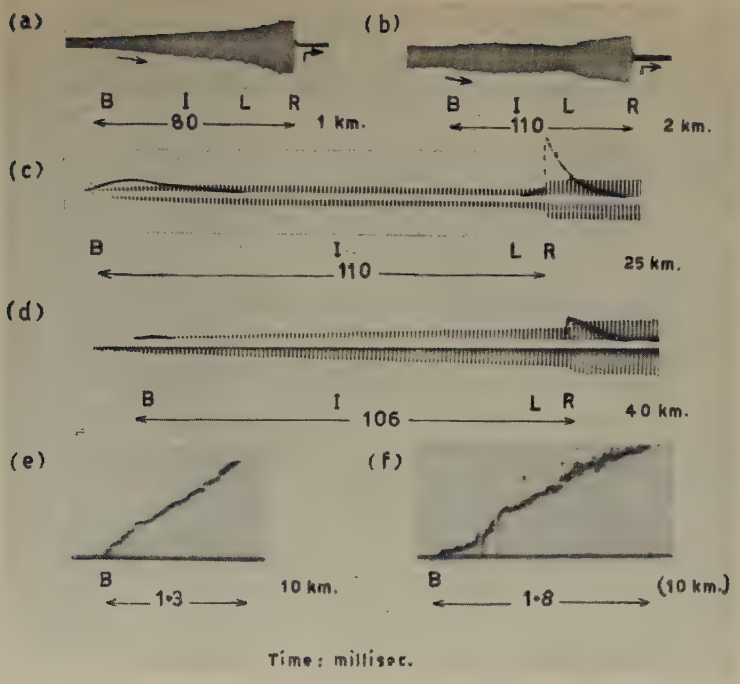

Figure 2. Records of electrostatic field-changes.

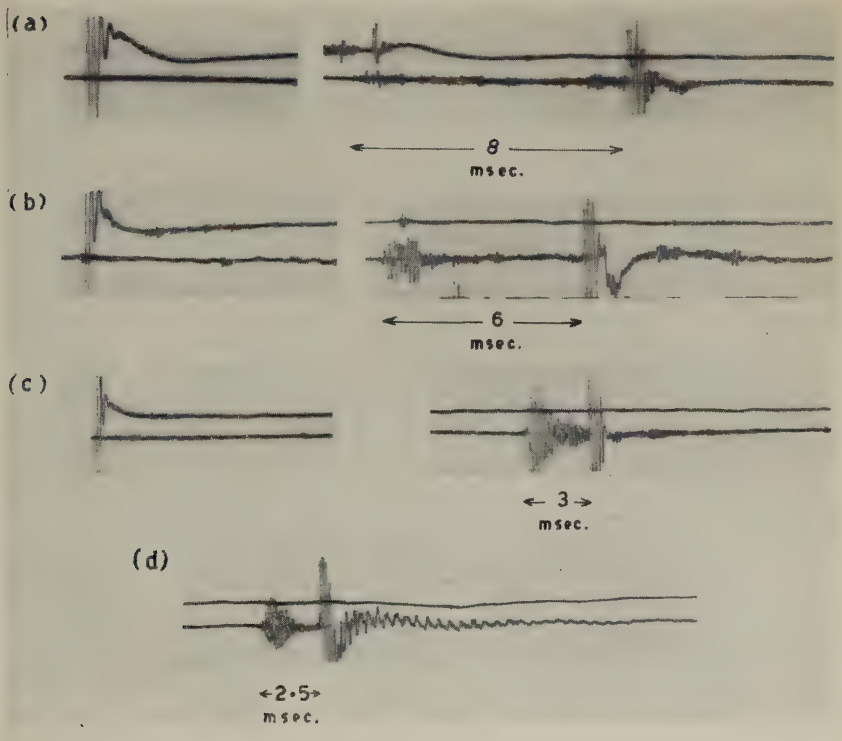

Figure 4. Records of radiation field-changes.

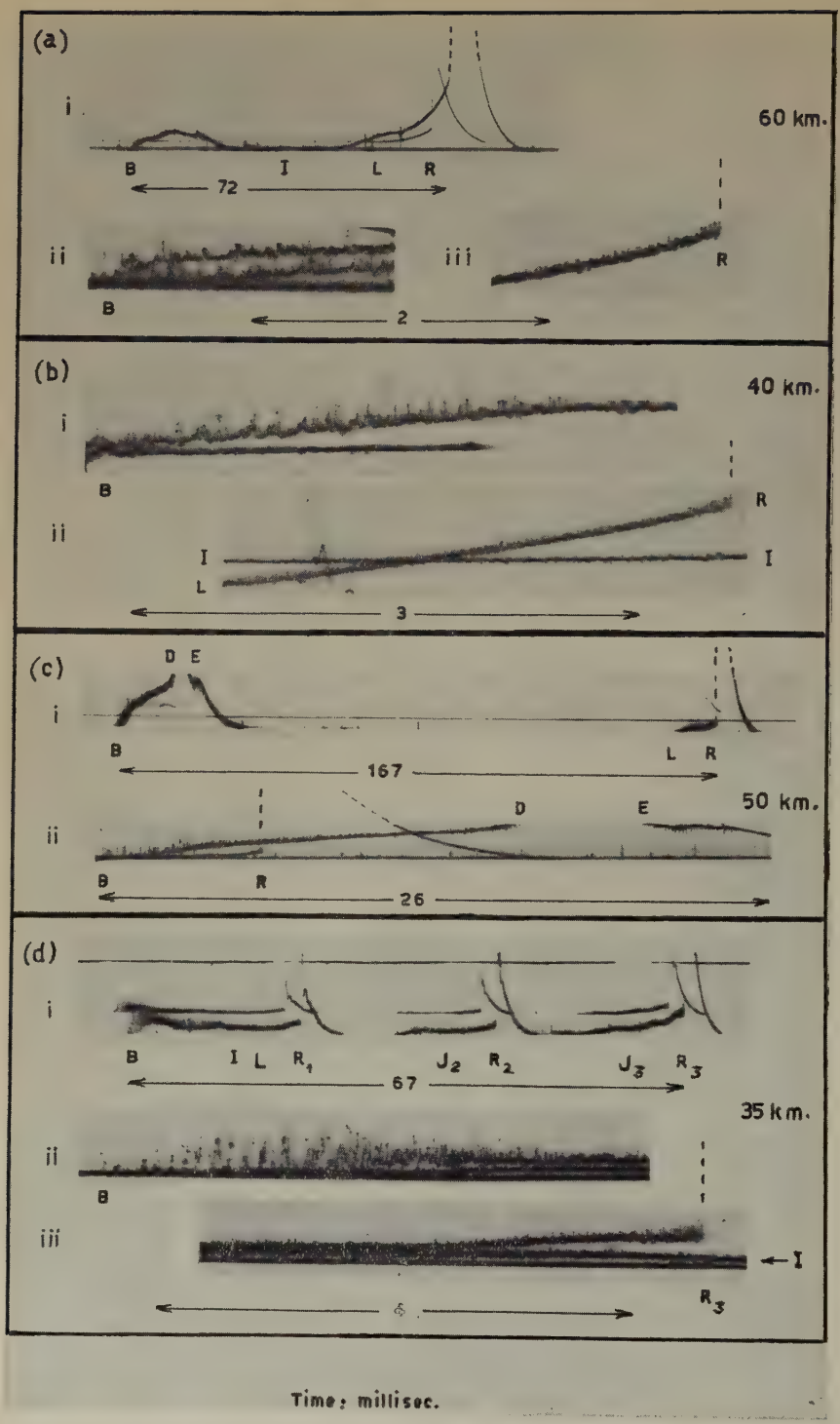

Figure 3. Records of rapid field-changes from discharges at distances up to 60 km.

Further light is thrown on the mechanism of the B discharge by the field changes depicted in Fig. 2 (e) and (f). These two B field changes were recorded at such a high amplification that the beam of the oscilloscope moved off-scale in 1·3 and 1·8 millisec respectively. They show that rapid stepwise increases of field, separated by irregular time intervals varying from 50 to 200 μsec, are superimposed upon a steady rise of field. Fig. 2 (f) also shows rapid pulses which will be discussed in § 4.

(*b*) *The electrostatic* I *field change*

The B field change is followed by a slow intermediate or I field change. During this part of the discharge the rate-of-change of field is either fairly uniform as in Figs. 2 (a) and (d), or variable as in Fig. 2 (b).

(*c*) *The electrostatic* L *field-change*

As can be seen at L in Fig. 2, the rate-of-change of field again starts to increase at a time which lies between 4 and 30 millisec before the incidence of the return stroke R. As these periods are of the same order of magnitude as the photographically observed durations of stepped leaders (Fig. 5), they suggest that only the L parts of the preliminary field changes are due to stepped leaders. Further justification for this conclusion will be given in § 5.

4. Rapid components of field change at distances up to 80 km

When an amplifier having high amplification and a frequency response up to 300 kc/sec is used for storms nearer than about 80 km, rapid pulsations of field are observed which also consist of three distinct B, I and L phases.

The technique of recording has been described in § 2 (iii). As the oscillograph spot may move off-scale under the influence of the relatively large and slow electrostatic field changes, these are counterbalanced by varying the time constant of the aerial circuit by preliminary trials. It is suggested that most of the small, high-frequency pulsations described in this paragraph have not been observed in detail by previous workers (Pierce 1955) owing to either insufficient amplification or too low a frequency response of the amplifiers used.

The four sets of records reproduced in Fig. 3 (Plate II) were recorded by method (iii), § 2, using a double-beam oscilloscope with different amplifications for the two beams. They were photographed by the double-drum camera described in § 2 and each set shows the slow-drum record at the top (i) and selected parts of the fast-drum record (ii) and (iii) below, except (b) which shows only fast-drum records. The slow records give both low and high-gain traces whereas, by selective screening of the oscillograph beams, the fast records were made to reproduce only the high-gain traces.

On the high-gain lower trace of Fig. 3 (a) i, the electrostatic field change of the preliminary discharge caused the beam to emerge at B, 72 millisec before R, whereas on the low-gain upper trace the beam emerged at L, 11 millisec before R, which clearly shows how the earlier parts of the preliminary field change may be completely missed by using an aerial circuit of short time constant and insufficient amplification. The lower trace of Fig. 3 (a) ii shows the first 2 millisec of the fast record of the B discharge (the upper trace belongs to a different flash) and iii the last 1·5 millisec of the L discharge.

The further examples shown in Figs. 3 (b) i and ii are respectively the fast-drum records of 3 millisec of the B and L field changes of another flash, the time interval

between B and R being 130 millisec. During this interval the recording drum made more than one revolution so that part of the intervening field change has also been recorded at I – I on (ii).

Figs. 3 (c) and (d), which illustrate additional features of these fields, will be discussed later.

(*a*) *The* B *pulsations*

As can be seen in Fig. 3 the discharges start with a train of large and predominantly positive pulses of varying and gradually decreasing amplitude. The interval between the pulses is irregular and varies from 80 to 200 μsec. The most frequent duration of the pulse train is between 2 and 4 millisec, the longest train observed lasting for 12 millisec, the durations corresponding with those of the electrostatic B field changes.

Since the electrostatic field is proportional to the electric moment M and the induction field to dM/dt (Eq. 1), a stepwise rise of the electrostatic field of the type shown in Figs. 2 (e) and (f) will give positive induction peaks. The radiation field which is proportional to d^2M/dt^2 will have positive and negative peaks. It thus seems that the predominantly positive pulses of Fig. 3 are mainly due to induction effects, although radiation effects are also present.

Small-amplitude pulsations whose time separations are between 5 and 10 μsec are often superimposed on the large low-frequency B pulses as can be clearly seen in Fig. 3 (d) (ii). They usually continue with varying amplitude up to the incidence of the return stroke.

(*b*) *The* I *pulsations*

The pulsations in the interval between the B and L stages are high-frequency pulsations of very small amplitude. Periodic spurts of isolated pulses, of amplitudes comparable with those of the B pulses, often occur during the I phase (I – I Fig. 3 (b) (ii)). These pulses are positive when the rate of change of electrostatic field increases and negative when the rate of change of field decreases. A clear example of the latter effect is shown in Fig. 3 (c). The rate of change of field is high from B to D after which it starts to decrease, the record having gone off-scale between D and E. Although the field seems to be falling to the right of E, this is only apparent and is caused by the small time constant of the aerial circuit; actually the field is still rising but at a slower rate than between B and D. The negative peaks appear to the right of E. Negative pulses associated with a decreasing rate of change of field are also shown between I – I in Fig. 3 (b) (ii).

When the return stroke follows the large B pulse train in less than 30 or 40 millisec (Fig. 3 (d)), the whole intermediate interval is occupied by the characteristic high-frequency L pulsations described in the next section, which suggests that in these cases the I stage is short or absent.

(*c*) *The* L *pulsations*

The field changes immediately preceding the return stroke consist of a train of steep and predominantly positive pulses following each other at 5 to 10 μsec intervals. Owing to insufficient resolution, the wave form of individual pulses could not be determined. Some of the pulses are of larger amplitude than those intervening. The larger pulses follow each other at intervals between 30 and 80 μsec, which is the same as the pause time between the bright steps of stepped leaders. The observation, however, that strokes subsequent to the first are often preceded by similar pulse trains (J_2, J_3 Fig. 3 (d)) indicates that they cannot wholly be due to the stepped process in the downward leader. It can be seen in Fig. 3 (d) (iii) that the pulsations in the interval preceding the third stroke R_3

are exactly similar to those preceding the first strokes R of Figs. 3 (a) (iii), (b) (ii) and (c) (ii). Since the effects in the intervals between the strokes of a flash must be due to J streamers (Malan and Schonland 1951a) it is reasonable to conclude that the similar field changes immediately preceding the first stroke are also mainly caused by streamer discharges inside the cloud, which supply charge to the advancing leader.

The pulses during the L part of the discharge are smaller in amplitude than the B pulses. The amplitude ratio of B to L pulses varies from 3 : 1 to 20 : 1, the higher the rate-of-change of the electrostatic field during the B stage, the larger this ratio. B pulses are not observed in 5 per cent of the records even with very large amplification. In these cases the return stroke is preceded by a steep and uniformly increasing electrostatic field upon which the characteristic L pulses are superimposed; the total duration of the preliminary field change is short and varies from 4 to 15 millisec. As this type of field change is usually observed in groups following each other on a series of records, it probably has some connexion with the type or stage of development of the storm.

5. Radiation fields

The field-changes to be described in this section originated from thunderstorms beyond 200 km, distances at which radiation fields are predominant (§ 1). The recording was first made on magnetic tape as described in § 2, (iv).

As this investigation was chiefly concerned with preliminary breakdown and leader field changes which are usually of much smaller amplitude than the return-stroke field changes (Hodges 1954), as large an amplifier gain as possible was used consistent with background noise from the tape recorder. Under these conditions the return-stroke field change usually saturated the tape so that it was not always possible to compare return-stroke amplitudes with those of the leader process.

(*a*) *Absence of radiation from* B *and* I *discharges*

Although very large amplification was used, no radiation effects which could be attributed to B or I field changes were observed on any of the 407 tape records examined. It is thus inferred that the radiation fields of these parts of the breakdown process are negligibly small in the frequency range between 200 c/sec and 20 kc/sec.

(*b*) *Radiation from* L *discharges*

Figs. 4 (a), (b) and (c) show three pairs of records of distant atmospherics.

The records on the left were obtained directly by triggering on the return stroke whereas those on the right are the corresponding tape records of the whole field change including the leader. By comparing the pairs of records it can be seen that although the tape, owing to its unsatisfactory low-frequency response, distorts the slow tail, it faithfully reproduces small oscillations of frequencies between 200 c/sec and 20 kc/sec.

These records which were obtained during the daytime illustrate three common types of radiation L fields.

(i) The α type having a small almost uniform train of pulsations whose amplitudes are often less than 1/100 of that of the return stroke.

(ii) The slow β type whose initial pulsations are slightly larger than the later pulsations, which resemble those of the α type.

(iii) The large-amplitude fast β type whose initial pulsations may have amplitudes up to half as large as the first return stroke pulsation.
Intermediate types are also obtained.

Table 1 gives the durations of the three types of leader trains. Norinder (1952) finds that the majority of leaders have durations less than 1 millisec but he states that owing to insufficient amplification he probably missed recording their initial parts.

TABLE 1. Duration of L radiation trains

Type	Extreme durations (millisecs)		Modal duration (millisecs)
	from	to	
α	2	25	7·0
slow β	3	19	5·5
fast β	1	7	3·5

The time intervals between the L pulsations vary from 30 to 100 μsec which indicates that they originate from stepped leaders (Schonland, Malan and Collens 1935).

Records taken with an amplifier having a response up to 300 kc/sec reveal that small pulsations of higher frequency are superimposed on the large leader ripples (Norinder 1952). They are not recorded on the tape owing to its low response above 20 kc/sec.

Night-time atmospherics show the same three types of leader, but the apparent time interval between the steps is smaller owing to successive ionospheric reflections. Fig. 3 (d) shows a night-time fast β leader and also the ionospheric reflection pulses following the return stroke.

On certain days β type leaders were predominant while on other days nearly all leaders recorded were of the small amplitude α type. Since radio-goniometers were not available for locating the storms, it was not possible to check to what extent the type of leader depends on the location of the storm or on other characteristics such as ' frontal ' or ' convective ' origin or intensity of precipitation. Since rain will tend to sweep away positive space charges which are responsible for β type leaders, the intensity of precipitation is probably the major factor in determining the leader type (Schonland, Hodges and Collens 1938).

(c) *The frequency of occurrence of stepped leader radiation*

Table 2 gives the frequency of occurrence of stepped leaders.

TABLE 2. Percentage of flashes preceded by stepped leader radiation

Fast β	Slow β	α	Doubtful	No leader observed	Total number of observations
16	21	38	16	9	407

Stepped-leader pulsations could be detected in 75 per cent of the observations. In 16 per cent there was some indication of pulsations but owing to background noise it was not possible to conclude definitely whether these were due to leaders. 9 per cent showed no leaders. It must be stressed that if smaller amplification had been used nearly all the α leaders and most of the slow β leaders figuring in Table 2 would not have been registered.

The brightest and the faintest stepped leaders as photographed by Boys cameras show the same characteristic steps and step intervals, these intervals being of the same durations as those observed between the electrical radiation pulsations whether they are large or small. As the luminous intensity of even the brightest stepped leaders is extremely low, it is reasonable to conclude that the radiation fields of many leaders were so small that they were missed, notwithstanding the high amplification used in the present research. Further independent support for this conclusion will be discussed in § 6.

6. General discussion of experimental observations

The experimental observations described in the last three paragraphs have been summarized in Fig. 1 which gives diagrams of (a) electrostatic field changes which are predominant at small distances; (b) rapid field changes superimposed on the slow electrostatic field changes as observed at 50 km and (c) radiation fields recorded during the daytime at distances of several hundred kilometres. The L and especially the I pulsations, which are extremely small on the actual records, have been slightly exaggerated in diagram (b) for reasons of clarity.

Fig. 5 gives the distribution curves for the times of commencement before the return stroke of the electrostatic field changes described in § 3 and the pulsations described in § 4 (Curve A, 234 observations) and the radiation field-changes described in § 5 (Curve B, 239 observations). Only the records taken for the purpose of this paper were considered; previous records taken at much lower amplification were not used in the computation of these curves. Curve C refers to the time taken by the leaders of first strokes to travel from the cloud base to the ground, as obtained from photographs with Boys and other moving-lens cameras.

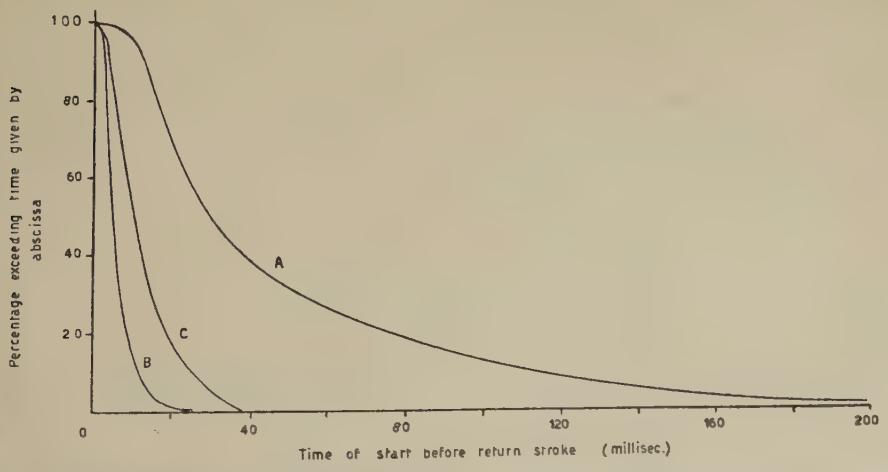

Figure 5. Distribution curves of the durations of: (a) preliminary electrostatic effects; (b) preliminary radiation effects; (c) visible stepped leader processes.

Since it was shown in § 5 that the radiation fields represented by curve (B) can be attributed to stepped leaders, it would be expected that curves (B) and (C) should coincide. The fact that curve (B), which has been calculated from the data in Table 2, gives shorter durations than curve (C), suggests that many slow stepped leaders must have been omitted from curve (B) because their radiation effects were too small to be detected. Since such unobserved leaders would have been among the flashes listed under the headings ' doubtful ' and ' no leader ' in Table 2, further indirect support is given to the view expressed in § 5 that probably all flashes to ground are preceded by stepped leaders.

According to curve (A), the initial electrostatic field changes generally precede the return stroke by time intervals far in excess of the time taken by stepped leaders to travel from the cloud base to the ground (curve C). For this reason there is strong justification for attributing only the later, or L parts of the field changes to stepped leaders (Fig. 1). It follows then that preparatory electrical discharges take place inside the cloud prior to the launching of the stepped leader.

This conclusion has been verified in a different way by one of us (Malan 1952, 1955). By using a specially designed camera which can discriminate between luminous processes inside and below the cloud, it has been established that the cloud becomes and remains luminous for intervals up to a hundred or more milliseconds before the emergence of the leader, which then proceeds to ground at the usual stepped leader velocity of about 2×10^7 cm/sec.

7. Suggested nature of the preliminary discharges

The field-change observations described in paragraphs 3, 4 and 5 give various clues as to the probable nature of the electrical processes which usually precede the stepped leader.

It was shown in § 3 that the variation with distance of the sign of the initial electrostatic B field change conforms with a discharge between the lower positive-charge centre p near the base of the cloud and the main negative-charge centre N. The irregular stepwise rise of the electrostatic field and its accompanying large pulses indicate that sudden intermittent spurts of current occur during the B stage.

Although, as stated in § 4 (c), the time resolution is not sufficient to show the detailed structure of the individual L pulsations observed at distances up to 80 km, the records do show that the large B pulsations have a longer period. The variation in relative amplitude of the B and L pulsations with distance also suggests that they must have different frequency contents. Further, since the radiation field produced at large distances by the B pulses is negligible compared with that produced by the L pulses, the rate of change of current during the main B pulses is probably much slower than that occurring during the bright pulses of the stepped leader. These arguments do not relate to the small high-frequency pulsations superimposed on both the B and L pulses. It follows that the initial breakdown inside the cloud must be entirely different from the stepped leader process.

The most likely mechanism of the electrical breakdown in the cloud is that described by Macky (1931) and elaborated further by English (1948). They found by laboratory experiments that in an electric field approaching 10^4 v/cm, a water drop with diameter of a millimetre or more, first elongates under the influence of its induced charges and then forms a long thin filament from its positive end. A glow discharge starts and the filament breaks up into a spray of minute positively charged droplets. By repeated filament formation a single drop can pass a current of 20 μa.

As was shown in § 3, the breakdown probably just as often starts upwards from the p as downwards from the N charge centre, so that the field near the boundary of either

charge centre must reach 10^4 v/cm to start the above breakdown process. This high field need only be very localized for, as Loeb (1953) has pointed out, ' it will require only one propitiously placed water drop to start a breakdown streamer.' Once a streamer has started it will easily propagate itself through the region of high water content between N and p and establish a conducting path between them. Neutralization of the smaller p charge can now follow.

The available data are not sufficient to show whether the stepwise change of field during the B stage is caused by the hesitant advance of a streamer or is due to secondary streamers branching out from the ends of an original streamer which has bridged the whole gap between N and p. The negative pulses which often succeed the steep B field change show that the integrated current does not diminish uniformly after the initial breakdown but falls in irregular steps. Such steps could be caused by the sudden fading out of branch streamers after the neutralization of pockets of high charge density.

The ensuing interval I (Fig. 1) between the B field change and the leader field change is characterized by a train of very small high-frequency pulses which are similar in nature to the pulses (J, Fig. 1 (b)) often recorded during the intervals between successive strokes to ground. This suggests that during the I stage, streamer discharges penetrate upwards and outwards into the negatively charged region. The slow, steady rise of field accompanying this stage further suggests that the highly conducting channel now existing from the negative-charge centre to the base of the cloud is being negatively charged. The charging will continue until the tip field immediately in front of the channel reaches the value required for the propagation of the stepped leader, which was estimated at 6×10^4 v/cm by Schonland (1953). The final breakdown to ground can now follow. These explanations are on similar lines to those suggested by Loeb (1953) on theoretical grounds.

The pulses observed at 5 to 10 μsec intervals during the stepped leader stage are of the same type as those of the I stage but are larger in amplitude. A further increase in amplitude usually occurs during the last 0·5 millisec of advance of the leader. In this time the leader traverses approximately the last 100 m to ground. Schonland, Malan and Collens (1935) found that the velocity of stepped leaders generally increases during the last 100 m before striking the ground, an effect which was ascribed to the increase in tip field as the leader approaches the ground.

Reasons were given in § 4 (b) for concluding that the high-frequency pulses observed during the L stage at distances nearer than 80 km were an indication of streamer discharges in the cloud rather than of downward leader steps. The increase in amplitude of the pulses at the beginning of the L stage thus seems to indicate that the advancing leader channel calls for an enhanced rate of supply of negative charge from the cloud. The further increase in amplitude of the pulses as the leader approaches the ground indicates an enhanced streamer activity in the cloud and suggests that the supply of charge to the leader channel is to a large extent regulated by the electric field in front of the leader tip.

Acknowledgments

We wish to thank the South African council for Scientific and Industrial Research for grants to purchase oscillographic and tape equipment. Our thanks are due to Dr. B. F. J. Schonland, Dr. D. B. Hodges and Dr. A. L. Hales for their interest and many helpful discussions. One of us (D.J.M.) would further like to express his appreciation of discussions with Dr. T. W. Wormell and Dr. E. T. Pierce while on a visit to Cambridge made possible by the reward of a bursary by the South African Council for Scientific and Industrial Research.

References

Appleton, E. V., Watson-Watt, R. A. and Herd, J. F.	1926	*Proc. Roy. Soc.* A, **111**, p. 654.
Appleton, E. V. and Chapman, F. W.	1937	*Ibid.*, **158**, p. 1.
Clarence, N. D. and Malan, D. J.	1951	*Proc. Phys. Soc.* B, **64**, p. 529.
English, W. N.	1948	*Phys. Rev.*, **74**, p. 179.
Hodges, D. B.	1954	*Proc. Phys. Soc.* B, **67**, p. 582.
Kitagawa, N., Iizuka, T., Murai, K. and Kobayashi, M.	1954	*Geophys. Mag.*, Tokyo, **25**, p. 237.
Lejay, P.	1926	*L'Onde Electrique*, **5**, p. 493.
Loeb, L. B.	1953	Report, Dept. Physics, University of California.
Macky, W. A.	1931	*Proc. Roy. Soc.* A, **133**, p. 565.
Malan, D. J. and Schonland, B. F. J.	1950	*Proc. Phys. Soc.* B, **63**, p. 402.
	1951a	*Proc. Roy. Soc.* A, **206**, p. 145.
	1951b	*Ibid.*, **209**, p. 158.
Malan, D. J.	1952	*Ann. de Geophys.*, **8**, p. 385.
	1954	*Ibid.*, **10**, p. 271.
	1955	*Ibid.*, **11**, p. 427.
Norinder, H.	1952	*Ark. Geof.*, **1**, p. 543.
Pierce, E. T.	1955	*Quart. J. R. Met. Soc.*, **81**, p. 211.
Schonland, B. F. J., Malan, D. J. and Collens, H.	1935	*Proc. Roy. Soc.* A, **152**, p. 595.
Schonland, B. F. J., Hodges, D. B. and Collens, H.	1938	*Ibid.*, **166**, p. 56.
Schonland, B. F. J.	1953	*Ibid.*, **220**, p. 25.
Simpson, Sir G.	1927	*Ibid.*, **114**, p. 376.
Wormell, T. W.	1952	*Nature*, **169**, p. 561.
	1953	*Quart. J. R. Met. Soc.*, **79**, p. 3.

551.510.534 : 551.521.63

The relation between an *umkehr* curve and the vertical distribution of atmospheric ozone

By G. F. WALTON
Queen's College, Dundee

(Manuscript received 1 November 1956)

SUMMARY

An expression is derived for the intensity-ratio for two wavelengths in the ultra-violet of primary scattered sunlight received from the zenith at the base of a plane-stratified atmosphere. The logarithm of the intensity-ratio is expanded in a series which reveals the nature of the relation between it and the vertical distribution of atmospheric ozone. The information on the vertical distribution given by zenith observations when the sun is high in the sky is discussed.

1. INTRODUCTION

Ozone is an important constituent of the atmosphere because of its particular vertical distribution and its absorption of infra-red and ultra-violet radiation. It could be used effectively as a natural tracer substance in the study of the general circulation, if regular three-dimensional pictures of the ozone distribution were obtained. The only routine ozone measurements on a world-wide basis to date have been those of the total ozone content, determined by the Dobson spectrophotometer, and it is necessary to supplement them by frequent determinations of the vertical distribution. Information on the vertical distribution of ozone can be obtained by the *umkehr* method from measurements of the clear zenith skylight, and such measurements using the Dobson spectrophotometer are now made with good accuracy (Dobson 1951). In order to make the fullest possible use of these measurements, the information which they yield needs to be carefully studied. The results of part of this study are contained in the present paper.

It was discovered by Götz (1931) that if two wavelengths in the ultra-violet were chosen such that one was absorbed by ozone strongly and the other weakly, the intensity-ratio of zenith-scattered light varied with the solar zenith distance and became a minimum at a zenith distance of about 75°. A curve depicting this variation is usually known as an *umkehr* curve. Theoretical *umkehr* curves for an atmosphere containing thin layers of ozone were calculated by Chalonge (1932) and Götz (1934). A study of these curves indicated that some information on the vertical distribution of atmospheric ozone could be expected from the analysis of an observed *umkehr* curve.

The problem of analysing an observed *umkehr* presents many difficulties, and in the past exact mathematical treatment has been abandoned in favour of approximate methods (Götz, Meetham and Dobson 1934, Götz 1951, Larsen 1955). The relation between the vertical distribution of ozone and the *umkehr* curve was studied by Chapman (1935), who calculated *umkehr* curves for several hypothetical vertical distributions of ozone. The results of this work suggested that the observed minimum value of the intensity-ratio would give an approximate estimate for the height of the centre of gravity of the ozone.

In this paper the problem is reconsidered. For simplicity, the atmosphere is regarded as plane-stratified and the effects of secondary and higher orders of scattering are neglected. Attention is confined to the part of the *umkehr* curve corresponding to small zenith distances of the sun, for which a series expansion for the logarithm of the intensity-ratio is valid. The information on the vertical distribution of ozone which can be obtained from this part of the curve is discussed.

2. Symbols and definitions

The following notation is mainly that of Chapman (1935) :

z = angular zenith distance of the sun
h = vertical coordinate
$\rho_0(h)$ = density of ozone at a height h
$\rho(h)$ = density of air at a height h
$m_0(h)$ = fraction of mass of ozone above a height h
$m(h)$ = fraction of mass of air above a height h
λ = wavelength
α = absorption coefficient, per unit mass of ozone, for a particular wavelength λ
σ = scattering coefficient, per unit mass of air, for a particular wavelength λ
a = total absorption coefficient of ozone, for a particular wavelength λ
s = total scattering coefficient of air, for a particular wavelength λ
$I(z)$ = intensity of primary scattered light, of wavelength λ, received at the ground from the zenith when the solar zenith distance is z.
$Z = \sec z - 1$

$$J(Z) = \int_0^1 e^{-Z(am_0 + sm)}\, dm \quad . \quad . \quad . \quad . \quad . \quad . \quad . \quad (1)$$

Primed symbols, e.g., a', s', $I'(z)$, I_∞', $J'(Z)$ will refer to a second wavelength λ'.

From these definitions we have

$$m_0 = \int_h^\infty \rho_0(h)\, dh \Big/ \int_0^\infty \rho_0(h)\, dh, \quad \text{and} \quad m = \int_h^\infty \rho(h)\, dh \Big/ \int_0^\infty \rho(h)\, dh, \quad . \quad . \quad (2)$$

whence

$$dm = -\rho(h)\, dh \Big/ \int_0^\infty \rho(h)\, dh. \quad . \quad . \quad . \quad . \quad (3)$$

Also

$$a = \alpha \int_0^\infty \rho_0(h)\, dh, \quad \text{and} \quad s = \sigma \int_0^\infty \rho(h)\, dh. \quad . \quad . \quad . \quad (4)$$

3. The intensity-ratio

Considering a wavelength λ, the intensity of the solar beam at height h in the atmosphere will be

$$I_\infty\, e^{-\int_h^\infty [\alpha\rho_0(h) + \sigma\rho(h)] \sec z\, dh.}$$

Suppose a fraction $k\sigma\rho(h)$ of this light is scattered vertically downwards towards the observer. According to the scattering theory of Rayleigh (1871) k depends only on z, but an explicit value is not required here since k will disappear from the expression for the intensity-ratio. This primary scattered light proceeding to the ground is also attenuated, the intensity being reduced by a factor

$$e^{-\int_0^h [\alpha\rho_0(h) + \sigma\rho(h)]\, dh.}$$

Combining the contributions of the primary scattered light from all heights we have

$$I(z) = k\sigma I_\infty \int_0^\infty \rho(h)\, e^{-\int_h^\infty [\alpha\rho_0(h) + \sigma\rho(h)] \sec z\, dh - \int_0^h [\alpha\rho_0(h) + \sigma\rho(h)]\, dh}\, dh. \quad . \quad (5)$$

Using (2), (3) and (4) we may rewrite (5) as follows

$$I(z) = ks\, I_\infty\, e^{-(a+s)} \int_0^1 e^{-(am_0 + sm)(\sec z - 1)}\, dm. \quad . \quad . \quad (6)$$

From (6) and a similar expression referring to a second wavelength λ' we have

$$\frac{I(z)}{I'(z)} = \frac{s\, I_\infty\, e^{-(a+s)} \int_0^1 e^{-(a\, m_0 + s\, m)(\sec z - 1)}\, dm}{s'\, I'_\infty\, e^{-(a'+s')} \int_0^1 e^{-(a' m_0 + s' m)(\sec z - 1)}\, dm}. \quad . \quad . \quad (7)$$

Dobson's spectrophotometer measures the logarithm of the intensity-ratio plus a quantity which is constant for all observations with one instrument. If we put

$$R = \frac{I(z)}{I'(z)} \Big/ \frac{I(0)}{I'(0)}, \quad . \quad . \quad . \quad . \quad . \quad (8)$$

then

$$R = J(Z) / J'(Z) = R(Z) \text{ say.} \quad . \quad . \quad . \quad (9)$$

We may regard $\ln R$ as an observable quantity, and the $(\ln R, Z)$ curve as the Götz *umkehr* curve.

The vertical distribution of ozone will be represented by the function $m_0(m)$. Since this function occurs in the integrands of $J(Z)$ and $J'(Z)$ there is no simple relation between the vertical distribution of ozone and the *umkehr* curve. Under certain conditions, however, the relation can be simplified to yield, from the *umkehr* curve, a single parameter characterizing the ozone distribution. The derivation of this relation, and an investigation of its possible usefulness, constitutes the remainder of this paper.

4. Series expansions

(a) *Series for* $J(Z)$

The integrand of (1) may be rewritten as the exponential series

$$\sum_0^\infty (-Z)^n (am_0 + sm)^n / n! \quad . \quad . \quad . \quad . \quad (10)$$

Since this series is uniformly convergent in the interval $0 \leqslant m \leqslant 1$, integration term by term is permissible. From (1) and (10) we have

$$J(Z) = \sum_{n=0}^\infty p_n Z^n, \quad . \quad . \quad . \quad . \quad . \quad (11)$$

where

$$p_n = \frac{(-1)^n}{n!} \int_0^1 (am_0 + sm)^n\, dm.$$

Expressing $(am_0 + sm)^n$ as the finite binomial series

$$\sum_{r=0}^n \frac{n!}{r!\,(n-r)!} (am_0)^{n-r} (sm)^r,$$

we then have

$$p_n = (-1)^n \sum_{r=0}^n \frac{a^{n-r} s^r}{(n-r)!\,(r+1)!} N_{n-r,r}, \quad . \quad . \quad (12)$$

where

$$N_{n-r,r} = (r+1) \int_0^1 m_0^{n-r} m^r\, dm. \quad . \quad . \quad . \quad (13)$$

We note that $N_{0,r} = (r+1) \int_0^1 m^r\, dm = 1$ for all r, and the first four coefficients are as follows :

$$p_0 = 1,\ p_1 = -(2a\,N_{1,0} + s)/2\,!,\ p_2 = (3a^2\,N_{2,0} + 3a\,s\,N_{1,1} + s^2)/3\,!,$$
$$p_3 = -(4a^3\,N_{3,0} + 6a^2\,s\,N_{2,1} + 4a\,s^2\,N_{1,2} + s^3)/4\,!,\ \text{and}$$
$$p_4 = (5a^4\,N_{4,0} + 10a^3\,s\,N_{3,1} + 10a^2\,s^2\,N_{2,2} + 5a\,s^3\,N_{1,3} + s^4)/5\,!\,. \qquad (14)$$

(b) *Series for* $\ln J$

Using (11) and (14) we write

$$\ln J = \ln\left(1 + \sum_1^\infty p_n Z^n\right) = -\sum_{t=1}^\infty \left\{t^{-1}\left(-\sum_{n=1}^\infty p_n Z^n\right)^t\right\}. \qquad (15)$$

The logarithmic series (15) is valid if $0 < J \leqslant 2$. This condition is satisfied for finite positive values of Z, which we wish to consider, since $0 \leqslant am_0 + sm < \infty$ whence, from (1), $0 < J \leqslant 1$. Expanding (15) we have

$$\ln J = \sum_1^\infty q_n Z^n, \qquad (16)$$

where, for example,

$$q_1 = p_1 = -(a\,N_{1,0} + \tfrac{1}{2}\,s),$$
$$q_2 = p_2 - \tfrac{1}{2}\,p_1^2 = \tfrac{1}{2}\,a^2\,(N_{2,0} - N^2{}_{1,0}) + \tfrac{1}{2}\,as\,(N_{1,1} - N_{1,0}) + s^2/24,$$
$$q_3 = p_3 - p_1\,p_2 + \tfrac{1}{3}\,p_1^3 \quad \text{and}$$
$$q_4 = p_4 - p_1\,p_3 - \tfrac{1}{2}\,p_2^2 + p_1^2\,p_2 - \tfrac{1}{4}\,p_1^4. \qquad (17)$$

(c) *Series for* $\ln R$

From (9) and (16) we get

$$\ln R = \sum_1^\infty (q_n - q_n')\,Z^n, \qquad (18)$$

where q_n' corresponds to q_n with a and s replaced by a' and s' respectively. Expressions for $(q_n - q_n')$ $(n = 1, 2, 3, 4)$ may be obtained from (17).

5. The meaning of $N_{1,0}$

It follows from (17) and (18) that when Z is sufficiently small

$$\ln R \simeq -Z\,[(a - a')\,N_{1,0} + \tfrac{1}{2}\,(s - s')]. \qquad (19)$$

Then, for given values of Z, a, a', s and s' the value of $\ln R$ depends only on $N_{1,0}$. Since $\ln R$ can be measured by the spectrophotometer, $N_{1,0}$ can in principle be determined.

A physical meaning for $N_{1,0}$ can be obtained by writing it in the form

$$N_{1,0} = \int_0^1 m_0\,dm \Big/ \int_0^1 dm, \qquad (20)$$

which agrees with the definition (13), since $\int_0^1 dm = 1$. Thus $N_{1,0}$ equals the mean value of m_0 with respect to m, or with respect to pressure p, since from (3) and the hydrostatic equation we have, assuming constant gravitational acceleration g,

$$dm = dp/g \int_0^\infty \rho\,(h)\,dh.$$

Chapman (1935) noted that for a number of hypothetical distributions of ozone the values of R at a zenith distance of 75° decreased as the height of the centre of gravity of the ozone increased. The preceding analysis shows that it is the value of $N_{1,0}$ rather than the height of the centre of gravity which affects the value of R when Z is small. Consequently for two different distributions having the same height of centre of gravity the corresponding *umkehr* curves will not be identical if the values of $N_{1,0}$ are different. This is exemplified by two pairs of distributions considered by Chapman (1935, 7·413, 7·2 and 7·32, 7·4) for which the values of $N_{1,0}$ are calculated to be 0·368, 0·333 and 0·967, 0·957 respectively. It is also noted that two different distributions may have the same value of $N_{1,0}$, e.g., for each of the hypothetical distributions characterized by

$$\left.\begin{array}{ll} m_0 = 0, & 0 \leqslant m \leqslant m_1 \\ m_0 = (m_1 - m)/(m_1 - m_2), & m_1 \leqslant m \leqslant m_2 \\ m_0 = 1; & m_2 \leqslant m \leqslant 1 \end{array}\right\} \quad . \quad . \quad (21)$$

and by

$$\left.\begin{array}{ll} m_0 = 0, & 0 \leqslant m < m_1 \\ m_0 = \frac{1}{2}, & m_1 < m < m_2 \\ m_0 = 1; & m_2 < m \leqslant 1 \end{array}\right\} \quad . \quad . \quad (22)$$

we find that $N_{1,0} = 1 - \frac{1}{2}(m_1 + m_2)$.

In the case of (21) the ozone is distributed with constant concentration between the levels m_1 and m_2, assuming an exponential atmosphere, i.e., assuming $m = e^{-h/H}$, H being the scale height. In the case of (22) it is present in two thin layers, situated at levels m_1 and m_2, each containing half the total amount of ozone. The expressions for $N_{2,0}$, $N_{1,1}$ etc., are not however identical in the two cases, so that the contributions to $\ln R$ from higher terms of (18) are different, producing a difference between the two *umkehr* curves as Z increases. This is also exemplified by two actual distributions of ozone considered in the following section.

6. Application to typical ozone distributions

In Fig. 1 (a) are shown four vertical distributions of ozone (two in the Spring and two in the Autumn, at intervals of about one week) obtained by Paetzold (1954) from balloon ascents at Weissenau, Germany. In Fig. 1 (b) are shown the corresponding m_0 (m) curves, which were derived from data kindly supplied to the author by Dr. Paetzold. As the ascents only gave information over limited ranges of height, e.g., 2 to 20 km, the data were extrapolated to ground level (shown by the dotted portions of the curves) and also in the region above the top of each ascent, to facilitate intercomparison. Values of m required for Fig. 1 (b) were taken from standard atmosphere tables (Diehl 1925, Warfield 1947).

TABLE 1. Values of $N_{1,0}$, $N_{1,1}$ etc., for four distributions of Paetzold

Distribution	Date	$N_{1,0}$	$N_{1,1}$	$N_{1,2}$	$N_{1,3}$	$N_{2,0}$	$N_{2,1}$	$N_{2,2}$	$N_{3,0}$	$N_{3,1}$	$N_{4,0}$
1	10.4.52	0·891	0·953	0·972	0·981	0·816	0·912	0·946	0·755	0·875	0·703
2	18.4.52	0·891	0·954	0·972	0·981	0·816	0·914	0·946	0·755	0·878	0·705
3	23.10.53	0·940	0·974	0·982	0·986	0·900	0·949	0·964	0·862	0·925	0·828
4	28.10.53	0·914	0·974	0·985	0·990	0·861	0·950	0·971	0·819	0·929	0·784

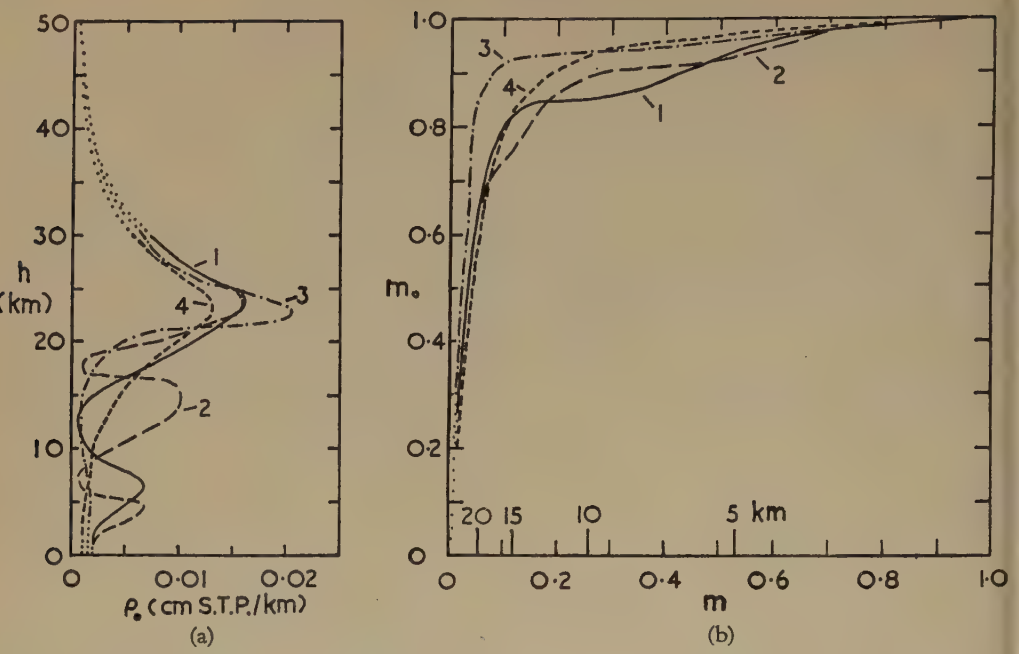

Figure 1. (a) Vertical distributions of ozone obtained by Paetzold on the following dates : (x = total amount of ozone in cm STP). (1) 10 Apr. 1952, $x = 0{\cdot}311$; (2) 18 Apr. 1952, $x = 0{\cdot}321$; (3) 23 Oct. 1953, $x = 0{\cdot}209$; (4) 28 Oct. 1953, $x = 0{\cdot}208$. (b) The corresponding $m_0(m)$ curves. An auxiliary scale of height is given.

It will be seen from Figs. 1 (a) and 1 (b) that large changes in the vertical distribution may produce relatively small changes in the $m_0(m)$ curve, the area beneath which is almost unity. This is also exemplified by the values given in Table 1, which were obtained from (13) by numerical integration. It may be noted that although the vertical distributions of 10 April and 18 April 1952 are markedly dissimilar below 20 km, and that the corresponding $m_0(m)$ curves do not wholly coincide, the values of the N's are almost identical in the two cases.

TABLE 2. VALUES OF THE COEFFICIENTS OF THE SERIES (18)

Distribution	$q_1 - q_1'$	$q_2 - q_2'$	$q_3 - q_3'$	$q_4 - q_4'$
1	− 0·8603	+ 0·05715	+ 0·006377	− 0·00005954
2	− 0·8839	+ 0·05910	+ 0·006983	+ 0·00005996
3	− 0·6466	+ 0·03359	+ 0·002950	+ 0·00007943
4	− 0·6298	+ 0·04304	+ 0·004591	− 0·00004020

It is of interest to know how rapidly the series (18) converges. Table 2 contains the values of $q_n - q_n'$ ($n = 1, 2, 3, 4$), which were calculated from the data of Table 1, adopting the following values (to base e) of the absorption coefficients and total scattering coefficients :

$$\alpha = 2{\cdot}83, \quad s = 1{\cdot}092; \quad \alpha' = 0{\cdot}18, \quad s' = 0{\cdot}840.$$

These values refer to the wavelengths Cλ 3112 Å and Cλ' 3323 Å used in routine measurements with a Dobson spectrophotometer. The results show, for example, that three terms of the series (18) suffice to calculate $\ln R$ correct to the second decimal place if Z does not exceed about 2·8 (i.e. if $z \leqslant 75°$).

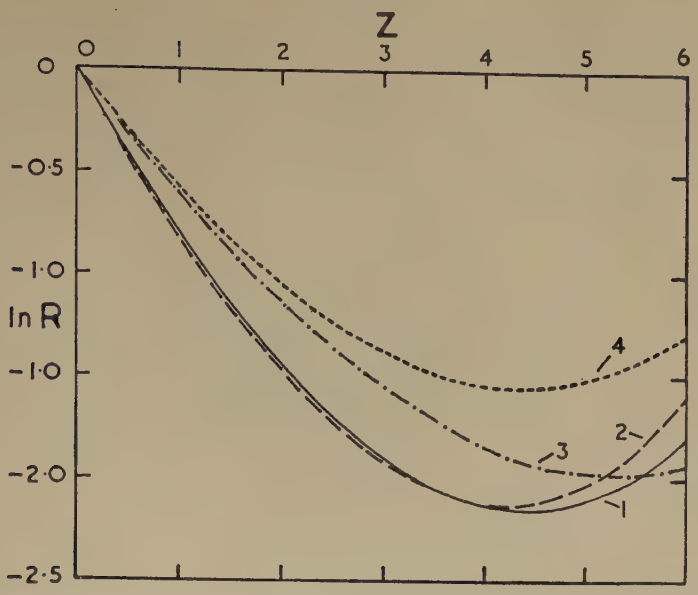

Figure 2. Calculated *umkehr* curves for the four ozone distributions shown in Fig. 1.

The *umkehr* curves derived from the data of Table 2 are illustrated in Fig. 2. It will be seen that when $Z < 4$, the difference between the *umkehr* curves 1 and 2 is very small; in fact this difference mainly results from the difference in the total ozone amount which enters a and a'. It would be near the limit of detection of the Dobson spectrophotometer, which is estimated to measure the log. intensity-ratio to 0·005, i.e. 0·012 in $\ln R$. Greater differences occur when Z is about 5 or 6, and it would be necessary to make measurements in this region to distinguish between the distributions 1 and 2. Also such measurements would be better than those for smaller values of Z in distinguishing between the distributions 3 and 4, which here refer to the same ozone amount (0·2 cm approx.), but which do not share the same values of the N's, since the difference between the curves 3 and 4 increases as Z increases.

7. Conclusions

It has been shown that any given vertical distribution of ozone may be represented by an m_0 (m) curve, from which the N's may be calculated, the series (18) evaluated, and an *umkehr* curve constructed in the region correponding to small zenith distances of the sun. It should be emphasized that the effects of secondary and higher orders of scattering on the *umkehr* curve have been neglected. A study of these effects based on multiple scattering theory (Walton 1955) is being made by the writer.

Even if these effects were negligible, or if allowance could be made for them, the converse problem of determining the vertical distribution of ozone from the high-sun portion of the *umkehr* curve presents further difficulties. For instance, suppose the coefficients $(q_1 - q_1')$ and $(q_2 - q_2')$ were determined from an observed *umkehr* curve. It follows from (17) and (18) that $N_{1,0}$ is completely determined, also $(a^2 - a^2)(N_{2,0} - N^2{}_{1,0}) + (as - a's')(N_{1,1} - N_{1,0})$. Thus in order to determine both $N_{2,0}$ and $N_{1,1}$, observations using a third wavelength, or a second wavelength-pair, are required. Even if the N's could be determined by making observations with several wavelengths, the function m_0 (m) could not be determined explicitly. Nevertheless it would be possible to decide whether or not any considered vertical distribution could be the actual vertical distribution.

It follows from these results that, in practice, no useful information can be obtained from the low-Z part of an observed *umkehr* curve. This suggests that attention should now be given to the higher-Z part of the *umkehr* curve in the hope that it can be made to yield more information of the vertical distribution of ozone than hitherto. The possibility of utilizing measurements of the scattered light received from various directions in the sky should also be explored.

References

Chalonge, D.	1932	*J. Phys. Radium*, **3**, p. 21.
Chapman, S.	1935	*Phil. Trans.* A, **234**, p. 228.
Diehl, W. S.	1925	*N.A.C.A. Rep.*, No. 218.
Dobson, G. M. B.	1951	*Quart. J. R. Met. Soc.*, **77**, p. 491.
Götz, F. W. P.	1931	*Beitr. Geophys.*, **31**, p. 147.
	1934	*Z. Astrophys.*, **8**, p. 270.
	1951	*Compendium of Meteorology*, Amer. Met. Soc., p. 281.
Götz, F. W. P., Meetham, A. R. and Dobson, G. M. B.	1934	*Proc. Roy. Soc.* A, **145**, p. 416.
Larsen, S. H. H.	1955	*J. Atmos. Terr. Phys.*, **6**, p. 46.
Paetzold, H. K.	1954	*Naturwiss*, **14**, p. 319.
Rayleigh, Lord	1871	*Phil. Mag.*, **41**, p. 107.
Walton, G. F.	1955	*Ibid.*, **46**, p. 281.
Warfield, C. N.	1947	*N.A.C.A. Tec. Notes*, No. 1200.

551.573 : 551.586 : 631

Water losses from various land surfaces

By N. E. RIDER

Meteorological Office, London, and School of Agriculture, University of Cambridge

(Manuscript received 22 October 1956)

SUMMARY

An account is given of observations designed to evaluate the daily water losses from surfaces carrying crops of different size and shape which were transpiring at their potential rates. The losses were obtained by the familiar aerodynamic method, the observations being made over bare soil, brussels sprouts, peas and grass. It is shown that the differences in the water losses from the various surfaces are too large to be accounted for by likely errors in the observations or method. Typical losses for sunny days in the period May to July 1955 were : peas, 2·5 to 7·5 mm; grass, 2 to 3 mm; brussels sprouts about 4 mm.

1. INTRODUCTION

Penman's (1948) method for the calculation of evaporation from land surfaces has led to the adoption of a scheme for the computation of irrigation need which is finding application in day-to-day farming practice (Pearl and others 1954). In the present paper it is not proposed to discuss the basis of Penman's method for the calculation of the potential transpiration from grass, that is the transpiration rate when the water supply is not limiting, by the substitution of meteorological data in semi-empirical equations. This has already been done by Pasquill (1950a). Here we shall be concerned with the results of an experimental study of the variation of the rates of water loss from nearby areas carrying different crops. The investigation was undertaken to test on a field scale the adequacy of the assumption, made in the general application of Penman's work, that the potential transpiration is the same as that from grass, provided that the crop has the same colour as grass and completely covers the ground. The aim of irrigation is to add just sufficient water to any crop to maintain the actual transpiration at its potential level since there is evidence that maximum growth takes place when this condition is satisfied. At present it is the practice to irrigate crops of very different size and character equally, once the irrigation point, which may differ from crop to crop owing to differences in the appropriate root constants, is reached. The root constant is defined as the maximum soil-moisture deficit, usually expressed in cm or in., which can be built up before transpiration is checked. Irrigation is started when this deficit is reached.

In the work to be described the aerodynamic method is used to evaluate the daily water losses. This method has been under investigation at Cambridge for a number of years and the physics underlying it, together with the limitations and precautions that must be observed in its use, are now fairly well understood. It will be recalled that the validity of the Thornthwaite and Holzman (1939) equation, as modified by Pasquill (1949a),

$$E = \frac{\rho k^2 (u_2 - u_1)(q_1 - q_2)}{\left[\ln \frac{z_2 - d}{z_1 - d}\right]^2} \quad . \quad . \quad . \quad (1)$$

in which E is the rate of evaporation, k is von Kármán's constant, ρ the air density, d the zero-plane displacement and u_1, u_2, q_1, and q_2 are the wind speeds and specific humidities at the heights z_1 and z_2, has been demonstrated (Pasquill 1949a, 1950b, Rider 1954a) and that a summary of these investigations together with some discussion of the difficulties and accuracy to be expected in its application has been given by Rider (1954b).

2. Observational aspects

A site about 6 mi NW of Cambridge was used. It was in level open country and throughout the period covered by the observations a pasture and a fallow field were generally available. At various times it was possible to expose apparatus in a field of peas and in a field of fully-grown brussels sprouts. The latter field was being allowed to run to seed. All these sites were within a circular area of some 500 m diameter and therefore exposed to the same weather. The soil type of each was the same. The initial plan for the observations, which had to be modified from day to day to meet ruling conditions, was to undertake a series of six-day runs, the first and last two days of each series being occupied by control observations. It was hoped to get a number of such observations at intervals of four weeks throughout the growing season, but it proved impossible to maintain a strict schedule, as this work had to be done in fine weather, as well as to give way to normal farming operations. In the event, three periods were covered. The first extended from 19 May to 7 June, the second from 16 to 24 June and the third from 7 to 14 July 1955. There was also an initial day's observation on 9 to 10 May 1955 to test the apparatus, three sets of which were built for the investigation. The sites on which the apparatus was exposed during these periods can be seen by referring to Table 1. Initially on 9 May the pasture had a grass length of about 15 cm. The grass grew steadily throughout the first period of observation until on 7 June it had reached a height of about 30 cm. Cattle were then sent into the field and when work recommenced on 18 June the grass had been reduced to a fairly uniform height of 10 cm, after which it again grew steadily until the observations finished. These changes in grass length are reflected in the values of the zero plane displacement, d, given in Table 1. The bare soil was harrowed before observations started and occasionally during the following weeks it was 'cultivated' to keep weeds down. The surface consisted of parallel ridges and troughs having an amplitude of about 20 cm. The brussels sprouts were fully grown plants about 1 m high and when the apparatus was placed over them they were on the point of flowering. Although the stems of these plants were fairly widely spaced the tops were bushy and formed a complete cover over the ground. The peas were just coming into flower on 18 June and had a height of 60 cm. They covered the ground with a dense mat of green vegetation and when in pod in July this cover was even denser although there was no apparent increase in height.

The minimum requirements for the calculation of the rate of evaporation by the use of Eq. 1 are the measurement of humidity at two heights and the measurement of wind speed at three heights, the wind speed at the third height being required for the determination of d, since the latter can theoretically be obtained by the use of the equation

$$\frac{u_3 - u_2}{u_2 - u_1} = \frac{\ln (z_3 - d) - \ln (z_2 - d)}{\ln (z_2 - d) - \ln (z_1 - d)} \quad . \quad . \quad . \quad (2)$$

when neutral conditions of stability hold in the layer of air concerned. However, previous experience when working over an oat field (Rider 1954c) has led to the conclusion that it is essential to have measurements of wind speeds at more than three heights in order to arrive at reliable values of d as it is not possible to measure the wind speed with sufficient precision for use in Eq. 2 and a graphical method in which smoothing is possible has to be used. For this, wind speeds at five or more heights are desirable and in the majority of observations this number of anemometers was exposed with each set of apparatus at heights up to 2·5 m. The anemometers were the sensitive cup type arranged to operate electromagnetic counters at some distance from the point of exposure. These counters were photographed every hour to provide a record of the runs of wind and hence of the mean hourly wind speeds. Each humidity mast carried two psychrometers, the latter

each having a dry- and wet-bulb thermo-electric thermometer which were aspirated at 3 m/sec. The thermometers were arranged in ' tandem ' along the axis of a copper tube with the dry bulb in front of the wet bulb. The arrangement is shown in Fig. 1. Outside the inner tube a second copper tube was mounted co-axially with the first, and in use the air passed down the space between the two tubes at the same rate as over the bulbs. All metal surfaces were plated and the thermometers had a lag coefficient of about 75 sec. These housings were designed to overcome some undesirable features found in those used previously (Rider 1954c) for this type of work which were based on Pasquill's (1949b) design. In that design rectangular section tufnol tubes were used and it was found that when solar radiation fell on one side of this housing a difference of temperature of up to 0·5°F could occur between two dry-bulb thermometers mounted in it when the aspiration rate over the thermometers was as high as 3 m/sec. In the present housing the thermometer bulbs are mounted symmetrically with respect to the walls and the much higher conductivity of the copper tends to even up the temperature differences around the housing when sunshine is falling on one side. The one precaution to be taken is that the housing must not be directed at a low sun. No temperature differences have been detected between two dry bulbs exposed in this housing in test runs and, further, the absolute radiation errors, although of secondary importance in this application, are considerably less than in the Pasquill type.

The housings are arranged to plug into tufnol collars which are attached to the mast. Each collar is provided with a butterfly valve which is locked in position after being adjusted to provide the required rate of aspiration, the latter being arranged to be the same at each of the four mounting positions, which were 25 cm apart in height. The two positions not in use at any time were closed by corks, and the overall heights of the masts could be adjusted when necessary by lengthening the supports. The masts themselves were hollow to provide the links between the psychrometers and the aspiration fans. The thermo-electric thermometers at the greater height were each provided with two thermo-junctions and one dry and one wet junction were used in conjunction with a

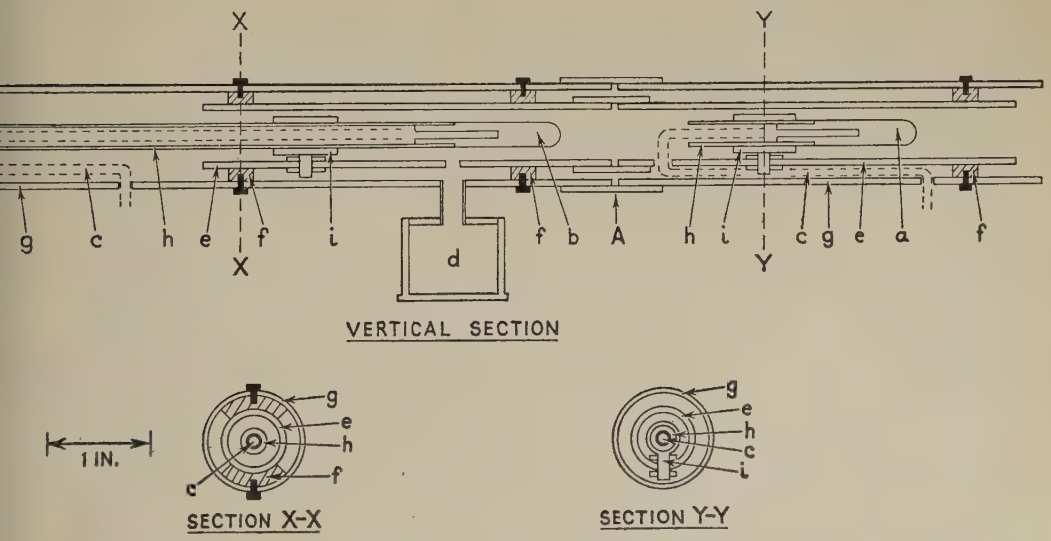

Figure 1. Sectional views of the psychrometer housing. (a) dry bulb, (b) wet bulb, (c) p.v.c. tubing insulating thermo-couple wires, (d) water holder, (e) inner copper tube, (f) tufnol spacers (g) outer copper tube, (h) paxolin tubes, (i) thermometer holders. The housing can be parted at A, the ' dry ' section being a tight push fit into the ' wet ' section.

standard junction kept in melting ice. The two other junctions were connected in series with the corresponding junctions in the lower psychrometer. The details of the wiring and recorders have been given previously (Rider 1954c, Fig. 2). It is sufficient to recall here that two classes of recorder are used. The first is a comparatively insensitive type which provides a record of the dry- and wet-bulb temperatures at the greater height (t_2 and t_2'), and the second is a sensitive photographic recorder which provides a record of the dry- and wet-bulb temperature differences between the two heights, $(t_1 - t_2)$ and $(t_1' - t_2')$. The temperatures are recorded to 0·1°F and the temperature differences to 0·01°F. These limits of measurement enable the vapour pressure differences $(e_1 - e_2)$ to be obtained to 0·01 mb. The masts and recorders were calibrated as single units in the usual way and on the site the wind and temperature recorders associated with each of the three sets of apparatus were grouped together in a hut placed at one corner of the pasture. Cables, 200 m long, enabled the apparatus to be moved from site to site as required. The main difficulties experienced in the observational work arose from the lack of a mains power supply and the enforced reliance on motor generators and batteries, and from the rather small areas of brussels sprouts (3 acres) and peas (4 acres) available for the observations. The small areas of these crops made it necessary to site the apparatus near the downwind side of the fields to obtain an ample fetch of wind over a uniform surface and changes in wind direction of more than about 45° during a run made it necessary to abandon the run and resite the apparatus for a further attempt. The time taken to move the apparatus from site to site was considerable.

3. Calculation of the water loss and discussion of the results.

Eq. 1 is strictly only valid in neutral conditions of atmospheric stability, its use in unstable and stable conditions leading to an underestimation and an overestimation of the rates of evaporation respectively. However, since the degree of departure from neutral conditions is controlled by the vertical wind shear as well as by the departure from the adiabatic lapse rate it is possible to keep the systematic errors which arise if the stability effect is neglected to a minimum by siting the apparatus at a low height above the vegetation (see, e.g., Pasquill 1949a). It has been estimated that above an oatfield and a pasture, provided this precaution is taken, the underestimates in the daily totals of water loss will not exceed 15 and 10 per cent respectively. Moreover in this instance, we are endeavouring to compare water losses from surfaces which are exposed to the same weather, so that when an overestimation or an underestimation occurs for one site it will, in general, occur for another. However, since the effective height of exposure of the apparatus on the various sites was not always the same and, as will be seen, important differences in the micro-environments were experienced the magnitude of the errors was somewhat different for the various sites. Other equations are available for the more precise evaluation of evaporation rates in non-neutral conditions but they contain parameters which are extremely difficult to determine with any confidence for a cropped surface.

From the records, mean values of the temperatures, temperature differences and wind speeds were easily obtained, and it only remained to obtain values for d before the hourly mean rates of evaporation and hence the daily water losses could be calculated from Eq. 1 which for practical use is conveniently written as

$$E = \frac{3{\cdot}46 \times 10^{-5} (e_1 - e_2)(u_2 - u_1)}{T \left[\ln \frac{z_2 - d}{z_1 - d} \right]^2}$$

in which e, the vapour pressure, is in mb, u is in cm/sec, z and d are in cm, T is the absolute temperature and E is in g cm^{-2} sec^{-1}. The method used for the determination of d was to select 'neutral' hours by referring to the records of $(t_1 - t_2)$ and to plot the values of u_z against $\log_{10}(z - d)$ using likely values of d. For this purpose 'neutral' hours were considered to be those for which $(t_1 - t_2)$ did not exceed $\pm 0{\cdot}05°F$, the psychrometer heights z_1 and z_2 being always 25 cm apart. When more than one hour on a particular day was suitable, more weight was given to the determination for the hour with the higher wind speeds. When a number of suitable hours occurred a mean wind-speed ratio plot was drawn and an average value for d obtained. An example is given in Fig. 2, in which plots for a few single hours as well as mean plots are given for the peas and grass. Table 2 contains some details from two observations from which the scatter experienced in the individual determinations of d can be judged. When working over a tall cereal Rider (1954c) found that the values of d found as outlined above showed a variation with wind speed, d increasing with increasing speed up to the maximum experienced (about 5 m/sec at 2 m). This was considered to be the result of the waving and bending of the crop and it added a complication to the evaluation of E. Similar effects have been reported by Inoue (1955). In the present investigation stiff crops were deliberately chosen in the hope that this feature would not be found. This proved to be the case, as while there was some variation in the values calculated for d from the various suitable hourly observations there was no indication of a systematic variation with wind speed. One value of d has therefore been used for each day of observation for each surface and these are set out in Table 1 together with the daily water losses computed from the hourly values of E. The influence of the likely errors in the values of d on the daily water losses is discussed later. In observations 1 to 4, 8, 9, 13, 14 and 19 the three sets of apparatus were exposed over either bare soil or grass and the 24-hr water losses were computed independently from the results provided by each set. It will be seen that the water losses were in reasonable agreement except when the losses were small. The worst case occurred in observation 8 when the gradients of temperature were very small. The instrumental errors which arise in the main from stray e.m.fs. in the thermo-electric circuits tend to produce absolute errors in the computed vapour-pressure differences and hence in the values of E, and when the evaporation is small the relative errors are large. If it had been realized at the start that the evaporation from bare soil would be so small on many occasions compared with that from grass, more effort would have been made to restrict the control observations to the grass surface. Observation 9 is of interest since although the psychrometers were exposed at different heights for each set, the losses for the day were in reasonable agreement. Some details from one of the control runs are given in Fig. 3. In this figure the mean hourly values of the dry- and wet-bulb temperature differences, $(t_1 - t_2)$ and $(t_1' - t_2')$, between the psychrometer heights z_1 and z_2 of 25 and 50 cm, and the values of $(e_{25} - e_{50})$ which were obtained from these differences and the recorded values of t_{50}' are shown for observation 14. The three sets of apparatus were placed about 4 m apart in line across wind. It will be noted that quite small differences in the values of the dry- and wet-bulb temperature differences produce appreciable differences in the vapour-pressure gradients over the height interval which when multiplied by the wind-speed differences give surprising variations in the hourly values of E. The mean hourly wind-speed differences do not themselves vary much from set to set, nor do the values of t_{50}'. The variations in the dry- and wet-bulb temperature profiles are probably due in part to genuine point-to-point differences as well as to deficiencies in the apparatus. The whole series of control observations suggest that, except when evaporation is small, the three sets of apparatus give consistent results to within about 20 per cent in the daily water losses.

TABLE 1. Surfaces and periods of exposure, psychrometric heights, values of zero-plane displacement and daily water losses

Observation No.	24 hours commencing GMT	Apparatus set 1 Surface	Psychrometer heights (cm)	d (cm)	Water loss (mm)	Apparatus set 2 Surface	Psychrometer heights (cm)	d (cm)	Water loss (mm)	Apparatus set 3 Surface	Psychrometer heights (cm)	d (cm)	Water loss (mm)
1	1400 9 May	grass	25, 50	10	2·0	grass	25, 50	10	2·3	grass	25, 50	10	2·2
2	1200 19 May	grass	25, 50	12	1·7	grass	25, 50	12	1·9	grass	25, 50	12	1·6
3	1700 20 May	grass	25, 50	—	—	grass	25, 50	12	1·9	grass	25, 50	12	2·1
4	1600 25 May	grass	50, 75	15	1·7	grass	50, 75	15	2·5	grass	50, 75	15	2·1
5	2000 26 May	grass	50, 75	20	2·2	sprouts	125, 150	60	3·6	soil	25, 50	10	1·2
6	2300 27 May	grass	50, 75	20	0·7	sprouts	125, 150	60	1·2	soil	25, 50	10	0·5
7	0900 6 June	grass	50, 75	20	2·3	sprouts	125, 150	60	4·3	soil	25, 50	10	0·3
8	1200 16 June	soil	25, 50	10	0·2	soil	25, 50	10	0·3	soil	25, 50	10	0·4
9	1400 17 June	soil	25, 50	10	0·4	soil	75, 100	10	0·5	soil	50, 75	10	0·5
10	1600 18 June	grass	25, 50	5	0·6	peas	75, 100	25	7·4	soil	25, 50	10	0·4
11	1100 21 June	grass	25, 50	5	1·1	peas	75, 100	25	2·3	soil	25, 50	10	1·4
12	1200 22 June	grass	25, 50	10	1·2	peas	75, 100	25	5·0	soil	25, 50	10	—
13	1500 23 June	soil	25, 50	10	0·3	soil	25, 50	10	0·4	soil	25, 50	10	0·6
14	1600 7 July	grass	25, 50	10	2·3	grass	25, 50	10	2·9	grass	25, 50	10	2·6
15	0900 9 July	peas	75, 100	25	4·4	soil	25, 50	10	1·9	grass	25, 50	10	2·7
16	1000 10 July	peas	75, 100	25	3·3	soil	25, 50	10	0·4	grass	25, 50	10	2·3
17	1100 11 July	peas	75, 100	25	2·6	soil	25, 50	10	1·1	grass	25, 50	10	2·0
18	1200 12 July	peas	75, 100	25	2·9	soil	25, 50	10	1·7	grass	25, 50	10	1·9
19	1500 13 July	soil	25, 50	10	0·4	soil	25, 50	10	0·6	soil	25, 50	10	0·4

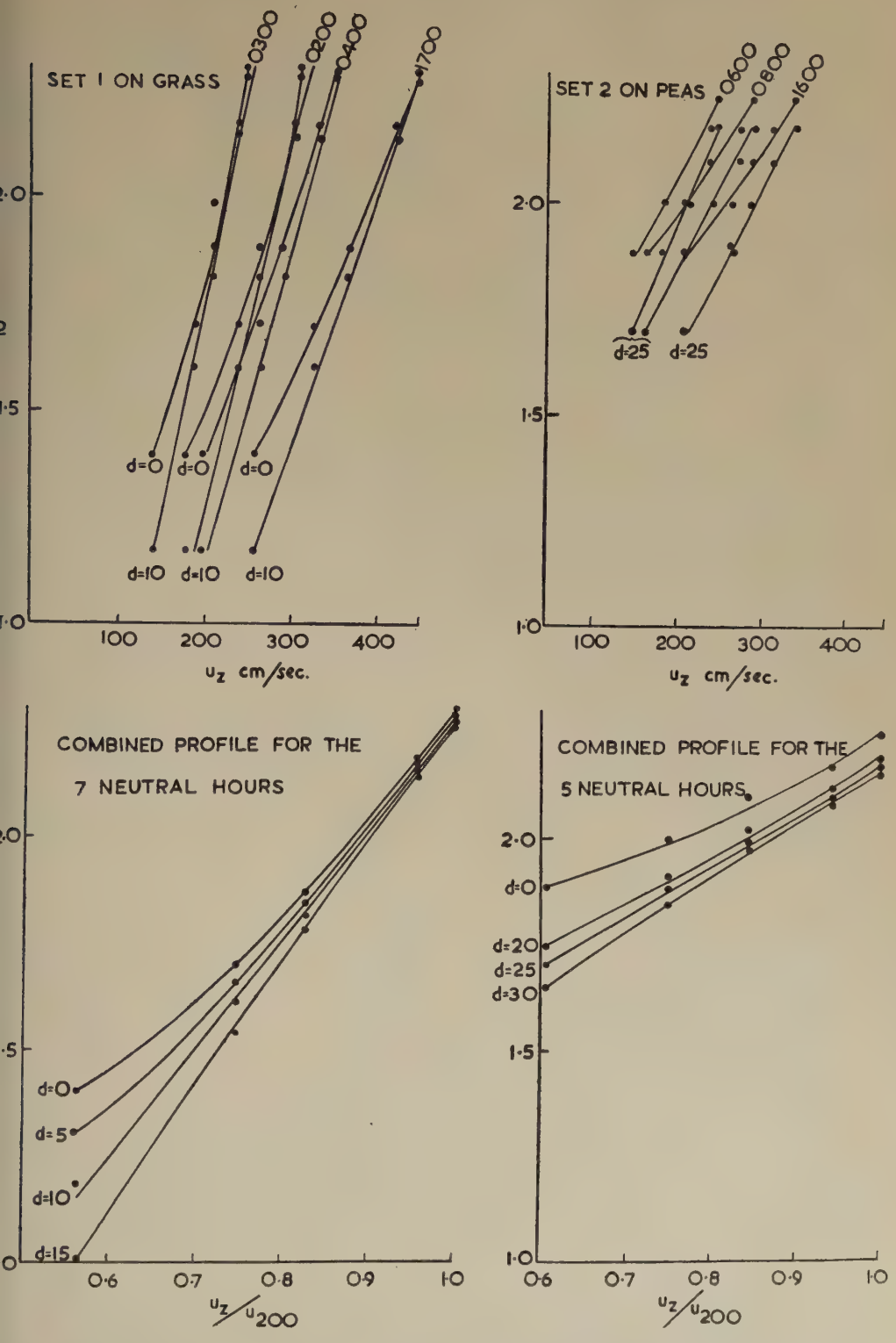

Figure 2. Determination of the zero-plane displacement, d, in observation No. 12, 22-23 June 1955.

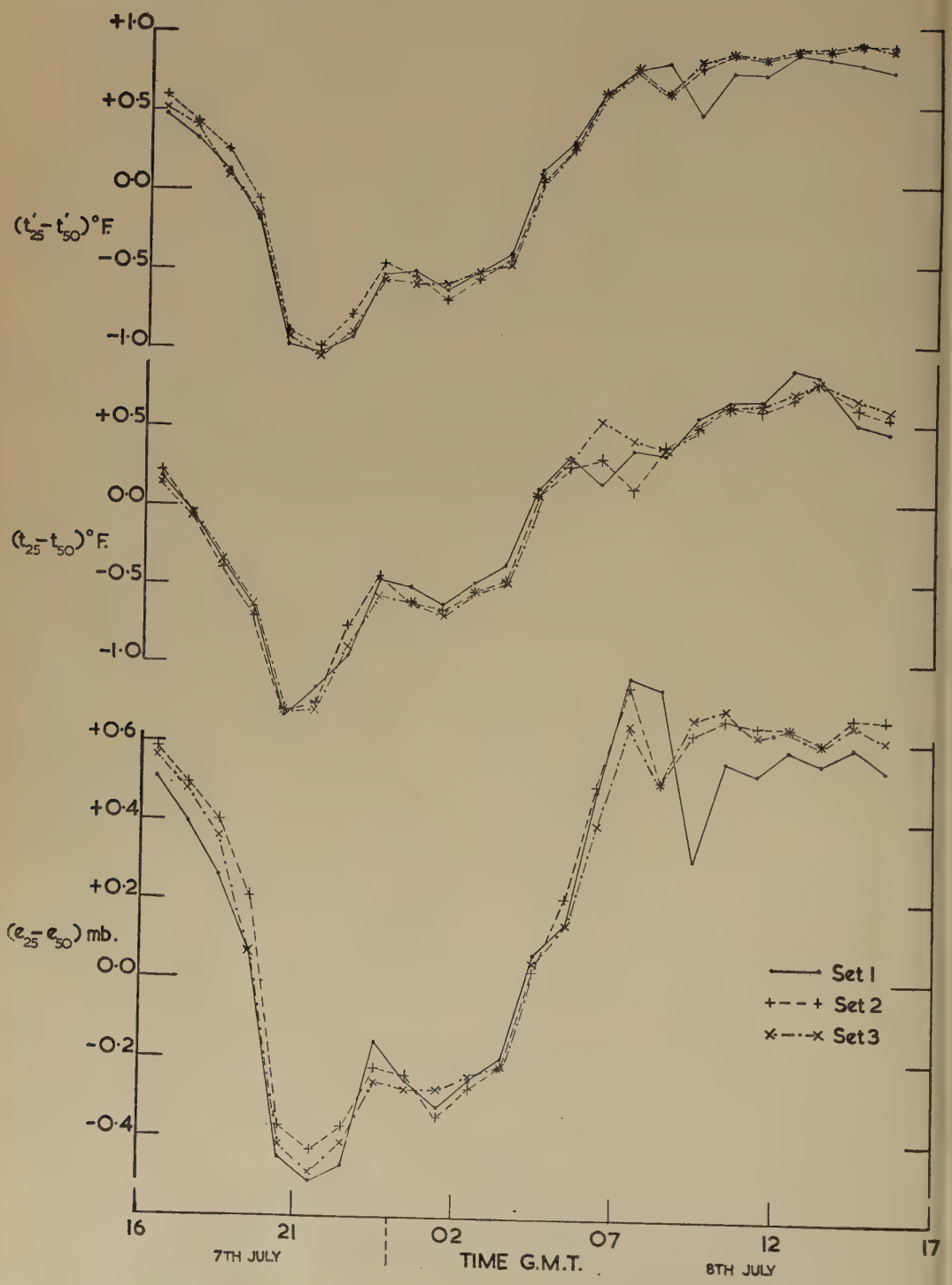

Figure 3. Comparison of humidity-mast performance in observation 14. The three sets of apparatus were exposed over grass, the psychrometer heights being 50 and 25 cm for each.

Turning now to those days on which the three sets were exposed over different sites we see, from Table 1, that the loss was greater from peas or brussels sprouts than from the pasture in every instance by a factor which varied from day to day and which reached a maximum of about an order of magnitude in observation 10. This latter observation is illustrated in Fig. 4. It is evident that the elements follow the expected daily variations but the differences from site to site are large. In general the vapour-pressure gradients are greater over the peas than over the pasture and this, together with the differences in the effective heights of exposure of the anemometers and psychrometers, leads to the much higher values of E for the peas. By far the greatest hourly rates of water loss experienced in the whole programme of observations occurred from 1600 to 1900 GMT from the peas on this occasion, reaching a maximum of about 40×10^{-6} g cm^{-2} sec^{-1}. The highest rate observed during the rest of the whole series was 17×10^{-6} g cm^{-2} sec^{-1}, again over the peas during the hour ending at 1400 GMT on 22 June. A rate of evaporation of 40×10^{-6} g cm^{-2} sec^{-1} corresponds to an energy consumption of about 100 mw cm^{-2}, and although no records of solar radiation, other than sunshine duration which was continuous during the hours in question, are available at or near the site it may be safely assumed that only about half the required energy could have been provided directly by the sun during this hour. The intensities of solar radiation on a horizontal surface recorded at Kew (about 60 mi S of the site) in the hours ending 1700, 1800 and 1900 GMT were 45, 28 and 11 mw cm^{-2} respectively. On these considerations it is tempting to reject the observation on the grounds of probable instrumental error. Tests of the apparatus on the following day revealed no such convenient explanation of these very high rates of evaporation and the details for this observation have been given in preference to those for another day in which the results were not out of accord with current energy balance ideas. No satisfactory explanation can be provided but we may note one or two interesting features revealed by the curves of Fig. 4. The dry-bulb temperature over the peas was lower than that over the grass, and the air over the bare soil was hotter than that over the other two surfaces. This remains true when a correction is applied, on the basis of the measured height variation, to obtain the approximate temperatures at the same effective heights, that is the actual height as measured from the ground minus the appropriate zero-plane displacements. Further the lapse of temperature over the peas between 1600

TABLE 2. EXAMPLES OF THE SCATTER EXPERIENCED IN THE DETERMINATION OF THE ZERO-PLANE DISPLACEMENT

Observation No.	Set number and surface	'Neutral hour' commencing GMT	Wind speed u_z at height z		Deduced d (cm)	Value of d (cm) used in computing evaporation
			z (cm)	u_z (cm/sec)		
6	1 grass	0500	200	210	20	
		1300	200	354	20	20
		1400	200	287	18	
6	2 sprouts	0500	200	182	65	
		1300	200	317	55	60
		1400	200	244	60	
		1500	200	271	60	
6	3 bare soil	0100	150	128	8	
		0300	150	131	12	10
		1700	150	268	10	
10	2 peas	1900	200	370	28	
		0400	200	142	25	
		0500	200	213	23	25
		0600	200	313	22	
		1400	200	259	19	
		1600	200	193	27	

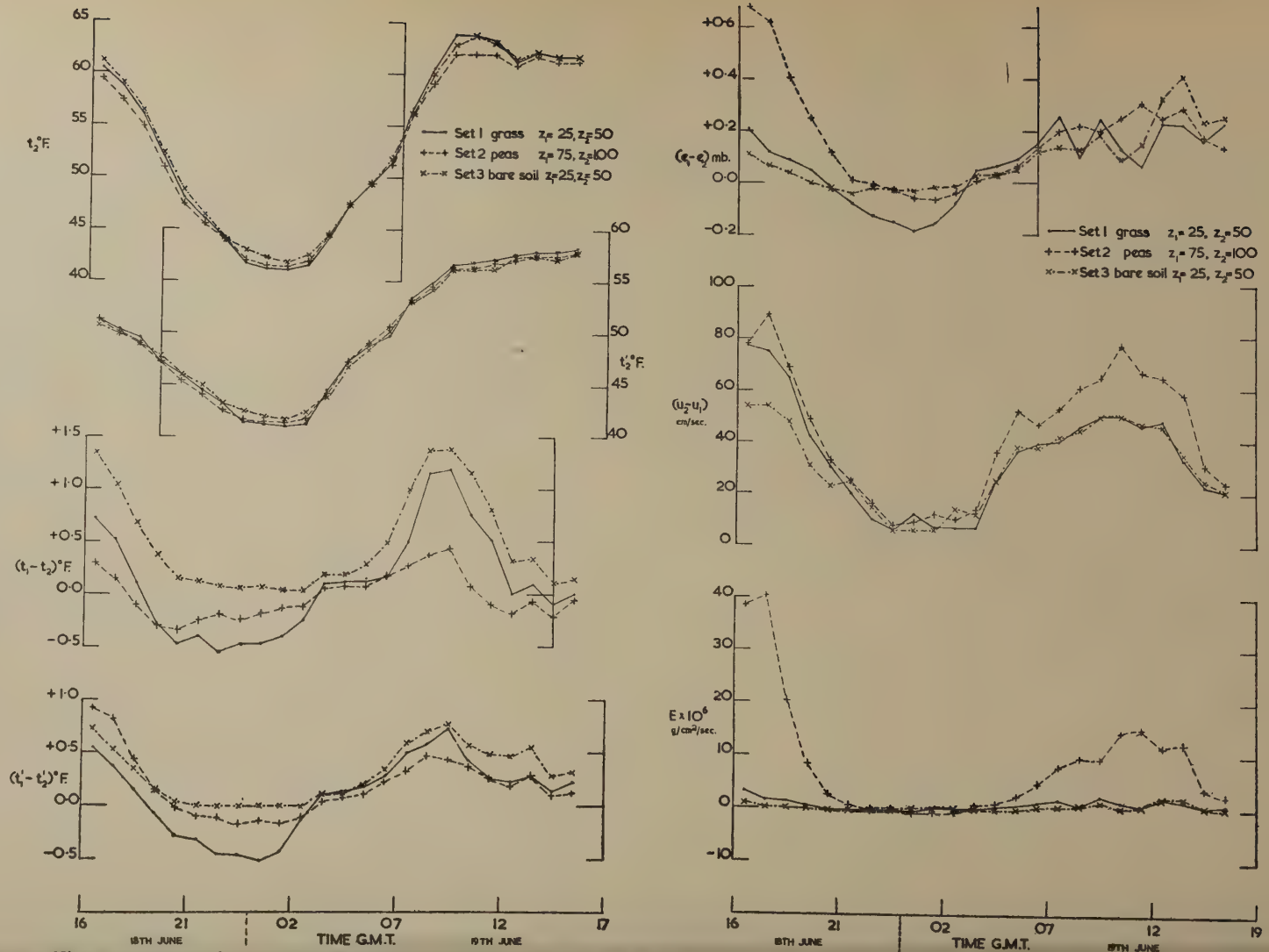

Figure 4. Dry- and wet-bulb temperature (t_2 and t_2'), dry- and wet-bulb temperature differences ($t_1 - t_2$) and ($t_1' - t_2'$), vapour pressure

and 1800 GMT was about a sixth of that over the bare soil and in the hour ending at 1900 GMT, when the E for the peas was 20×10^{-6} g cm^{-2} sec^{-1}, there was an inversion of temperature over the peas whereas a strong lapse persisted over the bare soil. Advection of energy from surrounding areas and the supply of energy from the air appears a possibility. Similar but less well-marked features can be detected from the observations for other days.

TABLE 3. ACCUMULATED WATER DEFICIT UNDER TURF.

1955	Accumulated deficit (in.)
30 April	1·6
30 May	2·2
15 June	2·5
30 June	3·6
15 July	5·0
30 July	7·5

It is necessary to produce evidence that the crops were transpiring at their potential rates during the period covered by the observations. Some support may be had here from calculations based on Penman's method for the computation of the accumulated water deficit for the turf-covered surface. The accumulated deficit is the excess of potential transpiration loss over rainfall and these figures for the dates of interest are given in Table 3. According to Pearl and others (1954) a deficit of from 3 to 5 in. can occur under turf before the transpiration falls below its potential value and for deeper-rooted crops the deficit is larger when transpiration is checked. Thus it appears that up to and including observation 13 we were definitely measuring potential transpiration from the grass and may have been doing so throughout the whole series as the accumulated deficit did not amount to 5 in. until after the last day of observation. The peas and brussels sprouts have a root constant which is probably at least equal to that of grass, and they too were probably transpiring at their potential rates. If the root constants for these two crops are smaller, then we must conclude from the results that a rate of transpiration less than the potential rate is greater than the potential rate from turf.

TABLE 4. INFLUENCE OF CHANGE IN THE ZERO-PLANE DISPLACEMENT, d, ON THE CALCULATED DAILY WATER LOSSES FOR THREE OBSERVATIONS

Observation No.	Apparatus-Set No.	Surface	d (cm)	Water loss (mm)
5	1	grass	20	2·2 ∓ 0·3
5	2	sprouts	60	3·6 ∓ 0·9
5	3	soil	10	1·2 ∓ 0·2
10	1	grass	10	0·6 ∓ 0·1
10	2	peas	25	7·4 ∓ 1·2
10	3	soil	10	0·4 ∓ 0·1
15	1	peas	25	4·4 ∓ 0·8
15	2	soil	10	1·9 ∓ 0·4
15	3	grass	10	2·7 ∓ 0·6

The greatest source of uncertainty in the results given in Table 1 arises from the lack of a precise knowledge of the values to be given to the zero-plane displacements. It is safe to assume that the values given were reliable to the following limits;

grass and bare soil	$\pm$ 2·5 cm
peas	$\pm$ 5 cm
brussels sprouts	$\pm$ 10 cm

These figures are suggested by the scatter in the individual determinations. Table 4 shows the change in the calculated daily water losses for three observations which arise from the range of uncertainty in the values to be given to d. It is apparent that any likely errors do not affect the general conclusion that must be drawn, namely that the potential transpiration is not the same for all crops which have roughly the same colour and completely cover the ground.

Another and disappointing feature of the results is that there is no steady relationship between the water losses from the various surfaces. As far as bare soil is concerned this is easily explained, the rate of loss being controlled by the time that has elapsed since the last fall of rain as well as by the weather. For example, during observation 17 there was a heavy thunderstorm from 1700 to 1730 GMT on 11 July and the rate of evaporation on 12 July was comparatively high while the soil surface remained wet. By 14 July the surface had dried out and the rate of loss fell to near its value before the storm. The change in the ratios of the daily water losses from the grass, peas and sprouts is not easily explained. The ratios of the wind-speed differences over the 25-cm height intervals are reasonably constant but the vapour-pressure profiles vary in an erratic way from site to site and hour to hour. The changes in the dry- and wet-bulb temperature profiles from lapse to inversion and vice versa do not occur at the same time over the different sites, and it is even possible to have evaporation from one site and condensation on another at the same time. Fig. 4 shows that no inversion occurred over the bare soil during the last hours of 18 June, whereas over the other two surfaces one did occur and was much larger over the grass than over the peas. This type of variation in the profiles was noted repeatedly and it is thought to be, at least in part, a reflection of the role that soil heat plays in the control of microclimate. During the preceding daylight hours the soil temperature under the bare surface reached much higher values than under the cropped surfaces and a relatively large reservoir of heat was available for liberation at night. This heat was released sufficiently quickly and proved large enough to offset the inversion which would have otherwise been present.

4. Conclusion

This paper has been written to suggest that the concept of equal potential transpiration irrespective of crop size or character be approached with the utmost caution. While the solar energy available to a large area, itself a reflection of weather and season, must control the overall rate of water loss and a balance must be maintained for such an area for reasonable lengths of time, it appears that different crops covering areas of several acres can so modify the general weather that real differences in water loss take place. It is readily admitted that the figures given in Table 1 are liable to be in error but in the opinion of the author no criticism, whether from the point of view of the validity of the method, of the computations of zero-plane displacement, of the apparatus or method of observation can invalidate the conclusion that real differences exist.

Acknowledgments

The author wishes to express his thanks to the Director and Staff of the National Institute of Agricultural Botany for providing the site facilities and to the Director of the Meteorological Office for permission to submit this paper for publication. He would also like to thank the members of the Meteorological Office Unit at Cambridge, and in particular Mr. E. L. Evans, without whose help this programme of observations could not have been undertaken.

References

Inoue, E.	1955	*J. Agric. Met.*, Tokyo, **11**, p. 18.
Pasquill, F.	1949a	*Proc. Roy. Soc.* A, **198**, p. 116.
	1949b	*Quart. J. R. Met. Soc.*, **75**, p. 239.
	1950a	*Air Ministry, Met. Res. Ctee.*, M.R.P., No. 579.
	1950b	*Quart. J. R. Met. Soc.*, **76**, p. 287.
Pearl, R. T., Hoare, E. R., Mathews, R. H., Penman, H. L., Skillman, E. E. and Smith, L. P.	1954	*Min. Agr. Fish. Tech. Bull.*, No. 4.
Penman, H. L.	1948	*Proc. Roy. Soc.* A, **246**, p. 120.
Rider, N. E.	1954a	*Phil. Trans.* A, **246**, p. 61.
	1954b	*Assoc. Internat. Hydrologie Publ.*, No. 38, Vol. III, U.G.G.I., Rome, p. 135.
	1954c	*Quart. J. R. Met. Soc.*, **80**, p. 198.
Thornthwaite, C. W. and Holzman, B.	1939	*Mon. Weather Rev.*, U.S.W.B., **67**, p. 4.

551.524.4 : 59

The vertical distribution of aphids in the air and the temperature lapse rate

By C. G. JOHNSON
Rothamsted Experimental Station, Harpenden, Herts.

(Communicated by H. L. Penman; manuscript received 8 April 1956, in revised form 9 January 1957)

Summary

Aphid density diminishes with height above the ground; the linear regression coefficient, $-b$, of log density on log height is an approximate expression of the vertical density profile. A low negative value of b suggests a relatively high degree of upward transport, and a high value the reverse.

From May to October 1948, aphid densities were estimated simultaneously at 6 heights from 50 to 2,000 ft over 2-hr periods during the day: lapse rates to 2,000 ft were also measured. The regression coefficient, $-b$, of log density on log height was inversely correlated with the mean lapse rate between months; September and October were associated with low lapse rates and steep density gradients.

Correlation coefficients of b with lapse for 2-hr periods were negative above a lapse of 10°F/2,000 ft and became statistically significant in the afternoon. Below the 10° value no significant correlation existed, probably because low lapse rates occurred usually in the early morning when densities were low and factors other than atmospheric mixing could affect the profile.

Two examples of the change in the vertical profile from hour to hour throughout the day are given to illustrate the association of high lapse rates with high-altitude dispersal and the limitation of upward transport when lapses are low: but biological factors also play a part in determining the form of the profile and these are briefly discussed.

1. Introduction

It has been recognized, often on *a priori* grounds alone, that the dispersal of many insect populations in the air is associated with atmospheric instability: but there has been no adequate demonstration of varying degrees of upward transport of insects with the vertical stability of the air.

In this paper it is shown that the relative density of aphids at different heights in the air is sometimes correlated with the temperature lapse rate. Aphids are particularly suitable insects for this work for they occur in relatively high aerial densities, they are fairly uniform in size, shape and habits, and being very weak fliers (maximum air-speed, 2-3 ft/sec) they are affected by slight air currents.

2. Methods

Aphids, unlike locusts, are very small insects and cannot be seen in the sky: nor do they, apparently, form well-defined swarms like locusts but become generally dispersed through the air, their aerial densities generally decreasing with altitude. Volume densities of aphids show about the same range as those of locusts: an extremely high aphid density is about $1{\cdot}8/m^3$ ($1/20\ ft^3$) and the lowest our largest traps detect is about $8 \times 10^{-5}/m^3$ ($1/450{,}000\ ft^3$). But even the low densities can add up to extremely high numbers over a wide area.

Thus the aerial life of these insects cannot be studied visually and gradients of density have to be estimated with traps which operate simultaneously at different heights on a tower or a barrage-balloon cable: this has been done over fairly level country at Cardington, near Bedford.

Such a static system, suspended in air moving horizontally (and with it an insect-density gradient) has its limitations: for example, insects caught at different altitudes no doubt come from different sources. There is no single point source but an almost infinite number of sources scattered over a very wide area. The discharge of aphids into

he air is periodic and very variable during the day and from day to day. There are numerous different species, not always in the same proportions : and in this paper data for many species of aphids have been pooled. Also we can usually study only the lower part of the distribution because the balloon has a limited lifting power and our apparatus is heavy (Johnson and Taylor 1955a). We have not been able to estimate the highest altitudes reached by the insects and to associate this with the height of the convection top.

TABLE 1. LOG (APHID DENSITY + 1) ESTIMATED WITH TOW-NETS AT CARDINGTON, 1948.
Density = No. per 10^6 ft^3 per 2 hr. Trapping periods (GMT), 0730 to 0930 (1), 1030 to 1230 (2), 1330 to 1530 (3) (after 1 October, 1 hr later).

Date		Ht (ft) Period	50	250	500	1000	1500	2000	*b*	Mean lapse rate (3 to 2,000 ft) (°F)
May	21	2	2·24	1·86	1·89	1·56	1·61	1·38	− 0·49	13·7
		3	2·94	2·64	2·52	2·27	2·07	1·97	− 0·60	12·9
	27	2	1·69	1·18	1·08	0·78	0·85	0	− 0·83	11·4
June	8	2	2·43	1·59	1·26	1·30	1·26	0·90	− 0·84	11·2
	11	3	1·71	1·40	0·78	0·78	0	0	− 1·11	10·0
	23	2	2·05	1·67	1·43	1·28	1·08	0·70	− 0·76	12·6
		3	1·95	1·38	1·38	1·00	0·78	0·30	− 0·90	12·4
	24	3	2·55	2·04	1·85	1·91	1·18	1·08	− 0·86	14·0
July	2	1	1·60	1·23	1·04	0·85	0·48	0	− 0·88	9·6
		3	2·32	1·63	1·28	1·04	1·11	0·85	− 0·88	10·9
	6	3	2·29	1·89	1·15	1·04	0·85	0·78	− 1·00	11·5
	7	3	1·71	1·40	1·20	0·60	0·60	0·48	− 0·82	6·4
	9	3	0·95	0·70	0·60	0·30	0	0	− 0·62	10·8
	16	1	1·69	1·36	0·95	0·60	0·78	0·48	− 0·75	11·5
	20	2	1·91	1·51	1·18	1·20	1·04	0·60	− 0·70	11·6
		3	1·94	1·49	1·18	0·85	0·90	1·04	− 0·66	12·1
	22	3	1·57	1·36	1·00	0·30	0	0·30	− 1·00	10·7
	23	1	1·74	1·78	1·54	0·60	0·48	0	− 1·10	10·1
		2	2·27	1·63	1·08	1·04	0·48	1·08	− 0·94	12·1
		3	2·17	1·77	1·04	1·20	1·00	0·85	− 0·82	11·5
	26	3	2·13	2·56	1·54	1·36	1·38	0·95	− 0·79	10·8
	29	2	1·63	1·93	1·51	1·36	1·28	1·20	− 0·33	13·2
		3	1·32	1·32	1·18	1·15	1·00	0·85	− 0·27	13·1
	30	3	2·55	2·37	2·01	1·51	1·36	1·15	− 0·91	15·1
August	5	2	1·48	0·95	0·85	0·48	0·70	0	− 0·76	10·1
	6	1	1·41	1·00	0·48	0·48	0·30	0·30	− 0·73	7·2
	9	3	1·54	1·26	0·70	0·48	0	0	− 1·03	12·8
	24	2	0·95	0·95	0·60	0	0·30	0	− 0·64	10·3
		3	1·00	0·48	0·60	0·30	0	0·30	− 0·51	12·2
September	9	3	1·60	1·23	0·95	0·70	0	0	− 1·03	12·5
	10	1	1·79	1·26	1·26	0·78	0·60	0·48	− 0·81	2·9
	22	3	2·17	2·02	1·26	0·60	0	0	− 1·51	12·1
	29	1	1·59	1·56	1·30	0·60	0·30	0	− 1·02	7·2
		3	2·14	2·04	1·41	0·60	0·48	0	− 1·37	10·2
	30	3	2·04	1·93	1·36	1·04	0·48	0·48	− 1·07	12·5
October	1	1	2·03	1·71	1·00	0·95	0·60	0	− 1·16	3·8
		2	2·12	2·14	1·52	1·00	1·00	0	− 1·18	7·0
		3	2·48	1·97	1·80	0·95	0	0·30	− 1·53	9·9
	4	2	2·21	2·18	1·68	0·70	0·48	0·60	− 1·23	12·4
	5	3	2·36	2·45	1·32	1·26	0·60	1·04	− 1·09	11·2
	6	3	3·25	2·51	1·48	0	1·15	0	− 2·01	10·5
	7	3	2·29	2·24	1·36	0·48	0·70	0	− 1·46	10·6
	8	3	2·11	2·34	1·65	0·90	0·48	0	− 1·36	11·2
	12	1	2·17	2·01	1·18	0·85	0·30	—	− 1·39	8·6
	15	2	1·28	1·46	1·04	0·48	0·30	0·30	− 0·74	9·4

Max. log (density + 1), i.e., 3·25 corresponds to a catch of 44 aphids. The other catches are not in proportion : this varies with the wind speed. Thus for the third period on 1 October, 176 aphids were caught at 50 ft.

The data in this paper are mainly from catches made in 1948 when densities were exceptionally high and prolonged, and trapping was successful for an exceptional number of days from May to October. The density at each height, (50, 250, 500, 1,000, 1,500 and 2,000 ft) was estimated by tow-net over a 2-hr period at 0730 to 0930, 1030 to 1230 and 1330 to 1530 hr GMT. Tow-nets are not as accurate as the suction traps used in later experiments, especially at low wind speeds. But most of the present data were obtained in moderate winds and evidently are good enough to show general trends. The operation of tow-netting and the estimation of aerial density (allowing in the present data for the run of wind through the nets but not for errors at low wind speeds revealed by suction traps) is described elsewhere (Johnson 1951).

In addition, however, a limited amount of data from suction traps in 1953 and 1955 is given to illustrate the kind of change occurring in the density profile from hour to hour throughout the day.

Temperatures in 1948 were measured at 3 ft with a thermograph (aspirated screen) and at 2,000 ft with a thermocouple, every 15 min throughout each 2-hr trapping period. Mean lapse rates for the 15-min period within the 2 hr were obtained. Table 1 gives the data.

3. The vertical distribution of aphids and the lapse rate

Past workers showed that, in general, insect density diminishes with altitude : but the relation was not studied systematically. For the present purposes it is convenient to plot log density on log height : or when no insects are caught at one of the heights to use log (density + 1). Though the graph is not strictly linear it is, in general, near enough straight to fit a linear regression whose coefficient b gives a simple measure of the density profile.

A high negative value of b means that the profile is steep and suggests that the mixing processes are relatively weak : a low b value suggests the reverse. These mixing processes are partly biological, partly meteorological, and a simple dependence of b on weather is not to be expected.

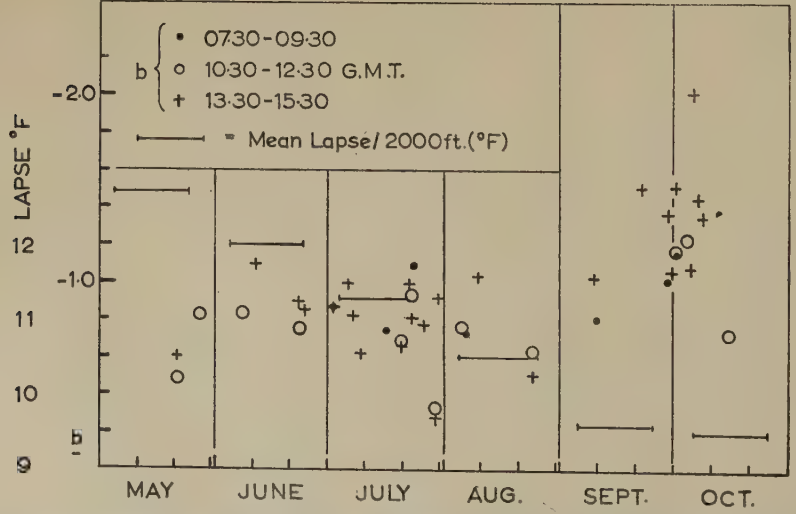

Figure 1. The regression coefficient $-b$ of log (aphid density + 1) on log height from 50 to 2,000 ft for 2-hr periods, May to October 1948 at Cardington, together with mean lapse rates °F/2,000 ft/15 min for the month.

(*a*) *Variation in the density profile during the year in 1948*

There were 151 2-hr periods of trapping in 1948, but only 45 of these have been used here. The remaining 106 occasions were when aphids were caught in small numbers at only one or two heights and the continuous profile could not be measured, or when the temperature record was defective, or when the profile was extremely irregular and could not be expressed by a linear graph. This last situation commonly occurred when densities were very small in the early morning when the profile was building up (sometimes with the addition of small densities of insects apparently remaining in the air from the previous day) or in the evening when the profile was decaying; these irregular profiles need special consideration and are not dealt with here. The present selection therefore is of profiles presumed to be in the quasi-steady state and these account for most of the insects caught in the 151 periods.

Fig. 1 shows values of b throughout the year. High values in September and October indicate relatively high densities at low altitudes and suggest a minimum of mixing (though the rate of production from terrestrial sources also affects this): low b values in the summer suggest the reverse. The mean value of b for September and October is $-1{\cdot}25 \pm 0{\cdot}31$ and for May to August it is $-0{\cdot}78 \pm 0{\cdot}21$ and the difference is statistically significant. The seasonal changes in b and in lapse rate are clearly opposed (Fig. 1) as might be expected if lapse rate is a measure of mixing; but simple correlation of long term means can be misleading.

(*b*) *The vertical distribution in lapse rates above and below the dry adiabatic*

When b for each 2-hr period is plotted against the mean lapse for the period there is much scatter (Fig. 2) but two trends are discernable. For lapse rates smaller than the dry adiabatic, $-b$ increases with lapse rate though the correlation coefficient is not significant. For larger lapse rates $-b$ decreases with increase in lapse rate, and above 10°F/2,000 ft the correlation *is* significant ($r = -0{\cdot}37$, $n = 35$, $P < 0{\cdot}05$). The mean values for b above and below the dry adiabatic are also statistically significantly different (for mean lapse rates of 12·4° and 8·9°F/2,000 ft mean b values were $-0{\cdot}85 \pm 0{\cdot}30$ and $-1{\cdot}05 \pm 0{\cdot}35$ respectively).

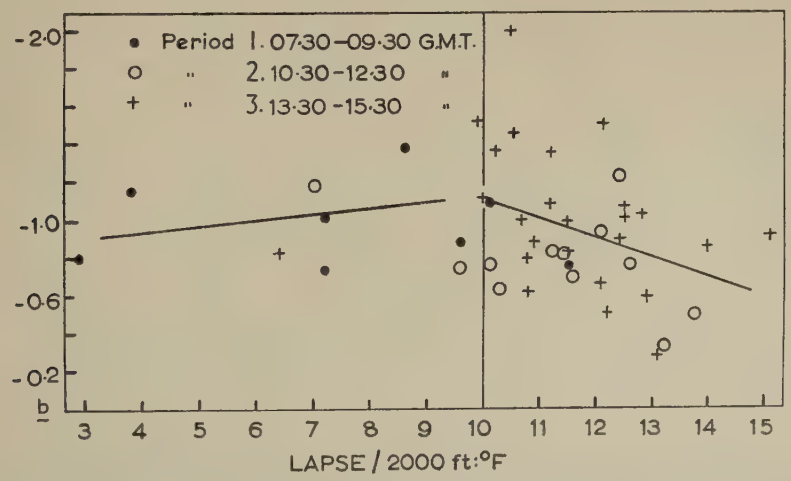

Figure 2. Correlation of $-b$ with lapse rate for 2-hr periods May to October 1948 at Cardington.

Lack of correlation of b with lapse rate below the dry adiabatic is associated with the large proportion of first periods (0730 to 0930 hr) in this range (Fig. 2). As mentioned previously, other factors than atmospheric mixing determine the form of the profile. Later in the day the correlation coefficients are larger and the lapse for later periods is more frequently super-adiabatic. For the third period the correlation is statistically significant ($r = -0{\cdot}46$, $n = 24$, $P < 0{\cdot}02$) provided the single apparently aberrant point for 7 July ($b = -0{\cdot}82$, lapse $= 6{\cdot}4°$, Fig. 2) is omitted from the correlation. On this day the aphid densities and the temperature were both low and little change in a very shallow profile occurred up to 1230 GMT. Evidently the effects of this persisted into the third period in spite of a low lapse rate. The cause of this original condition has not been elucidated.

(c) *Changes in the vertical density profile from hour to hour*

Two examples have been chosen to illustrate more precisely the kind of change in vertical distribution of aphids which may occur during the day. In these, suction traps which break up the catch automatically at hourly intervals were used; 12 in. and 30 in. enclosed cone traps sampling 1,385 and 7,500 ft^3/min respectively were used, the former on a tower up to 56 ft, the latter on the balloon cable (Johnson and Taylor, 1955a and 1955b). All densities in Figs. 3 to 5 are from hourly catches.

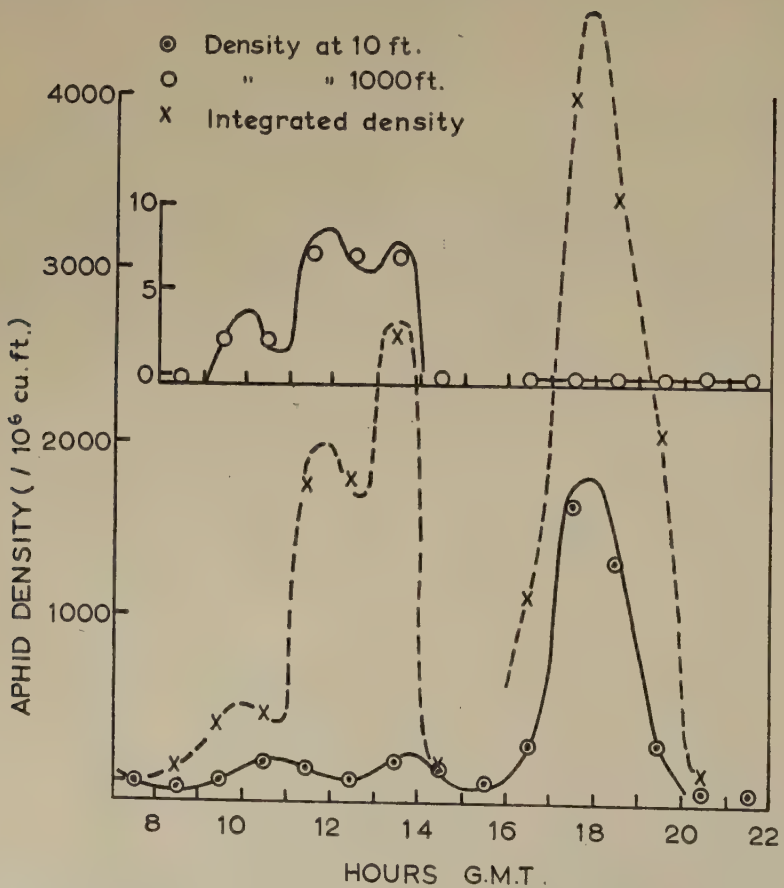

Figure 3. Hourly aphid densities (/10^6 ft^3) at 10 and 1,000 ft with integrated profiles for 8 August 1955, at Cardington. The scale on the ordinate should be multiplied by 20 for integrated values which represent numbers in the air over an area $10^3 \times 10^3$ ft^2: the profiles were extrapolated for integration to 1600, 3700 and 10,000 ft for the periods 0900 to 1000; 1100 to 1300; 1300 to 1500 hr GMT (other times, see Fig. 4).

There are frequently two main waves of aphid aerial density during the day, particularly at the breeding site. These are principally due to the changing rate at which aphids leave such a site. On 8 August 1955 these two waves were well marked and showed especially in the integrated gradient expressing total numbers in the air at all heights (Fig. 3).

Aphids in the first wave were well distributed vertically to at least 1,000 ft and the densities measured at 10 ft, were accordingly reduced. By 1400 to 1500 hr the peaks at 10 ft, 1,000 ft and the integrated curve had declined almost to zero. The evidence indicates that the atmosphere was unstable up to about 1500 hr, the surface temperature at Cardington increasing from 59°F at 0900 hr to 69°F at 1400 hr with a dry adiabatic lapse rate to 6,000 ft at 1400 hr (recorded at Crawley). At about 1500 hr however a steady cooling of the atmosphere began, and the atmosphere over the whole trapping range (10 to 1,000 ft) rapidly cleared of the aphids in the first wave.

The second wave began at about 1530 hr, reached its maximum density by about 1730 hr, and declined almost to zero by 2030 hr. This second wave coincided with the establishment of a stable atmosphere (wind speed at 135 ft decreasing from 12 to 4 mi hr^{-1} between 1700 and 1830 hr) and an inversion developing from the ground from about 1600 hr. The second wave of aphids, greater in total numbers than the first wave, was confined to a much shallower layer of air, for no aphids were detected at 1,000 ft (i.e., density was less than 1/450,000 ft^3) although some were caught at 250 ft (see profiles in Fig. 4).

It is not easy to assess the role of atmospheric stability in the first spectacular decline in aerial numbers at 1400 to 1500 hr and later after about 1800 hr. Although the densities in the air began to decline at about the very beginning of the stable period, it is doubtful if the loss of aphids from the higher altitudes can be attributed solely to the onset of

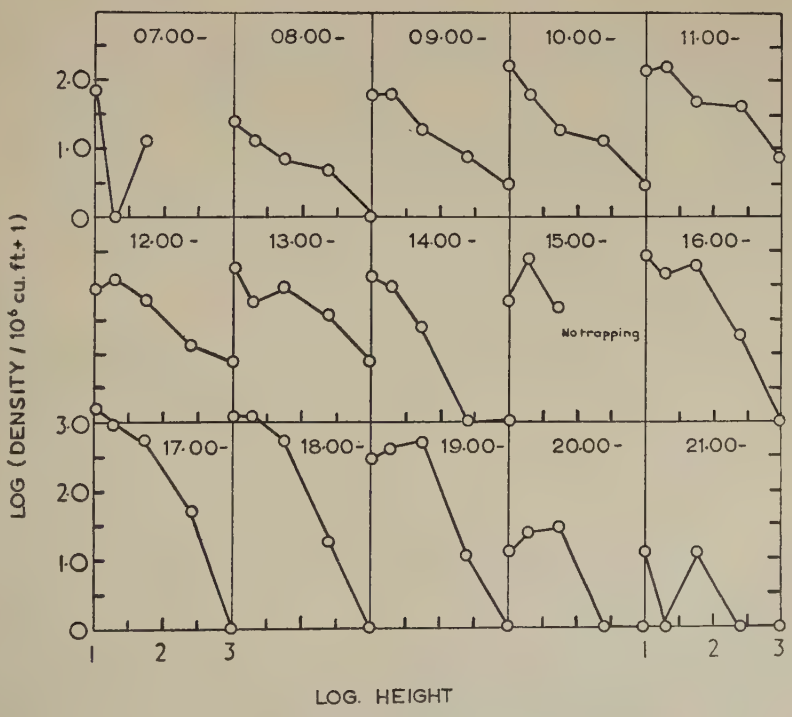

Figure 4. Hourly profiles of log density on log height for 8 August 1955. Traps at 10, 20, 50, 250 and 1,000 ft.

stability, though Rainey's results with locusts suggest that it may at least be a contributary cause. Undoubtedly the insect's capacity for sustained flight also is important and the diminution of numbers taking off at the terrestrial source also plays a part.

That the number of aphids in the air may decrease generally even while some upward transport might be expected is suggested by the example on 8 October 1953 (Fig. 5). The first wave of aphids at 10 ft began at 0400 hr, reached a maximum at about 0630 hr and then declined. Only after this decline had begun were any aphids caught at 500 ft (0730 hr) where the wave reached its maximum at about 0900 hr. The air during this period was cool with little buoyancy (surface temperature 49°F until about 0830 hr wind 2 mi hr^{-1} and 3 mi hr^{-1} at 135 and 1,000 ft respectively and a lapse rate of 1·8°F/1,000 ft at 0745 hr). After this (1000 hr) aphid densities at all altitudes had reached a minimum although buoyancy tended to increase.

The second wave of aphids at 10 ft began at about 1000 hr and the density reached a maximum at 1200 hr. The insects were carried up to at least 500 ft without delay, for at this time the air was becoming more buoyant, the lapse rate increasing to the dry adiabatic (5·2°F/1,000 ft at 1200 hr and wind-speeds 2 mi hr^{-1} and 5 mi hr^{-1} at 135 and

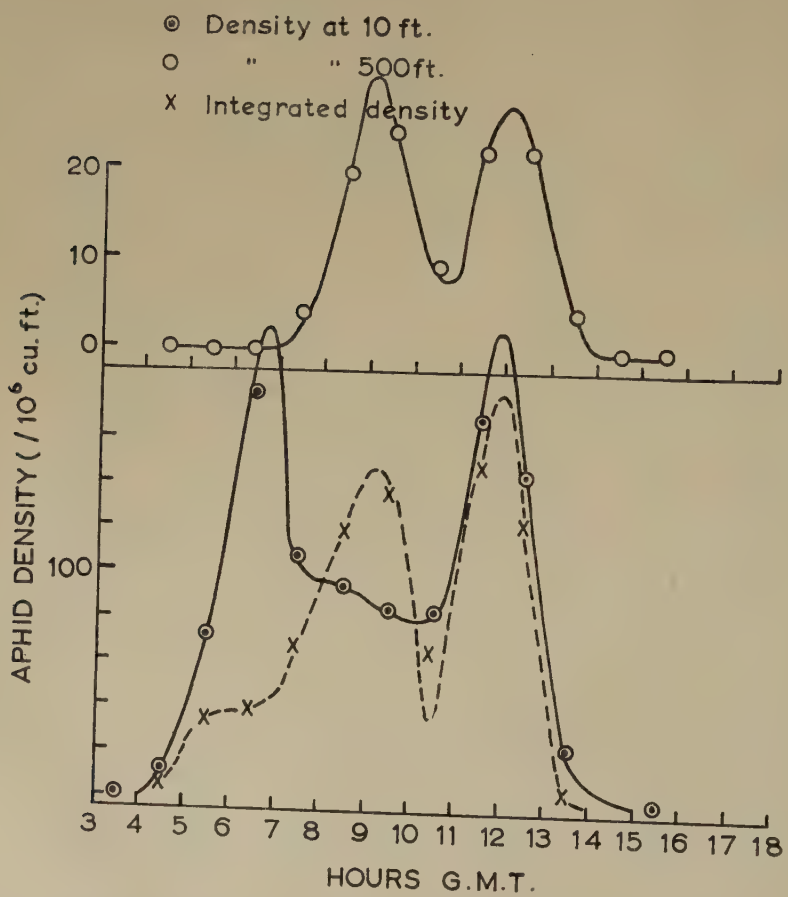

Figure 5. Hourly aphid densities (/10^6 ft^3) at 10 and 500 ft with integrated profiles for 8 October 1953. The scale on the ordinate should be multiplied by 250 for integrated values. The profile was extrapolated for integration to 1,000 ft between 0700 and 1300 hr GMT: extrapolation and integration to 4,000 ft gave a similar curve. It is doubtful if insects reached heights much beyond 4,000 ft for there was an inversion of 10° between 4,000 and 4,250 ft from 0800 to 1200 hr.

,000 ft respectively, surface temperature 55·9°F). After 1500 hr the general decline n density coincided with a lapse rate decreasing below the dry adiabatic and with a diminishing supply of aphids from terrestrial sources.

Thus about a 2½ hr difference exists between the times of maximum density at 10 and 500 ft in the first wave : this coincides with a lack of buoyancy. In the second wave the immediate transfer of aphids from 10 to 500 ft coincides with increased buoyancy.

It is tempting to suppose that the first wave showed a delay in upward transport associated with weak turbulence as contrasted with convective activity during the second wave. While this idea may be true it remains speculative for the biological facts may not support it.

It must be emphasized that each successive point on the aphid-density graph probably represents a new flush of insects from a terrestrial source (Johnson 1954). Their flight was probably of a relatively short duration, for the surface temperature at the time (49°F) is almost the threshold for active flight and it is highly doubtful if the individual insects sustained a flight of 2½ hr; the very low densities also suggest this. It seems more than likely that the first wave at 10 ft subsided before 0730 hr and that the populations at 500 ft were derived from other insects flying at 10 ft at about 0800 to 1100 hr.

Thus although Fig. 5 suggests a *delay* in upward transport it is questionable if this actually occurred : also the shape of the integrated curve does not suggest a delay. Such points may be settled when these data, and many other similar sets now available, are analysed for individual species.

These two examples show other points which are of interest mainly to entomologists. The shape of the characteristic double peak of aphid density seen at the lowest altitudes near surface sources may be greatly modified by atmospheric stability. The sudden appearance of swarms at low altitudes may be causally associated with the onset of atmospheric stability together with increased take-off rates; it is common to see aphid swarms only in still air, notably in the evening calm, though it cannot yet be stated how much of this is due to descent or to the failure of insects to rise in the air. The rapid clearance of the upper air as stability increases suggests that the average duration of flight of individual aphids may be comparatively short : that is, well within the cycle of a single wave and perhaps of the order of 2 to 3 hr. One can visualize a continuous descent of individuals which would be masked as long as the supply from the ground and upward transport continued, but the onset of stability and diminution of supply at terrestrial sources would leave only the factor of descent and lead to a swift clearing of the air.

Acknowledgments

I wish to thank the staff of the Research and Development Establishment, Cardington, Mr. R. H. Pedlow of the Meteorological Office, and Dr. H. L. Penman and Mr. L. R. Taylor of Rothamsted for help received.

References

Johnson, C. G. 1950 ' The comparison of suction trap, sticky trap and tow-net for the quantitative sampling of small airborne insects,' *Ann. appl. Biol.*, **37**, pp. 268-85.

1954 ' Aphid migration in relation to weather,' *Biol. Revs.*, **29**, pp. 87-118.

Johnson, C. G. and Taylor, L. R. 1955a ' The measurement of insect density in the air,' *Lab. Practice*, **4**, pp. 187-92 and pp. 235-9.

1955b ' The development of large suction traps for airborne insects,' *Ann. appl. Biol.*, **43**, pp. 51-61.

551.508 : 551.58

Instruments for micro-meteorology

By I. F. LONG
Rothamsted Experimental Station, Harpenden, Herts.

(Manuscript received 8 November 1956, in revised form 7 January 1957)

SUMMARY

Several instruments suitable for long-term recording of temperature, humidity and wind gradients among growing crops have been constructed. Practical details are given of the use of thermistors and miniature nickel resistance thermometers as wet- and dry-bulb psychrometers, and of the use of these units for direct recording of both dew point and dew-point gradient. Modifications of the sensitive cup anemometer, appropriate circuits and details of a ' hot-bulb ' anemometer using a resistance thermometer, are described.

1. INTRODUCTION

In the course of work on the measurement of the physical environment of growing plants it has been necessary to modify standard equipment or make special equipment for use in small spaces. Many of the innovations have been obvious, and most of them have been simple, but requests for information about them have been sufficiently numerous to justify the setting out of a brief permanent record of what has been done.

The primary interest has been in finding out what is the ' weather ' experienced by plant pathogens, and the dominant problem the humidity balance of a potato crop and the effect that it has in the development of fungus disease.

2. PORTABLE THERMISTOR BRIDGE (PENMAN AND LONG 1949)

With a full description available it is sufficient to note here that Standard Telephones Type F thermistors were used as wet- and dry-bulb resistance thermometers, with the sensitive element enclosed in a metal cylinder 18 mm long and 4 mm diameter, to provide thermal damping of response. A Type L thermistor, with its glass sheath removed, was used as a ' hot-bulb ' anemometer with an effective range of 0 to 4 mi hr^{-1}. A comment on its stability appears in the next sections: here two general points are noteworthy.

(*a*) *The thermometers*

The bulk of the effective sensing element increased the need for screening against radiation and as forced ventilation was undesirable because it would disturb the conditions to be measured, a compromise had to be accepted between adequate exposure to the air and adequate screening from sources of radiation. A hemicylinder of copper gauze 4 cm long and 1·5 cm radius was, and is, used, the screen and the rest of the instrument being painted white. Calibration in full sunlight against an Assmann psychrometer showed that the shield was adequate except when a low sun shone into the end of the unit, or when ventilation was below 1 m/sec. Under conditions of low ventilation and full sunlight, the dry-bulb temperature may rise to a maximum of 0·1°C above ambient temperature, but the corresponding rise of the wet-bulb temperature is only 0·05°C, with the result that the derived dew-point temperature is almost unaffected. The addition of an antiradiation screen below the thermometers was found to increase, rather than to decrease, the radiation effects in sunlight, and to reduce the ventilation of the system.

Use of this instrument by Penman in very bright sunshine under semi-arid conditions n Australia, and of a similar instrument by Smith (1953) in the West Indies, showed that he shielding was not adequate under these conditions. Smith tried many other forms of shield without finding one that could be trusted in full tropical sunshine. At Rothamsted Belgian worker – M. Michel Frère of I.N.E.A.C. – experimented with a wide variety of shields, and though none was completely satisfactory the first choice was as good as ny under temperate conditions.

(*b*) *The anemometer*

This instrument has proved more reliable in use than was expected. After use by Broadbent (1950) in the field it was used intermittently in a wind tunnel for measuring very low wind speeds during spore dispersal experiments (Gregory 1951). Seven years after being built it was recalibrated in a wind tunnel at Imperial College, London, and its response was unchanged.

3. Continuous recording of wet- and dry-bulb temperatures

(*a*) *Phase 1. Thermistors*

Biological interest shifted from daytime spot readings to obtaining night and early morning records at times that could not be predicted in advance. Continuous recording was needed. The recorder available (a twelve-point Kent Multelec resistance recorder) had a designed range of 50°C for a change in thermometer resistance of 18 ohms in about 86 ohms. The thermistor units had a resistance of about 5,000 ohms at 0°C, about 2,000 ohms at 20°C and 700 ohms at 50°C. To use them it was necessary to reduce the sensitivity greatly, and to straighten out the response curve. In simple theory the latter cannot be achieved : in practice it was closely approximated by an arrangement of series-parallel resistors. A resistor, R_s, is put in series with the thermistor and another, R_p, in parallel with the combination. Values are :

$$R_p = \left(\frac{R\,(r_t + r)\,(r_0 + r)}{r_0 - r_t}\right)^{\frac{1}{2}} \simeq 206 \text{ ohms}$$

and $R_s = r - R_p \simeq 794$ ohms

where R_p = parallel resistor

R_s = series resistor

R = 18 ohms for Multelec recorder with 50°C range

r = 1,000 ohms for thermistor type F. 2311/300

r_0 = resistance of thermistor at 0°C

r_t = resistance of thermistor at 50°C.

When building such thermistor units it is important to note that the resistance of the field leads to the thermistor is included in resistance R_s, and that the resistors R_p and R_s must be correct to within 0·1 per cent. When using thermistors it is not necessary to employ temperature compensation for field leads of less than 200 yd since the temperature coefficient of the leads is negligible compared with that of the thermistor. The negative temperature coefficient is easily allowed for by shifting the recorder zero and placing the thermistor unit, with its resistance network, in the arm of the bridge circuit opposite to the normal one. Since the thermistor unit has about twice the overall resistance for which the recorder was designed, increased sensitivity of the recorder null mechanism is required, and this can be achieved by a standard sensitivity adjustment in the recorder.

Unit assembly, size and shape were standardized in this phase : such new information as is needed is given in the paragraph below. The equipment was used during two summers (Hirst, Long and Penman 1954) in and above a potato crop, and it is estimated that mean air temperatures were correct to 1/20°C and derived dew-point temperatures were corrected to 1/10°C. Each thermistor unit was individually calibrated and any slight variation from linearity, never more than 0·2°C, corrected during analysis of the records. Frequent checks were made with an Assmann psychrometer, and were absolutely essential because the thermistors were not stable in continuous use. Fortunately nearly all the changes detected were large and abrupt, being clearly seen on the printed record. The instability of the thermistors, however, made analysis of the records a laborious task, and it was decided to change to nickel resistance thermometers.

(*b*) *Phase 2. Nickel resistance thermometers*

In the absence of suitable commercial instruments nickel-wire elements were wound to match the recording instrument and with the same external geometry as the thermistor elements. Enamelled nickel wire (45 s.w.g.) was non-inductively wound on a perspex bobbin (max. diameter 3 mm, core diameter 1 mm, length 10 mm) mounted in the end of quill tubing (3 mm diameter, 65 mm long) through which connecting copper leads were brought to the pins on a standard octal valve base (Fig. 1). Over the bobbin and part of the glass was fitted a brass sheath 18 mm long, 4 mm external diameter, the cavity being filled with Ceemar embedding resin FR264, which gave on setting a water-tight seal that has withstood up to two months' continuous immersion in water during calibration and other testing operations. Mounted in pairs, with standard antiradiation screen, and painted white, the nickel units were visually indistinguishable from the thermistor units it is presumed that response characteristics dependent on external geometry will be the same. All calibrations have been made with the units connected to the recorder by the cable to be used in the field, a three-wire system giving a compensation lead.

The temperature coefficient of resistivity of nickel increases with temperature, but over a small range of temperature a near linear relationship of temperature and resistance may be assumed for practical purposes. If the average temperature coefficient over the range 0 to 30°C is used, the errors of temperature are given in Table 1. Over a period of three years no changes in the nickel thermometer characteristics (0·36 ohm/°C; resistance at 0°C = 68 ohms) have been detected.

TABLE 1. Error of nickel thermometer elements

Actual temperature °C	Indicated temperature error °C
30	− 0·1
25	− 0·05
20	0·0
15	0·0
10	0·0
5	− 0·1
0	− 0·2

Tests in still air (wind < 5 cm/sec) showed that the time-lag constants, λ, the time required for difference in temperature between the thermometer and its surroundings to fall to 1/e of its initial value (Spilhaus 1936) were :

as a dry-bulb thermometer, $\lambda = 90$ sec.

as a wet-bulb thermometer, $\lambda = 70$ sec.

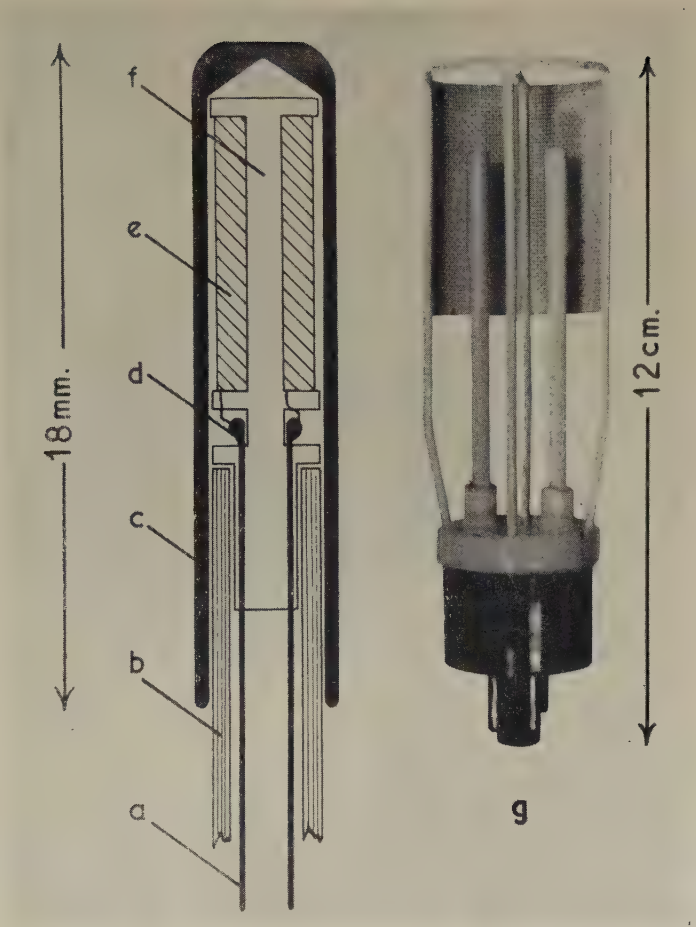

Figure 1. Construction of standard nickel-thermometer unit. (a) Copper leads. (b) Glass tube. (c) Brass sheath. (d) Soldered joint. (e) Nickel wire coil. (f) Perspex bobbin. (g) Standard psychrometer unit.

(i) *Soil thermometers*

A similar set of elements has been made with the same sensing unit but mounted on the end of a pliable polythene tube (100 cm long) instead of a glass tube, for ease of insertion into holes bored in the exposed face of a pit dug into the soil. Eleven such units are being used to give a continuous record of soil temperatures in the top 2 ft of soil.

(ii) *Leaf thermometers*

Miniature units have been constructed for experiment. With some difficulty it has been possible to wind 50 s.w.g. enamelled nickel wire on a copper former (38 s.w.g.), and to machine a metal sheath so that the external dimensions of the sensing element are 0·8 mm diameter and 5 mm long. As in the larger units, the nickel resistance coil was embedded in a thermal setting resin within the metal sheath. The units are small enough to be inserted in the thicker part of a potato leaf after making a hole with a number 18 hypodermic needle. One of these elements is being used as a ' surface ' thermometer in the soil observations.

The sensitivity of these thermometers is the same as that of the larger units. Tests in still air gave a time-lag constant λ of 9 sec.

4. Humidity

(a) *Standard assembly of nickel units as wet- and dry-bulb thermometers*

The unit is mounted horizontally : the elements, necessarily parallel, are about 1·5 cm apart. The line is north-south so that low morning or evening sun does not shine directly on the elements. One element has a close-fitting muslin sleeve 22 mm long (i.e. covering all the metal sheath and a little of the glass) from the underside of which four threads of cotton wick lead to a reservoir mounted alongside. This is J-shaped, the longer, fatter arm being closed at the top and having a capacity of about 12 cm^3 water – at least enough for one day's supply in dry summer weather. The threads are long enough to pass right round the bend (an essential condition for maintained flow) and experience indicates that the exposed length between the open short end of the reservoir and the muslin should be constant. The standard length used is 5 mm.

The unit is plugged into a socket mounted in a resin-filled cylindrical base forming the field termination of the cable. The joint is filled with ' Henley Plastic Compound ' and is not broken except when there is need for replacement of the unit. The cylindrical base has on one side a clip for attachment to a vertical post, and on its other side another clip to hold the water reservoir for the wet bulb.

In the field, behaviour has been encouraging. On damp nights the two traces merge into one with less than 0·02°C difference between them, (this is about the smallest difference measurable on the chart) when there is good reason to regard the air as saturated. At other humidities spot checks with an Assmann psychrometer have confirmed that the laboratory calibrations can be trusted to yield derived dew-point temperatures to within 0·1°C. A laboratory determination of the psychrometric constant at different wind velocities yielded the data of Fig. 2, and has been used where needed.

To speed psychrometric analysis a transparent scale has been devised (Long 1956) by which relative humidity and vapour pressure can be read directly from the charts. In the absence of suitable tables for mb and °C a complete set has been computed for all the important humidity parameters over a wide range of temperatures. A copy has been deposited in the Meteorological Office library at Harrow.

Six pairs of elements are in use in and above a potato crop, and another set in and above a wheat crop; both sets have given satisfactory service during a period of three years.

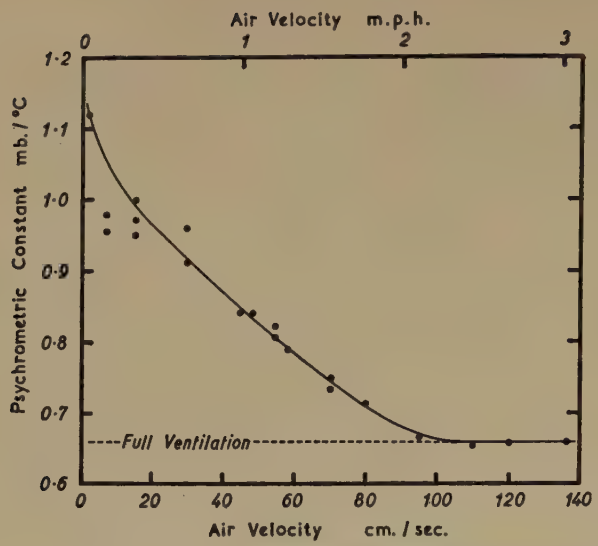

Figure 2. Psychrometric constant of standard nickel-thermometer unit at low air flow.

(*b*) *Non-standard units : humidity gradient*

For temperatures around 10°C and humidities not too far from saturation the wet-bulb temperature is approximately mid-way between the air temperature and the dew-point temperature : or, in self-evident symbols

$$Tw \simeq \tfrac{1}{2}(Ta + Td)$$
$$Td \simeq 2\,Tw - Ta.$$

Thermometers have been wound with twice the standard length of nickel wire (within the same external sheath dimensions) and used as wet-bulbs on one side of the bridge circuit of the recorder with a standard dry-bulb element and a fixed resistor in the other, so reading an approximate *Td* direct on the chart. This gives a picture, admittedly somewhat crude, of the daily trend of absolute humidity at the observation level. A pair of such units, at two levels, wired in the bridge circuit so that their deflections are in opposition, gives a much more accurate measure of humidity gradient, showing at a glance (from a fixed reference line on the chart) the direction of vapour transfer at any time of day. If the two levels are 1 and 2, the recorder deflection on the chart is measuring $Td_1 - Td_2$ where :

$$Td_1 - Td_2 = (2\,Tw_1 + Ta_2) - (2\,Tw_2 + Ta_1).$$

The overall sensitivity is such that $\Delta\,Td$ over 50 cm height interval can be measured with ease to 0·1°C, and the sign can be detected to better than 0·05°C. The error at about 75 per cent relative humidity is that $\Delta\,Td$ is underestimated by about 10 per cent : at 95 per cent humidity and above, when the device is needed for studies of incidence and ending of condensation the error is < 2 per cent underestimate in $\Delta\,Td$. The change of wind speed with height introduces a smaller error of opposite sign when wind speed is < 100 cm/sec.

The above estimates of error, in underestimate of $\Delta\,Td$, are for the range 5°C to 15°C, and a gradient of 10°C in *Ta* over a height interval of 50 cm has been assumed; this would be an extreme case. In practice the gradients are very much smaller and therefore the errors in $\Delta\,Td$ are much less.

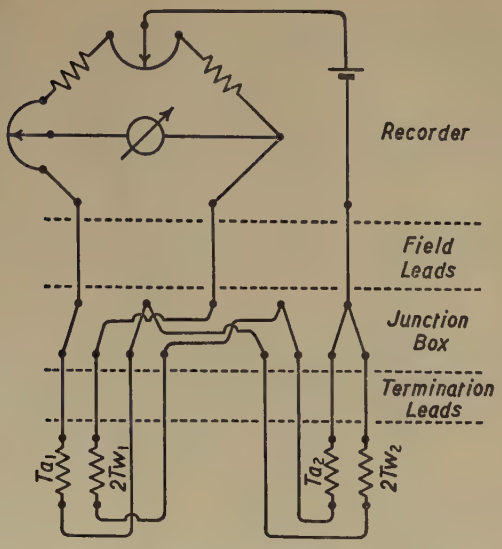

Figure 3. Dew-point gradient recorder circuit.

A practical wiring diagram of the $\Delta\ Td$ recorder showing the method of lead compensation between the units at two levels and the units to recorder is shown in Fig. 3. The $\Delta\ Td$ recorder has been in use for two summers in a potato crop at Rothamsted, two 50-cm interval gradients being measured : one from above the crop to crop surface, and the other from crop surface to the crop interior. On the same recorder chart the soil temperature at 10 cm depth, the soil surface temperature, the leaf temperature at crop level and leaf temperature within the crop are continuously recorded. These data together with the standard wet- and dry-bulb records enable the time of onset and finish of dew deposition to be determined direct from the charts to within 5 min, the times agreeing with those obtained from two mechanical ' dew balances ' (Hirst 1954, Jennings and Monteith 1954) both of which were installed in the crop.

Apart from the simplicity of installation and its negligible effect on the local environment the $\Delta\ Td$ recorder has several advantages :

(i) Periods of dew can be determined without analysis of the recorded data, the characteristic traces standing out clearly, so that periods of short duration are not obscured (periods of dew lasting only 10 min have been recorded).

(ii) Periods of extremely light dew (which may not be recorded on a mechanical type dew-balance) are clearly recorded.

(iii) Recording of the two gradients gives an approximate indication of the relative magnitudes of dewfall from above the crop and dew formed by distillation from the ground.

(iv) A rough estimate of the intensity of the dewfall or its total amount may be determined. (Air-flow gradients necessary for this estimation are recorded on a separate instrument).

(v) The conditions for dew formation are clearly recorded and are not obscured by events which may have preceded or followed it, as in the case of deposition before or after rain, or deposition on a surface already wetted.

(vi) Physiological phenomena, such as guttation, which may be mistaken by an observer for dew, will not be recorded.

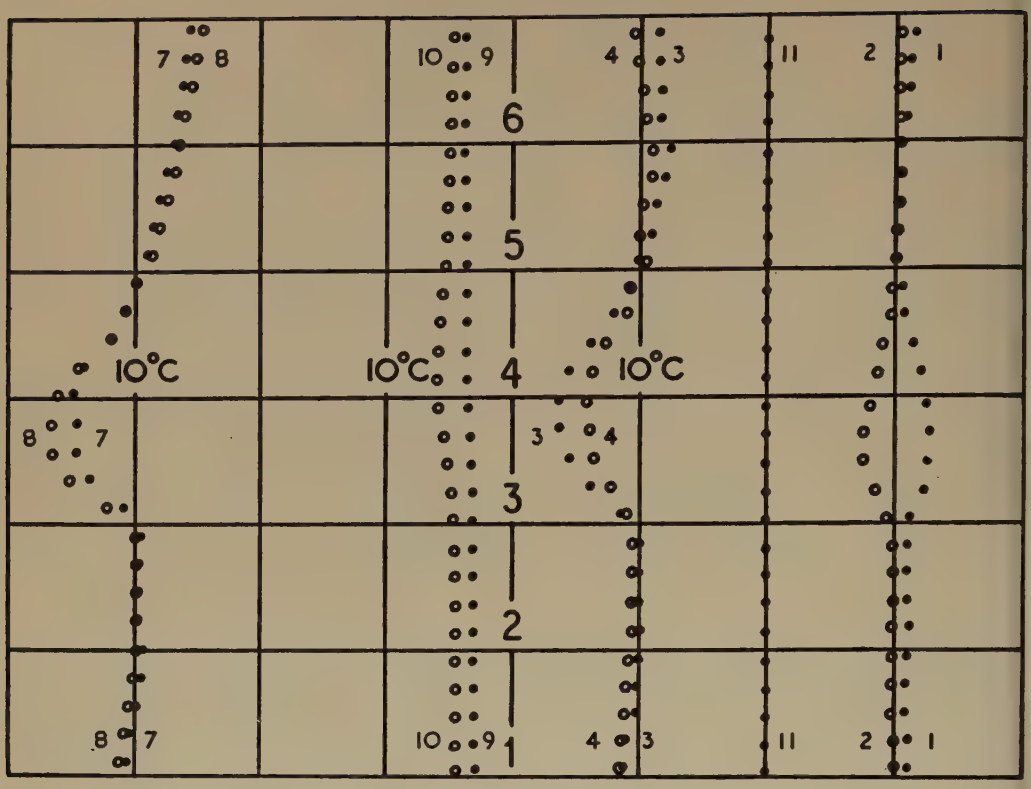

Figure 4. Tracing of record from Δ *Td* recorder. Alternate points are omitted.

A tracing of a typical record of dew obtained from the Δ *Td* recorder, when placed in a potato crop at Rothamsted during the night of 31 July to August 1 1956, is reproduced in Fig. 4. One division on the chart equals 5°C, the three pairs of traces to the left of the chart being displaced from each other by 10°C as indicated on the figure. The numbers are for identification of the trace, and reading from left to right the traces represent :

7. Leaf temperature, interior of crop.
8. Leaf temperature, upper surface of crop.
9. Soil temperature at 10 cm depth.
10. Soil surface temperature.
3. Dew-point temperature 10 cm below crop surface.
4. Dew-point temperature 40 cm above crop surface.
11. A reference trace to check the recorder.
1. *Td* gradient from crop interior to crop surface (50 cm).
2. *Td* gradient from crop surface to upper air (50 cm).

Traces 1 and 2 have a positive gradient to the right (i.e., water vapour in transit from lower to upper level), and a negative gradient to the left.

The night, part of which is here recorded, was mainly overcast with the exception of a short period lasting just over 1 hr from 03 hr, when a gap in the clouds resulted in an increase of outgoing radiation. A separate recorder showed that the relative humidity

at 2 m rose in 20 min from 94-97 per cent, at 1 m from 95-98 per cent and at crop level from 96-100 per cent in 10 min. Average air-flow during the period was 73 cm/sec at 2 m, 30 cm/sec at 1 m and < 20 cm/sec in the crop.

Traces 1 and 2 show the sudden change in the vapour pressure gradients and clearly indicate that conditions suitable for dew formation existed between 03 hr and 0430 hr. The leaf temperature, 8, and dew-point temperature, 3, indicate that dew was formed on the upper leaf surfaces from about 03 hr to 04 hr. Some drop in temperature at the soil surface also took place although there was an almost complete foliage cover.

(c) *The resistance recorder*

The resistance thermometer systems described have all been designed to work into a linear resistance recorder of the double-slide-wire bridge type; non-linear recorders of the out-of-balance-current type being unsuitable. The recorder used was a Kent Multelec Mark II, twelve-point Wheatstone bridge temperature recorder (3-wire type), in which the following modifications were carried out.

(i) To decrease the current through the resistance thermometers, (to avoid self-heating) the voltage applied to the bridge network was reduced by increasing the value of the resistance in series with the bridge voltage power supply; the values being chosen to suit the particular thermometer system in use.

(ii) Reduction of the bridge voltage supply necessitated an increase in the sensitivity of the recorder galvanometer and mechanical null system. This was achieved by replacing the existing 20 ohm galvanometer and its suspensions (Kent, 3·5 yellow) by an 80 ohm coil and lighter suspensions (Kent 3·0 green). Appropriate changes of the galvanometer damping resistances were also made. Provision for increase in sensitivity of the mechanical null system is incorporated in the recorder.

With these two modifications the maximum power dissipated in the nickel wire thermometers is 1·3 mW and in the thermistor units 0·65 mW. Laboratory experiments in still air gave no detectable rise of temperature from self-heating of the thermometers.

5. Wind

(a) *Large cup anemometers*

To give a continuous record of run-of-the-wind from cup anemometers, step-by-step motors have been built (largely from Meccano parts). The first two of these (Long 1951) were used with switch type anemometers (M.O., Mark III), full-scale deflection on a weekly chart 3 in. wide corresponding to a run of 50 mi of wind. There are two records per instrument, and two of these instruments have been in continuous use for six years with the cups of the anemometers at 6, 20, 40 and 80 ft above the ground.

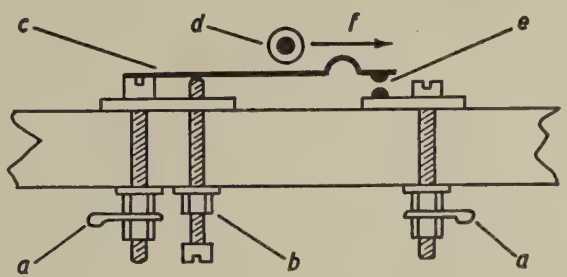

Figure 5. Switch mechanism for modified anemometer. (a) Soldering tag. (b) Locknut. (c) Shim brass strip. (d) Anemometer arm. (e) Platinum contacts. (f) Direction of motion of anemometer arm.

(b) *Small cup anemometers*

The sensitive cup anemometer (Sheppard pattern) carrying a pointer has been modified to work into a similar kind of recorder. (When used for this purpose it is necessary to lock the free-wheel clutch of the anemometer reduction-gear system). The ordinary pointer is removed and replaced by a four-arm unit made of two crossed pieces of non-annealed copper wire (20 s.w.g.), the ends of each arm being covered with fine glass tubing for electrical insulation and to reduce friction. The glass window of the anemometer is removed and replaced by a piece of perspex of the same dimensions. On this perspex, at zero on the dial, is mounted a light contact made from a strip of shim brass (20 mm long, 2 mm wide and 0·002 in. thick) on the end of which is fitted a platinum contact, the strip being soldered on to the head of a 10 B.A. brass screw bolted to the perspex face. Beneath this strip and bolted to the perspex is another platinum contact mounted on a small rigid brass strip; clearance between the contacts being effected by the use of an adjustable screw with lock-nut (Fig. 5). For protection against the weather, the switch mechanism and face of the anemometer is enclosed in a clip-on water-tight cover with transparent window. As the anemometer arm sweeps by, it presses the light contact down on the other, and the making of this contact actuates the impulse motor of the step-by-step recorder. The 100 impulses for full-scale deflection (25 complete revolutions of the pointer) represent a run-of-the-wind of approximately 4 mi : a daily chart is used and, when needed, average wind speeds over a period of 15 min can be estimated to within 2 cm/sec (for speeds above 30 cm/sec).

Precautions have been taken against contact trouble. To keep the retarding action on the rotating arms within a negligible amount the pressure must be very light, and it is necessary to ensure that the system will work for a very high resistance contact. Further, it must give only one impulse if the contact chatters, and it must not give more than one impulse in the event of the contact remaining closed during a calm. The pulse discriminator and lengthening circuit of Fig. 6 satisfied these conditions.

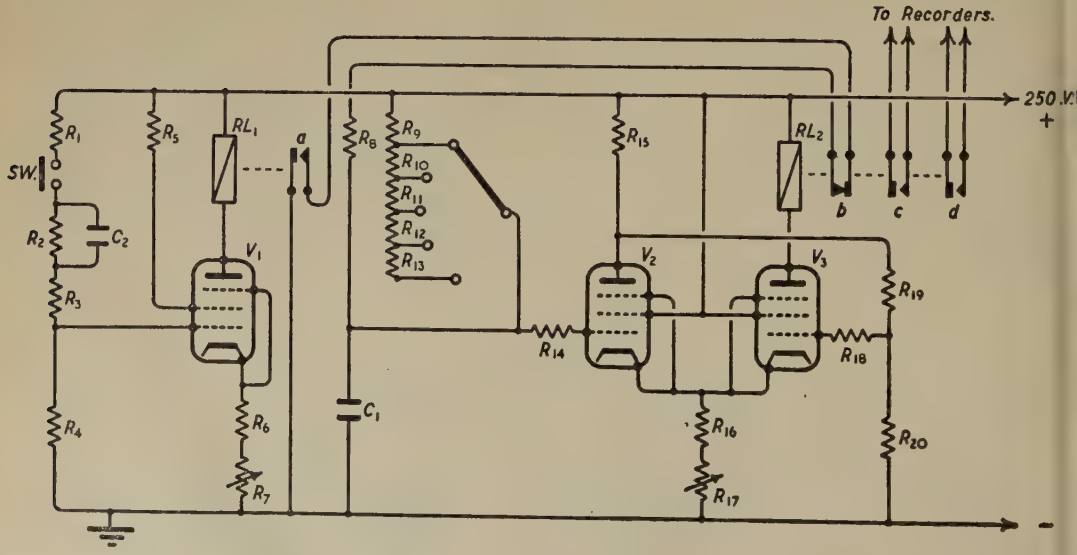

Figure 6. Pulse discriminator and lengthening circuit. Circuit values: R_1, 56 KΩ. R_2, 50 MΩ. $R_{3,4}$, 2·2 MΩ. R_5, 22 KΩ. R_6, 5 KΩ. $R_{7,17}$, 10 KΩ. R_8, 1 KΩ. $R_{9,10,11,12,13,14,19}$, 1 MΩ. $R_{15,16}$, 10 KΩ. R_{18}, 10 KΩ. R_{20}, 1·5 MΩ. C_1, 1 μF. C_2, 0·002 μF. RL_1, RL_2, 2,000 Ω Type 3,000 G.P.O. V_1, V_2, V_3, EF 50.

(i) In the event of dirty contacts, the unit will act when the short circuit of the input is as high as one megohm. The current through the anemometer contacts never exceeds 50 μA, and when the contacts are continuously closed the current is reduced to < 5 μA.

(ii) When the anemometer contact SW is closed, the side of the condenser C_2 connected via R_3 to the grid of V_1, is momentarily raised for a period determined by the time constant of C_2, R_3, R_4, to about 100 v positive; the relay RL_1 then operates. When the condenser C_2 becomes fully charged, the voltage on the grid of V_1 falls to a value determined by the potentiometer network R_1, R_2, R_3, R_4, and the relay RL_1 then opens.

(iii) If the anemometer contact SW remains closed (in a calm) then the condenser C_2 remains charged and no further action can occur.

(iv) When the contact SW opens then the condenser C_2 will discharge at a rate determined by the resistance R_2; and until it is partly discharged, no further closing of the contact SW will induce sufficient positive voltage to appear on the grid of V_1 to actuate the relay RL_1. With the circuit values given, 3 sec must occur between the opening and closing of the contact SW before the relay RL_1 can again operate (which means that wind speeds up to 50 mi hr^{-1} can be handled).

(v) The time of operation of the relay RL_1, and hence the relay contacts (a), is insufficient in length to operate the impulse motor of the step-by-step recorder. To overcome this difficulty a pulse lengthening circuit comprising V_2 and V_3 has been added. With the values of C_1 and R_{9-13}, settings of 1-5 sec are available; normally the unit is run on a 2 sec impulse length.

(vi) Optimum point of operation of the relay RL_1 is obtained by adjustment of R_7, and calibration of the ' pulse length ' period by adjustment of R_{17}.

(vii) Contacts (c) are for operation of the step-by-step recorder, and contacts (d) are included for operation of a G.P.O. counter so that long-period values of run-of-the-wind can be obtained at chosen intervals.

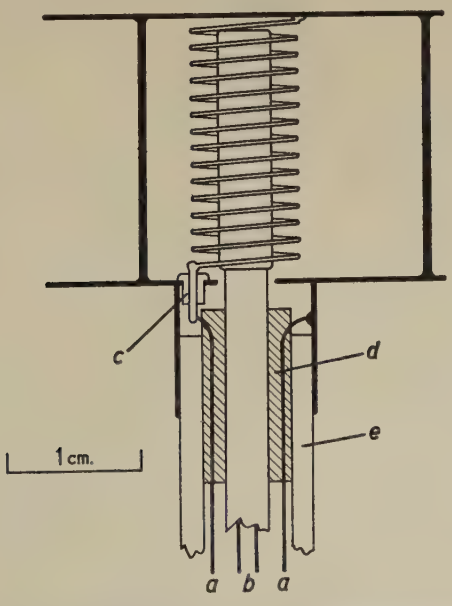

Figure 7. Hot-bulb anemometer. (a) Heater coil leads. (b) Nickel thermometer leads. (c) Perspex bush. (d) Rubber tubing. (e) Tufnol tubing.

(c) *Hot-bulb anemometer*

A slow response, semi-integrating 'hot-bulb' anemometer has been constructed for continuous recording of low air flows at distances up to 100 yd from the experimental site. The anemometer has a useful near-linear range of 5 to 70 cm/sec; below 5 cm/sec self-convection from the heating coil gives spurious results. The anemometer is ideal for recording the low air speeds encountered in crops during light winds, and has been built as an aid in the study of air movement during the still conditions of dew formation.

The instrument consists of two identical thermometer units wound with 45 s.w.g. enamelled nickel wire, having the same dimensions as the standard units but with a copper instead of perspex bobbin and a sensitivity of 0·72 Ω/°C, their resistance at 0°C being about 134 Ω. Around one thermometer is placed a heating coil (8 mm diameter, 18 mm length, 15 turns) of 26 s.w.g. manganin wire, the length of wire having a resistance of 1·3 Ω. The heater coil is suitably supported in an anemometer shield so that the thermometer is central and does not come into contact with the coil. The shield consists of two thin brass discs (diameter 3 cm, and 2 cm apart) which are separated by three copper wire supports (22 s.w.g.). One end of the heating coil is soldered to the upper disc, and the other to a copper wire supported in the lower disc by a perspex bush (Fig. 7). The anemometer shield gives some protection from light rain, keeps the crops from coming into contact with the anemometer, and acts as a return path for the current supply to the heater coil. The other thermometer unit is placed in a standard radiation screen and acts as a partial compensation for changes in ambient temperature.

The two units are placed in opposition in a wheatstone bridge circuit (Fig. 8). The bridge circuit is indicated by the thick lines and the power supply system by the thin lines.

The power supply is obtained from any conventional 24-30 v direct current supply, battery or mains unit. The power dissipated in the anemometer heater coil is kept constant by the use of a barretter valve, B, which maintains the current in the circuit steady at 1·7 a.

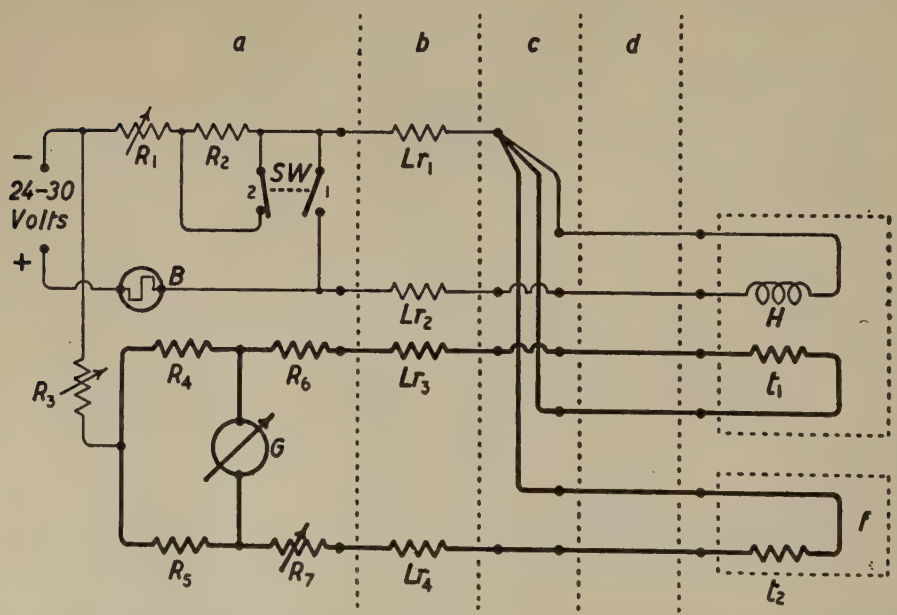

Figure 8. Recording hot-bulb anemometer circuit. (a) Recorder unit. (b) Field leads. (c) Junction box. (d) Termination leads. (e) Hot-bulb anemometer. (f) Ambient temperature-compensation thermometer. Circuit values, R_1, 3 Ω. R_2, see text. R_3, 500 Ω. $R_{4,5}$, 150 Ω. R_6, 5 Ω. R_7, 10 Ω. G, recording galvanometer.

Power supply for the bridge circuit is obtained from the voltage drop across the lead resistance Lr_1 (about 4 Ω for 100 yd of cable) and variable resistance R_1 which is adjustable so that some control over the bridge voltage is available.

To set the anemometer for use the switch SW is first switched to ' Balance cold.' In this position SW_1 is closed and shorts the supply to the heater coil H : SW_2 is open and the resistance R_2 (equal in value to Lr_1) is in circuit. R_2 compensates for loss of bridge supply voltage, since in this position Lr_1 is out of circuit. The bridge is now balanced by the adjustment of the potentiometer, R_7, for zero deflection of the recording galvanometer G (0-1 ma). The anemometer is next shielded against air flow and SW switched to the ' Balance hot ' position. The heater current is now on, the unit heats up and the bridge becomes unbalanced. At equilibrium, the out-of-balance current is set for full scale deflection of the galvanometer, G, by adjustment of the potentiometer R_3. The anemometer is now ready for use.

In an air current the temperature change caused by heat loss tends to bring the bridge circuit back to balance, and therefore to reduce the galvanometer deflection. This reduction in deflection, when suitably calibrated, serves as a measure of the air flow. A series of test runs in a small wind-tunnel at Rothamsted yielded the calibration curve of Fig. 9.

No attempt has as yet been made to find the effect on the calibration of turbulent air flow, but it is assumed that a rough integration of the air flow will be obtained so long as the peak air flow does not exceed 70 cm/sec. A check on the ambient temperature compensation afforded by the thermometer unit has, to date, only been possible over a small temperature range. The anemometer was placed in a steady air flow of 15 cm/sec for a period of 48 hr, during which time the temperature in the wind tunnel varied from 9 to 18°C and the relative humidity from 60 to 98 per cent: no change in the deflection of the galvanometer was detected. The thermal lag coefficient, λ, of the anemometer is slightly greater than that of the standard thermometer units, being about 100 sec in an air-flow of 5 cm/sec.

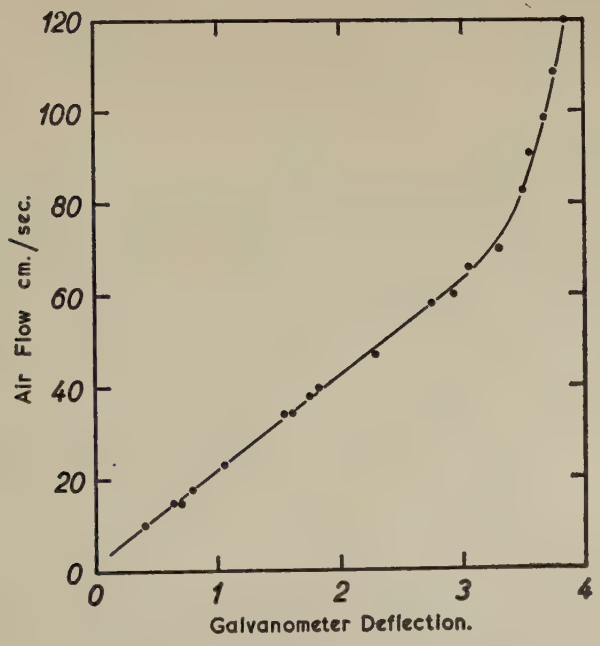

Figure 9. Hot-bulb anemometer calibration.

Acknowledgment

The author wishes to thank Dr. H. L. Penman for guidance, advice and helpful discussion during the course of this work.

References

Broadbent L.	1950	*Quart. J. R. Met. Soc.*, **76**, p. 439.
Gregory, P. H.	1951	*Ann. App. Biol.*, **38**, p. 357.
Hirst, J. M.	1954	*Quart. J. R. Met. Soc.*, **80**, p. 227.
Hirst, J. M., Long, I. F. and Penman, H. L.	1954	*Proc. Toronto Met. Conf. 1953*, p. 233.
Long. I. F.	1951	*Proc. Inst. Elec. Eng.*, **98**, Pt. II, p. 458.
	1956	*J. Sci. Inst.*, **33**, p. 199.
Jennings, E. G. and Monteith, J. L.	1954	*Quart. J. R. Met. Soc.*, **80**, p. 222.
Penman, H. L. and Long, I. F.	1949	*J. Sci. Inst.*, **26**, p. 77.
Smith, G. W.	1953	*Ibid.*, **30**, p. 414.
Spilhaus, A. F.	1936	*Trans. Roy. Soc. S. Africa*, **24**, p. 185.

551.557.5 : 551.513.1 : 608.4

Jet stream and long waves in a steady rotating-dishpan experiment : structure of the circulation

By HERBERT RIEHL and DAVE FULTZ
University of Chicago

(Manuscript received 14 August 1956)

SUMMARY

The three-dimensional structure of the flow of water in a steady rotating three-wave dishpan experiment is computed and compared with the atmosphere.

At first the experiment and methods of comparison between dishpan and atmosphere are described. Then motion and vorticity at the top surface are shown; trajectories leading from equatorial to polar rim of the pan are found. Next the three-dimensional temperature field is determined, and from this the geostrophic motion at all depths.

The flow pattern resembles the basic features of the middle-latitude atmosphere in a remarkable way. Mobile long waves in a jet stream near the top overlie cyclonic and anticyclonic vortices farther down. There is, however, neither the counterpart of tropopause nor stratosphere in the temperature field, indicating that these features are not necessary for development of the basic flow pattern. Further, the distribution of momentum sources and sinks differs from that of the atmosphere, as momentum is given off to the inner (and possibly to the outer) cylinder, while most of the bottom acts as source. This throws doubt on the importance of momentum balance considerations for explanation of the principal flow features.

Vertical motions are calculated in the interior of the fluid with the adiabatic assumption. Values again compare well with those of the atmosphere as does the distribution of centres of ascent and descent relative to long waves and cyclones. A positive correlation between temperature and vertical motion exists along the jet axis, hence there is release of potential energy. If averaging is performed along the jet-stream axis, one finds that the centre of ascent lies equatorward, and the centre of descent poleward of the axis. If *zonal* averaging is performed, however, the centre of ascent appears north of the zonal wind maximum, and the centre of descent on its equatorward side. This calculation uncovers a weakness of zonal averaging as a tool in studying the general circulation.

Absolute vorticity is calculated on constant temperature surfaces in the interior of the liquid. It is found that the theorem of conservation of absolute vorticity is nearly fulfilled in the jet-stream layer with wave motion; in the lower layer with vortices, validity of the theorem of conservation of potential vorticity is indicated qualitatively. The regions of convergence and divergence, as inferred from the vorticity changes along the relative stream-lines, agree qualitatively with the vertical motion distribution.

1. INTRODUCTION

The remarkable similarities noted between the circulations of the upper troposphere and the surface of the water in rotating-dishpan experiments (Fultz 1950, 1952, 1956, Corn and Fultz 1955) have encouraged extension of these experiments to determine the three-dimensional structure of the dishpan circulations. At the present stage of technical development in these experiments this is made possible through the discovery by Hide (1953, 1956) and Fultz (1952, 1956) that when the liquid is contained between two concentric cylinders, the inner of which is a cold source and the outer a heat source, steady-state wave motion may be developed over a range of experimental conditions. In a coordinate system moving at the rate of propagation of the waves the field distribution of motion, temperature, etc., remains unchanged. Because of this steady state one can measure the entire three-dimensional temperature field with only one or two measuring elements which are placed at a number of different locations. ' Thermograph ' traces of the time variation can then be converted to longitude variation.

For a first try a case with three steady long waves was chosen. As shown by Hide (1956) and Fultz *et al.* (1956), the surface-flow pattern for any given pan size, inner cold-source cylinder size, and depth, is determined by the rate of rotation of the pan and the rate of energy supply. In the experiment to be described the pan had a radius of 15·6 cm,

the water depth was 4 cm and the rate of revolution 0·30 sec^{-1}. A heat source with nominal intensity of 150 w was applied at the equatorial rim, and a central cylindrical cold source with radius of 6·5 cm provided for heat balance. Actual heat transport to the cold source was measured at about 64 w; this is probably about 20 per cent too high because of extraneous gains at the cold source. The mean temperature of the water in the pan was about 19·5°C and the temperature of the circulating water in the cold source about 10°C. Given these physical conditions a pattern of three long waves on a continuous jet stream emerges when steady state is attained. Fig. 1 (Plate IV) shows the top-surface flow pattern, made visible by photography of aluminium powder floating at the surface.

The objectives of the investigation were (a) to determine the structure of the circulation in the dishpan and to compare it with the atmosphere; (b) to calculate the heat and momentum budgets; (c) to ascertain, as far as possible, the mechanism governing maintenance of long waves and jet stream, and their role in the general circulation.

This report deals mainly with the first of these objectives.

2. Data

The observations consisted of (a) surface-velocity measurements made from the original of Fig. 1 and (b) temperature measurements made at different radii and depths so that the three-dimensional temperature field could be analysed. Fultz *et al.* (1956) have discussed the details in making these measurements.

The three waves of Fig. 1 are quite symmetrical; thus only one wave need be analysed. Some subordinate microstructure was present, evident especially along the equatorial margin of the pan. This microstructure, an unsteady part of the flow, was eliminated by averaging velocity and temperature fields over all three waves.

Some of the features of the flow encountered during the analysis were subsequently checked and verified at least qualitatively by repeating the experiment.

3. Comparison of dishpan and atmosphere

If circulations on bodies of such different size as dishpan and earth are to be compared successfully, the variables must be properly selected. Rossby (1947) accomplished this for the motion variables when he found from data on earth and sun that the equatorial velocity of a rotating body provides a pertinent reference velocity, in terms of which other velocities may be expressed. One may think of relative velocities, for example, expressed non-dimensionally as ratios to this reference speed or, what is equivalent, expressed with the equatorial velocity as the unit.

Different types of experiment have amply verified the validity of Rossby's deduction. Given the relative wind u, the angular rotation ω and the radius r_0 of any rotating system, the ratio $R = u/r_0\,\omega$ expresses the wind speed as a fraction of the equatorial velocity $C_e = r_0\,\omega$. This method of representing the wind is one of a number of more or less equivalent choices of similarity variables; it is particularly convenient for practical reasons. Fultz (1951) and others have called R the ' Rossby number ' when u is a representative relative velocity. If we express $R = \dfrac{u}{r_0\,\omega} = \dfrac{u^2}{r_0\,u\omega} = \dfrac{u^2}{r_0}\Big/u\omega$, we see that R is also a measure of the ' convective ' acceleration as a fraction of the Coriolis acceleration. This is the really significant aspect for dynamic similarity of the experiments to the atmosphere since it expresses one of the most important typical force ratios involved, i.e., of inertia forces to Coriolis forces. The interpretation of u^2/r_0 holds as long as r_0 is of the order of a typical wave length or other typical horizontal scale for the motion (Charney 1948, Fultz and Frenzen 1955).

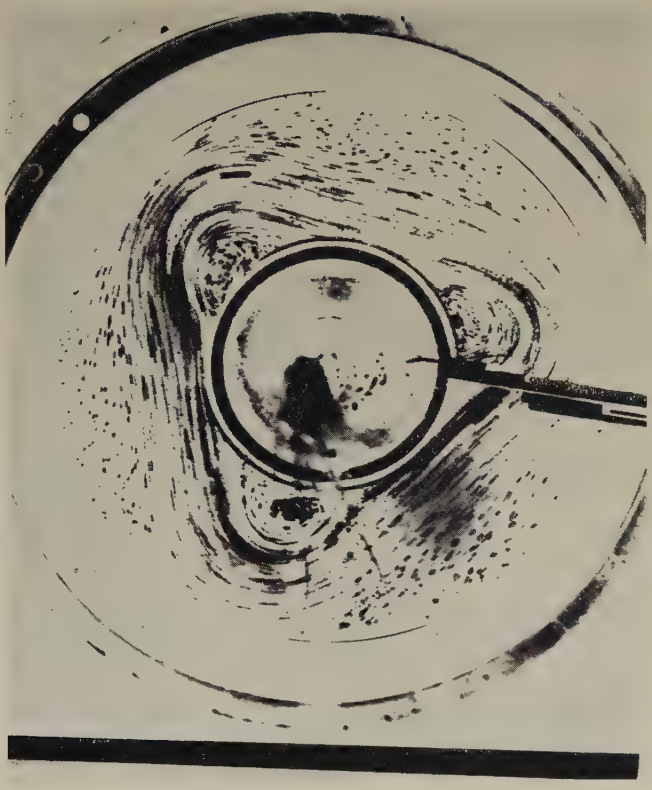

Figure 1. Photograph of top-surface flow.

The smaller R, the more nearly geostrophic will be the flow. In the present case, the highest value of R is 0·2. Hence the motion to be treated is quasi-geostrophic, though 0·2 is attained over relative areas considerably larger than in the high troposphere. Consequently the experimental system is somewhat more ageostrophic than the atmosphere. We may note here that the reference velocity $r_0\,\omega$ for the earth is about 1000 mi hr^{-1} and also that the experimental work mentioned earlier, at least for some broad aspects of the experiments, shows that the geometrical distortion from spherical shape does not vitiate direct comparison of velocity fields, etc., on the kinematic basis.

While it is not the intention of the present discussion to consider in detail the question of model similarity for the experiment, it is well to note also the similarity situation with respect to at least two of the parameters that depend on the temperature and density fields driving the whole system. The driving force, due to the average horizontal temperature gradient, is represented in a significant way by the resulting thermal wind difference, u_T, between top and bottom. If this wind is expressed in terms of $r_0\,\omega$ as $u'_T = \dfrac{u_T}{r_0\,\omega}$, we obtain the 'thermal Rossby number' of the system (Fultz 1956, Fultz *et al.* 1956). Its value for this experiment is about 0·18 and consequently is substantially higher than typical atmospheric values of middle latitudes which lie near 0·03. This is consistent with the higher 'kinematic Rossby number' in the jet (0·2) and the somewhat less geotrophic character of the motion previously mentioned.

The second parameter of particular interest is the large-scale Richardson number that appears, for example, in the baroclinic wave theories of Eady (1949) and others. This number is a ratio of vertical stability to the square of the vertical wind shear (for which we use the thermal wind shear). In the experiment its value is about 8, compared to a typical range of from 40 to 140 in middle latitudes.

The detailed implications of these and differences in other parameters are in many cases not yet clear. For general discussions of the methods of analysis see, e.g., Langhaar (1951) and for the meteorological experiments, Fultz *et al.* (1956).

4. Top surface flow

In general, the observed motions will be described in a coordinate system rotating with the speed of the pan. However, much importance attaches to the motion of the water *relative* to long waves and jet stream; in particular there is the question whether fluid

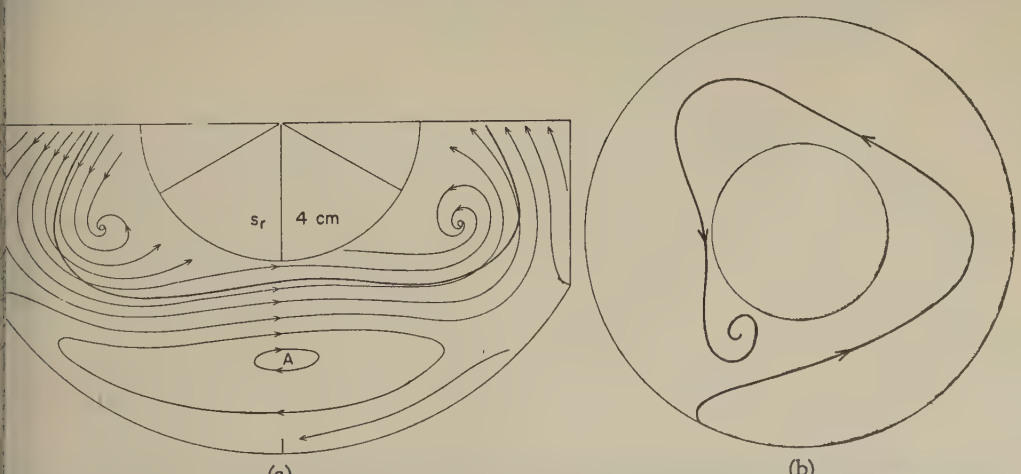

Figure 2. (a) Relative streamlines on top surface. Heavy solid line is jet-stream axis. (b) Typical path followed by water from heat source to cold source on top surface.

passes across the jet-stream axis to produce a so-called ' cross-stream circulation.' The waves seen in Fig. 1 travel at a regular rate of 25° longitude per revolution (or per day) relative to the pan. They thus complete a circuit around the pan in fifteen revolutions travelling with more than twice the speed of 'short' waves in the upper westerlies of the troposphere. Because of the regular progression, the linear wave speed may be subtracted vectorially from all winds, allowing for the radial variation of this speed. The residual is the motion *relative* to the waves.

Fig. 2 (a) shows relative streamlines at the surface computed in this manner. We observe closed paths in the ridge, a sink near the cold source in the trough and a source at the equatorial rim, also in the trough. From this source the relative streamlines spiral inward gradually. A typical streamline reaches the polar sink after passing through all three waves, i.e., it terminates in the same trough in which it starts (Fig. 2 (b)). Thus water does cross the jet stream axis from equatorial to polar side. All crossing takes place in the troughline and just to its east. This feature of the analysis – crossing of the jet – however is rather delicate and could easily be affected by experimental errors in the velocity measurements. Confirmation was obtained in repeat experiments subsequent to the analysis by using tracer-ink bands in the interior of the liquid. The motion of these bands is not subject to some of the difficulties of the aluminium powder measurements (Fultz *et al* 1956).

The field of wind speed depicts the jet stream clearly (Fig. 3). A broad band with speed of 20 per cent (comparable to 200 mi hr^{-1}) extends almost uniformly along the jet axis. Although two speed centres have been drawn, no importance can be attached to this feature which is well within the margin of error of the observations. As in the atmosphere the cyclonic shear greatly exceeds the anti-cyclonic shear. Generally, however, the shears are much weaker than those observed on weather maps. This becomes evident when the field of absolute vorticity is computed (Fig. 4).

The absolute vorticity $\xi_a = 2\omega + \xi_r$, where ξ_r is the relative vorticity. In order to reduce ξ_a to values comparable to the atmosphere, we divide by the angular rotation of the pan. This is consistent with the method of expressing velocities in terms of $r_0\,\omega$. Denoting non-dimensional quantities with primes, $\xi_a' = 2 + \xi_r'$ where the number 2 denotes the value of the Coriolis parameter. In Fig. 4 the line, $\xi_a' = 2$, closely parallels the jet-stream axis, but its amplitude is greater because of the variation of streamline curvature along the axis. A band of minimum vorticity lies equatorward of the core but values are only some 40 per cent less than the Coriolis parameter; zero absolute vorticity is approached nowhere. Similarly, the highest cyclonic vorticities on the poleward side of the axis exceed the Coriolis parameter by only 120 per cent. As demonstrated by

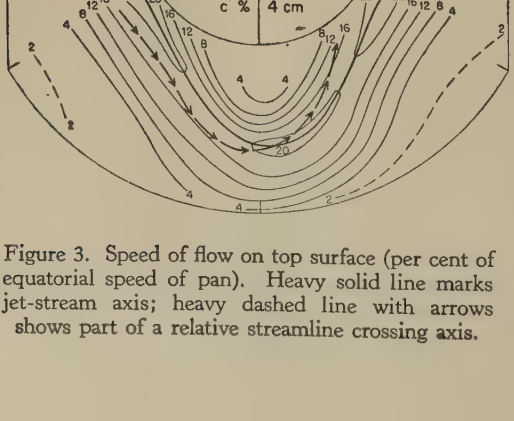

Figure 3. Speed of flow on top surface (per cent of equatorial speed of pan). Heavy solid line marks jet-stream axis; heavy dashed line with arrows shows part of a relative streamline crossing axis.

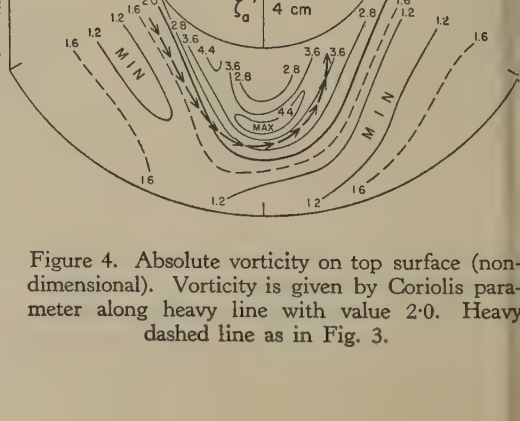

Figure 4. Absolute vorticity on top surface (non-dimensional). Vorticity is given by Coriolis parameter along heavy line with value 2·0. Heavy dashed line as in Fig. 3.

Fultz *et al.* (1956) vorticity fields that resemble those of the atmosphere more exactly are generated in experiments with higher rotation rates.

A portion of a relative streamline from Fig. 2 which crosses the jet has been entered in Figs. 3 and 4. As the water approaches the core of the jet it accelerates, then decelerates strongly after crossing the axis. The motion is directed toward increasing vorticity; as will be shown later, descent takes place below the area where the vorticity increase occurs.

5. Temperature field

A mean radial cross-section of temperature (temperatures are given as departures from 16°C), (Fig. 5a), obtained by averaging over all meridians, shows a poleward directed temperature gradient at all heights. This gradient is strongest at the bottom (6°C) and diminishes upward, with temperatures generally increasing with height, as is the case with potential temperature in the atmosphere. At the top we still observe a temperature drop of approximately half the strength of that at the bottom : tropopause and stratosphere do not exist. This suggests that these features of the atmospheric temperature field are not needed for production and maintenance of a jet stream and long waves.

In the interior of the water the stratification is very stable; even so, the stability is less than in the atmosphere as shown by the low Richardson number. Near top and bottom the vertical temperature gradient reverses, hence a convective regime prevails in relatively thin layers near these boundaries. At the bottom this is owing to the fact that the heat source at the rim was not insulated, so that heating also spread along the bottom. At the top some evaporation took place under the laboratory air conditions prevailing at the time of the measurements. The evaporation, measured from the volume loss, was sufficient to produce a heat loss rate of about 8 w.

Fig. 5 (a) may be averaged radially to yield a standard temperature-depth curve (Fig. 5 (b)). Between 0·5 and 3·5 cm the mean vertical temperature gradient is linear and amounts to 1°C per 0·5 cm.

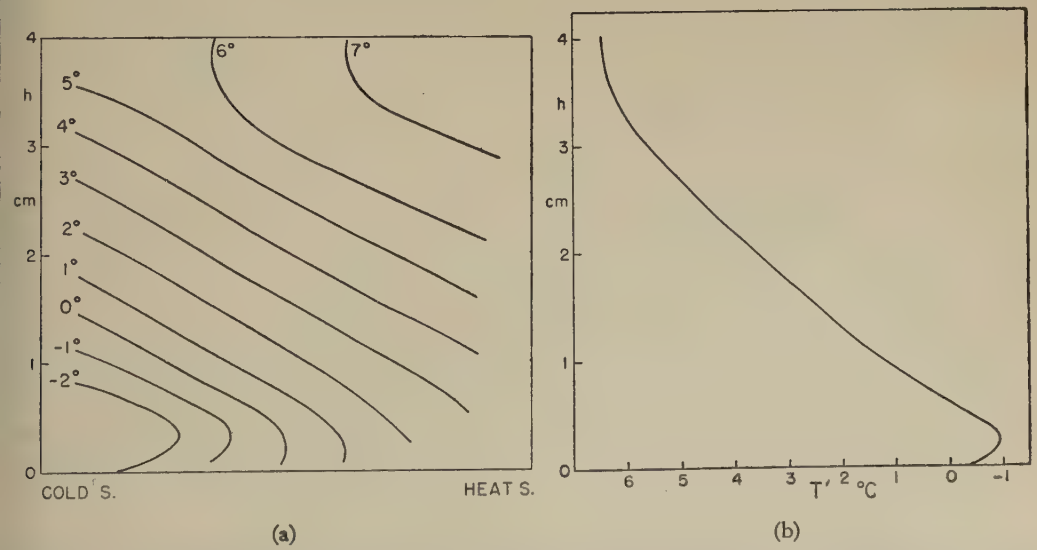

Figure 5. (a) Zonally-averaged distribution of temperature (departure from 16°C) with radius and height above bottom (cm). (b) Standard temperature-height curve for experiment.

Looking at a selection of horizontal temperature charts (Figs. 6 (a), (b), (c) and (d)) we observe in some measure what Rossby (1942) once termed a quasi-uniform swaying north and south of a very deep atmospheric layer. The phase shift with depth is slight, but the amplitude of the isotherm waves decreases downward. At the top surface the influence of evaporation is pronounced as seen from comparison with Fig. 2; in the region of closed anticyclonic streamlines in the ridge, where the same water circulates slowly for a long time, a secondary minimum of temperature is located. The inward-spiralling streamlines pass toward lower temperatures; therefore there is relative advection of warm water. Evaporation and convection in the unstable top layer provide for maintenance of the steady temperature field.

6. Pressure and wind-field

Because the density of the water is a function of temperature alone, under the conditions of the present experiment, i.e., the pressure compressibility of the water is very low, the vertical pressure distribution can be calculated in any column given the bottom pressure or configuration of the top surface. Neither of these data was available, although it is hoped to obtain at least one of them in future experiments. As the only remaining alternative, the surface configuration was computed from the wind-field. This was done from the complete equation of motion, and also geostrophically. The difference between the two contour fields was small; since later the contour fields at higher pressures or greater depth were used to calculate geostrophic flow, the geostrophic contour field was finally adopted also for the top surface, to be consistent. It should be noted that the contour field in question is that of heights relative to the level surfaces of ' apparent ' gravity for the rotating-pan coordinate system. These surfaces are the same as those of the equilibrium paraboloid $z = z_0 + \frac{\omega^2 r^2}{2g}$ of a free surface of liquid rotating rigidly with the pan.

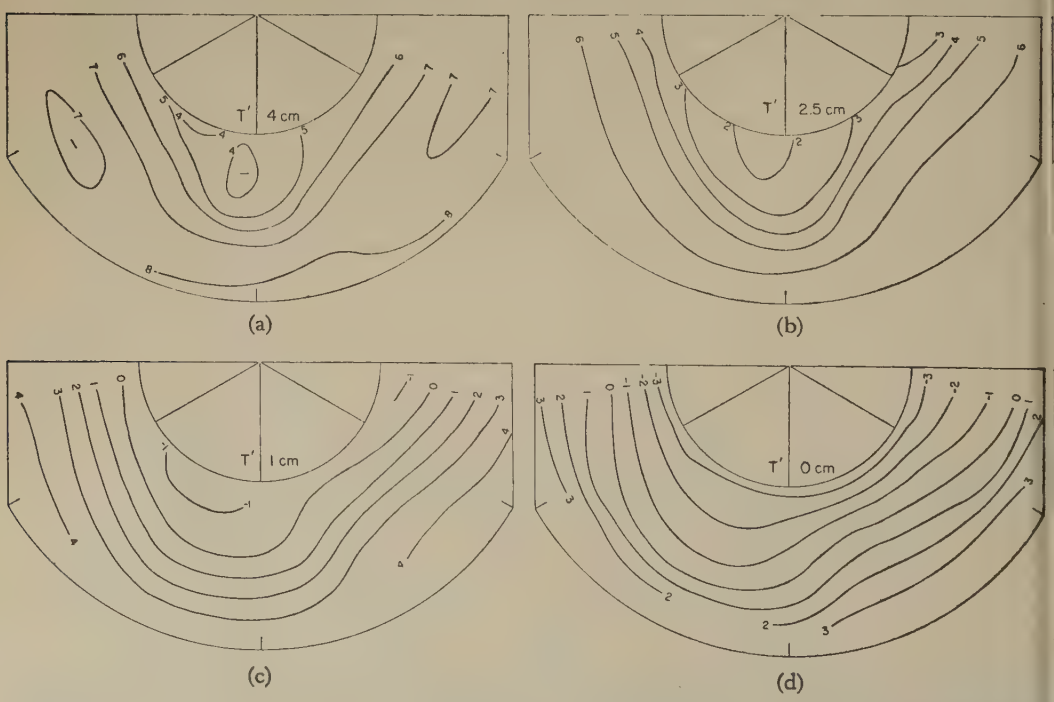

Figure 6. (a), (b), (c) and (d): Isotherms (departure from 16°C) at four selected levels; heights are indicated on diagrams.

For the low rotation value of 0·30 sec^{-1}, the rise at the rim of a level surface from a plane tangent to it at the axis is only 0·011 cm. Since the location of temperature measuring elements was known only to about 1 mm there was no need to allow for the curvature of the level surfaces in locating temperature points for calculations.

The geostrophic flow (c_g) on a constant-pressure surface is calculated from the well-known formula $f c_g = -g \frac{\partial D}{\partial n}$, where g is the acceleration of gravity, D the altimeter correction and n the horizontal axis normal to the wind, taken positive toward the left of the wind looking downstream. For non-dimensional calculation this equation becomes, after division by $r_0 \omega^2$,

$$c_g' = -\tfrac{1}{2} \frac{\partial D'}{\partial n'}, \qquad . \quad . \quad . \quad . \quad (1)$$

where $n' = n/r_0$ and $D' = gD/C_e^2$. Generally, we shall express distances as fractions of r_0 such as n'. The quantity D' is obtained from the hydrostatic equation. Given the pressure interval $\delta\rho$ between two isobaric surfaces, the specific volume α and the thickness between the isobaric surfaces δz, $\alpha\, \delta\rho = -g\, \delta z$. In standard water, denoted by the subscript 's,' $\alpha_s\, \delta p = -g\, \delta z_s$. Then $\alpha/\alpha_s = \delta z/\delta z_s$. Solving for δz and integrating from the top down, the height of any constant pressure surface

$$h = h_{top} - \bar{\alpha}/\alpha_s\, \delta z_s, \qquad . \quad . \quad . \quad . \quad (2)$$

where $\bar{\alpha}$ is the pressure-averaged specific volume. This equation assumes a very convenient form if we choose $\alpha_s = 1$, $\delta z_s = 1$. The specific volume $\bar{\alpha}$ is obtained from Dorsey's (1940) Tables on the expansion of water. Since $D = h - h_s$, the field of D' is readily determined from Eq. 2, given the topography of the top surface.

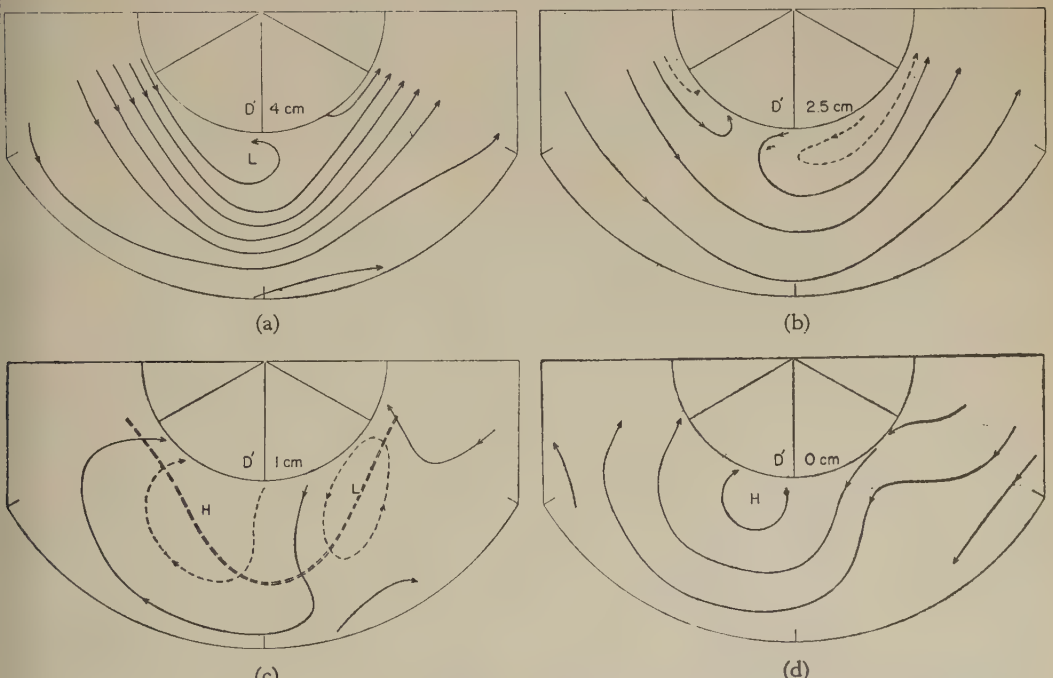

Figure 7. (a), (b), (c) and (d): Contours on four selected isobaric surfaces (D') shown as stream function of geostrophic velocity. Double-dashed line at 1 cm is jet-stream axis at top surface (heights are indicated on diagrams).

Figs. 7 (a), (b), (c) and (d) contain the analysis of selected constant-pressure charts, expressed as a stream function of the geostrophic wind. (Since the altimeter corrections involved have the order of magnitude of microns, it is still permissible to refer to the charts in terms of constant height for convenience). In general, the lines could be drawn with ease but some smoothing proved necessary near 1 cm where gradients are weak and where the pattern changes rapidly with depth.

The jet stream decays downward and goes over into a system of vortices below 2 cm. At 1 cm the jet-stream axis has been entered for reference. We observe a cyclone and an anticyclone directly under the jet, with centres near southwest and northwest inflection points of the surface current. This then is the analogue of the atmospheric sea-level chart, but it is not the bottom chart in the dishpan where we find a sinusoidal easterly current, much as we would obtain in the atmosphere in middle latitudes after downward extrapolation to, say, 1200 mb.

Owing to the influence of the frictional boundary layer there were some winds at the bottom in the region under and just ahead of the upper trough not indicated by the geostrophic analysis. These were mainly north-westerly winds that occurred in a narrow sector behind a shallow cold front, which appeared to lie on the average 10° longitude ahead of the upper trough. This front extended only slightly above 0·5 cm height; the evidence for its existence was given by much sharper breaks downward in the temperature traces than occur anywhere else even where, in the upper layers, larger ranges of temperature were observed as the waves pass. Both this front and some smaller temperature breaks farther west which resemble secondary cold fronts, were somewhat variable in exact location and were smoothed out in the averaged analysis. The *local and shallow nature* of the near-discontinuity surface compared to the upper-temperature gradients in the jet certainly *suggests a minor role for the front in the overall mechanics of the waves*; perhaps it is no more than a minor result of the distribution of temperature advection.

The differences between dishpan and atmosphere arising from the predominant bottom easterlies will be discussed in detail in another report. Here it should merely be mentioned that they are explained readily from momentum-balance considerations. All interaction between atmosphere and earth must take place at the ground, while in this dishpan experiment the water loses momentum to the inner and possibly also the outer

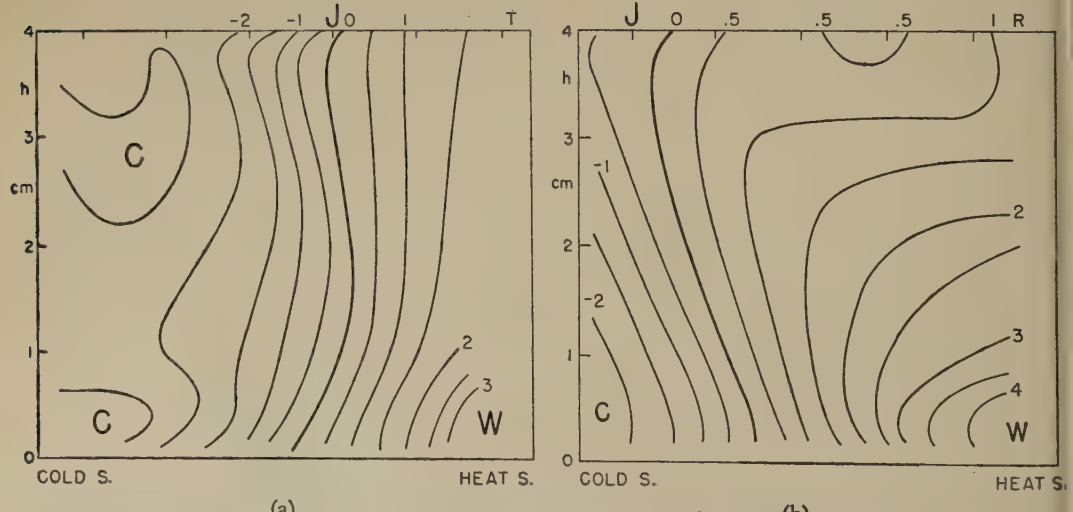

Figure 8. (a) and (b) Temperature anomaly from standard water (Fig. 5 (b)) in trough (T) and ridge (R).

ylinder. The whole bottom thus becomes a momentum source. It is significant that in spite of this difference in arrangement *a replica of the atmospheric sea-level chart occurs*, and that altogether we see in Fig. 7 *the principal features of the atmospheric long and short waves merged into one simple basic pattern.* Clearly, momentum balance considerations should be very cautiously used in deriving insight into the reasons for the occurrence of the observed general circulation, since essentially the *same* circulation becomes established with such a *different* distribution of momentum sources and sinks.

7. Vertical cross-sections

Because of the great stability of the water the significant features of the temperature field are best brought out through subtraction of the mean temperature-depth curve of Fig. 5 (b) from the temperature cross-sections (Fig. 8 (a), (b)); cf. isotherms on Figs. 9 (b), (c). Along both trough and ridge the stability decreases from polar to equatorial

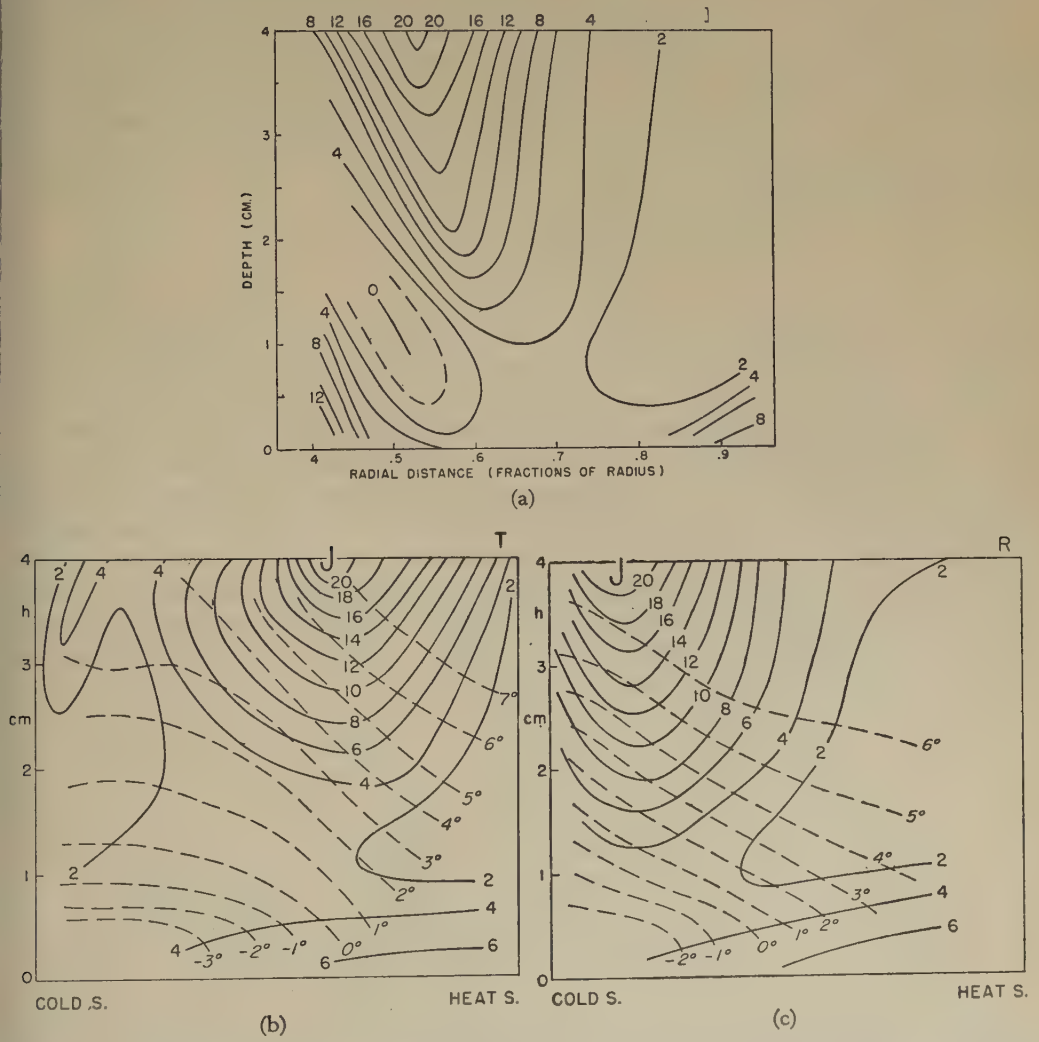

Figure 9. (a) Vertical cross-section of speed of flow (per cent) at south-west inflection point. For location of section see Fig. 10. (b) Vertical cross-section of flow speed (per cent) and temperature (departure from 16°C) in trough (T). (c) Same as Fig. 9 (b) for ridge (R).

latitudes. In the trough, almost the whole meridional temperature gradient above the bottom layer is concentrated near the jet stream and, as is typical for the atmosphere, the jet-stream centre is located in the middle of the gradient near the zero anomaly line. Such a position of the core is also observed near the surface in the ridge. At greater depths in the ridge, however, the anomaly lines slope equatorward indicating greater vertical stability and smaller vertical slope of the isotherms than in the trough under the jet.

The wind-field at the south-west inflection point (Fig. 9 (a)) is spectacular and differs from atmospheric vertical sections only in the strong easterly velocities near the bottom. The horizontal cyclonic shear is much greater than the anticyclonic shear through a deep layer. Figs. 9 (b), (c) show vertical cross-sections of wind and temperature in trough and ridge.

8. Vertical motion

Quantitative observation of vertical displacements was not possible under the conditions of the experiment, but the main features of the calculated vertical motion pattern to be described were later verified qualitatively by dropping dye in the interior of the pan and following the motion of the coloured water visually. Vertical motions were computed with the assumption of conservation of heat, i.e., temperature. This assumption is clearly inapplicable near all four boundaries; there, however, the condition applies that the vertical motion must vanish. In the interior, molecular diffusion alone can produce changes in heat content. As the lapse rate is almost linear (c.f., Fig. 5 (b)) such diffusion can be shown to be without importance.

Because of the steady state, the substantial derivative

$$\frac{d}{dt} = c_r \frac{\partial}{\partial s_r},$$

where c_r is the three-dimensional velocity relative to the waves and s_r is along the three-dimensional relative streamline, (also a trajectory since the motion is steady in the wave coordinate system). c_r may be approximated by c_{rg}, the relative geostrophic velocity in the horizontal plane since we may expect the vertical velocities to be at least one order of magnitude less than the horizontal velocities. The relative streamline distance s_r however cannot be so treated. The ratio of vertical to horizontal extent of the water is 1 : 4, while in the atmosphere the corresponding ratio is 1 : 1000. Thus three-dimensional relative streamlines had to be constructed on constant-temperature surfaces for the dishpan. This was no easy task and several techniques of construction were tried out. Most satisfactory was Fultz's adaptation for the dishpan* of Montgomery's (1937) isentropic geostrophic potential plus further modification for relative motion. Some of the relative streamline maps computed by this method are shown in Fig. 16.

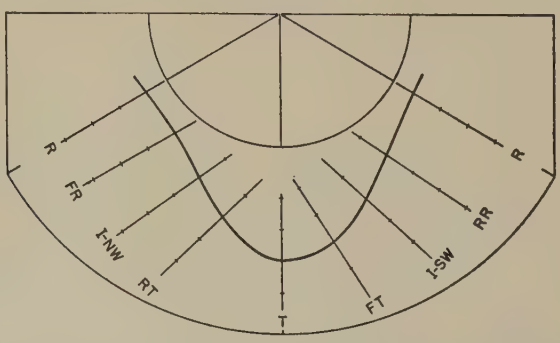

Figure. 10. Scheme of cross-sections normal to jet-stream axis on top surface.

* To be published.

The vertical velocity

$$w \equiv \frac{dz}{dt} = c_{rg} \frac{\partial z_T}{\partial s_r},$$

and after division by C_e

$$w' = c_{rg}' \frac{\partial z_T'}{\partial s_r'}, \qquad . \quad . \quad . \quad . \quad (3)$$

where z_T is the height of the constant temperature surface and $s_r' = s_r/r_0$. Given the fields of c_{rg}', s_r' and the topography of the isothermal surfaces, w' can be computed. Such computations were made on seven surfaces 1°C apart. Some adjustment for vertical consistency proved necessary; all adjustments however were relatively minor and nowhere altered the computed pattern substantially. The results will be shown at first with vertical cross-sections (Fig. 11) as laid out in Fig. 10. The unit of vertical motion is per mille (of $r_0\,\omega$). Because the relative vertical extent of the dishpan is 250 times that of the atmosphere, all values must be divided by 250 for comparison. Thus 5 per mille is equivalent to 1 cm/sec, and we see from Fig. 11-13 that the magnitude of vertical speeds in the

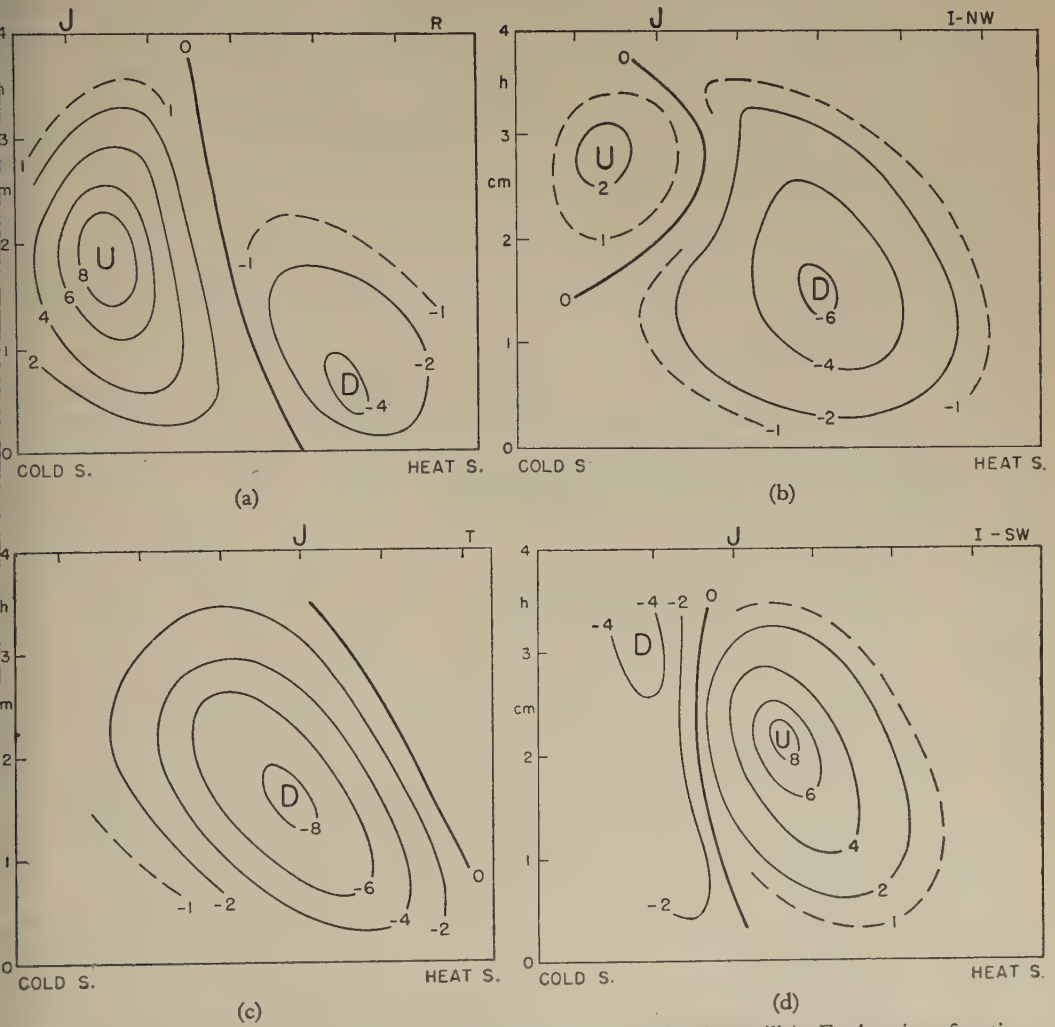

Figure 11. (a), (b), (c) and (d) Vertical cross-sections of vertical motion (per mille). For location of sections see Fig. 10.

dishpan, just as that of horizontal speeds, compares satisfactorily with the atmosphere. This method of comparison amounts to treating the vertical exaggeration by using total depth as the reference quantity for vertical distances and $z\omega$ instead of $r_0\,\omega$ for the vertical component of velocity. Rossby (1926) and Fultz *et al.* (1956) have discussed conditions necessary for this to be valid; mainly, that the hydrostatic approximation for the vertical equation of motion applies.

In the ridge (Fig. 11a) we observe ascending motion under the jet and descent in the warmer water toward the equatorial rim. Thus the circulation is solenoidally indirect over most of the cross-section; but the centre of ascent lies to the right of the jet-stream axis, looking downstream, so that the vertical circulation is direct at the core. The analysis has been extrapolated to top and bottom where the vertical velocity must vanish; it has been terminated a few millimeters from heat and cold sources where visual observation of coloured water shows strong ascent, or descent, in accord with expectations. This procedure has been followed on all cross-sections and charts.

The vertical circulation is definitely indirect about the jet axis in the north-westerly flow (Fig. 11 (b)). General descent takes place in the trough (Fig. 11 (c)), with the centre of descending motion situated under and slightly to the left of the jet stream core. Finally, at the south-west inflection point (Fig. 11 (d)) strong direct circulation prevails. In summary the sense of the vertical circulation about the jet-stream axis is not uniform. Direct circulation occurs in the south-westerly part of the flow and indirect circulation in the north-westerly part. However, the direct portion is the stronger and also occupies a longer distance along the axis. It is of interest that direct and indirect branches appear even though there is no concentrated velocity maximum along the core, hence no entrance and exit zones. These branches must therefore be related to the wave motion.

Fig. 12 shows a vertical cross-section along the core, obtained by averaging the vertical motion in each normal cross-section over a distance of 0·1 r_0 on both sides of the core. Centres of ascent and descent lie slightly east of the ridge and west of the trough. The zero lines extend nearly vertically at the north-west inflection point and somewhat west of the south-west inflection point. Broadly, descent takes place in the region of cyclonic flow curvature at the top surface, ascent in the region of anticyclonic curvature. In view of the flow pattern on the 1-cm surface (Fig. 7) one can also say that descent occupies the area of northerly flow at that level between cyclone and anticyclone, ascent the area of southerly flow, in excellent agreement with the atmosphere.

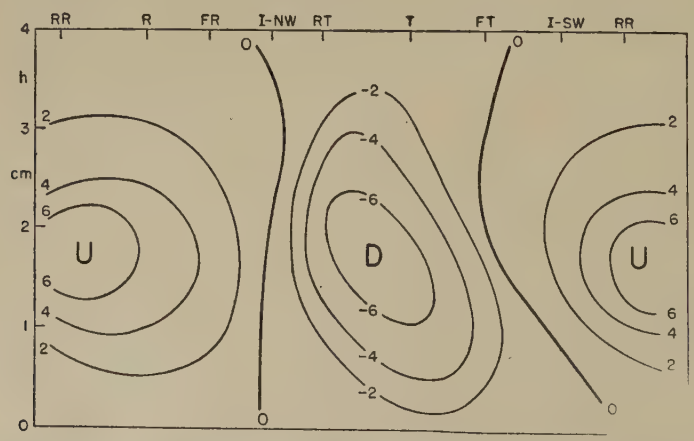

Figure 12. Vertical cross-section of vertical motion (per mille) following jet-stream core on top surface. Horizontal axis determined from Fig. 10.

In water, the level of non-divergence corresponds almost to the level of strongest ertical motion; according to Fig. 12 it is situated therefore in the mean slightly below he 2-cm surface which divides the mass in equal halves. This corresponds well with the verage position of the level of non-divergence near 600-500 mb in the atmosphere. As the atmosphere, however, non-divergence is not found near the centre of the mass verywhere, but, as shown by Fig. 11, there are sloping surfaces of non-divergence which each from bottom to top of the pan. The slope is always poleward and, as suggested by he patterns of Fig. 13, the surfaces of non-divergence start near the equatorial rim of the an and from there spiral toward the poleward rim with counterclockwise curvature.

Figs. 13 (a), (b), (c) and (d) depict the vertical motion on four horizontal charts; he jet-stream axis has been added for reference. We observe the features already noted rom the vertical sections : strong ascent to the right and strong descent to the left of the xis in the south-westerly flow, and a weaker reverse circulation west of the trough. Vertical notion gradients are strongest at the position of the cyclone at 1 cm, and the areas of ascent nd descent spiral inward cyclonically from the outer rim.

Since the temperature field is steady in the wave-coordinate system, horizontal dvection must compensate for vertical temperature advection. Except near top and bottom he temperature increases upward everywhere, so that colder water is moved upward nd warmer water downward by the vertical displacements. Steady state demands that elative to the waves horizontal advection of warm water takes place in the areas of ascent nd advection of cold water in the areas of descent. Further, since the speed of the flow ncreases upward everywhere above the bottom layer of easterlies, the water accelerates s it rises and decelerates as it sinks. As in the atmosphere, individual particles do not onserve their energy; increases, or decreases, of potential and kinetic energy are coupled. t also follows that acceleration takes place in areas of relative horizontal advection of varm water and deceleration in areas of relative cold advection.

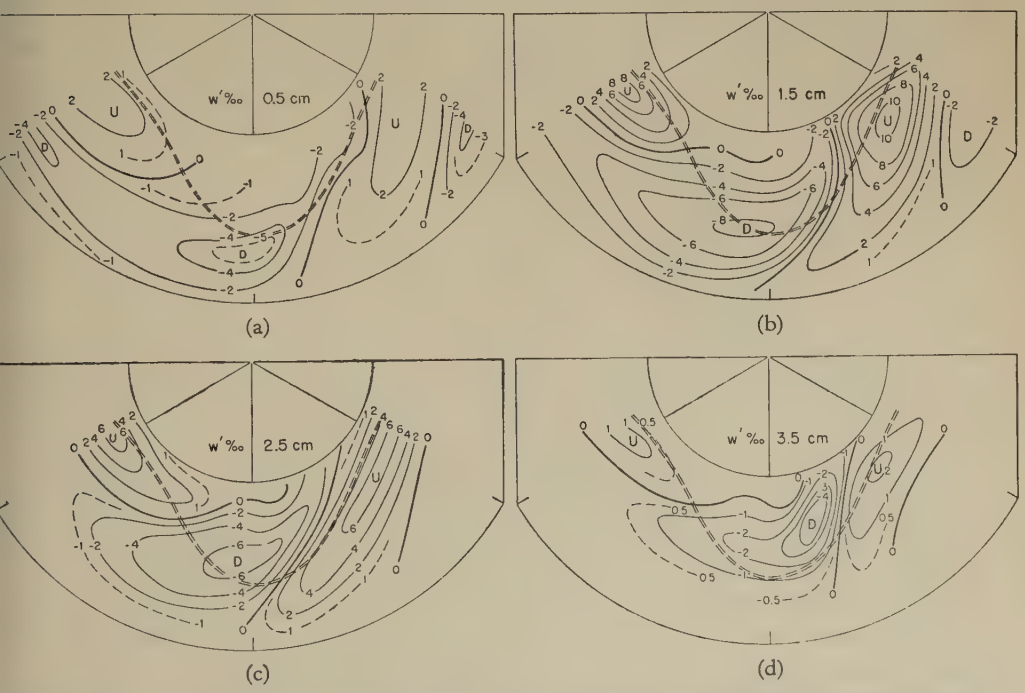

Figure 13. (a), (b), (c) and (d) : Vertical motion (per mille) on four selected levels with heights indicated on diagrams. U denotes centre of ascent and D centre of descent; double-dashed line is jet-stream axis.

Regional distributions of temperature, wind and vertical motion are often summarized in general circulation studies in cross-section form after averaging around the globe. Fig. 13 shows that much caution is necessary in performing the averaging so that proper deductions can be drawn. A preferred method is zonal averaging. In Fig. 13 the area of strongest ascent lies poleward of the area of strongest descent. If one averages zonally one will inevitably arrive at a picture with ascent poleward of the descent (Fig. 14 (a)). If the horizontal flow is also averaged zonally, the mean zonal flow distribution of Fig. 14 (b) is obtained. This leads to the apparent result that ascent takes place north of the strongest westerlies, and descent to their south; if Fig. 5 (a) is also considered one might reason that the cold water rises and the warm water sinks. When downward motion at the cold source and upward motion at the heat source are added to the pattern of Fig. 14 (a) the classical atmospheric three-cell structure emerges.

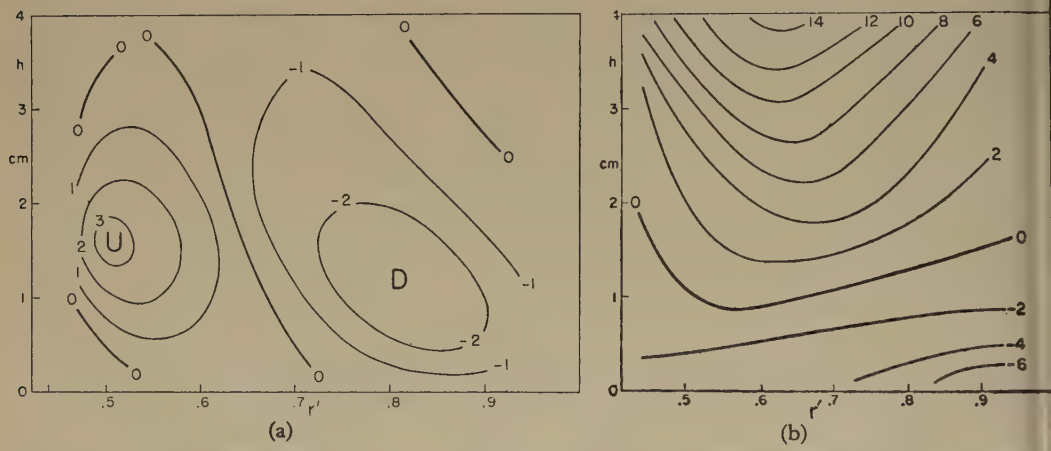

Figure 14. (a) Zonally-averaged distribution of vertical motion (per mille) with radius and depth. (b) Zonally-averaged distribution of horizontal flow speed (per cent) with radius and depth. Distance r' at bottom as fraction of r_0.

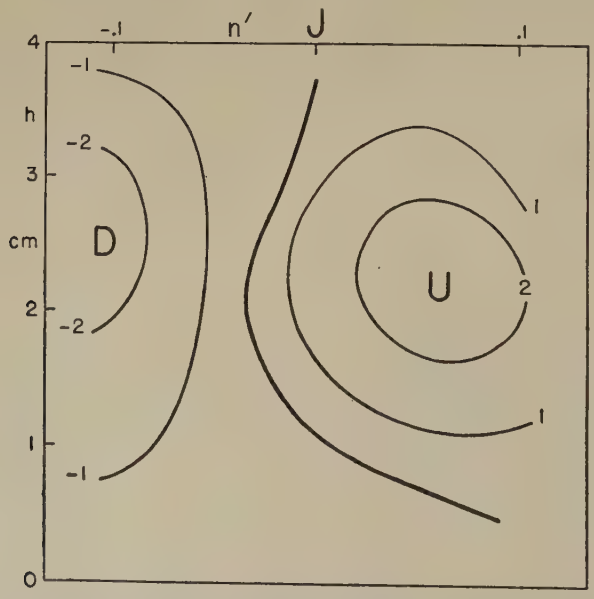

Figure 15. Distribution of vertical motion (per mille) averaged following jet-stream axis on top surface. Distance normal to jet axis expressed as fraction of r_0 at top (n').

Fig. 14 (a), of course, is not incorrect and truly represents the zonally-averaged distri-ıtion of vertical motion. As the foregoing has demonstrated, however, a simple interpre-tion by comparison with Figs. 5 (a) and 14 (b) is not permissible. The technique of ›nal averaging has arisen basically from the concept of small perturbations superimposed ı a broad zonal current. Both in dishpan and atmosphere, however, the perturbations e large and calculations based on coordinate systems implying small perturbations for ieir significance, lose much of their meaning. Analogous to Fig. 13, the ' reverse ' middle-titude circulation cell of the atmosphere can be taken to signify little except the well-ıown fact that in cyclones the ascent above warm fronts takes place north of the descent ehind cold fronts. As in the dishpan it does not follow that cyclones are energy-consum-ıg systems; rather the reverse is known to be true. What does follow is that zonal averag-ıg can, to great advantage for solving many problems, be replaced by averaging following ıe large perturbations, in our case the jet stream, as it traces out the long-wave pattern. Vhen this is done, we obtain the vertical motion pattern of Fig. 15 which immediately ıggests that the jet-stream zone may be a region of potential-energy release. This subject ill be explored fully in a further report.

9. Vorticity field

The vorticity field was calculated to determine whether the theorem of conservation f potential vorticity is the dynamic law guiding the motion. We also hoped that this alculation would shed some light on an apparent difference between dishpan and atmos-here. Long waves occur in both systems. In the atmosphere their appearance has been scribed to variation of the Coriolis parameter with latitude (Rossby 1940): in the dishpan owever the Coriolis parameter is constant.

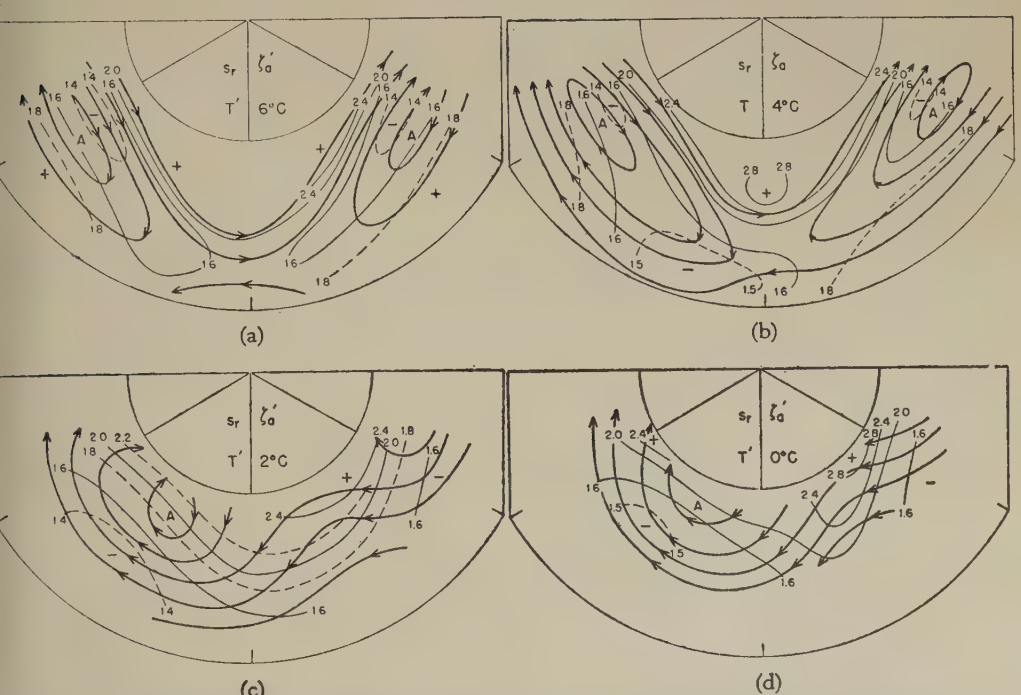

Figure 16. (a), (b), (c) and (d): Relative streamlines s_r (with arrows) and isolines of absolute vorticity ξ_a' non-dimensional) on four selected constant-temperature surfaces. The value 2·0 denotes Coriolis parameter.

As various recent studies have shown, the vorticity in the atmosphere is logical computed on isentropic surfaces when the motion is adiabatic. Except for the top surfac (Fig. 4), this is even more true for the dishpan because of the relatively great depth the water. Figs. 16 (a), (b), (c), (d) shows analyses of absolute vorticity on four constan temperature surfaces. Of these, the upper two (6° and 4°C) indicate conditions in th layer with waves, the lower two (2° and 0°C) in the layer with vortices. The relativ streamlines have been added so that the motion of the water through the vorticity fiel can be followed. Since the relative streamlines are geostrophically computed, they ar not quite comparable to Fig. 2 where the total motion, including non-geostrophic flow is depicted. Hence the vorticity variation along the relative streamlines, while given approximately, will not be exact; this comment also holds for the preceding calculatio of vertical motion.

The analysis could not be carried above the 3·5-cm level because of non-adiabati motion near the top, so the 6°C and 4°C surfaces do not reach the jet-stream core. The enter the jet stream sufficiently to permit several deductions, however. Near the jet stream axis the water conserves its absolute vorticity in the north-west flow; in the troughl line and to its east the vorticity increases somewhat, in accord with Fig. 4. The tota vorticity variation is very small, however, actually within range of error of the analysis It follows that with some approximation *conservation of absolute vorticity is the applicabl dynamic law in the layer with wave motion.* This is surprising since at first sight one would judge from Fig. 1 that the vorticity of individual particles increases from ridge to troughl and decreases from trough to ridge. But, as seen from Fig. 8, the vertical slope of the isot therms is smaller in ridge than in trough. Therefore the anticyclonic shear equatorward of the jet-stream axis is smallest in the ridge because the constant-temperature surface pass through a smaller fraction of the vertical wind shear than in the trough (Figs. 9 (b) (c)). The increase of anticyclonic shear from ridge to trough compensates for the chang from clockwise to counter-clockwise flow curvature. On the left of the jet-stream axis similar consideration applies. There the constant-temperature surfaces cross the isotach at a larger angle in ridge than in trough so that the cyclonic shear is greatest in the ridge whereas the shear may be zero or even small anticyclonic in the trough (Fig. 9 (b)). I follows that variations of the slope of the isotherms along the jet-stream core in the dishpan take the place of variations of the Coriolis parameter in the atmosphere in order to maintain the same type of motion.

Equatorward of the jet-stream region marked vorticity changes occur. On the 6°C surface we find anticyclonic relative streamlines curving toward decreasing vorticity in the southwesterly flow. This is the region where strong ascent takes place as the water enters the jet stream from the equatorial side. West of the trough-line the descending water acquires higher vorticity. On the 4°C surface the same type of pattern is still present but no longer with the same clarity, as this surface drops well below the 2-cm level in the equatorial portions. A completely different regime prevails on the two lower surfaces. All relative motion is easterly. The current acquires cyclonic vorticity as it moves toward the area of the cyclone found on the 1-cm surface (Fig. 7). It loses vorticity during passage from cyclonic to anticyclonic centre.

These results are satisfactory and show the mechanism of maintenance of the vortices. Looking at upper and lower surfaces jointly, the water moves toward higher vorticity east of the cyclone at low levels and toward lower vorticity at high levels. The vertical motion is upward, with largest speeds at intermediate heights. West of the cyclone, inverse conditions obtain. Qualitatively, then, the *theorem of conservation of potential vorticity is applicable.* We also attempted to calculate the potential vorticity (ξ_p) directly from the relation $\xi_p = \xi_a/\Delta$, where Δ is the depth of the column considered. The potential vorticity

should be constant along the relative streamlines. This calculation failed because Δ could not be measured with sufficient accuracy. The mean thickness of a column between two constant-temperature surfaces 1°C apart is only 0·4 to 0·5 cm (Fig. 5 (b)); the analysis of the topography of the surfaces can be considered correct only within 0·2 cm. This is a small error compared to the vertical extent of the temperature surfaces which is 2 to 3 cm in the layer with adiabatic motion. The error, however, has the percentual magnitude of the vorticity variations, precluding valid computations of potential vorticity.

Conclusion

This report has shown that the three-dimensional structure of long waves and jet stream in the dishpan, indeed the structure of all major features, resembles the atmosphere in basic pattern and relative magnitude of the motions to a high degree. In a further report (in course of preparation), the mechanisms of the general circulation, including production and maintenance of kinetic energy, will be discussed.

Acknowledgments

The writers are indebted to Dr. G. W. Platzman, University of Chicago, for discussion of various aspects of the calculations, and to a number of their co-workers and assistants for help in the voluminous evaluations and computations. The research was carried out with the support of the Office of Naval Research, United States Navy, and the Geophysical Research Directorate, U.S. Air Force.

References

Charney, J. G.	1948	*Geofys. Publ.*, **17**, No. 2.
Corn, J. and Fultz, D.	1955	*Geoph. Res. Pap.*, No. 34, AFCRC, Cambridge, Mass.
Dorsey, N. E.	1940	*Amer. Chem. Soc. Monogr.*, No. 81, New York (Reinhold).
Eady, E. T.	1949	*Tellus*, **1**, p. 33.
Fultz, D.	1950	*Proc. First Midwest Conf. Fluid Dynam.*, p. 279.
	1951	*J. Met.*, **8**, p. 262.
	1952	*Ibid.*, **9**, p. 379,
	1956	*Proc. First Sympos. Geophys. Models, Baltimore* 1953, ' Fluid models in geophysics,' pp. 27-63, U.S. Govt. Printing Off., Washington.
Fultz, D. and Frenzen, P.	1955	*J. Met.*, **12**, p. 332.
Fultz, D. *et al.*	1956	' Studies in experimental hydrodynamics applied to large-scale meteorological phenomena,' Pt. I., *Dept. Met., Univ. Chicago.*
Hide, R.	1953	*Quart. J. R. Met. Soc.*, **79**, p. 161.
	1956	*Proc. First Sympos. Geophys. Models Baltimore*, 1953, ' Fluid models in geophysics,' pp. 101-116, U.S. Govt. Printing Off., Washington.
Langhaar, H. L.	1951	*Dimensional analysis and theory of models*, New York (Wiley).
Montgomery, R. B.	1937	*Bull. Amer. Met. Soc.*, **18**, p. 210.
Rossby, C.-G.	1926	*Mon. Wea. Rev.*, **54**, p. 237.
	1940	*Quart. J. R. Met. Soc.*, **66**, Supplement, p. 68.
	1942	*Dept. Met., Univ. Chicago Misc. Rep.*, No. 5.
	1947	*Bull. Amer. Met. Soc.*, **28**, p. 53.

551.509.313 : 551.509.317

Objective analysis in numerical forecasting

F. H. BUSHBY and VERA M. HUCKLE
Meteorological Office, Dunstable

(Manuscript received 24 November 1956)

SUMMARY

This paper describes an objective technique for analysing sets of upper-air data. The analyses resulting from the application of this technique to four sets of data for the NE Atlantic and Europe were compared with those produced subjectively by an analyst, and no marked differences were apparent.

Numerical forecasts for twenty-four hours ahead based on both subjective and objective analyses were computed for these four situations and the results compared with the actual developments. Only slight differences were noticed between the forecasts based on the subjective analyses and those based on the objective analyses in three of the four situations, but in the fourth situation the numerical forecast based on the objective analysis was much the better.

1. INTRODUCTION

The recent results obtained from the production of prognostic charts by numerical integration of systems of equations relating to various models of the atmosphere have been very encouraging. Indeed, in America and Sweden forecast charts are already being produced on a routine basis under operational conditions. This has only been made possible by the use of electronic computing machines, and it is natural to consider whether or not it is desirable to use these machines for any of the preliminary work prior to the actual integration calculation.

At present, most if not all of the integration procedures make use of the calculus of finite differences, and it is necessary to know the initial fields of the basic variables at mesh points of a grid. This is normally done by plotting observations on a map and drawing isopleths of the required variable. A grid is superimposed on the map and the initial values of the variable (such as 500-mb height) are read off from the map at grid points by interpolation by eye from the isopleths. This is a subjective process and Gilchrist and Cressman (1954) and Bergthorrson and Döös (1955) have suggested how this can be done objectively by computation. The advantages of this technique of analysis are that it is objective, and that it is time-saving when fast electronic computing machines are available. A possible disadvantage is that the conventional analyst often puts into his analysis something as a result of his experience (especially where observations are scanty), and it is difficult for an objective technique to make use of this kind of experience.

It was therefore decided to analyse objectively a few 500-mb charts and 1,000-500-mb thickness charts in order to ascertain whether or not a satisfactory technique could be evolved which would not be dependent upon a dense network of observations. This report describes the method used and the results of these computations. Numerical forecasts for twenty-four hours ahead, based on both subjective and objective analyses, were computed for four situations and the results compared.

2. THE OBJECTIVE-ANALYSIS TECHNIQUE

Bergthorrson and Döös (1955) obtained the contour heights at grid points by first forming a weighted mean of forecast and climatological normal heights for the point, then modifying this by the observed heights at neighbouring observing stations in an empirical manner. The technique proposed by Gilchrist and Cressman (1954) was the

finding of the best quadratic surface to fit the observations over a limited area. In each case the geostrophic approximation was used to enable wind observations to be taken into account.

The method of computing 500-mb contour heights which was tested in the Forecast Research Division, Dunstable, is one which has something in common with both these techniques. Each grid point is dealt with individually, and essentially the method consists of finding, by the method of least squares, the quadratic or cubic surface which best fits the observed 500-mb contour heights and winds and the forecast 500-mb contour heights. Different weights are given to observed heights and winds and to forecast heights. The method differs from that of Gilchrist and Cressman in that it makes use of forecast values and it differs from the method of Bergthorrson and Döös in that a best fitting surface is found. The techniques can be applied to data for thickness charts and to data for other isobaric surfaces. The computations were carried out by the Ferranti electronic computer at Manchester University.

We denote by H_s the height of the surface (quadratic or cubic) which best fits the observations and forecasts over a limited area of the chart where

$$H_s = F(x, y) \quad . \quad . \quad . \quad . \quad (1)$$

F being a quadratic or cubic function of x and y. Then the expression E which we minimize in order to obtain the best fitting surface is given by

$$E = \sum_{r=1}^{m} \{p\,(H_s - H_0)^2\}_r + T^2 \sum_{r=1}^{n} \{p\,(\mathbf{V}_s - \mathbf{V}_0)^2\}_r + \sum_{r=1}^{l} \{q\,(H_s - H_F)^2\}_r \quad . \quad (2)$$

where H_0 and $\mathbf{V}_0$ represent the observed 500-mb contour height and wind respectively, H_F represents a forecast 500-mb height, $\mathbf{V}_s$ is the geostrophic wind obtained from the surface represented by Eq. (1), p and q are weighting factors depending upon the distance of the observation or forecast from the grid point for which interpolation is being made, T^2 is a weighting factor relating the fitting of the wind observations to the fitting of the height observations, and m, n and l denote the number of height observations, wind observations and forecast heights used to determine F.

One of the purposes of the work described in this paper was to decide what values of p, q and T^2 gave the best results and whether the use of a cubic form of F gave any improvement over a quadratic form. It was hoped to be able to decide upon a value of q such that forecast heights would have no appreciable effect in regions of dense networks of reporting stations, but such that they would be of importance when there were only a few observations, or none. If we represent the polynomial $F(x, y)$ by

$$F = \Sigma\, \alpha_{jk}\, x^j\, y^k \quad . \quad . \quad . \quad . \quad (3)$$

where $j \geqslant 0$, $k \geqslant 0$, in both cases and $j + k \leqslant 2$ for the quadratic case and $j + k \leqslant 3$ for the cubic case, we determine α_{jk} by solving the set of simultaneous equations

$$\frac{\partial E}{\partial \alpha_{jk}} = 0 \quad . \quad . \quad . \quad . \quad . \quad (4)$$

In order to determine the 500-mb height at each grid point, the machine selected the six nearest observing stations at which either a 500-mb height or wind or both were reported. Only those stations within a radius of 1,000 mi of the grid point were used, and sometimes the number of stations chosen was less than six; indeed on rare occasions there could be no stations available. The information available from these stations therefore consisted of m contour heights and n winds where m and n are both integers and $0 \leqslant m \leqslant 6$ and $0 \leqslant n \leqslant 6$. When m or n is equal to zero then the appropriate summation term in Eq. (1) is zero.

The forecast heights used in this experiment were read from the forecast 500-mb charts prepared by the Forecast Division at Dunstable, and they were 21-hr forecasts issued for a time 3 hr before the time for which the objective analysis was made. No correction was made for this discrepancy. If this technique was being applied on a routine basis, twice daily, then numerical forecasts would be available for this purpose and would be based on information only 12 hr old. For the purpose of evaluating the final term in Eq. (2) we took $l = 9$, i.e. the summation was effected over the nine grid points nearest to the one in question. Thus in the quadratic case we have enough information to determine F at a grid point even if no observations are available. This is not so in the cubic case, and in these circumstances we simply make $H_s = H_F$ at the grid point.

The values of p and T^2 were chosen in accordance with work by Johnson (1956). Two expressions for p were used, and these are shown in Fig. 1 as functions of the distance from the grid point at which interpolation was being carried out. It is convenient to express H_s, H_F and H_0 in feet, $\mathbf{V}_s$ and $\mathbf{V}_0$ in ft sec^{-1}; then the unit of T is a second. In the first trials a value of T^2 equal to 2 sec^2 was used for the quadratic surface and a value of T^2 equal to 16 sec^2 was used for the cubic surface. Later, $T^2 = 16$ sec^2 was used for the quadratic surface. Two expressions for q were tried; $q = p/4$ and $q = p/16$. On the Ferranti Mark I machine at Manchester University the computation took 40 sec per point for the quadratic case and 60 sec per point for the cubic case.

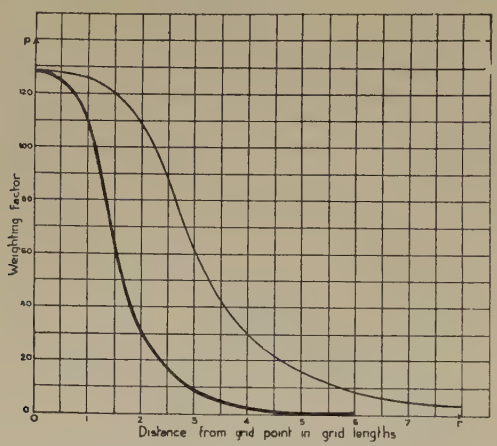

Figure 1. Distance weighting factors :

——— $p = \dfrac{128}{1 + 2^{-29} \times 10^8 r^4}$; ——— $p = \dfrac{128}{1 + 2^{-33} \times 10^8 r^4}$.

3. The examination of some objective analyses

The three situations used for the preliminary experiment were those for 15 GMT on 12 September 1955, 15 October 1955 and 31 October 1955. These situations were chosen because the forecasts of the 500-mb contours for 12 GMT on those days were substantially in error over some part of the area. They were not chosen as being typical of everyday differences between forecast and actual charts, because in this experiment it was necessary that there should be differences between the forecast and the corresponding observations in order to assess the effect that each was having on the objective analysis.

The objective analyses were made for the 18 × 14 grid used for previous work by the Forecast Research Division at Dunstable, but the computations were done firstly for the European half of the grid and secondly for the Atlantic half. Since the effect of varying the parameters was similar for each of the three situations, only one case, that of 15 GMT, 12 September 1955, is described in detail.

Most of the 500-mb observations used in this computation are shown in Fig. 2 (a), ogether with the forecast of the 500-mb contours produced for 12 GMT, 12 September 955, but certain observations outside the area covered by the background map were lso used. A subjective analysis of the 500-mb chart is shown in Fig. 2 (b). It can be een that the forecast contained appreciable differences in the Atlantic and central Medi- erranean from both the actual observations and the subjective analysis. Also, the trough n the vicinity of the British Isles was not sharp enough in the forecast chart.

In the first experiment T^2 was taken as 2 sec^2, $p = p_1 = 2^7 (1 + 2^{-29} \times 10^8 r^4)^{-1}$ where r is the distance in grid lengths of the reporting station from the grid point, $= q_1 = p_1/4$, and a quadratic surface was used. From the results of this and similar omputations using the other two sets of data it was obvious that the forecast heights vere being given too much weight in all areas except where the network of reporting tations was very dense. The objective analyses were therefore repeated using $= q_2 = p_1/16$. In general there was some improvement over Europe in areas of few eporting stations. For instance, the cut-off low actually centred over Sardinia was now omputed to be nearer its correct position than in the original computation. Over the Atlantic there was also a change away from the forecast values towards the conventional nalysis. However, it was equally clear that results were unsatisfactory over the Atlantic owing to the introduction of short-wavelength irregularities to accommodate isolated bservations which were different from the smooth forecast values.

The computations were therefore repeated using $p = p_2 = 2^7 (1 + 2^{-33} \times 10^8 r^4)^{-1}$, p_2 representing a weighting factor which decreases less rapidly with distance than p_1, so hat each observation has an influence over a greater area than when p_1 was used. Over Europe only very slight changes occurred, whereas marked improvements occurred over he Atlantic. Nevertheless, there was still some slight distortion around the ship observa- ions. The computations over the Atlantic sector were therefore repeated using T^2 equal o 16 sec^2, which has the effect of increasing the weight of the wind observations relative o the observed and forecast heights. The results of this computation for 12 September 1955 are shown in Fig. 2 (c), although the European values plotted are still for a value of $T^2 = 2$ sec^2, as there did not appear to be any purpose in repeating the calculations for that sector.

In order that the reader may assess the smoothness of the results for himself, the value for each grid point has been plotted on Fig. 2 (c) to the nearest ten feet with the ten-thousand figure omitted. An inspection of Figs. 2 (b) and 2 (c) shows very little difference between them. The central value of the cut-off low is not quite low enough on the objectively analysed chart. There is also a small oscillation on Fig. 2 (c) in the 18,600-ft contour line in the south-western approaches to the British Isles which does not occur in Fig. 2 (b). This is probably due to the apparently incorrect observation at Brest, which was not excluded from the raw data.

One set of computations for each of the three situations was completed using a cubic rather than a quadratic surface, with $T^2 = 16$ sec^2, $p = p_2$ and $q = q_2$. In all three cases, there were no significant differences between the results obtained from the use of a cubic surface and those using the quadratic surface with the best choice of parameters.

Having thus decided that the quadratic-surface method was apparently adequate when $T^2 = 16$ sec^2, $p = p_2$ and $q = q_2$, 1,000-500-mb thickness charts were computed for the three situations for which 500-mb charts had already been computed. In each case the objectively-analysed thickness chart was very similar to the one produced by the subjective analysis.

A 500-mb chart (Fig. 3 (a)) and a 1,000-500-mb thickness chart (Fig. 3 (b)) were also produced by this technique for 15 GMT on 30 January 1952. This was a situation

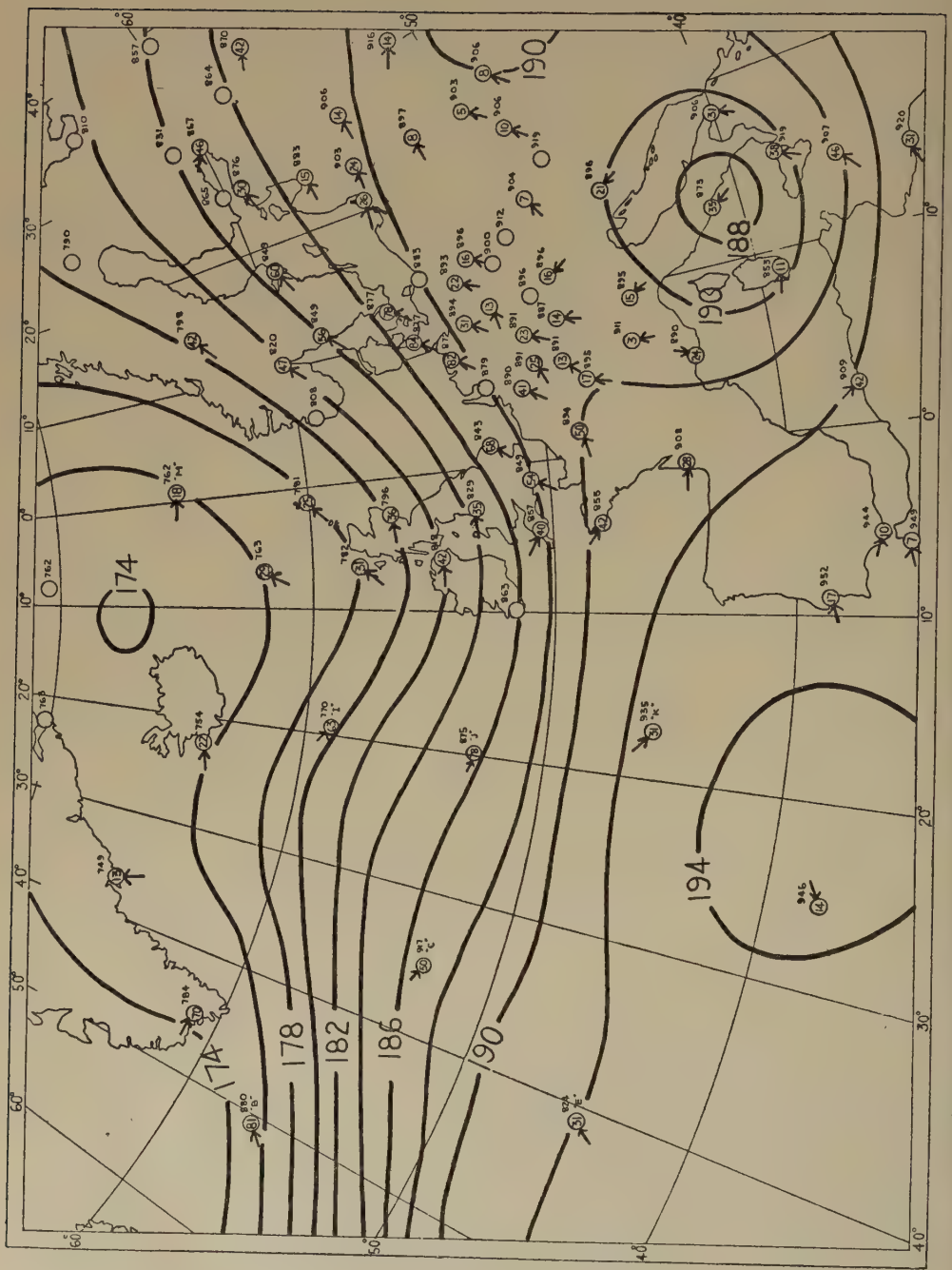

Figure 2 (a). 500-mb observations for 15 GMT and forecast 500-mb contours for 12 GMT on 12 Sept. 1955.

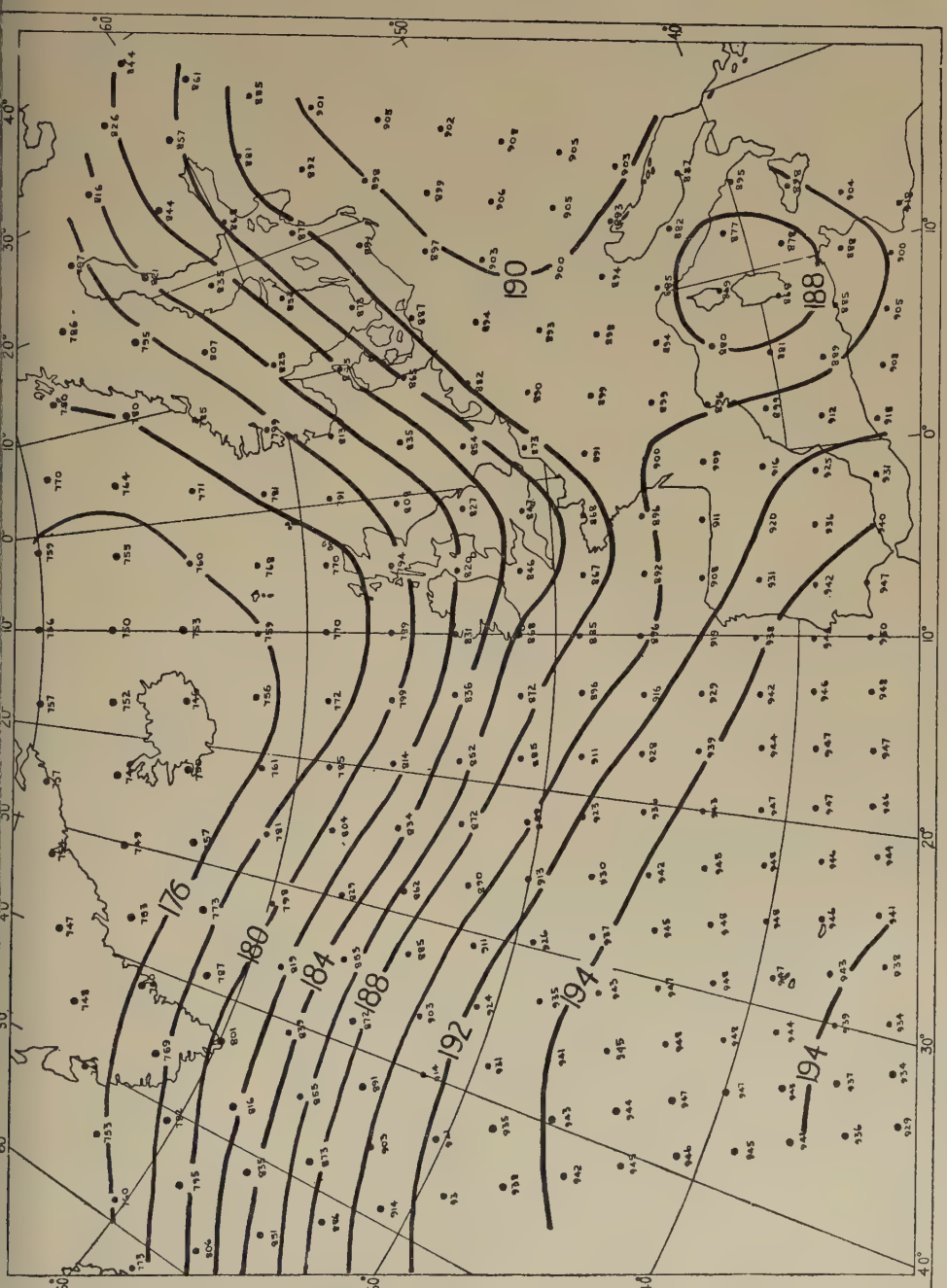

Figure 2 (c). Objective 500-mb analysis for 15 GMT on 12 Sept. 1955. $p = p_{21}$, $q = q_{21}$, $T^2 = 16$ sec^2 (2 sec^2 over European half).

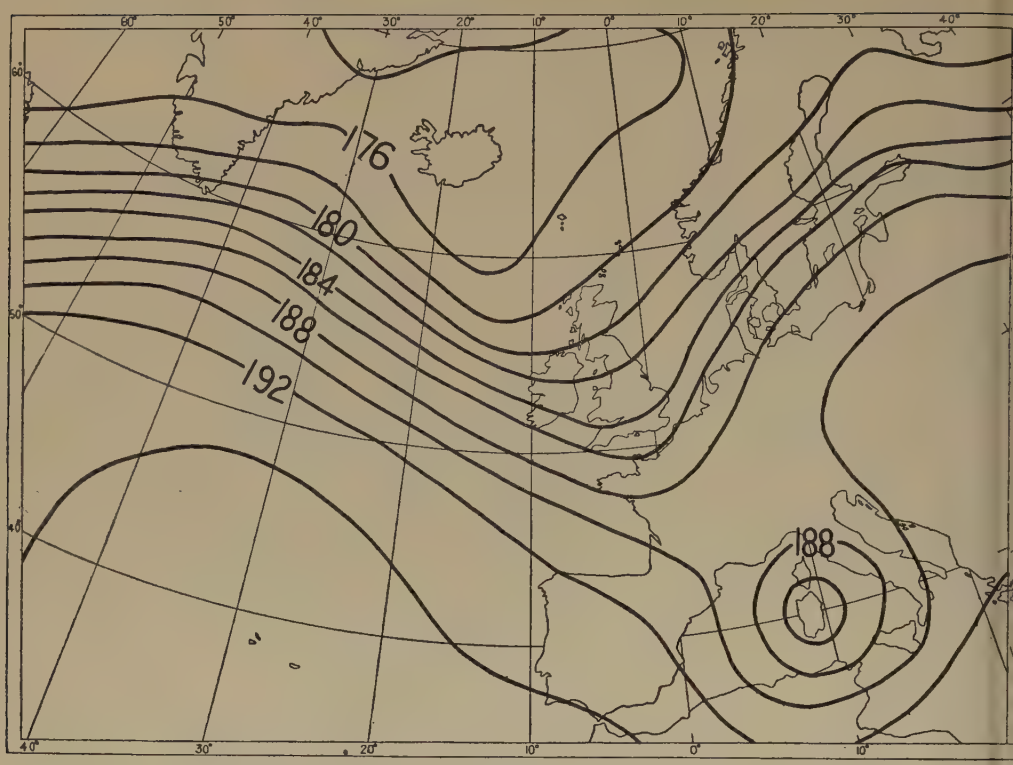

Figure 2 (b). Subjective 500-mb analysis for 15 GMT on 12 Sept. 1955.

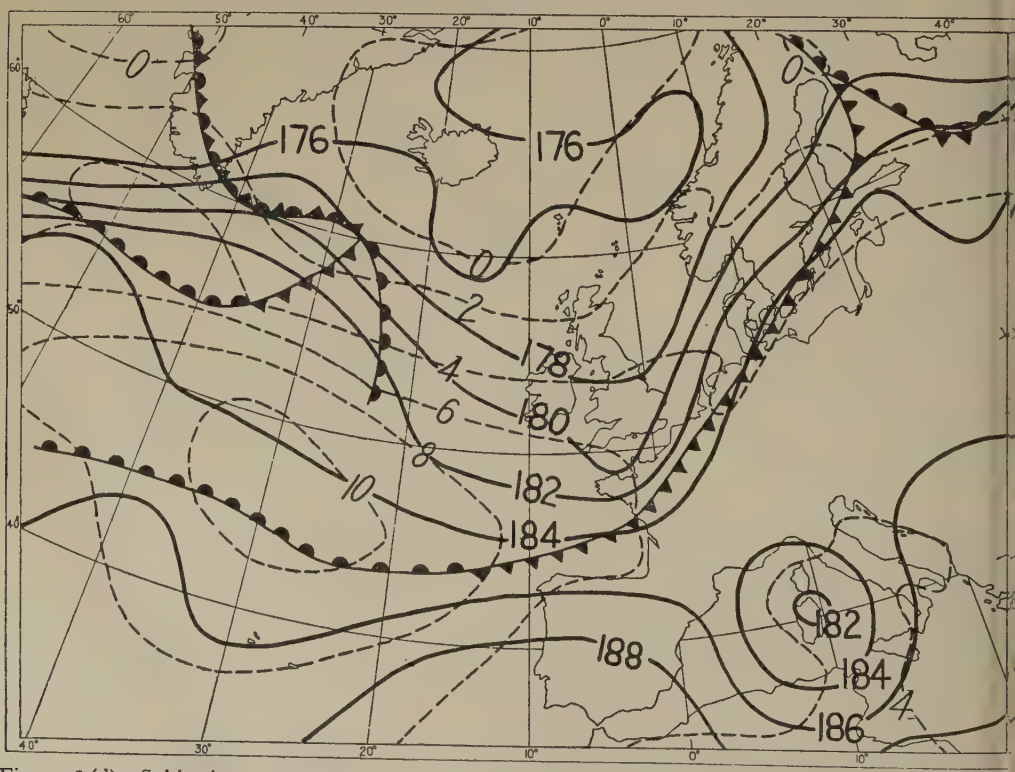

Figure 2 (d). Subjective 1,000-500-mb thickness (———) and 1,000 mb (– – – –) analyses for 15 GMT 12 Sept. 1955.

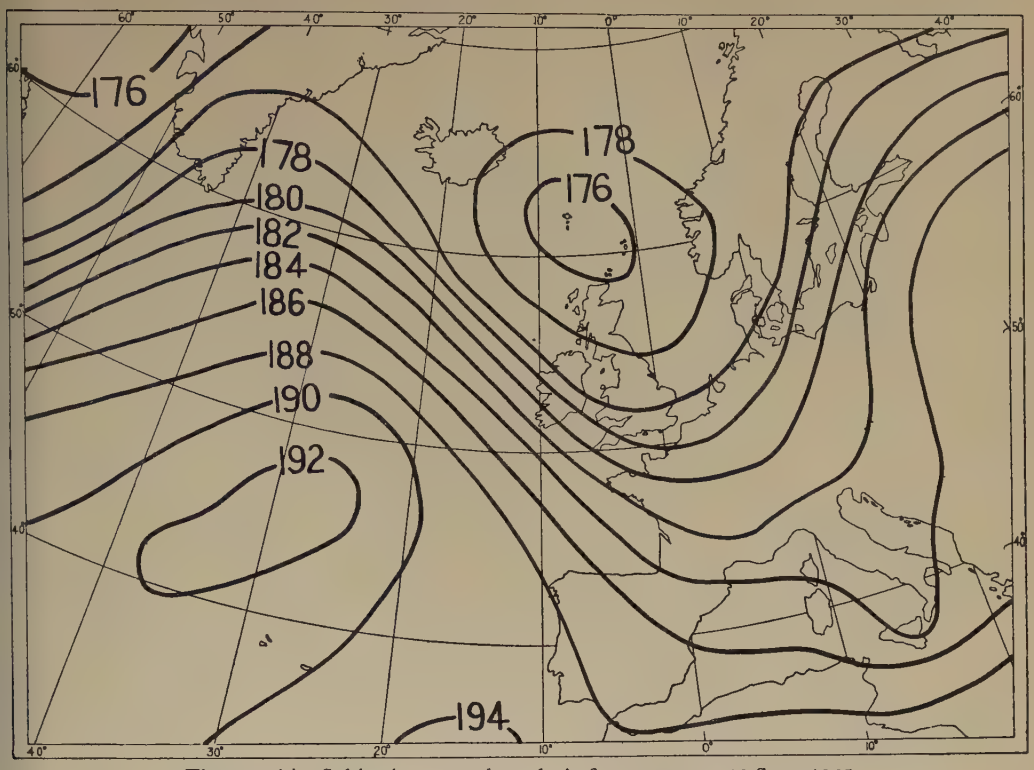

Figure 2 (e). Subjective 500-mb analysis for 15 GMT on 13 Sept. 1955.

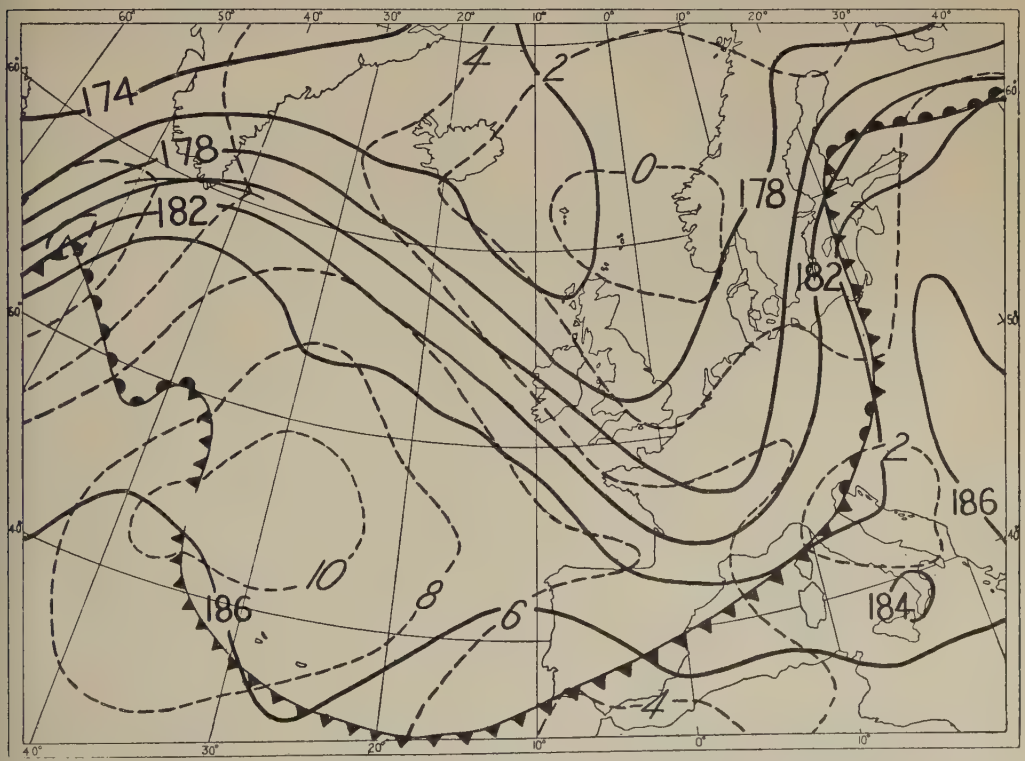

Figure 2 (f). Subjective 1,000-500-mb thickness (———) and 1,000 mb (– – – –) analyses for 15 GMT on 13 Sept. 1955.

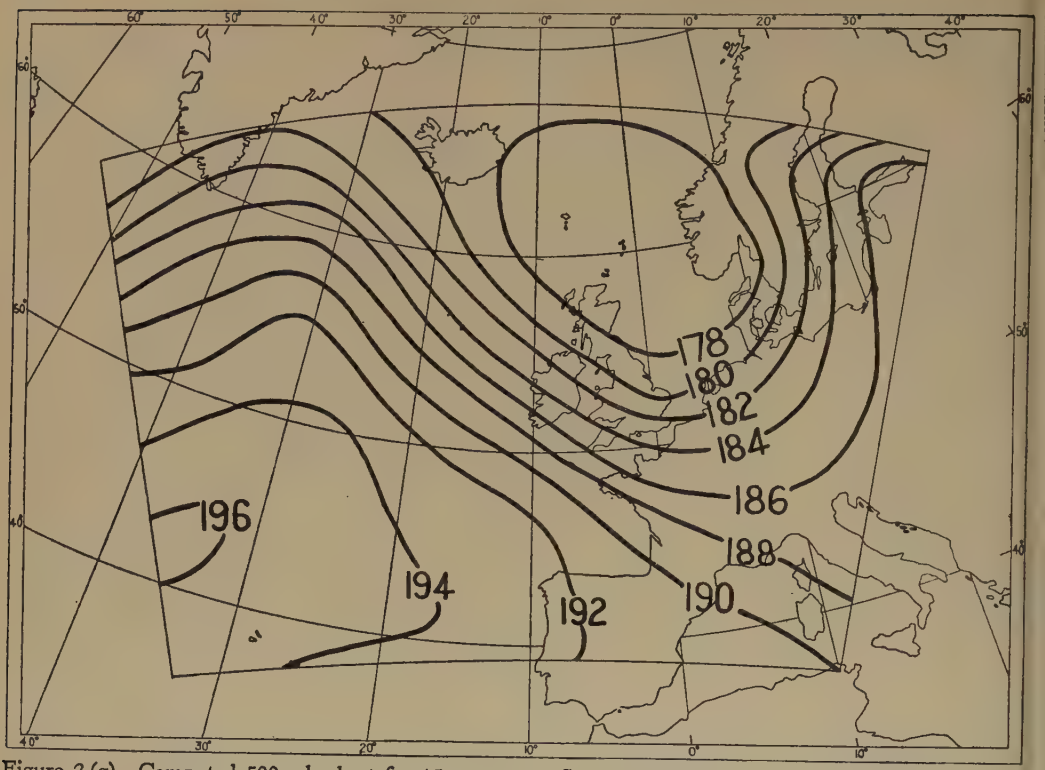

Figure 2 (g). Computed 500-mb chart for 15 GMT on 13 Sept. 1955 based on subjectively-analysed data.

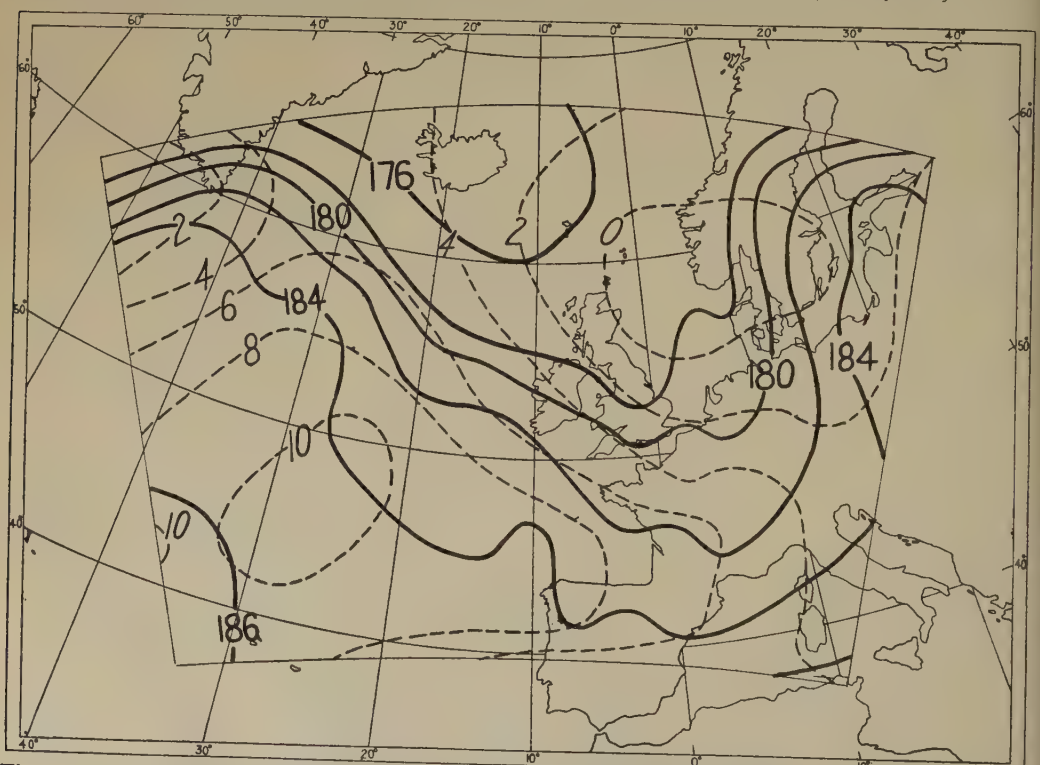

Figure 2 (h). Computed 1,000-500-mb thickness (———) and 1,000-mb contours (- - - -) for 15 GMT on 13 Sept. 1955 based on subjectively-analysed data.

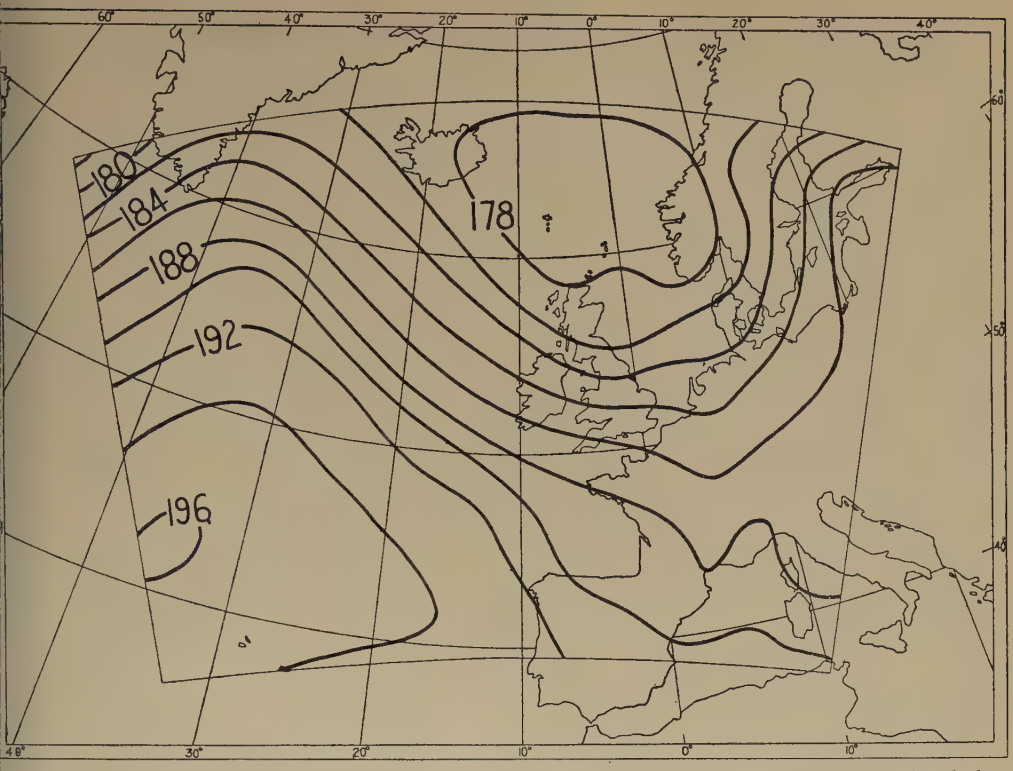

Figure 2 (i). Computed 500-mb chart for 15 GMT on 13 Sept. 1955 based on objectively-analysed data.

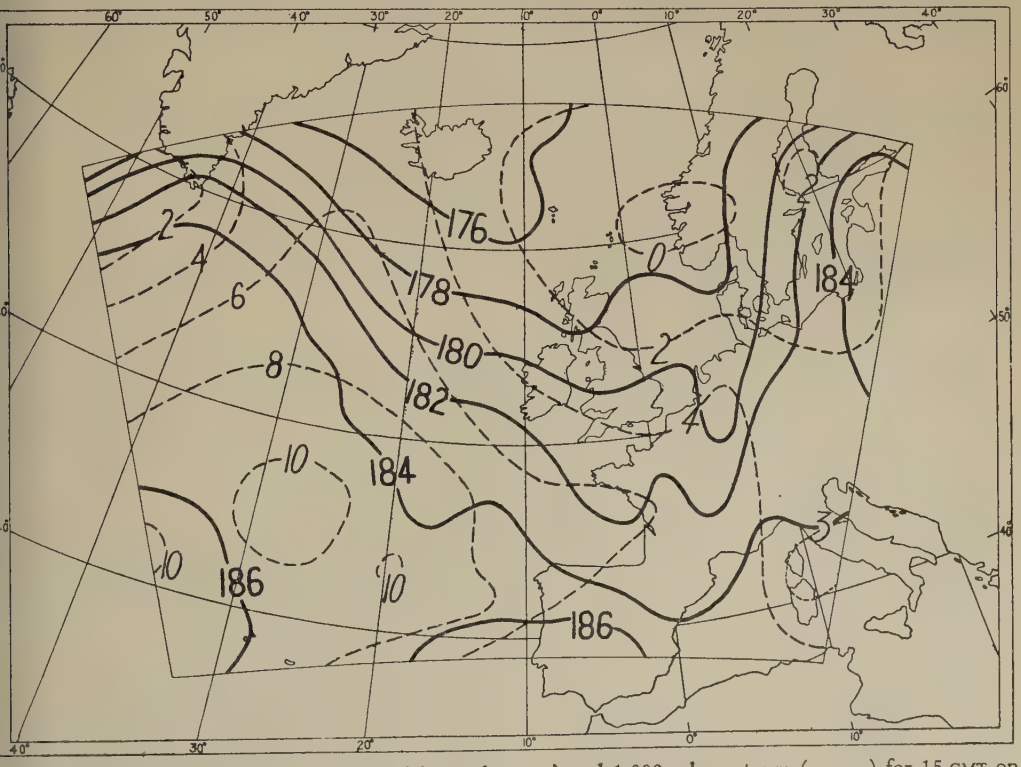

Figure 2 (j). Computed 1,000-500-mb thickness (———) and 1,000-mb contours (- - - -) for 15 GMT on 13 Sept. 1955 based on objectively-analysed data.

in which a strong jet stream in Mid-Atlantic extended across the British Isles within th next 24 hours. Subjective analyses of both the thickness and 500-mb contour charts a this time have been reproduced in a paper by Bushby and Huckle (1956). A compariso of the two techniques of analysis shows no apparent difference in the results obtaine for this situation, a rather surprising fact in view of the strong gradients involved.

4. Time integration based on subjective and objective analyses

(a) General

Twenty-four hour forecasts were computed on both subjectively- and objectively analysed data for the four situations mentioned in the previous section. The computation were based on the Sawyer-Bushby (1953) two-parameter model atmosphere. The actua changes of the parameters on the boundary were used as boundary conditions, and th effect of sea-surface heating was included (Bushby and Hinds 1955). The 600-mb leve was taken as the level which best represented the mean horizontal flow of the atmosphere.

TABLE 1. Correlation and regression coefficients

Date 15 GMT	Method of analysis	500 mb			1,000-500 mb			1,000 mb		
		r	a	b	r	a	b	r	a	b
12 Sept. 1955	Subjective	0·95	0·96	− 3·40	0·91	1·10	0·70	0·87	0·72	− 3·50
	Objective	0·92	0·71	− 4·30	0·85	1·04	− 1·14	0·89	0·92	− 3·50
	Subjective prebaratic	–	–	–	–	–	–	0·83	1·46	− 3·14
15 Oct. 1955	Subjective	0·82	0·98	− 6·9	0·90	0·77	− 5·4	0·81	0·90	− 3·60
	Objective	0·90	0·99	− 8·4	0·88	0·74	− 4·2	0·81	0·92	− 6·60
	Subjective prebaratic	–	–	–	–	–	–	0·34	0·33	− 5·68
31 Oct. 1955	Subjective	0·93	1·21	− 8·1	0·83	1·01	− 5·37	0·86	1·29	1·65
	Objective	0·92	1·14	2·09	0·85	0·91	− 3·80	0·85	1·30	8·56
	Subjective prebaratic	–	–	–	–	–	–	0·67	1·23	− 3·83
30 Jan. 1952	Subjective	0·47	0·40	− 28·20	0·72	0·69	− 5·5	0·58	0·63	− 26·9
	Objective	0·60	0·69	− 35·20	0·86	0·72	− 5·4	0·76	0·80	− 31·6
	Subjective prebaratic	–	–	–	–	–	–	0·79	0·92	− 1·6*

r = correlation coefficient; a, b are the regression coefficients of the best fitting straight line giving the actual change (Y in tens of feet or millibars*) in terms of the forecast change (X in tens of feet or millibars*) in the form $Y = aX + b$, where b is in tens o feet or millibars*.

The correlation coefficients given in Table 1 show little difference between the computations based on subjectively- and objectively-analysed data in three of the four situations, but in the computations based on data for 15 GMT, 30 Jan. 1952 the correlation coefficients imply that the calculations which used the objectively-analysed data gave much better results than those using the subjective analysis. This case is therefore described in detail in sub-section 4 (c). However, although Table 1 suggests that the computations for the other three situations were not significantly affected by the choice of initial analysis, an inspection of the resulting charts did show some differences of detail. The results for one of these situations, that of 15 GMT, 12 Sept. 1955, are therefore also described in detail (sub-section 4 (b)).

It is also worth noting that the surface prebaratics prepared by the conventional forecaster for 18 GMT on 16 Oct. 1955 and for 18 GMT on 31 Oct. 1955 were less accurate than the 1,000-mb numerical forecasts for 15 GMT on those days. The conventional surface forecasts for the other two situations were of the same order of accuracy as the numerical forecasts, although the numerical forecast for 15 GMT on 31 Jan. 1952 based

on subjectively-analysed data was less accurate than both the conventional forecast and the numerical forecast based on objectively-analysed data.

(*b*) *12 September 1955*

On the 500-mb chart for 15 GMT, 12 Sept. 1955 (Fig. 2 (b)) there was the suggestion of a double trough, the northern one to the west of the British Isles and the southern one over the British Isles. Twenty-four hours later (Fig. 2 (e)) there was a very broad irregular trough from Scotland across Europe to Italy, with still a slight suggestion of a double trough. There was a very strong flow from Greenland to the British Isles. The computation (Fig. 2 (g)) based on subjectively-analysed data gives a trough east of the actual position and not broad enough. There is a strong flow across the Atlantic from Greenland to the British Isles but it continues round the trough whereas there was actually a diffluence. The values of the contours are too high in the south-west of the area and over Ireland. The computation based on objectively-analysed data also gives the heights too high, those over Ireland being higher than in the previous computation. As a result of this, the flow in the Atlantic is not strong enough. The trough is in the right position and is very broad, but owing to the height error it appears as a shallow trough and the double trough is over-emphasized.

On the 1,000-500-mb thickness charts (Figs. 2 (d) and 2 (f)), a broad trough just west of the British Isles became stronger and moved to the east of the British Isles, a ridge forming in the Atlantic, south of Greenland. The computation (Fig. 2 (h)) based on subjective analysis gives a ridge over southern Greenland and a broad trough over the British Isles with small-scale oscillations superimposed on it. These may be due to computational instability. The values of the height agree fairly well with the actual chart. The chart (Fig. 2 (j)) produced from objectively-analysed data is very similar to the one mentioned above. The irregularities are more marked and the thickness is wrong by about 200 ft over the British Isles.

On the 1,000-mb charts (Figs. 2 (d) and 2 (f)) there was an almost stationary anticyclone in the Atlantic with a depression moving south-east from Iceland. There were two troughs associated with the depression, one being a frontal trough and one connected with the thickness trough. The computation (Fig. 2 (h)) based on subjectively-analysed data gave an anticyclone of the right intensity in the right position and a depression of the right intensity but too far east. Two troughs appeared but they were not emphasized enough. The objective analysis produced a similar chart (Fig. 2 (j)). The frontal trough was correctly placed and there was a more pronounced ridge over the Low Countries. The values were too high over the British Isles in both computations, that based on objectively-analysed data giving the higher values.

(*c*) *30 January 1952*

This case has been computed using several variations of the basic two-parameter method. The computation based on subjectively-analysed data using the same method as was used for the other three cases mentioned in this report is described by Bushby and Huckle (1956). At 500 mb the computation based on subjectively-analysed data has a strong jet stream terminating in a diffluent trough that is much too far east. The jet stream is not intense enough and is too far north. Over Southern England, the heights are 1,200 ft too high. When the computation was repeated on objectively-analysed data (Fig. 3 (c)) the diffluent trough was placed much nearer its actual position. The jet stream is still not intense enough and too far north, the height over Southern England in this case being 1,000 ft too high. In the computation based on subjectively-analysed data, the axis of the thickness trough was computed to be too far north and east and not

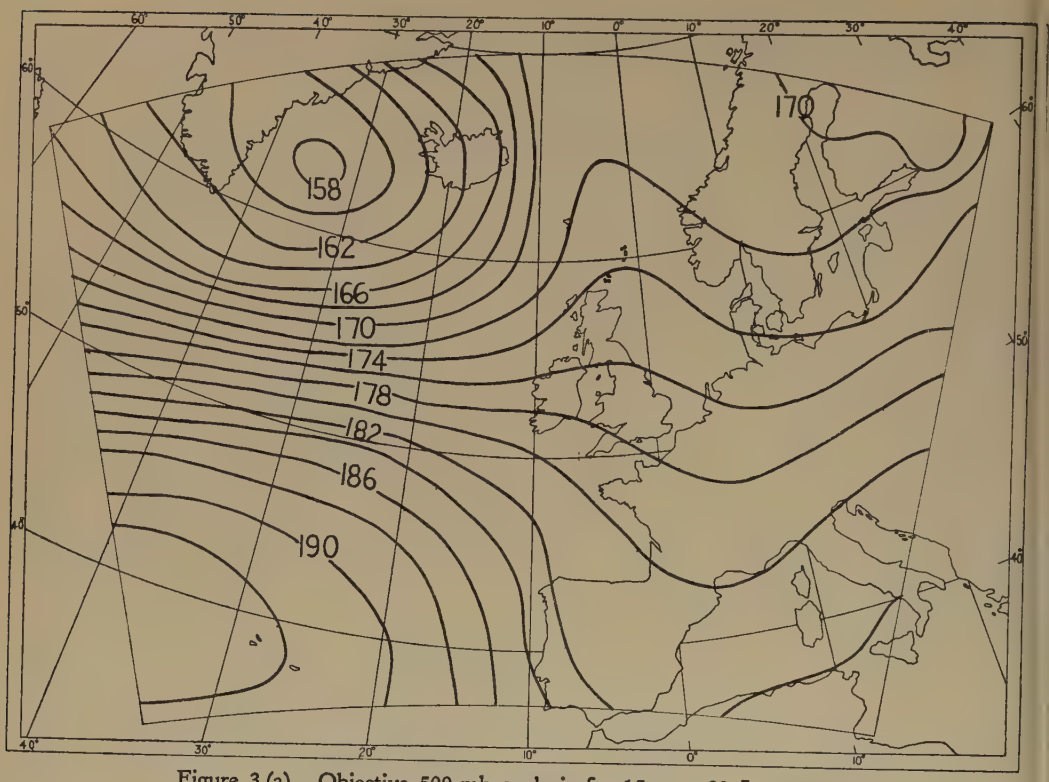

Figure 3 (a). Objective 500-mb analysis for 15 GMT, 30 Jan. 1952.

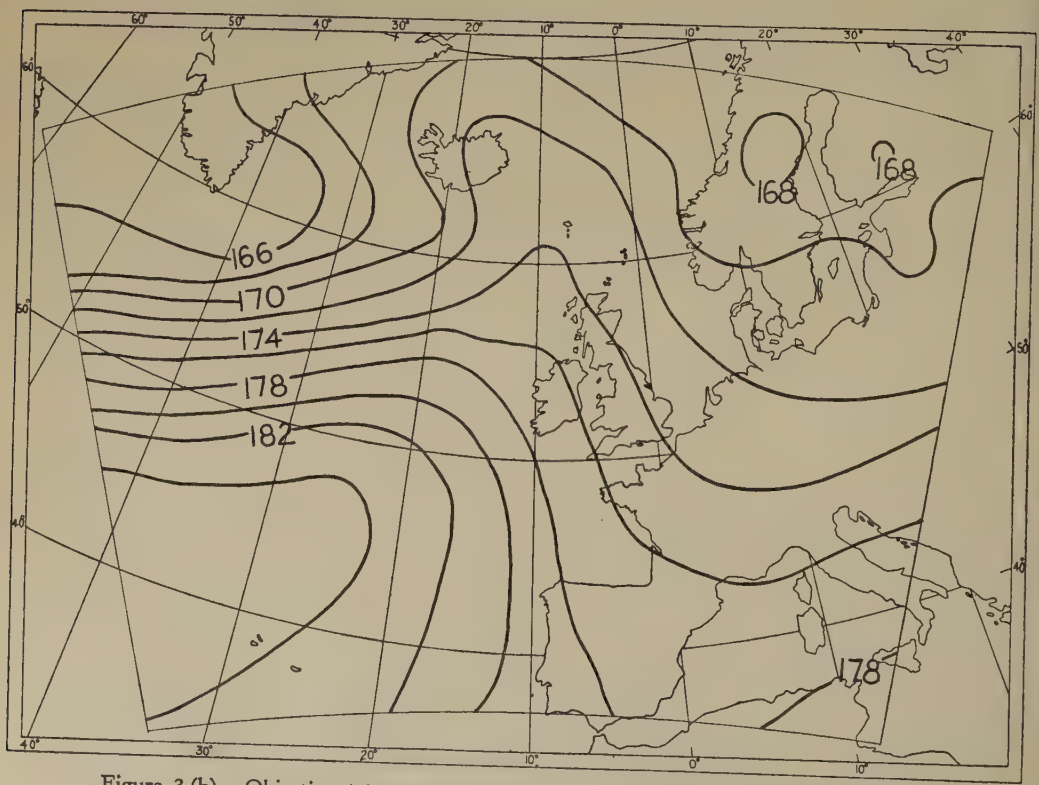

Figure 3 (b). Objective 1,000-500-mb thickness analysis for 15 GMT, 30 Jan. 1952.

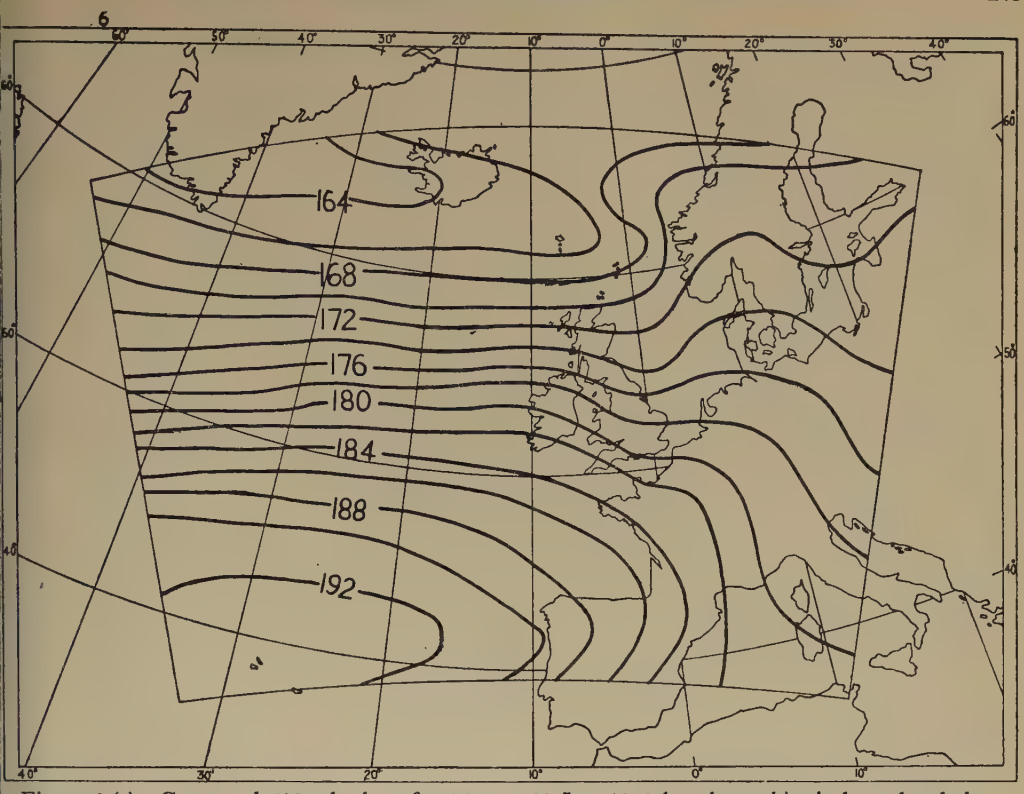

Figure 3 (c). Computed 500-mb chart for 15 GMT, 31 Jan. 1952 based on objectively-analysed data.

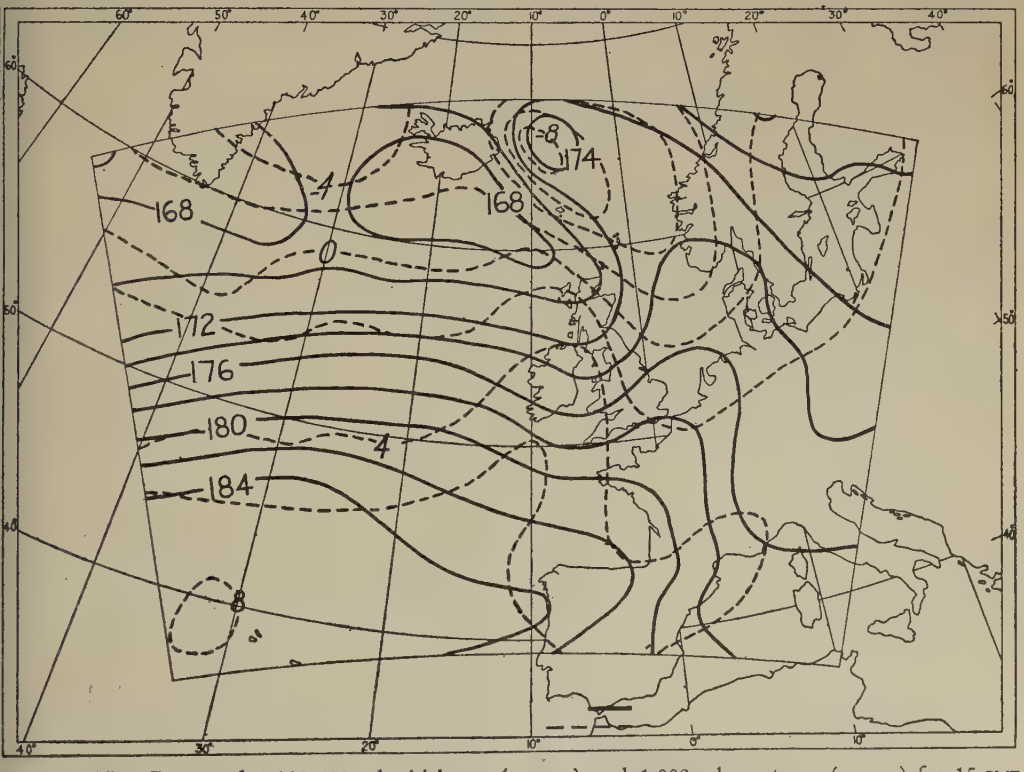

Figure 3 (d). Computed 1,000-500-mb thickness (———) and 1,000-mb contours (– – – –) for 15 GMT, 31 Jan. 1952 based on objectively-analysed data.

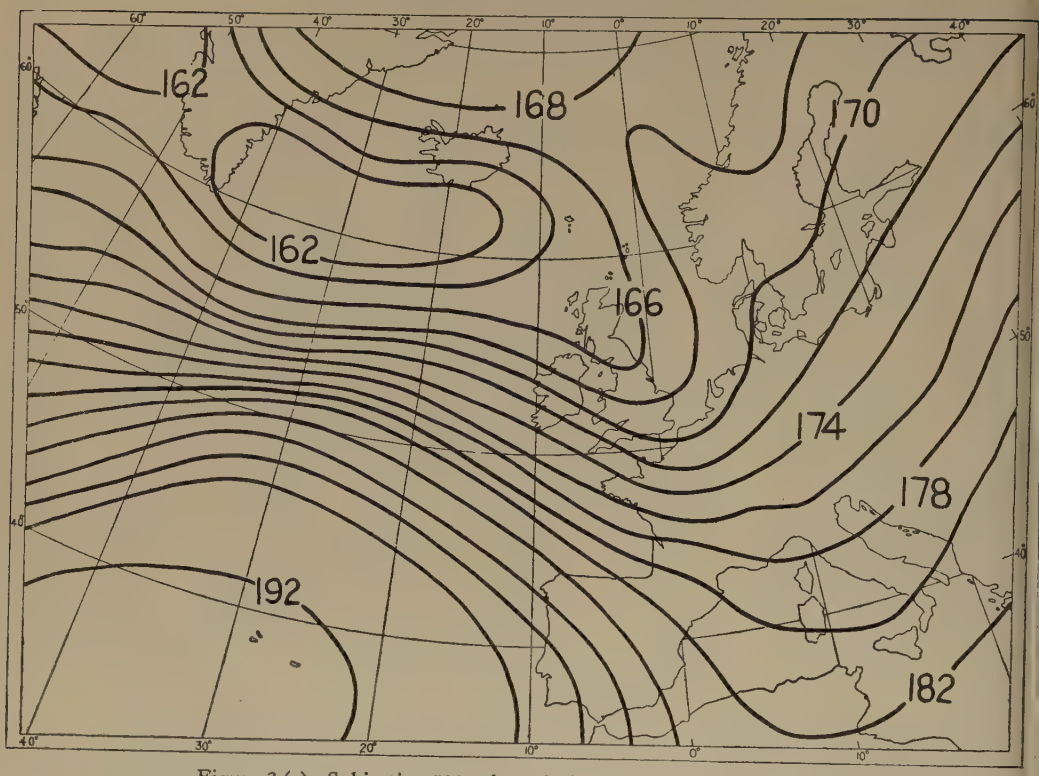

Figure 3 (e). Subjective 500-mb analysis for 15 GMT, 31 Jan. 1952.

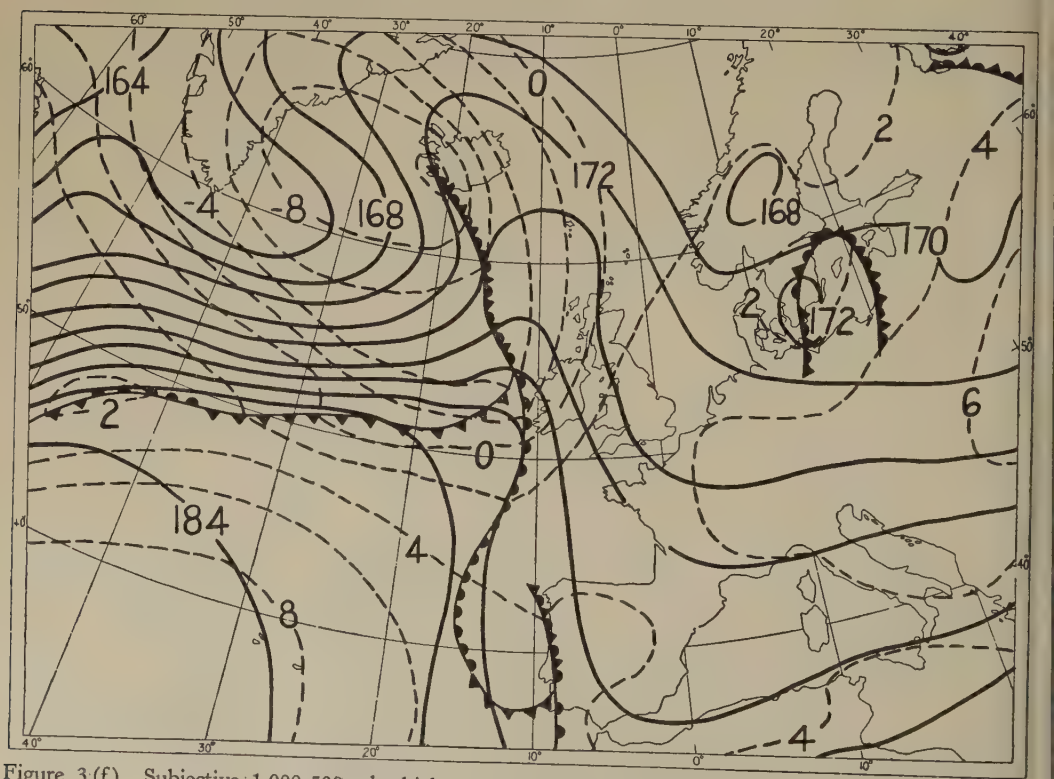

Figure 3 (f). Subjective 1,000-500-mb thickness (———) and 1,000-mb contours (– – –) for 15 GMT, 31 Jan. 1952.

rving enough. The ridge near it was also wrongly situated and shaped. In the com-
tation based on objectively-analysed data (Fig. 3 (d)) the position and shape of the
ough and ridge are very near the actual position and shape. The values are only 400 ft
high over the British Isles. The computation based on subjectively-analysed data for
00 mb gave a series of ridges and troughs right across the Atlantic, with the main
ough over Europe and the ridge over the North Sea, instead of an almost straight flow
ross the Atlantic with a ridge west of Ireland and a trough over the North Sea. In the
mputation based on objective analysis (Fig. 3 (e)) there was a much smoother flow
ross the Atlantic with a ridge over Ireland and a trough down the North Sea.

5. Conclusions

It is evident that for the four situations under consideration, a good analysis can
e produced objectively by fitting a quadratic surface to the observations and forecast
lues. The best values for the constants appear to be $T^2 = 16$ sec^2, $p = p_2$ and $q = q_2$,
though $T^2 = 2$ sec^2 is satisfactory over Europe. There does not appear to be any
dvantage in increasing the length and complexity of the computations in order to use a
ubic surface. Indeed in one or two areas it appears that the quadratic surface probably
ves a better answer than the cubic surface as it introduces a greater measure of smoothing.
he cubic surface with its extra degrees of freedom is able to fit more closely both the
bservations and forecast values, and this is not necessarily a good thing in regions not
ear a reporting station.

The results of the numerical forecasts based on the objective analyses show that the
bjective-analysis technique is a practical method for obtaining the initial values of the
arameters required for the time integrations. The initial values can be obtained in a
uitable form for further numerical work much more quickly by using the objective-
nalysis technique than by using subjective analysis. In general, the results of the numerical
orecasts indicate that small-scale features are sometimes lost when objective analysis is
sed, although the main features are dealt with quite accurately. On one occasion the
bjective analysis of the data has resulted in a better numerical forecast than that produced
y using subjectively-analysed charts.

It appears from these four situations that the objective-analysis technique described
n this paper will produce an analysis good enough for use as a basis for numerical fore-
asting. The results of the numerical forecasts computed from these data are only
lightly different from those produced from subjectively-analysed initial data in three
ut of the four situations. It seems likely that in regions of strong gradients the objective-
nalysis technique may well provide a necessary degree of smoothing and thus produce
etter numerical forecasts than would be obtained by using data interpolated from
ubjective analyses produced under practical working conditions.

Acknowledgments

The authors wish to acknowledge the permission of the Director of the Meteorological
Office to publish this paper and they also wish to thank those members of the Forecast
Research Division staff at Dunstable who have prepared the data in a suitable form for
he machine.

References

ergthorrson, P. and Döös, B.	1955	*Tellus*, **7**, p. 329.
ushby, F. H. and Hinds, M. K.	1955	*Quart. J. R. Met. Soc.*, **81**, p. 396.
ushby, F. H. and Huckle, V. M.	1956	*Ibid.*, **82**, p. 409.
ilchrist, B. and Cressman, C. P.	1954	*Tellus*, **6**, p. 309.
ohnson, D. H.	1956	*Air Ministry, Met. Res. Ctee.*, M.R.P., No. 965.
awyer, J. S. and Bushby, F. H.	1953	*J. Met.*, **10**, p. 54.

551.558.3

Air motion over a heated land mass : II

By R. C. SMITH
Imperial College, London

(Manuscript received 17 May 1956, in revised form 18 February 1957)

SUMMARY

In a previous paper (Smith 1955), the problem of the resultant theoretical velocity field that arises from the diurnal variation of heating of a land mass with an initially stationary air mass was considered. The present paper considers the same problem with an initial overall velocity. Henceforth the first paper (Smith 1955) will be referred to as Part I.

The same heat function is used as in Part I for the time and horizontal variations, but the vertical variation is amended for closer approximation to the different circumstances. The difficulty of the boundary condition at infinite height is overcome by associating the solutions with those of Pt. I.

The resulting surface temperatures and vertical velocities at different times are shown in tables and graphs.

1. INTRODUCTION

The situation differs from that considered in Part I. The air, as it is heated, is continually carried away from its source out to sea. There is an additional form of energy in the kinetic energy of the original air current, and the whole model has lost its symmetry with respect to x, since cool air is being brought in over one coast and heated air taken out over the other.

2. LIST OF SYMBOLS USED

B_+ defined by Eq. (13)

C, D arbitrary constants

f twice the vertical component of the earth's rotation

g gravity

H_0 numerical constant

σ, k wave numbers in time and distance

n constant determining the exponential rate of decrease of heating in the vertical

p_0 pressure

T constant determining the rate of heating

U_0 initial overall velocity perpendicular to the coast

W vertical velocity

x, y, z horizontal coordinates perpendicular and parallel to the coast, and vertical coordinate

β stability; $\beta \times$ temperature = adiabatic lapse rate − actual lapse rate

τ_0, Γ reciprocal of potential temperature and disturbance thereof

ρ_0 density

$\rightleftharpoons$ real part of

The following symbols are those used for the variable when it refers to one pair of alues of σ, k :

(z, x, t) heating function
H_1 defined by Eq. (10)
p disturbance of pressure
u, v horizontal velocities perpendicular and parallel to the coast
w_+, w_- vertical velocities proportional to $\exp\{-i(kx + \sigma t)\}$ and $\exp\{i(kx - \sigma t)\}$ respectively
λ defined by Eq. (13)
Σ_+, Σ_- defined by Eq. (8)
ρ disturbance of density
τ disturbance of reciprocal of potential temperature

3. The initial equations

p_0 is a function of y and z only. The three equations of motion, taking

$$\frac{\partial}{\partial y} = 0 \quad . \quad . \quad . \quad . \quad . \quad (1)$$

xcept in so far as

$$\frac{\partial p_0}{\partial y} = -\rho f U_0$$

ecome, ignoring terms of the form $u\frac{\partial u}{\partial x}$ compared to $\frac{\partial u}{\partial t}$ and $U_0\frac{\partial u}{\partial x}$, and omitting Coriolis orces as in Part I :

$$\frac{\partial u}{\partial t} + U_0\frac{\partial u}{\partial x} = -\frac{1}{\rho_0 + \rho}\frac{\partial p}{\partial x} \quad . \quad . \quad . \quad . \quad (2)$$

$$\frac{\partial v}{\partial t} + U_0\frac{\partial v}{\partial x} = 0 \quad . \quad . \quad . \quad . \quad . \quad (3)$$

$$\frac{\partial w}{\partial t} + U_0\frac{\partial w}{\partial x} = -\frac{1}{\rho_0 + \rho}\frac{\partial}{\partial z}(p_0 + p) - g \quad . \quad . \quad . \quad (4)$$

Neglecting the variation of density in the equation of continuity, we write

$$\frac{\partial u}{\partial x} + \frac{\partial w}{\partial z} = 0 \quad . \quad . \quad . \quad . \quad (5)$$

Physically the neglect of the $\frac{1}{\rho}\frac{D\rho}{Dt}$ term only becomes important when we are dealing ith the diurnal variation of temperature over a land mass more than 1,000 km wide. he author (Smith 1954) showed this more fully, but the demonstration is of considerable ength and for that reason is omitted from the present paper.

The equation of added heat

$$\frac{D}{Dt}(\tau_0 + \tau) = H(x, z, t)$$

ecomes, neglecting the smaller terms,

$$\frac{\partial \tau}{\partial t} + U_0\frac{\partial \tau}{\partial x} + w\frac{\partial \tau_0}{\partial z} = H(x, z, t) \quad . \quad . \quad . \quad (6)$$

The modified pressure is introduced as in Pt. I, Eq. (7), and the solution of th problem is represented by a Fourier integral. The variables are taken as proportiona to $\exp\{\pm ikx - i\sigma t\}$ where σ and k are wave numbers for the time and distance respect ively, and are substituted in Eqs. (2) to (6).

Thus we get :

$$\frac{\partial^2 w_+}{\partial z^2} + \frac{(g\beta - \Sigma_+^2)}{\Sigma_+^2} k^2 w_+ + \frac{gH k^2}{\Sigma_+^2} = 0 \quad . \quad . \quad . \quad (7a$$

for variables proportional to $\exp\{-ikx - i\sigma t\}$ and

$$\frac{\partial^2 w_-}{\partial z^2} + \frac{(g\beta - \Sigma_-^2)}{\Sigma_-^2} k^2 w_- + \frac{gH k^2}{\Sigma_-^2} = 0 \quad . \quad . \quad . \quad (7b$$

for variables proportional to $\exp\{ikx - i\sigma t\}$ where

$$\Sigma_+ = \sigma + U_0 k, \qquad \Sigma_- = \sigma - U_0 k \quad . \quad . \quad . \quad (8$$

The coefficient of $\frac{\partial w}{\partial z}$ in the differential equation is β ($= 10^{-2}$ km^{-1}) and thus its elimination by substitution introduces a factor $e^{\beta z}$. This, by inspection, negligibly affects e^{-nz} ($n = 2$ km^{-1}) and can also be shown to affect negligibly the other part of the solution even at infinity. Thus the term in $\frac{\partial w}{\partial z}$ has been omitted from Eqs. (7a) and (7b).

We will now proceed to discuss the heating function.

4. The heating function

For our present example we are going to take the velocity of our deep and steady current to be 10 m/sec. This means that the air takes 2×10^4 sec or $5\frac{1}{2}$ hr to cross the 200-km wide land mass and does not attain such a high temperature as was the case in Part I. This in its turn implies that the depth of the heated layer is not so great as it was in the first case, since the bubbles of heated air only reach a height determined by their size and potential temperature and both these quantities are reduced by an overall velocity. It is reasonable therefore to reduce the virtual depth of our heated layer in the heating function by introducing e^{-4z} instead of e^{-2z}. In this case $\frac{6}{7}$ of the heat is put in below $\frac{1}{2}$ km height and $\frac{3}{5}$ below $\frac{1}{4}$ km.

It would appear also that there should be some relation between the horizontal and vertical distributions of the heating function since the air near the ground has to move some distance inland before it acquires a sufficient potential temperature to reach the required height. This is indeed true for the perfect case of no surface friction but, when this is active, we have a thin layer of heated air close to the surface or held in sheltered pockets in the topography. These bubbles would be released at periodic intervals. If they were rising at $\frac{1}{2}$ m/sec they would take 1,000 sec to rise to the $\frac{1}{2}$ km, level and in that time they would have moved 10 km inland. A similar situation arises on the leeward coast, where the bubbles from the heated land mass reach a height of $\frac{1}{2}$ km, 10 km out to sea. However, we may allow for these two discrepancies by choosing the same horizontal distribution of the heating function as we had in Part I and assuming that the land mass, instead of extending from + 100 km to − 100 km, extends from + 105 km to − 95 km. This would give a good approximation to what we want.

The variation of heating with time is also taken to be identical with that in Part I. Of course, the actual temperature distribution will not be the same as in Part I, as will be seen, but it is reasonable to assume that the heating, by means of insolation and convection, will take a similar form.

Thus our heating function is given by

$$H_2 = -i H_0 e^{-nz} \int\int_0^\infty \frac{e^{-\sigma\tau - i\sigma t}(e^{ikx} - e^{-ikx})}{k} d\sigma\, dk$$

$$\left[\equiv -i e^{-nz} \int\int_0^\infty H_1 (e^{ikx} - e^{-ikx})\, d\sigma\, dk\right] . \quad . \quad (10)$$

as in Part I Eq. (15b), where H_1 is defined and H_0 is a numerical constant.

5. Mathematical evaluation of W

We must first examine the magnitudes of Σ_+^2, Σ_-^2 and $g\beta$. As was shown in Part I, for a static stability which corresponds to a lapse rate 3°C/km less than the dry adiabatic in the lowest kilometre, the value of $g\beta$ is 10^{-4} sec^{-2}. It was also shown in Part I that $\sigma > 10^{-3}$ sec^{-1} corresponded to periods of heating of less than $\frac{1}{2}$ hr and affected our equations negligibly. We now have an additional term $U_0 k$. For this to exceed 10^{-3} sec^{-1}, k must exceed 10^{-1} km^{-1} which implies that we are concerned with distances considerably less than 10 km. This is not so in the present paper as the final calculations are made over steps of 20 km so that we may neglect Σ_+^2 and Σ_-^2 compared to $g\beta$ in Eqs. (7a) and (7b). This gives us :

$$\frac{\partial^2 w_+}{\partial z^2} + \frac{g\beta k^2 w_+}{\Sigma_+^2} + \frac{gH_1 k^2 e^{-nz-ikx}}{\Sigma_+^2} = 0 \quad . \quad . \quad . \quad (11a)$$

$$\frac{\partial^2 w_-}{\partial z^2} + \frac{g\beta k^2 w_-}{\Sigma_-^2} + \frac{gH_1 k^2 e^{-nz+ikx}}{\Sigma_-^2} = 0 \quad . \quad . \quad . \quad (11b)$$

The solution to (11a) is :

$$w_+ = \frac{B_+ e^{-nz}}{n^2 + \left(\frac{\lambda}{1+\lambda}\right)^2} + C e^{\frac{i\lambda z}{1+\lambda}} + D e^{-\frac{i\lambda z}{1+\lambda}} . \quad . \quad . \quad (12)$$

where

$$B_+ = -\frac{gH_1 k^2 e^{-ikx}}{\tau_0 \Sigma_+^2}, \qquad \lambda = \frac{(g\beta)^{\frac{1}{2}} k}{\sigma} = \frac{10^{-2} k}{\sigma} = \frac{U_0 k}{\sigma} \quad . \quad . \quad (13)$$

and C and D are arbitrary constants. Similarly for w_-.

6. Boundary conditions

On examining Eq. (12) we see that as in Part I we are faced with the difficulty of finding the second arbitrary constant; putting $w = 0$ at $z = \infty$ once again yields nothing.

The boundary condition $w = 0$ at $z = 0$ still gives us one relation between the constants. In effect we have the same choice that faced us in Part I and in this case it seems impossible to verify our choice in the same way (Part I, p. 389, 2nd paragraph) since we have a coefficient of w, $\frac{\lambda^2}{(1+\lambda)^2}$ which, when λ is made an imaginary quantity, not only changes sign but introduces an imaginary term. Thus our second method of evaluation as in Part I, which transformed the coefficient of w into a negative quantity and gave a solution of the form $e^{\pm\lambda z}$, breaks down.

We can however overcome the difficulty by another method. In the initial equations we neglected terms like $u\frac{\partial u}{\partial x}$ in comparison with $\frac{\partial u}{\partial t}$ and $U_0 \frac{\partial u}{\partial x}$. If, on the other hand,

we state that $u\frac{\partial u}{\partial x}$ was neglected only in comparison with $\frac{\partial u}{\partial t}$ even though it may be small compared with $U_0\frac{\partial u}{\partial x}$ we may assume that the solutions for the transition from $U_0 = 0$ to $U_0 = \text{const.}$ are continuous and say that our present solution must be identical with that of Pt. I when $U_0 = 0$. Thus we have found the arbitrary constants by choosing a solution for the $U_0 = 0$ case (Part I first solution of w), showing by another method that this was indeed the solution (Part I, second solution of w), and then making the assumption that the present solution must be identical with that of Part I when U_0 is put equal to zero.

This leads to the solution

$$w_+ = \frac{B_+}{n^2 + \left(\frac{\lambda}{1+\lambda}\right)^2}\left\{e^{-nz} - e^{-\frac{i\lambda z}{1+\lambda}}\right\} \quad . \quad . \quad . \quad (14a)$$

$$w_- = \frac{B_-}{n^2 + \left(\frac{\lambda}{1-\lambda}\right)^2}\left\{e^{-nz} - e^{-\frac{i\lambda z}{1-\lambda}}\right\} \quad . \quad . \quad . \quad (14b)$$

On substituting for B_-, B_+ and H_1 and integrating over σ and k in the manner given by the initial heating function we get for the final vertical velocity

$$W = \frac{ig\,H_0 \cdot 10^4}{\tau_0}\int\int_0^\infty \frac{\lambda^2 e^{-\sigma T - i\sigma t}}{k}\left\{\frac{e^{ikx}\left(e^{-nz} - e^{-\frac{i\lambda z}{1-\lambda}}\right)}{n^2(1-\lambda)^2 + \lambda^2} - \frac{e^{-ikx}\left(e^{-nz} - e^{-\frac{i\lambda z}{1+\lambda}}\right)}{n^2(1+\lambda)^2 + \lambda^2}\right\} d\sigma\, dk\,. \quad (15)$$

By substituting for k in terms of λ from Eq. (13) we may integrate directly over σ.

By using the theory of residues we may split the λ-integration into two parts to make the numerical work simpler, and we obtain two terms similar in form to Eqs. (23) and (24) in Part I but a good deal more lengthy. For that reason they have been omitted from the present paper.

The integrand of Eq. (15) shows, as would be expected, that the values of the vertical velocity for $+x$ and $-x$ are now completely different and not antisymmetrical as in Part I.

We will now find the time rate of change of the inverse of potential temperature at the ground, $\frac{\partial \tau}{\partial t}$, by using Eq. (6) at $z = 0$

$$\frac{\partial \tau}{\partial t} + U_0\frac{\partial \tau}{\partial x} = H(z, 0, t) \quad . \quad . \quad . \quad . \quad (16)$$

For the different functions $\exp\{\pm ikx - i\sigma t\}$ we then get

$$\tau_+ = \frac{H_1 e^{-ikx}}{-i(\sigma + k\,U_0)} \quad . \quad . \quad . \quad (17a)$$

$$\tau_- = \frac{H_1 e^{ikx}}{-i(\sigma - k\,U_0)} \quad . \quad . \quad . \quad (17b)$$

where τ_+ corresponds to the $\exp\{-i(k\,x + \sigma\,t)\}$ part and τ_- to the $\exp\{i(k\,x - \sigma t)\}$ part.

Thus we get that $\frac{\partial \Gamma}{\partial t}$, where Γ is the final value of the inverse of potential temperature after integration over σ and k has been performed, is given by

$$\frac{\partial \Gamma}{\partial t} = -i H_0 \int\int_0^\infty \frac{e^{-\sigma T - i\sigma t}}{k} \left(\frac{e^{ikx}}{1-\lambda} - \frac{e^{-ikx}}{1+\lambda} \right) d\sigma \, dk$$

$$= \frac{200 \pi H_0 Tx (t - 50x)}{(T^2 - t^2 + 100xt)^2 + 4T^2 (t - 50x)^2} \quad . \quad . \quad . \quad (18)$$

7. Numerical evaluation

The values of the constants and variables used were the same as in Part I except those mentioned below.

$x = -300, -280$, then in steps of 20 km to . . . . 280, 300 km

$t = -5 \times 10^4, -4 \times 10^4 \ldots, 4 \times 10^4, 5 \times 10^4$ sec

$n = 4$ km^{-1}

By numerical integration and substitution the final vertical velocity field was evaluated. The results are given in Figs. 1 to 4.

8. Discussion of results

From Eq. (18) the values of $\frac{\partial (\text{temp})}{\partial t}$ at $z = 0$ were computed for a single heating pulse in time and are shown in Table 1. On examining this table there are two features which stand out immediately – the first most obvious one is that similar values are aligned diagonally apart from $x = 0$; the second is that the potential temperature of the air at the surface, equivalent to its actual temperature there, is changed before reaching the land mass. Now, the second of these is obviously not true in practice, for the effect of heating over a land mass cannot affect the potential temperature of the air an appreciable distance upstream of the land mass. Our model therefore appears to give incorrect results. However the key to the puzzle is found in the first feature noticed in the table. It can be seen on examining Eq. (16) that the solution for τ is not affected if we add a function $f(x - U_0 t)$ to it. This also applies to the integrated temperature changes we have found, so that to our table we may add any such function to make it more consistent with fact. This we can do by making all the temperature changes at $z = 0$ on the windward side of the land-mass zero and amending all the others by adding the same function. The values in Table 1 are for a single heating pulse in time and to get our final results, appropriate to the diurnal variation, we have to add and subtract them in the fashion indicated by Eq. (12) in Part I, to give Table 2.

TABLE 1. Values of $\frac{\partial (\text{temp})}{\partial t}$ in °C/hr at $z = 0$ for a single heating pulse in time as given by Eq. (18)

				x (km)			
	− 300	− 200	− 100	0	100	200	300
t (10^4 sec)							
− 2	0·8	0	− 0·8	− 0·2	0·14	0·06	0·03
− 1	0·4	0·8	0	− 0·2	0·4	0·14	0·06
0	0·14	0·4	0·8	1·0	0·8	0·4	0·14
(09 hr)							
1	0·06	0·14	0·4	− 0·2	0	0·8	0·4
2	0·03	0·06	0·14	− 0·2	− 0·8	0	0·8
3	0·02	0·03	0·06	−0·1	− 0·4	− 0·8	0

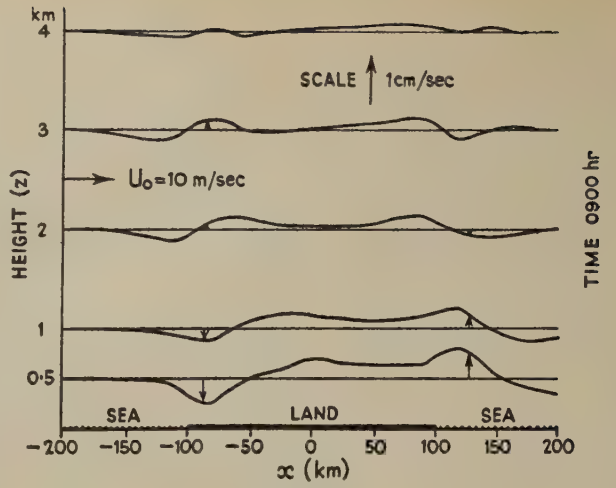

Figure 1.

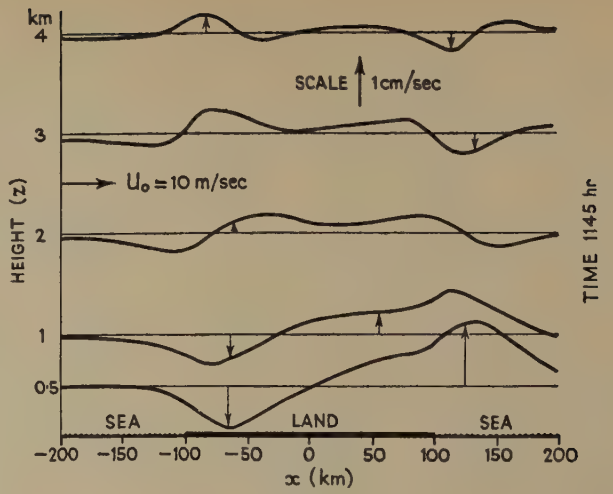

Figure 2.

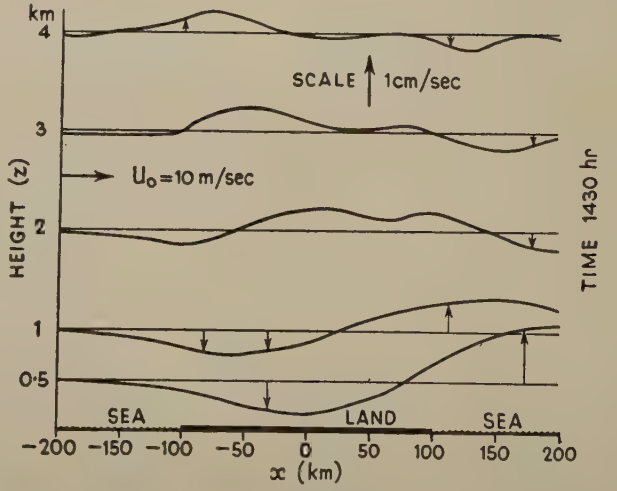

Figure 3.

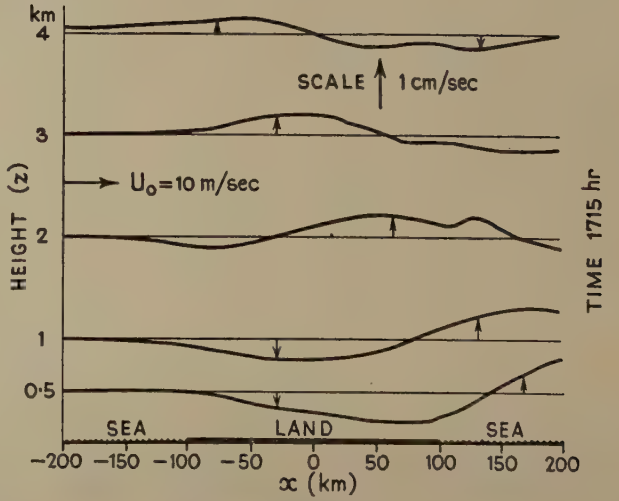

Figure 4.

Figures 1 to 4. Vertical velocities at heights of 0·5, 1, 2, 3, 4 km at the various stations

TABLE 2. VALUES OF $\frac{\partial (\text{temp})}{\partial t}$ IN °C/HR AT $z = 0$ FOR THE HEATING FUNCTION WE HAVE CHOSEN

				x (km)			
	− 300	− 200	− 100	0	100	200	300
t (10^4 sec)							
− 2	0·0	0·0	0·0	− 0·03	− 0·12	− 0·08	− 0·04
− 1	0·0	0·0	0·0	0·35	0·78	− 0·12	− 0·08
0	0·0	0·0	0·0	1·11	1·85	0·78	− 0·12
(09 hr)							
1	0·0	0·0	0·0	− 1·03	0·1	1·84	0·78
2	0·0	0·0	0·0	− 0·73	− 1·74	0·1	1·84
3	0·0	0·0	0·0	− 0·67	− 1·38	− 1·74	0·1

Table 2 shows a maximum temperature occurring over the centre of the land mass t about 1030 hr and over the leeward coast around midday. During the afternoon the emperature falls quite considerably. From the theory we can see why the temperature hanges are such. The temperature over the land mass is subjected to two conflicting nfluences during the morning and early afternoon. Firstly the wind is perpetually bringing n the cooler air from over the sea; this crosses the land mass in 5½ hr and is attempting o lower the temperature. Secondly, the heating function, representing the input of solar nergy, is attempting to raise the temperature, with a maximum rate of heating at 09 hr. n mid-afternoon the latter becomes zero; therefore at some time previous to that the wo must be in equilibrium and the time of maximum temperature reached. The rate f temperature change was evaluated at two other positions on the land mass and it was ound, as might have been expected, that the maximum temperature was lowest and arliest on the windward side of the land mass and higher and later as we progress to he leeward coast.

Another feature of Table 2 to be noted is that once the leeward coast has been eached the temperature change becomes once again a function of $(x - U_0 t)$ and thus his temperature pulse continues to infinity in the x-direction without change. This situation arises from the theory because there is no means by which the air, actually at our perfect surface, may be removed from it or allowed to transfer heat away from it; herefore measuring the temperature change at any point on the sea surface will produce he same variations. In the real atmospheric case, small-scale eddying primarily, and to a lesser extent conduction and radiation, will fairly rapidly remove this transient temperature pulse.

The resultant velocity profiles at different times are shown in Figs. 1 to 4. Fig. 1 shows the velocity distribution at 09 hr. The air descends at all levels as it approaches the windward coast. The descent starts well out to sea at the higher levels, giving a pronounced backward tilt to the velocity curves, and actually over the windward coast the air is rising at the 2 and 3 km levels whilst descending at the ½ and 1 km levels. The air rises over the whole land mass with the maximum of vertical velocities just off the leeward coast in the lowest kilometre, topped by descending air at the 2 and 3 km levels. At 1145 hr the vertical velocities have increased in magnitude, the air is descending over half the land mass in the lowest kilometre and we have an appreciable vertical velocity at a height of 4 km. The maximum upward velocity still exists just off the leeward coast.

At 09 hr the velocity curves at all levels have double maxima – this is in evidence only above 2 km at 1145 hr and at lower levels the velocity field exhibits the features of a miniature cold front crossing the land mass with a velocity equal to our original overall velocity. Comparison of temperature records with the present theoretical case on windy

days is very difficult for on such days the temperature trace is very irregular without any well-defined maximum. This irregularity is caused by the separate thermals which continually pass the recording station. These thermals originate in the lee of a tree belt or in the hollow of the terrain and are released at periodic intervals with a temperature far in excess of what one would expect had the land surface been smooth.

The situations at 1430 hr and 1715 hr are very similar in form, with the down-motion extending over all the land mass in the lower layers whilst at the higher levels the upward motion is over the windward coast with down-motion off the leeward shore.

The values of the horizontal velocity were also found (Smith 1954). It was found that at $z = 0$, as in Part I, the values were meaningless since they were comparable with the initial velocity U_0. Above this level however the values were much smaller and could be ignored compared to U_0. This applies to all heights depicted on the graphs.

To discern these motions by any cloud forms would be difficult for at 2, 3 and 4 km the air does not rise much more than 30 m in the case considered, so that the air would have to be near its condensation level. If such clouds did form then it might be a difficult matter to dissociate them from those formed from orographic features so that verification by this means seems almost impossible.

9. Conclusion

The results have, in general, shown us what we should expect when a wind blows across a heated land mass. Points which have been brought out more clearly are the movement across the land mass of a miniature cold front during the period and the reversal of the vertical velocity with height. One feature to note is that the vertical velocity falls off less rapidly with height than in the $U_0 = 0$ case, the perturbations being carried to a greater height in the moving air-stream.

Differential heating, whether of land and sea or of difference in latitude, is the major driving force of our atmospheric circulation. It is one of the problems we shall have to solve if we are to understand our atmospheric motions more fully. The two papers in this series give one method of tackling the problem. The major obstacle to progress at present is that Coriolis forces cannot be dealt with except on a localized scale (Pearce 1955). The introduction of these terms presents problems in the mathematics which are difficult to surmount. However if this could be done, we could get on to such problems as the perturbations of the air flow caused by the heating of large continents and oceans both on a diurnal and annual basis.

Acknowledgments

I would like to thank Dr. R. S. Scorer, under whose direction this work was carried out, for his advice and useful criticisms. During the course of this work I was in receipt of a London University Postgraduate Studentship.

References

Pearce, R. P. 1955 *Quart. J. R. Met. Soc.*, **81**, p. 351.

Smith, R. C. 1954 'Air motion due to the heating of a land mass,' Ph.D. Thesis, Imperial College, London.

1955 *Quart. J. R. Met. Soc.*, **81**, p. 382.

551.524.7 : 551.571.7

Some further observations from aircraft of frost point and temperature up to 50,000 ft.

By N. C. HELLIWELL, J. K. MACKENZIE and M. J. KERLEY
Meteorological Research Flight, Farnborough, Hants.

(Manuscript received 19 October 1956)

SUMMARY

During 1955, 46 measurements of frost point and temperature were made at varying altitudes up to about 50,000 ft using a Dobson-Brewer pressurized frost-point hygrometer and a flat-plate thermometer mounted on the Canberra aircraft of the Meteorological Research Flight. The general character of these ascents in the lower stratosphere confirms the conclusions of earlier papers (Murgatroyd, Goldsmith and Hollings 1955). The mean frost point at 48,000 ft for the ascents made in 1954 and 1955 is — 117°F and at 46,000 ft — 115°F, with a standard deviation of about 3°F in each case.

1. INTRODUCTION

The series of measurements of frost point in the upper troposphere and lower stratosphere, described by Murgatroyd, Goldsmith and Hollings (1955), was continued during 1955. The total number of ascents made was 46 and during the two years 1954 and 1955 the total number of ascents was 81.

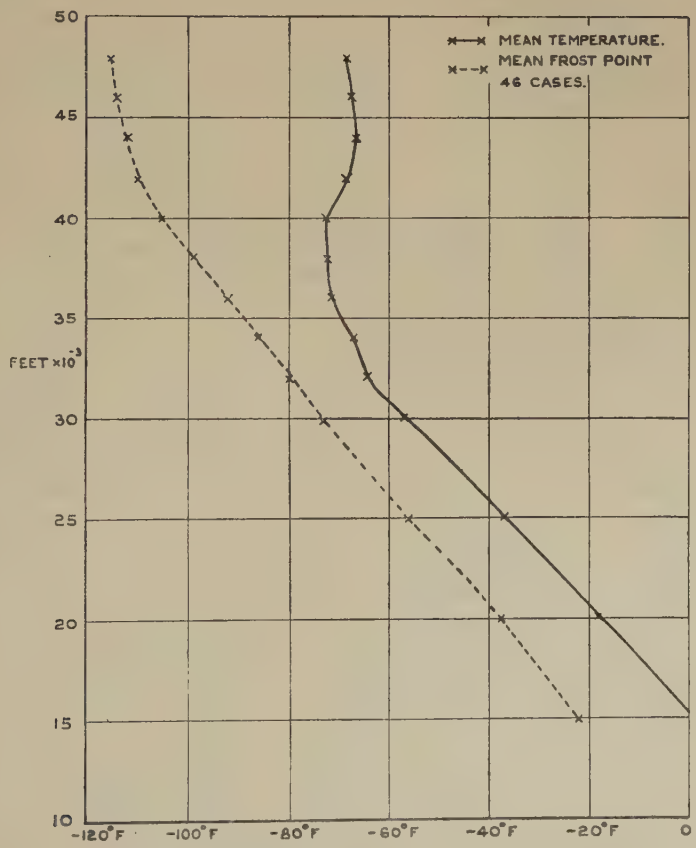

Figure 1. Mean temperature and frost point, 1955.

2. Observations

The observations are shown in detail in Table 1 but each individual ascent requires synoptic data to explain the detailed features; this paper will be concerned with the broad features of the ascents. Fig. 1 shows the arithmetic mean of the ascents made in 1955, the mean being taken only at levels where the number of observations is sufficient to justify the averaging process. The flights can be divided into two classes :

TABLE 1. Temperature and frost point (in brackets) °F, individual ascents (1955)

I.C.A.N. Height (ft)	Pressure (mb)	Dates: 3 Feb.	4 Feb.	7 Feb.	8 Feb.	8 Feb.	9 Feb.	10 Feb.	11 Feb.
		Times (GMT): 1350	1220	1505	1410	1015	0950	1020	1050
5,000	843	+24 (+08)	+29 (+16)	+37 (+33)	–	–	–	+23 (+10)	+14 (+08)
10,000	697	+08 (−23)	+12 (−17)	+24 (+06)	+16 (−33)	+19 (−04)	+15 (00)	+02 (−25)	+01 (−49)
15,000	572	−12 (−40)	−04 (−22)	+05 (−30)	+04 (−09)	+08 (+01)	−09 (−18)	−21 (−41)	−15 (−26)
20 000	466	−33 (−60)	−24 (−37)	−08 (−17)	–	−09 (−23)	−24 (−59)	−38 (−58)	−35 (−44)
25,000	376	−43 (−79)	−46 (−61)	−30 (−46)	−33 (−40)	−30 (−46)	−43 (−84)	−45 (−84)	−58 (−72)
30,000	301	−55 (−94)	−62 (−82)	−52 (−66)	−52 (−68)	−54 (−73)	−61 (−82)	−51 (−96)	−62 (−93)
31,000	287	–	–	–	–	–	–	–	–
32,000	274	–		–	–	−64 (−75)		−57 (−103)	–
33,000	262	−55 –		–	–	–		–	–
34,000	250	–	–	–	−69 (−77)	−71 (−75)	–	−53 (−106)	−61 (−102)
35,000	238	−50 (−100)	−65 (−100)	−73 (−77)	–	–	−65 (−96)	–	–
36,000	227	−51 (−108)	–	–	–	−80 (−79)	–	−57 (−108)	–
38,000	206	−49 (−113)	–	–	−76 (−96)	−82 (−92)	−64 (−107)	−58 (−110)	−60 (−110)
40,000	187	−52 (−115)	−55 (−113)	−74	−72 (−112)	−77 (−106)	−60 (−110)	−60 (−110)	−58 (−111)
42,000	170	−54	−59 (−117)	–	−66 (−115)	−70 (−115)	−58 (−111)	−55 (−115)	−60 (−112)
43,000	162	–	–	–	–	–	–	–	–
44,000	155	−52	−58 (−116)	–	−66 (−117)	−73 (−115)	−61 (−111)	−58 (−117)	−61 (−113)
45,000	147	–	–	–	–	–	–	–	–
46,000	140	−56	−57 (−114)	–	−71 (−118)	−76 (−117)	−66 (−113)	−59 (−119)	−63 (−114)
48,000	127	−56	−56	–	−66 (−118)	−69 (−118)	−65 (−114)	−63 (−119)	−64 (−117)
49,000	121	–	–	–	–	–	–	–	–
50,000	116	−62	−58	–	−67 (−119)	–	−65	−65 (−118)	−64 (−118)

I.C.A.N. Height (ft)	Pressure (mb)	Dates: 14 Feb.	15 Feb.	16 Feb.	28 Feb.	1 Mar.	2 Mar.	3 Mar.	4 Mar.
		Times (GMT): 1140	1205	1155	1205	1345	1055	1130	1125
5,000	843	+20 (+16)	+18	+25 (+07)	+29	–	–	+38	–
10,000	697	+11 (−55)	+08	+07 (−08)	+19	–	–	+23	+22
15,000	572	–	−09	−01 (−40)	+02	–	–	+08 (−16)	–
20,000	466	–	−30	−25 (−51)	−08 (−18)	–	–	−13 (−33)	−15
25,000	376	−46 (−49)	−46	−42 (−70)	−29 (−37)	–	–	−36 (−55)	−40
30,000	301	−63 (−81)	−60 (−78)	−61 (−81)	−53 (−68)	−54 (−60)	−57 (−69)	−59 (−73)	−61 (−70)
31,000	287	–	–	–	–	–	–	–	–
32,000	274	−69 (−91)	–	−64 (−90)	–	–	−67	–	−70 (−76)
33,000	262	–	–	–	–	–	–	–	–
34,000	250	−70 (−93)	–	−67 (−95)	–	–	–	–	−77 (−81)
35,000	238	–	−69 (−103)	–	−76 (−77)	−77 (−80)	−80 (−89)	−73 (−92)	–
36,000	227	−70 (−99)	–	−65 (−101)	–	–	–	–	−81 (−89)
38,000	206	−71 (−101)	–	−64 (−106)	–	–	−90 (−98)	–	−91 (−97)
40,000	187	−70 (−105)	−61 (−114)	−65 (−114)	−87 (−97)	−92 (−101)	−94 (−100)	−88 (−100)	−86 (−99)
42,000	170	−63 (−108)	−64 (−114)	−55 (−115)	–	–	−85 (−112)	–	−82 (−108)
43,000	162	–	–	–	–	–	–	–	–
44,000	155	−60 (−109)	−65 (−115)	−57 (−117)	–	–	−81 (−113)	–	−75 (−113)
45,000	147	–	–	–	−78 (−116)	−79 (−118)	–	−78 (−114)	–
46,000	140	−59 (−109)	−63 (−116)	−62 (−118)	–	–	−77 (−116)	–	−76 (−114)
48,000	127	−61 (−112)	−64 (−116)	−72 (−119)	−79 (−118)	–	−77 (−117)	–	–
49,000	121	–	–	−65 (−120)	–	–	−74 (−118)	–	–
50,000	116	−63	−62 (−118)	–	–	–	–	–	–

(1) Ascents made before 26 October 1955; (2) ascents made between 26 October 1955 and 1 December 1955.

The flights in the first class lasted about two hours, during which the aircraft travelled about 1,000 mi and consecutive readings in the vertical were not over the same point on the ground. The ascents of the second class were made between 13 and 15 GMT within a 30-mi radius of a radiosonde station, generally Crawley. In all the ascents the determination of each frost point takes about 5 min, during which the aircraft travels some 30 mi.

The measurements were made to the same accuracy as that quoted by Murgatroyd, Goldsmith and Hollings (1955). The observers found little difficulty in detecting the frost deposit,

TABLE 1 (*continued*)

C.A.N. Height (ft)	Pressure (mb)	Dates / Times (GMT) 9 Mar. 1615	10 Mar. 1140	10 Mar. 1620	11 Mar. 1205	14 Mar. 1150	15 Mar. 1150	16 Mar. 1525	18 Mar. 1145
5,000	843	+11	–	–	–	–	–	–	–
10,000	697	+04	–	–	–	–	–	–	–
15,000	572	−13	–	–	–	–	–	–	−04
20,000	466	−26	−22	–	–	−13	–	–	−21
25,000	376	−46	−42	–	−36	−34	–	–	−42
30,000	301	−64 (−73)	−63 (−70)	–	−61 (−70)	−59 (−65)	−61 (−70)	−64 (−62)	−64 (−73)
31,000	287	−66 (−79)	−67	–	−63 (−69)	−61	–	−66	−66 (−79)
32,000	274	−71 (−75)	−69	–	−68	−66 (−75)	−69 (−77)	−70	−69 (−85)
33,000	262	–	−72	–	–	–	–	−75 (−82)	–
34,000	250	−68 (−83)	−74	–	−75	−73 (−84)	−78 (−81)	−79 (−85)	−74 (−92)
35,000	238	–	−75 (−88)	–	−80	–	–	–	−75
36,000	227	−72 (−84)	−78	–	−83 (−89)	−81 (−88)	−85 (−90)	−85 (−91)	−79 (−95)
38,000	206	−67 (−90)	−75	–	−84	−90 (−100)	−88 (−94)	−90 (−93)	−76 (−101)
40,000	187	−66 (−93)	−76 (−98)	−77 (−99)	−86	−98 (−106)	−92 (−97)	−89 (−97)	−72 (−109)
42,000	170	−66 (−90)	−70	−71 (−103)	−84	−94 (−108)	−86 (−112)	–	–
43,000	162	–	–	–	−78	−86	–	–	–
44,000	155	−65 (−89)	−74 (−106)	−71 (−108)	−74	−83 (−114)	–	–	–
45,000	147	–	−69	–	−72	−80	–	–	–
46,000	140	−62 (−92)	−69	−71 (−111)	−70	−76 (−119)	–	–	–
48,000	127	−64 (−91)	−72 (−102)	−68 (−111)	−70 (−117)	−77 (−119)	–	–	–

C.A.N. Height (ft)	Pressure (mb)	Dates / Times (GMT) 18 Mar. 1605	21 Mar. 1115	28 Mar. 1510	30 Aug. 1025	31 Aug. 1025	29 Sep. 1445	4 Oct. 0805	12 Oct. 1440
5,000	843	+19 (+15)	+21 (−01)	–	+37	+50 +(26)	–	–	–
10,000	697	+13 (−11)	+12 (−14)	–	+34 (+16)	+27 (+19)	–	–	+29 (+14)
15,000	572	−03 (−20)	−02 (−44)	–	+19 (−13)	+09 (+01)	–	–	+14 (−06)
20,000	466	−24 (−53)	−20 (−49)	−28 (−66)	−01 (−23)	−05 (−26)	–	–	−06 (−09)
25,000	376	−44 (−67)	−40 (−70)	−46 (−49)	−24 (−26)	−26 (−61)	−17 (−37)	–	−25
30,000	301	−63 (−77)	−61 (−81)	−67 (−71)	−43 (−74)	−47 (−67)	−39 (−59)	−56 (−75)	−48 (−52)
31,000	287	–	–	–	−46	−52	–	–	−52
32,000	274	−70 (−83)	−68 (−85)	−73 (−77)	−51 (−78)	−56 (−77)	−49 (−69)	−62 (−78)	−57 (−62)
33,000	262	–	–	–	−54	−61	–	–	−61
34,000	250	−72 (−92)	−75 (−91)	−69 (−93)	−59 (−83)	−63 (−77)	−57 (−70)	−67 (−81)	−64 (−73)
35,000	238	–	–	–	−61	−63	−59	–	−68
36,000	227	−78 (−95)	−76 (−96)	–	−64 (−84)	−62 (−92)	−65 (−75)	–	−68 (−86)
38,000	206	−75 (−99)	−72 (−107)	–	−65 (−97)	−61 (−102)	−73 (−87)	–	−72 (−83)
40,000	187	−80 (−103)	−67 (−113)	–	−64 (−103)	−60 (−108)	−80 (−88)	−65 (−103)	−75 (−101)
42,000	170	−73 (−113)	−64 (−114)	–	−60 (−109)	−60 (−111)	−84 (−95)	–	−74
43,000	162	–	–	–	–	–	−82	–	−74
44,000	155	−77 (−116)	−63 (−116)	–	−59 (−114)	−63 (−116)	−82 (−107)	−67 (−114)	−72
45,000	147	–	–	–	–	–	–	–	−72
46,000	140	−70 (−116)	−61 (−117)	–	−66 (−117)	−63 (−118)	−87 (−111)	−64	–
48,000	127	−70 (−118)	−62 (−117)	–	−66 (−117)	−59 (−118)	−87 (−115)	−67 (−118)	–

even at the lowest temperatures; the compressor method due to Goldsmith (1955) wa consequently, not needed. It was, however, used a few times, as a check on the normal metho

The results generally confirm those of the 1954 series and may be briefly summarized :

(1) Frost point over Southern England decreases with height above the tropopause to reach value of about − 117°F at 48,000 ft;
(2) The lapse rate of frost point also decreases above the tropopause;
(3) High and low values of frost point in the lowest 10,000 ft of the stratosphere correspon well with high and low values at the tropopause but this correspondence disappears a higher altitudes where there is little variation of frost point.

TABLE 1 (*continued*)

I.C.A.N Height (ft)	Pressure (mb)	Dates 17 Oct. Times (GMT) 1045	18 Oct. 1045	18 Oct. 1510	20 Oct. 1445	26 Oct. 1530	28 Oct. 1345	31 Oct. 1345	1 Nov. 1350
5,000	843	+25 (+18)	–	–	+38	+38	+29 (+05)	+30 (−20)	+33 (−22)
10,000	697	+14 (−22)	+10 (−25)	–	+20 (+18)	+29	+09 (−14)	+20 (00)	+19 (−06)
15,000	572	–	–	–	+03 (−09)	+11	−04 (−56)	+02 (−16)	+02 (−12)
20,000	466	−13	−22 (−23)	−16 (−27)	−21 (−28)	−11	−18 (−53)	−15 (−27)	−19 (−27)
25,000	376	−41	−42 (−44)	−39 (−57)	−36 (−62)	−28	−41 (−66)	−37 (−54)	−41 (−54)
30,000	301	−54	−65 (−67)	−63	−56 (−72)	−48 (−62)	−60 (−77)	−59 (−71)	−61 (−81)
31,000	287	−61	−66	−68 (−72)	−60	−55	−62	−64	−65
32,000	274	−65 (−74)	−68 (−84)	−69	−59 (−80)	−60 (−62)	−63 (−88)	−67	−68
33,000	262	−69	−68	–	−57	−63	−63	−71 (−84)	−71
34,000	250	−69 (−85)	−68 (−92)	−68 (−93)	−51 (−95)	−68 (−73)	−65 (−92)	−74	−72 (−85)
35,000	238	−74	−66	–	−48	−73	−69	−79	−74
36,000	227	−70 (−93)	−65 (−103)	−71 (−97)	−46 (−102)	−76 (−84)	−70 (−95)	−83 (−90)	−74
38,000	206	−72 (−99)	−62 (−107)	−66 (−107)	−48 (−105)	−84 (−88)	−69 (−101)	−85 (−90)	−71 (−103)
40,000	187	−64 (−104)	−58 (−110)	−61 (−111)	−51 (−108)	–	−67 (−105)	−83 (−101)	–
42,000	170	−66 (−108)	–	−61 (−111)	−56 (−109)	–	−61 (−112)	–	−71 (−109)
43,000	162	–	–	−63	–	–	–	−73 (−113)	–
44,000	155	−66 (−112)	–	−60 (−112)	−57 (−109)	–	−67 (−115)	–	−71 (−112)
45,000	147	–	–	−62	–	–	–	–	–
46,000	140	–	–	−62 (−114)	−56 (−111)	–	−68 (−116)	−73 (−113)	−71 (−114)
48,000	127	–	–	−64 (−114)	−63 (−112)	–	−66 (−117)	−72 (−116)	−69 (−116)

I.C.A.N. Height (ft)	Pressure (mb)	Dates 8 Nov. Times (GMT) 1000	11 Nov. 1130	22 Nov. 1335	28 Nov. 1335	29 Nov. 1335	1 Dec. 1125
5,000	843	+41 (+33)	–	+28	–	+38	–
10,000	697	+22 (+19)	+25	+15 (−13)	+26	+25	–
15,000	572	+05 (−12)	+07	+04 (−46)	+08	+06	–
20,000	466	−16 (−54)	−13	−18 (−36)	−14	−14	−20
25,000	376	−41 (−51)	−33 (−43)	−33 (−59)	−35	−27	−42
30,000	301	−61 (−72)	–	−50 (−77)	−59	−50 (−82)	−56 (−88)
31,000	287	−63		−53	−63	−55	–
32,000	274	−67	–	−57	−66	−58 (−88)	−60 (−88)
33,000	262	−71 (−74)	–	−60	−71 (−79)	–	−62 (−92)
34,000	250	−70	–	−64	–	−64 (−90)	−61
35,000	238	−70	−82 (−86)	−68 (−91)	–	–	−61
36,000	227	−69 (−94)	−79 (−86)	−73	−80 (−85)	−77	−61 (−99)
38,000	206	−66 (−101)	−78 (−95)	−74	−79	−72 (−95)	−61
40,000	187	−66 (−107)	−66 (−106)	−75 (−103)	−79 (−99)	−83	−65 (−111)
42,000	170	–	–	−78	−76 (−110)	−74 (−112)	−65
43,000	162	−64 (−112)	–	–	–	–	−64
44,000	155	–	–	−77 (−112)	–	−74	−67 (−114)
45,000	147	–	–	–	–	–	−67
46,000	140	−64 (−113)	–	−79	−74 (−114)	−76 (−116)	−68
48,000	127	−66 (−115)	–	−79 (−115)	−74 (−117)	−76 (−117)	−70 (−120)

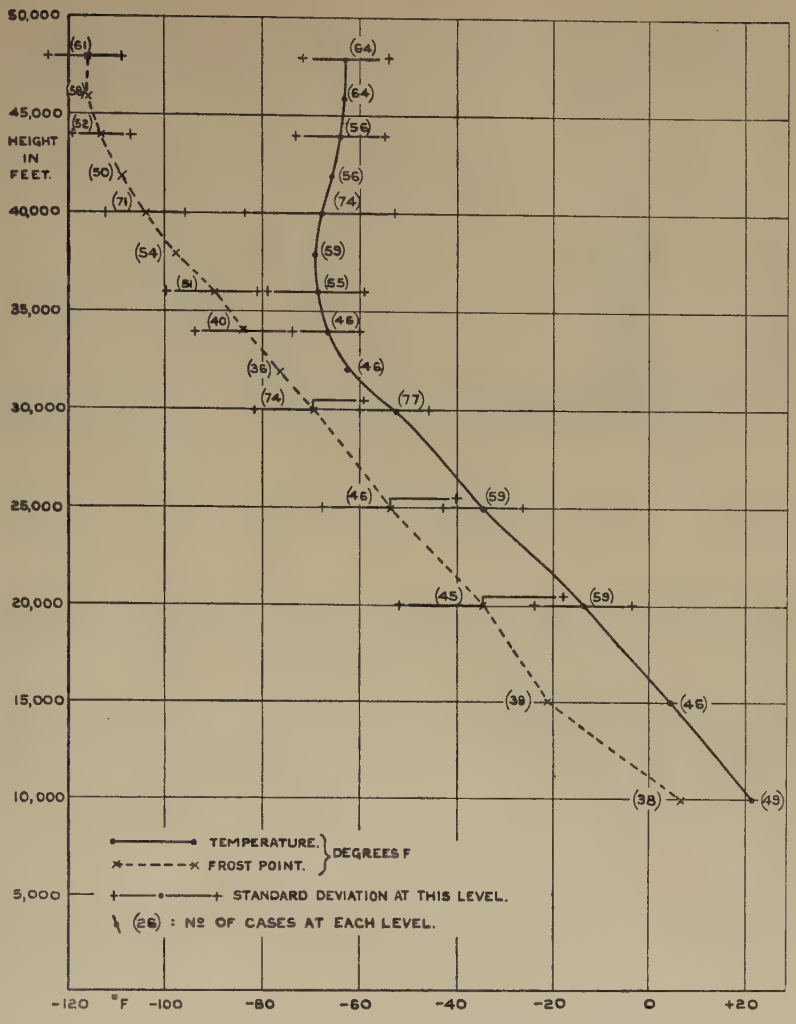

Figure 2. Mean for 1954 and 1955 ascents (81 cases).

3. Combination of observations for 1954 and 1955

Fig. 2 shows mean curves of frost point and temperature using the values obtained in 1954 nd 1955 combined at selected levels. The 1955 observations were made only in restricted periods f the year but in 1954 observations were made in most months and were more uniformly spaced.

TABLE 2. Mean values of temperature (°F) and frost point (°F), with standard deviations, for selected levels for 1954 and 1955

Height (ft)	Mean temperature (°F) 1954 and 1955	1955	1954	Standard deviation	Mean frost point (°F) 1954 and 1955	1955	1954	Standard deviation
20,000	− 14·4	− 18·2	− 7·7	10	− 35	− 38	− 32	17
25,000	− 35·2	− 37·6	− 30·2	8	− 54	− 56	− 50	14
30,000	− 53·3	− 57·0	− 48·0	7	− 70	− 74	− 65	11
34,000	− 66·9	− 67·9	− 64·0	7	− 84	− 86	− 79	10
36,000	− 68·9	− 71·8	− 64·5	10	− 90	− 92	− 87	9
40,000	− 67·4	− 72·6	− 60·8	15	− 104	− 105	− 103	8
44,000	− 64·2	− 67·2	− 60·3	9	− 113	− 112	− 113	6
48,000	− 63·5	− 68·2	− 58·4	9	− 116	− 115	− 116	7

Table 2 compares mean values for selected levels for the two years. One interesting featur of Table 2 is that although there is sometimes a difference of 10°F in the mean at lower level the frost point between 40,000 ft and 48,000 ft shows little variation in the mean from year t year.

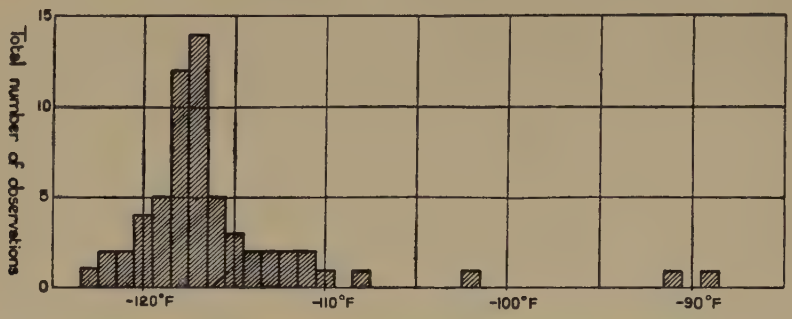

Figure 3. Histogram : frost points at 48,000 ft (61 cases).

When individual observations at 48,000 ft were compared with the mean value and standar deviation it was noted that the latter value was rather large. Fig. 3 shows the observations a 48,000 ft arranged in steps of 1°F. It will be seen that the majority are grouped fairly symmetrically about a temperature of — 117°F but that three observations — 102°F, — 91°F and — 89°F appear to be anomalous. Two of these occurred on consecutive days and Mackenzie (1956) has suggested that they may be due to moisture carried into the stratosphere by a nuclear explosion If this view is accepted and the three high values are rejected as being due to unnatural causes the mean frost point at 48,000 ft becomes — 117°F and that at 46,000 ft — 115°F, each having a standard deviation of 3·2°F.

4. Further work

In view of the relative constancy of stratospheric frost points over southern England, measure ments are being extended to other latitudes in the hope that further information can be obtained on the general circulation and associated problems.

Acknowledgment

The authors are indebted to the Director of the Meteorological Office for permission to publish this paper.

References

Bannon, J. K., Frith, R. and Shellard, H. C. 1952 *Met. Off., Geophys. Mem.*, London, No. 88.
Brewer, A. W., Cwilong, B. M. and Dobson, G. M. B. 1948 *Proc. Phys. Soc.*, **60**, p. 52.
Goldsmith, P. 1955 *Quart. J. R. Met. Soc.*, **81**, p. 607.
Murgatroyd, R. J. and Goldsmith, P. 1953 *Air Ministry, Met. Res. Cttee.*, M.R.P., No. 833.
Murgatroyd, R. J., Goldsmith, P. and Hollings, W. E. H. 1955 *Quart. J. R. Met. Soc.*, **81**, p. 533.
Mackenzie, J. K. 1956 *Met. Mag.*, **85**, p. 233.

551.508.765

The detection and measurement of water droplets

By H. F. LIDDELL and N. W. WOOTTEN

Chemical Defence Experimental Establishment, Ministry of Supply, Porton, Wilts.

(Manuscript received 14 December 1956)

SUMMARY

The use of a dyestuff (Naphthol Green B) in gelatine, coated on the slides of a cascade impactor, provides a method for determining the drop-size distribution of fogs and water sprays which is easy to apply in practice and gives a permanent record for subsequent microscopic analysis. Calibration of the stain remaining after evaporation of a droplet impacting on the slide shows it to be, on the average, 2·5 times the diameter of the droplet. The method can be readily used for droplets of less than 1 μ diameter.

1. INTRODUCTION

In order to measure the drop-size distribution in a natural fog or a water spray there is need for a method of sampling which is easy to perform and which gives a permanent record of the droplets for subsequent measurement. The use of the cascade impactor (May 1945) provides a ready means of sampling. Air containing the droplets is drawn through a series of jets at increasing velocity and the droplets impact upon plates behind the jets according to their inertia. The largest drops impact on the first slide and the smallest on the last slide. This gives a size grading of the droplets making microscopic analysis easier than for measurement of a large range of sizes on one slide. The limitations of this method of sampling, hitherto, have been in the capture of the very small droplets, of the order of 1 μ, and their retention for examination.

The original methods described by May of making permanent records of traces left by small drops of water, which are too volatile to persist long enough for direct measurement of their size, are : (a) *the absolute method* and (b) *the magnesium-oxide method*. In the former method the drops are captured in oil on the slides, which are quickly removed from the impactor. The sample is then covered with an oiled cover-slip before the drops evaporate. A viscous oil is required on the slides if it is not to be blown aside by the stream of air through the jets, but such an oil on the cover-slip requires warming before it will flow around the water drops and capture them. This is not possible under field conditions. In the magnesium-oxide method the drops make craters in a film of MgO coated on the slides. This method is not suitable for measuring, to the required accuracy, drops smaller than 10 μ diameter and high air velocities destroy the sensitive layer.

A *stain method* for the detection of droplets of certain organic liquids is described in May's paper. Provided that a suitable technique could be devised it seemed that this method offered the most promising way of overcoming the disadvantages of the other two methods for the detection of water droplets.

2. THE NAPHTHOL GREEN B FILM METHOD

The stain method depends on the displacement by a water droplet of the dyestuff contained in a very thin film of gelatine. The requirements of the dyestuff are that it should be :

(a) very readily soluble in water, so as to be sensitive to small droplets, many of which are likely to evaporate from the film in less than 1 sec,

(b) sufficiently soluble in water to produce a deeply-coloured effect in a thin film of gelatine, so that the impressions made by small droplets are easily distinguishable against the background,

(c) free from inorganic salts, as these will crystallize on the film,

(d) not liable itself to crystallize in the gelatine film at the concentration required.

So far as was known there was no commercial dyestuff which fulfilled these requirements, but Naphthol Green B, Colour Index No. 5 (Rowe 1924) seemed likely to have the properties needed for (a) and (b). A sample of Naphthol Green B.N.S. (I.C.I.) was purified by dissolving 10 g in 50 ml of water at the boil and salting out with 10 g powdered anhydrous sodium acetate. This was cooled and filtered and the filter cake was extracted with boiling ethyl alcohol until all the sodium acetate was removed. 1 g of this purified Naphthol Green B dissolved in 20 ml of warm distilled water, filtered and added to a 4 per cent aqueous solution of gelatine, was found to give a satisfactory film.

It was necessary that the slides of the cascade impactor should be free from grease before the green film was applied; this was achieved by boiling them in water with Teepol added, and drying with a clean cloth. The gelatine solution containing the dyestuff was warmed before applying it to the slides, which were also warmed. The solution was poured on to the slide, drained off from one edge and then gently heated to dry out and leave an even deposit. When this procedure was followed carefully there was no difficulty in obtaining a film free from holes and spurious particles. Fig. 1 (Plate V) shows a typical record obtained by the technique.

3. Stain-size calibration

A droplet impinging upon the film dissolves the dyestuff as it spreads and, upon evaporation, leaves a ring in which the concentration of the dyestuff is increased. When observed through a microscope with normal transmitted illumination these rings appear dark against a lighter background as illustrated in the plate, which was obtained from a photomicrograph. The outer diameters of the dark rings can be measured by the use of an eyepiece graticule and hence, if the spreading factor is known, the sizes of the original droplets are determined.

The spreading factor was found under laboratory conditions by simultaneously sampling a water spray by the absolute method and with the Naphthol Green B film. The spray was generated from a Collison atomiser (Collison 1935) in a manipulator box with the relative humidity at 99 per cent to avoid, as far as possible, evaporation of the droplets. One half of each slide of the cascade impactor was coated with a vaseline and liquid-paraffin mixture and the other half with a Naphthol Green B film. Immediately after taking the sample the slides were removed and the oil-coated half was covered by a warmed cover-slip similarly coated. The size distribution of the stains and of the droplets in oil was determined and plotted on logarithmic-probability paper from which the ratio of the mean sizes was readily calculated. The ratio of the mean diameter of stain to diameter of drop on slide 1 was 2·4 : 1 and on slide 2 it was 2·7 : 1. It can be seen from Fig. 2 that these values agree well for all drop sizes. Measurements by this method could not be made on slides 3 and 4 as the velocity of the air through the jets blew the oil aside and the droplets were lost, although the stains were visible on the Naphthol Green B film.

It was thought that the passage of the droplets through the impactor might affect their size, either by evaporation or by condensation during the expansion of the air through the jets. To determine if this were so a series of measurements was made, using clouds generated under identical conditions, in which successive stages of the impactor were removed. Any change of size of the droplets would appear in plotting the cumulative-number distribution curve for each stage removed. Fig. 3 illustrates that within the limits of experimental error there was no difference between the values obtained using all four stages and those using only one stage. From these observations it may be concluded that there is no change of size during sampling.

To obtain the relationship between drop-sizes and stain-sizes for the small drops, samples were taken simultaneously by a cascade impactor, using Naphthol Green B, and in a sedimentation cell (Green 1934), using the absolute method. Measurements were made on clouds produced by various methods giving mean drop diameters ranging from 2 μ to 11 μ. The total range occurring in these clouds was from less than 1 μ to 20 μ diameter. The value of the stain-diameter to drop-diameter ratio thus obtained was 2·5 : 1 with a standard deviation of 0·13. Stains down to 2 μ diameter (i.e., droplets of 0·8 μ diameter) are measurable and below this they can be identified but not accurately measured.

4. Use in fog sampling

The ease of manipulation and the permanence of the record makes this method particularly suitable for the measurement of drop-size distribution in natural fogs. The slides require no special treatment under normal conditions and will remain usable, and the stains remain visible, for months. If they are likely to be subjected to high humidity for long periods the slides should be stored in a sealed container or the film will develop a 'bloom.'

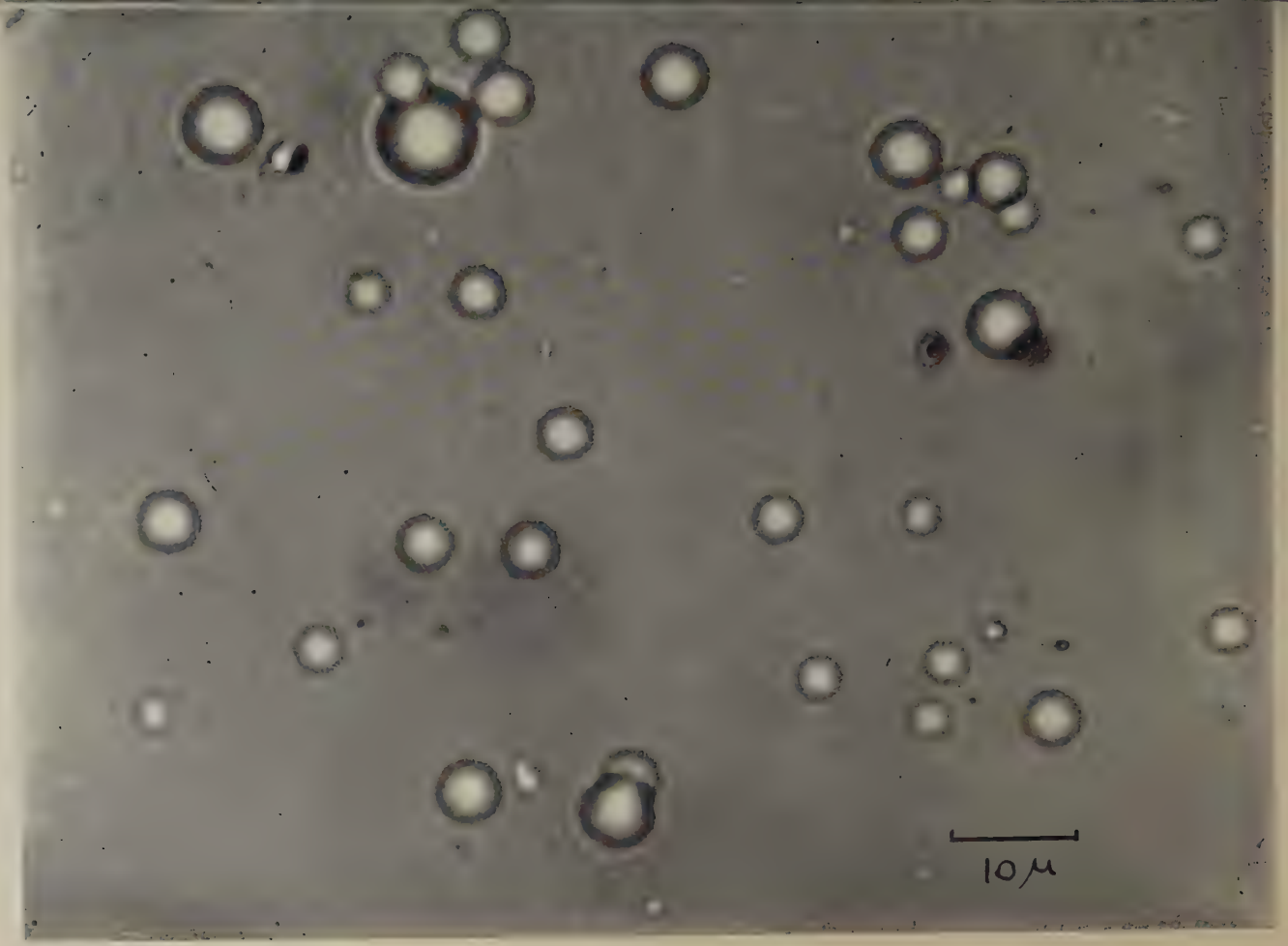

Figure 1. Typical stains of water drops on Naphthol Green B film from slide 3 of a cascade impactor.
(Crown Copyright reserved. Reproduced by the permission of the Controller, H.M.S.O.)

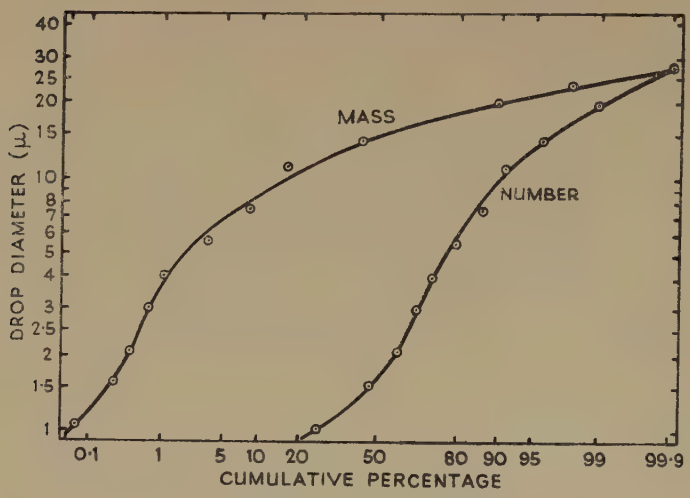

Figure 4. Drop-size and mass distribution of fog at Porton, 15 December 1954, 1540 hr.

Acknowledgments

Thanks are due to Imperial Chemical Industries (Dyestuffs Division) for supplying sample of Naphthol Green B.N.S.

References

Collison, W. E. 1935 *Inhalation therapy technique*, London (Heinemann).
Green, H. L. 1934 *J. Ind. Hyg.*, **16**, p. 29.
May, K. R. 1945 *J. Sci. Instr.*, **22**, p.187.
Middleton, W. E. K. 1952 *Vision through the atmosphere*, University of Toronto Press.
Rowe, F. M. (Ed.) 1924 *The colour index*, 1st Edn., Society of Dyers and Colourist
Stewart, K. H., 1956 Unpublished communication.

551.510.41 : 551.508.952 : 551.507.35

Ozone-concentration measurements from an aircraft in N. Norwa

By A. W. BREWER
Clarendon Laboratory, Oxford

(Manuscript received 18 October 1956)

1. Introduction

As a result of a suggestion of D. Tönsberg of the Nordlys Observatory at Tromsö, tha the Norwegian Air Force, would, if suitably approached, provide us with aircraft facilities, visit was made to N. Norway from April to July of 1955 to make measurements of the vertica distribution of ozone and water vapour. The work was part of a general programme to determin the world-wide distribution of ozone and represents an extension of the work of Kay (with Brewe and Dobson) in S. England (Kay 1953). There is especial interest in N. Norway because of it high geographical latitude (Tromsö is at 70°N) and the Nordlys Observatory has made there a long series of measurements of total ozone, and of *Umkehr* curves, from which some information about the vertical distribution of ozone can be obtained.

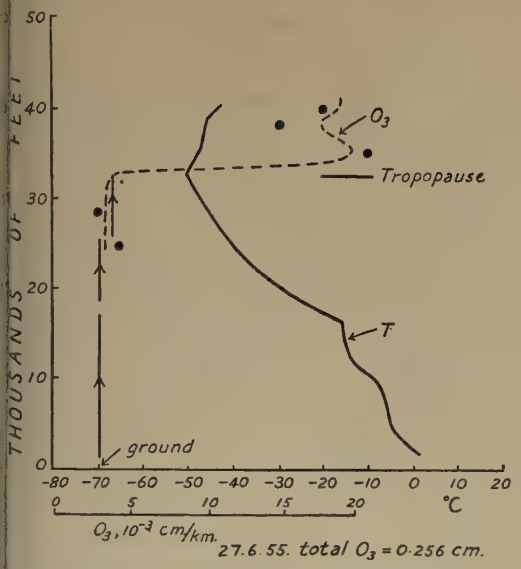

Figure 1.

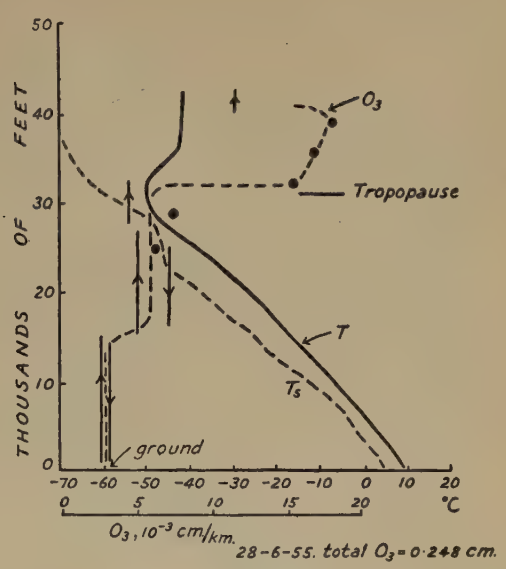

Figure 2.

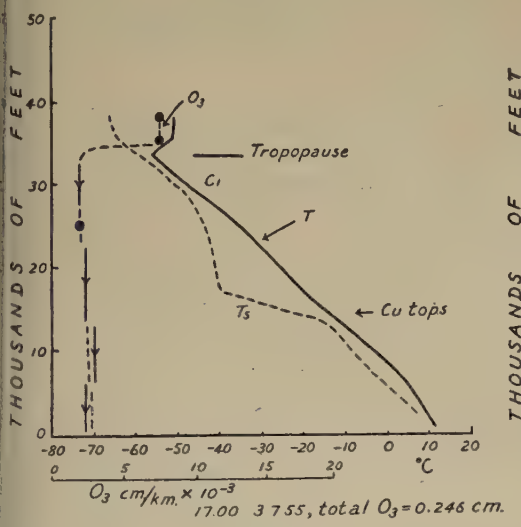

Figure 3.

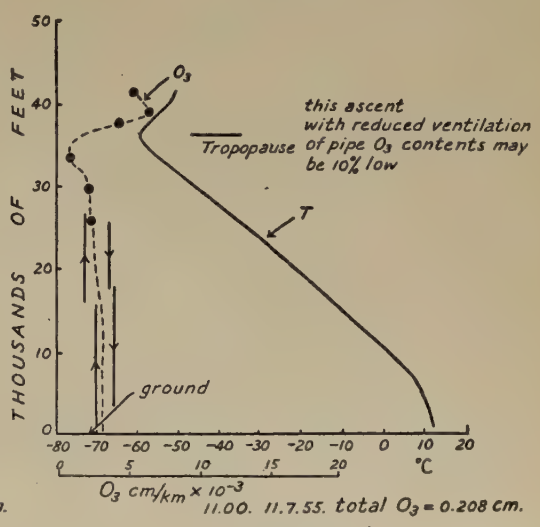

Figure 4.

O_3 concentration • - - - - •

O_3 concentration, measured while climbing or descending ↑ or ↓

Figures 1, 2, 3 and 4. Aircraft measurements of air temperature, T, dew or frost point, T_s, and ozone concentration, made at Bardufoss, N. Norway, 68°N, 18°E. The total ozone amounts were measured at Tromso, 69°34′N, 18°35′E.

2. Equipment used

The meteorological equipment taken was :

1. A standard M.O. pattern, balanced-bridge aircraft air-temperature thermometer.
2. An automatic dew-point hygrometer with pressurized test chamber, so that compressed air from the jet engine could be used.
3. The ozone sampler which was used by Kay.

The thermometer and the hygrometer were carried to provide simultaneous data so that the ozone concentration could be correlated with the temperature and humidity structure.

3. Installation in aircraft

The instruments were installed in a Vampire trainer (two seater), the only suitable aircra available. The installation was carried out by Royal Norwegian Air Force ground staff and i early May the aircraft and crews were moved from Trondheim, where the installation wor was done, to Bardufoss, near Tromsö, for the operational flights.

4. Flights

Initial flights suggested that no ozone was, in fact, reaching the sampling vessels, apparentl because of the absorption of ozone in the inlet system. This was of brass and copper. When firs made it had appeared satisfactory but, perhaps through spilling of the solutions at some time thereby contaminating the pipes, all the ozone was now being absorbed. The inlet system wa rebuilt of anodised aluminium and the fine metering capillary was drilled through gold. Carefu tests then showed that the ozone concentration measured by the aircraft at 1,500 ft during con vective conditions was substantially equal to that measured at the ground with a simple, all-glas sampler.

Four ascents were then made between 24 June 1955 and 12 July 1955. The results of these four ascents are given graphically in Figs. 1, 2, 3 and 4.

It will be seen that except for the ascent of 28 June the ascents show approximately constan concentration (cm/km or $\mu g/m^3$) up to the tropopause, corresponding to about a 3 to 1 increase in mixing ratio. On 28 June the concentration approximately doubled between 15,000 ft and the tropopause. All the ascents, but particularly those of 27 June and 28 June, show a large increase in ozone concentration at the tropopause, but the increase is much smaller on 11 July when the ascent was in an air stream of tropical maritime origin.

These results are to be compared with those of Kay (1953), who found that on the average there is no marked change in the ozone concentration at the tropopause. It is possible that this is a real geographical difference or it may be that Kay's results were affected by ozone absorption in the pipes of the sampler, and this point must be investigated. It is also possible that the accumulation of dirt in the pipes is responsible for the smaller amount of ozone recorded in the stratosphere in the last two flights when compared with the first and second.

The general feature of an increase in ozone concentration at the tropopause is of course a reasonable one and the increase observed is of about the correct amount to account for the observed correlation between total ozone amount and tropopause height. A very variable lower stratosphere concentration would account for the rather low correlation coefficients which are sometimes obtained.

If the changes of *stratospheric* ozone observed in these ascents in N. Norway are real they may be associated either with different air masses, or with the annual variations of ozone, or both, and it would be most desirable to learn more about the mechanisms involved. Observations in S. England may show something of the former but the annual effect could be best investigated in N. Norway where the total ozone has a large annual variation. In particular during December and January there is a very rapid increase in total ozone, and observations from an aircraft made at that time would show whether the increase is occurring in the lower stratosphere. Simultaneous temperature and humidity measurements would also form a useful investigation of the polar tropopause structure, about which we know so little.

Acknowledgments

The British Council and the British Air Attaché in Oslo made the arrangements for the visit and were most helpful in many ways during the course of the work. The Royal Norwegian Air Force provided the aircraft, carried out all the installation work, and provided all flying facilities, and helped in every way possible. It is a great pleasure to acknowledge the generous assistance which I received in every way and from everyone concerned in the R.N.A.F. It is also a pleasure to acknowledge the help I received from Professor Westin, National Technical High School, Trondheim and from Ing. Gisle Dyvik, also of the N.T.H.S., when I was in difficulties with the sampler. The Gassiot Committee of the Royal Society paid personal travelling expenses.

Reference

Kay, R. H. 1953 *Air Ministry, Met. Res. Cttee.*, M.R.P., No. 817.

Correspondence

551.510.42 : 551.551 : 551.558.1

The bent-over plume of hot gas

By G. Spurr

I have recently applied Dr. Priestley's formulae (*Q.J.*, **82**, p. 165, 1956) to calculate theoretically the plume rise from a chimney stack.

In contrast to the author's comments, I found great difficulty in obtaining the transition values by graphical means. As an alternative, these values can be calculated, the only difficulty being the rather tedious arithmetic involved in the solution of a cubic equation .

At the transition stage, the variables are given by the following equations in Dr. Priestley's paper.

$$w_1^3 = \frac{3Ag}{2\theta_e c^2}\left\{\frac{1}{z_1} - \frac{z_0^2}{z_1^3}\right\} + \frac{w_0^3 z_0^3}{z_1^3} \quad . \quad . \quad . \quad (1)$$

$$\theta_1' = \frac{A}{c^2 z_1^2 w_1} \quad . \quad . \quad . \quad . \quad . \quad . \quad (2)$$

and

$$-\frac{dw_1}{dz_1} = k - \frac{g\theta_1'}{\theta_e w_1} \quad . \quad . \quad . \quad . \quad (15)$$

In Dr. Priestley's paper Eq. 15 is given wrongly* as :

$$-\frac{dw_1}{dz_1} = k - \frac{g\theta_1'}{\theta_e}\Big)$$

If Eq. (1) is differentiated with respect to z_1

$$3\frac{dw_1}{dz_1} w_1^2 = \frac{3Ag}{2\theta_e c^2}\left\{-\frac{1}{z_1^2} + \frac{3z_0^2}{z_1^4}\right\} - \frac{3w_0^3 z_0^3}{z_1^4}$$

From this equation and from Eqs. (1), (2) and (15) it can be shown that

$$\frac{1}{k^3 z_1^4}\left\{\tfrac{3}{2}\frac{Ag}{\theta_e c^2} + \frac{1}{z_1^2}\left(w_0^3 z_0^3 - \tfrac{3}{2}\frac{Ag}{\theta_e c^2} z_0^2\right)\right\} = 1$$

This is a cubic equation in z_1^2 which can be solved by well-known techniques.

Having found z_1 then the ceiling height of the plume can be found from Priestley's formulae (Eq. (12)) without any recourse to graphical methods.

Central Electricity Authority,
Research Laboratories, Randall's Farm Lane,
Kingston Road,
Leatherhead, Surrey.
3 December 1956.

Reply

By C. H. B. Priestley

I am grateful to Mr. Spurr for drawing attention to the error in Eq. (15) of my paper. Fortunately this was only a transcription error and was not embodied in the calculations leading to Table 2.

The purpose of Fig. 2 was illustrative and I had not intended to imply that the transition point was determined by graphical means. Actually I located it by equating the slopes (dw/dz) of the two curves (1) and (15) by trial and error, which can be done quite quickly once the 'feel' of the computation has been obtained. Spurr's use of the cubic equation is not essentially different but may have practical advantages, particularly if the solutions could be tabulated over a useful

* See Corrigendum, *Q.J.*, Jan. 1957, p. 139.

range of the independent variables; however, the latter are more than two in number, so a single table does not appear practicable.

Division of Meteorological Physics,
C.S.I.R.O.,
Melbourne.
18 December 1956.

551.557.35 : 551.509.317

The zonal wind in the upper troposphere and weather at Singapore

By P. Peterson

I wish to refer to a Shorter Contribution by J. R. Scott in a recent issue of the *Quarterly Journal* (**82**, p. 340, 1956).

The theory propounded in this paper is briefly that, in certain seasons, air converges at low levels over the China Sea and Philippines. There is compensating divergence at 50,000 ft. The air at 50,000 ft then travels south-westward, conserving its momentum, and causes compensating convergence and strong winds at high levels over Singapore. By still further compensation, this causes low-level divergence and fine weather at Singapore.

The only evidence offered in support of this complicated theory is that there is a correlation between strong winds at 50,000 ft and fine weather at Singapore in the afternoons of the summer and autumn.

However, there is a simple physical reason for this correlation. Strong easterlies at 50,000 ft over Singapore in the northern summer and autumn are associated with westerly winds at intermediate levels (see I. E. M. Watts, *Q.J.*, **81**, p. 582, 1955 and R. F. M. Hay, *Weather*, July 1953, p. 206). They are also associated with high zonal index at low latitudes.

High zonal index and normal light surface winds at Singapore imply strong wind shear at some intermediate level(s). Under conditions of strong wind shear, particularly between 10,000 and 30,000 ft, the tops of cumuliform clouds tend to be sheared off and successive cumulus towers form in fresh dry air instead of in air moistened by the preceding cumulus tower and development of convective showers in the afternoon is inhibited.

There is also a possible physical explanation for Mr. Scott's failure to find a corresponding correlation between early morning storms and his 50,000 ft winds. The early morning storms in Singapore or ' sumatras ' differ from the afternoon showers in that they are often in the form of line squalls or roll clouds. They appear to have greater horizontal and often lower vertical development and they can probably grow more readily under conditions of strong wind shear. Moreover these storms dissipate rapidly after sunrise, often many miles off shore, and only affect Singapore under the influence of westerlies or south-westerlies at intermediate levels.

Royal Observatory,
Hong Kong.
13 December 1956.

Reply

By J. R. Scott

Mr. Peterson's physical reason, with its high zonal index at low latitudes, is, I confess, neither simple nor clear to me. However, it does appear that he anticipates association between above average zonal components at 50,000 ft and strong wind shear between 10,000 ft and 30,000 ft.

It is true of course that above-average winds at 50,000 ft are associated with larger than average mean shear between that level and the surface, where winds are usually light. However, my impression (not numerically investigated) from working with the wind data is that most of this excess shear is usually concentrated above 30,000 ft. In addition, later investigation showed no relation between weather and zonal component (even values greater than 70 kt) in other seasons.

Mr. Peterson's anticipated association requires the shear between 10,000 ft and 30,000 ft on days of strong zonal component to be distributed differently from that on other days. To test this I have measured zonal component of mean shear between these levels on each tenth day during the period investigated in the paper. This selection of almost certainly independent observations was divisible into two sets; one of ten days when the zonal component at 50,000 ft

exceeded 53 kt and the other of 18 days when this component was less than 40 kt. The difference between the averages of mean zonal shear between 10,000 ft and 30,000 ft of these two sets was tested by Student's *t*. The value of *t* found corresponded to a probability level of about 0·37; a value which does not support Mr. Peterson's anticipations. The actual difference between the averages was 6 kt per 20,000 ft, which, if significant (there is a reason stated above which suggests that, in spite of the *t* test, it might possibly be so) and representative, could hardly engineer his effect.

Mr. Peterson's impression that ' sumatras ' have lower vertical development than afternoon showers is one which I have neither read nor heard from any other source and with which I do not agree.

Meteorological Office,
P.O. Box 715,
Singapore.
29 December 1956.

551.558.21

Airflow Over Mountains

By R. S. Scorer

Professor Sheppard's question posed in the *Quarterly Journal* (**82**, p. 528, 1956) is one which seems to have haunted Sir Napier Shaw, and it certainly haunted me when trying to understand how the air managed to get through the Straits of Gibraltar with orographic cloud at the entrance. Shaw's solution of the problem of airflow over mountains was as follows : the air arriving at the mountain may not have enough kinetic energy to get it up to the top, consequently the energy will be expended in tilting the isentropic surfaces upwards over the mountain. The air following will find an already partly tilted path and will have to depart less from existing isentropic surfaces in order to get over the mountain. When a particle has managed to get over the crest an isentropic path over the mountain will have been paved; since particles can move in isentropic surfaces without effort, the air will be able to follow this path, and the problem is solved.

If this exposition seems inadequate it is at least partly because Shaw's own version was unsatisfactory. He ignored Bernoulli's equation and the equation of continuity. Professor Sheppard puts before us Bernoulli's equation using the total head of pressure and shows that there then arise problems of continuity. A slowing down of the air as it rises against gravity over the mountain is incompatible with the presence of the mountain which requires a speeding up.

The answer to the problem is in two parts. First of all it is assumed that one can take any airstream, A, and any mountain, M, and obtain by recognized hydrodynamical methods a solution to the problem ' what is the pattern of flow of A over M ? ' But A and M may be incompatible, and this is, I think, one of the reasons why the problem of the upper-boundary condition has not been properly solved. We may return to Shaw and ask what happens to the ' first ' air arriving at the mountain but which fails to get over it. It will move towards low pressure, across the geostrophic wind, thereby gaining kinetic energy. The deflection across the isobars may begin 50, 200, or even 1,000 mi upwind of the mountain, and in such a distance it would be possible for the airstream to acquire kinetic energy in order to get it over the mountain. This additional energy may appear as potential energy again by flow across the isobars towards high pressure on the lee side or in the form of lee waves superimposed on the stream. It is important to note that this kinetic energy does not necessarily appear in the layers below the mountain top only.

The second part of the answer is that wavy motions at high levels produce horizontal gradients of hydrostatic pressure in the direction of motion, and if the waves are not in the same phase at all heights over a point on the ground, a wave trough at high levels, by warming the air, can produce a pressure minimum at lower levels, which causes a speeding up of the low-level air coming towards that point. Perturbation theory *usually* predicts that if the air is statically stable the wave pattern will vary in phase over a mountain (but not in lee waves). But not *always*, because if the hypothesis is made that there is a rigid lid, or free-liquid surface, or inversion above which there is no motion, then these horizontal pressure gradients in the direction of motion can be maintained by conditions at the upper boundary at finite height.

Dept. of Meteorology,
Imperial College of Science and Technology,
London, S.W.7.
8 January 1957.

551.521.3 : 551.521.61 : 551.510.534 : 551.524

The influence of the 9·6 μ ozone band on the atmospheric infra-red cooling rate

551.521.61

The influence of the 15 μ carbon-dioxide band on the atmospheric infra-red cooling rate

By G. N. PLASS

(Read 19 December 1956. Presented by Prof. P. A. Sheppard. See *Q.J.*, **82**, p. 30 and p. 310)

Dr. R. M. Goody : I think Dr. Plass is to be congratulated upon two useful papers which will undoubtedly be put to good use in studies of the dynamics of the upper atmosphere.

I am, however, troubled by the method, particularly as applied to ozone. Epstein, Osterberg and Adel (1955) have treated statistically Summerfield's ozone data and find that the absorption area of the 9·6 μ band varies as a function of $w\,p^{0\cdot253\pm0\cdot023}$. Thus the data used by Dr. Plass are very far from being in the ' strong-line ' region. For the 15 μ carbon-dioxide band Howard, Burch and Williams (1955) find that band area varies as $w\,p^{0\cdot87}$ for their laboratory data. In this case therefore laboratory data are probably much more nearly in the strong-line region.

As I understand the method, it is assumed that there is either the ' strong-line ' case or the ' linear-law ' case or Doppler broadening. It is hard to say how this affects the final results. Special examples can be constructed where the mistaken use of the strong-line case instead of the linear-law case can lead to heating-rate errors of orders of magnitude. There is little comfort to be gained from the laboratory data. Walshaw (1954) made measurements on ozone over four orders of magnitude change in pressure and three orders of magnitude change of amount. He just reached the linear-law region, he hardly reached the Doppler region and he never reached the strong-line region. Thus almost all of Walshaw's observations were in regions for which the methods used in these papers would be inadequate.

Things may be rather better in the case of the 15 μ carbon-dioxide band. The results shown agree as closely as might be expected with computations made by a totally different method due to Curtis (1956) (see also Curtis and Goody 1956). The agreement must however be partly fortuitous for Curtis's method needs to be improved as Curtis himself is well aware.

Incidentally Dr. Plass's computations on carbon dioxide cease at a level of great physical interest, above which the fundamental assumption of Kirchoff's law is no longer valid (Curtis and Goody, 1956).

References

Curtis, A. R.	1956	*Proc. Roy. Soc.* A, **236**, p. 56.
Curtis, A. R. and Goody, R. M.	1956	*Ibid.*, **236**, p. 193.
Epstein, E. S., Osterberg, C., and Adel, A.	1955	*Sci. Rep. U.S. Air Force*, No. HA-7, Contract AF19 (122)-198.
Howard, J. N., Burch, D. L. and Williams, D.	1955	*Geophys. Res. Pap. U.S. Air Force*, Cambridge, No. 40.
Walshaw, C. D.	1954	Dissertation, Cambridge University.

Dr. L. Kaplan : I should like to compliment Professor Sheppard on an excellent presentation of Dr. Plass's papers.

In general I agree with Dr. Goody's remarks. Summerfield's data as given in Plass's diagram do not fit the ' universal curve ' within experimental error, since separate, smooth curves can be drawn through the constant-pressure points. This is to be expected from the great line-density in the ozone spectrum (Kaplan, Migeotte and Neven, *J. Chem. Phys.*, **24**, p. 1183, 1956). Over the main part of the 9·6 μ band, there are from ten to fifty lines per cm^{-1} with intensity greater than one per cent of that of the strongest line, so one can hardly consider the transfer to be due to line-wing absorption.

The carbon-dioxide lines are not as closely spaced, and I believe this to be the reason for the better fit of the data to a universal curve. But even in these data, systematic deviations can be observed, especially in the figures for the band wings. The agreement of Plass's cooling rates in the lower stratosphere with Curtis's results, as presented by Dr. Goody, is probably accidental, and due to Curtis's neglect of overlapping and of most of the weak lines. My values for cooling rates at these heights (*J. Met.*, **9**, p. 1, 1952), obtained by retaining the actual line-shape near the line-centres and without neglecting line-overlap, were half as large, indicating that absorption near the line-centres and overlapping must be taken into account in radiative heat-transfer calculations for the troposphere and lower stratosphere.

Mr. G. S. Callendar (*communicated*) : Amongst the many points of interest arising from Dr. Plass's calculations, I should like to refer to the thermal influence of CO_2 in the troposphere. Dr. Plass finds that its effect there would be a cooling of about 0·2°C per day at all levels, as no doubt would be the case in a very dry air mass. If, however, the radiation from water vapour is taken into account it will be found that the CO_2 actually causes a significant reduction of cooling rate in the lower troposphere of warm and temperate regions. This effect arises both from the rapid fall of water-vapour density with altitude, and from the relative absorption intensities of these gases in the spectral range of the CO_2 band.

Admittedly our knowledge of water-vapour absorption is still only approximate here, but there are sufficient data from Adel's (1940 and 1942) observations of atmospheric transmission on both wings of the CO_2 band, to show that its absorption divergence is very large over a range of the order of 2 to 0·2 g/cm^2. In consequence of this, and its distribution in altitude, there would be a strong upward flux of radiation in 13 to 17 μ from the warm, dense layers of water vapour at low levels were it not for the CO_2 absorption. The latter is strong, with relatively small divergence in altitude, so it would stop the direct escape of most of this water radiation, and thus reduce the cooling rate in the troposphere at levels below that corresponding to a temperature of around $-5°$ to $-10°$C. When clouds are present the thermal effect of CO_2 absorption is similar, although mainly localized at the upper surface of the cloud as the principal source of outgoing radiation.

Since this thermal effect of CO_2 is largely transferred from the surface to the lower troposphere when much water vapour or cloud is present, its overall influence on the temperature equilibrium should be similar for a wide range of climates, although more accurate values of water-vapour absorption in 13 to 18 μ are required to confirm such points as this.

Dr. Plass finds that surface temperatures would fall nearly 4°C as a direct result of halving the amount of CO_2 in the air. If, however, secondary effects, such as reduced water-vapour absorption in the colder air, and increased albedo from the spread of ice and clouds to lower latitudes, are taken into account this fall might well be increased by a factor of two or more in some regions. A further secondary effect which may be of great importance is suggested by Dr. Plass's remarks on the influence of CO_2 on cloud cooling, because any change of cloud cover, or albedo, alters the supply of solar heat.

References

Adel, A. 1940 *Astrophys. J.*, **91**, p. 481.
1942 *Ibid.*, **96**, p. 239.

Dr. G. N. Plass (*in reply, communicated*) : I would like to thank Prof. P. A. Sheppard for his presentation of my papers.

It appears from the remarks of Dr. Goody and Dr. Kaplan, that the procedure which was followed for my calculations is not entirely clear. This misunderstanding may have arisen because I was asked to shorten considerably this section of my original manuscript. Let me attempt to clarify this matter and to state here exactly how this portion of the calculation was done. The point at issue seems to concern the method which was used to obtain the transmission function between two different heights in the atmosphere.

In order to simplify the discussion, I will refer here only to the ozone band. The identical method was used for the carbon-dioxide band. The experimental data are plotted in Fig. 1 of my paper on ozone (referred to as Fig. 1 in the following discussion). A theoretical consideration of the problem (Plass 1952) shows without question that even in the most general case the absorption is a function only of pw (pressure times path length) for any given pressure when the path length is greater than a certain critical amount. When this condition is satisfied, I will refer to the resulting curve of absorption plotted against pw as the strong-line curve (instead of the expression ' universal curve ' which I have used on some previous occasions). All the experimental

data that are known to me support the above-mentioned theoretical conclusion. The results o the laboratory experiments give us the functional form of the absorption curve. In addition, they determine the critical path length, w_c, at which the absorption curve for a particular pressure p_c, begins to depart appreciably from the strong-line curve. For example, for ozone this occur when $\log pw = 2{\cdot}4$ for 58 mm pressure and when $\log pw = 1{\cdot}9$ for 25·8 mm pressure. Nov it is only necessary to determine from the experiments a relatively small number of pairs o values for p_c and w_c, since other pairs of values can then be calculated. I have shown (Plass 1954 that for various pressures $p_c = A\, w_c$, where A is a constant, when there is no appreciable over lapping of the lines, and by more complicated expressions when there is overlapping. For use in my calculations the value of w_c was determined for each pressure, p_c, either directly from the experimental measurements or by a straightforward theoretical calculation based on the experimental results. The strong-line approximation was only used in my calculations when $w > w_c$ at the pressure p_c, i.e., the strong-line approximation was only used in the region where experimentally it was found to be valid.

For short path lengths (I will refer to this as the linear region) the absorption is determined from the total band intensity by the method described in my article. If these curves are plotted in Fig. 1, for each pressure there is a separate absorption curve which has a slope of unity in the linear region. The separation of these curves for a given value of pw is the logarithm of the pressure ratio for the two curves. In this manner the absorption curve for a given pressure was determined in the linear and strong-line regions from the experimental data. Finally, an estimate of the absorption was made in the intermediate region between the two limits discussed above. In some cases the experimental measurements determined the absorption curve in this intermediate region when they indicated a departure from the strong-line curve. In the remaining cases it was necessary to connect the absorption curves in the linear and strong-line regions in the most reasonable manner possible; for this task use was made of the measured and calculated regions of validity and the experimentally-determined shape of the absorption curve at other pressures.

Thus the absorption was determined for all relevant values of p and w. Finally, these values of the absorption were changed into the appropriate values for the variable path conditions in the atmosphere by the method which I have previously described (Plass 1952). As an example of the procedure followed by the electronic computer, consider the problem of obtaining the transmission function from the surface of the earth to all higher levels in the atmosphere. For nearby levels, the path length is so short that the absorption follows the linear law. As the path length increased, the absorption was obtained from the appropriate constant-pressure curve in the intermediate region. For still greater path lengths, the machine tested the relevant values of p and w in order to determine whether the path length was sufficiently long so that the strong-line curve was applicable. This condition might or might not be satisfied when the upper level was near the top of the atmosphere, depending on the frequency interval under consideration. In any case the machine based its decision on the absorption curve that should be used entirely on the experimentally determined regions of validity, and always used the appropriate absorption values determined by the method described above.

In reply to Dr. Goody, it is not particularly relevant that the total band area in certain cases varies as a function of wp^a, where $a < 1$. The absorption of an actual band cannot be represented over an appreciable range of pressure and path length by such a simple function. Such representations of band spectra have only a limited range of usefulness. They certainly are not valid for either short or long path lengths; further, the region of validity of these results is not stated. Although I have not seen the report of Epstein, Osterberg and Adel, I feel sure that their low value of a ($a = 0{\cdot}253$) was obtained because they included the measurements at a pressure of one atmosphere, which depart considerably from the strong-line curve of Fig. 1. At one-atmosphere pressure the strong-line curve for ozone is valid only for path lengths greater than those shown in Fig. 1. In my calculations the experimental data are not used for the purpose of obtaining a simple approximate expression for the absorption with a limited range of validity, but rather to determine the actual values of the absorption regardless of their functional form over as wide a range of path lengths and pressures as possible.

In further reply to Dr. Goody, let me state that a Doppler region as such was never used in my calculation. The correction for the Doppler line shape was introduced continuously, as the altitude increased, from the equations of Plass and Fivel (1953). One reason for not extending these calculations to higher altitudes is that these corrections become too large to handle by this method. Another reason is that Kirchoff's law is no longer valid, as has been pointed out by Curtis and Goody in their most interesting paper.

In reply to Dr. Kaplan: in my method, separate, smooth curves were used for the absorption at various given values of the pressure when there was sufficient departure from the strong line curve to make an appreciable difference in the absorption. I am afraid that it is not correct to draw conclusions as he suggests about the wing absorption from a single parameter representing the number of lines per cm^{-1}. Regardless of how great this number may be, there will be wing absorption for a sufficiently long path length. The crucial question is to determine how long a path length is required. In my method this can readily be determined from the experimental results by inspection of the absorption data (Fig. 1). The experimentally determined dependence of the absorption on p and w shows unambiguously when most of the absorption in the interval comes from the wings of the lines.

Dr. Kaplan is to be complimented on his early work where he calculated the heat transfer from the carbon-dioxide bands, which I have followed with a great deal of interest (Kaplan 1952). However, it should be pointed out that the following assumptions were made in Dr. Kaplan's calculation: (1) the line strength is independent of temperature; (2) the half-width is independent of temperature; (3) the carbon-dioxide band can be represented by the Elsasser model of equally spaced and equally intense lines over appreciable frequency intervals; (4) the diffuse radiation can be obtained from the beam radiation by multiplication by the constant factor 1·66; (5) the old calculated values for the positions and intensities of the lines are correct (these have since been revised considerably by Dr. Kaplan); (6) many of the weak lines in the band can be omitted (Dr. Kaplan now states that these should be included in the calculations). I am not criticizing this pioneer work in the field, but I am merely pointing out that it is difficult to assess the accuracy of his results because of the many approximations that were used. In my calculations the following factors were taken into account: variation of line strength with temperature (for the carbon-dioxide band); variation of half-width with pressure and temperature; overlapping of the lines; the actual irregular variation of the strength and position of the spectral lines from line to line as it affects the experimentally measured absorption; the correction for the Doppler line shape at high altitudes; a variable multiplier depending on the transmission to obtain the diffuse radiation. The only approximation in my calculation that could introduce an error of more than 1 per cent in the calculated flux (aside from the experimental error associated with the absorption measurements) might conceivably arise from estimating the absorption in the intermediate region between the linear and strong line regions in the instances where this was not measured experimentally. I am sure that eventually it will be possible to perform a calculation similar to Dr. Kaplan's and to obtain more accurate results than I have obtained from the experimental data. However, this will require a much more accurate computation of the positions and intensities of the spectral lines than any that have been published to date. Even when these data are available, the calculation of the radiation flux will be a very complicated task even for a large electronic computer. I understand that Dr. Kaplan has already made some progress in this direction. However, in view of the many approximations that were made in Dr. Kaplan's original calculations, I do not feel that a comparison of our results leads to the conclusions drawn by him.

I would like to thank Mr. Callendar for his interesting observations about the influence of water vapour on the carbon-dioxide cooling rate and on the problem of climatic variation.

References

Kaplan, L. D.	1952	*J. Met.*, **9**, p. 1.
Plass, G. N.	1952	*J. Opt. Soc. Amer.*, **42**, p. 677.
	1954	*J. Met.*, **11**, p. 163.
Plass, G. N. and Fivel, D. I.	1953	*Astrophys. J.*, **117**, p. 225.

551.465 : 551.556

A determination of the relation between wind and sea-surface drift

By P. HUGHES

(Read 19 December 1956. See *Q.J.*, **82**, p. 494)

Miss S. A. Yeo : The variation of currents with depth near the surface is such that the trajectories of floating bodies of different size are often widely divergent. The direct wind action on any part of the floating body which is not submerged is also difficult to allow for. Both effects are difficult to assess, either experimentally or theoretically.

Some preliminary measurements on a smaller scale have been made, with the cooperation of the Metropolitan Water Board, at King George VI Reservoir at Staines, using 1 in. diameter polythene discs (density 0·93 g cm^{-3}) of various thicknesses and National Institute of Oceanography drift cards as used in the Oil Pollution Investigation. The technique is simple; the drifting body is released from a fixed pole in the centre of the reservoir and the time taken to drift a fixed distance is noted. The distance used is 30 m and it is marked by a circle of small buoys on light lines. Wind profiles are measured simultaneously by Sheppard anemometers mounted on the fixed pole.

Most runs so far have been made with $\frac{1}{8}$ in. discs. The ratio between drift speed and the wind speed at $\frac{1}{2}$ m is about 1/30; it appears to decrease slightly with increasing wind speed. The ratio of the speed of drift envelopes and of the $\frac{1}{8}$ in. discs is 1·4 at wind speeds below 2 m/sec, falling with increased wind speeds to about 1·1 at a wind speed of 5 m/sec.

The agreement Mr. Hughes claims with the work of Keulegan and van Dorn appears to be founded on a misconception : Keulegan's results were based on wind measurements at 10 cm or less above the water surface, and Hughes's are at 1,000 cm. The error thus made may, however, be largely compensated by the direct effect of wind on the cards so that there is a satisfactory agreement between surface-drift measurements on such different scales as the small laboratory tank and the open ocean.

Mr. J. R. D. Francis : The good agreement that Mr. Hughes finds between the direction of drift and the mean wind direction is the striking result of his investigation. There is, however, much more doubt about his wind-speed factor k. Not only could wind action on the above-water part of the envelope be important, but also the presence of currents caused by the ocean wind-system as a whole could give appreciable errors which might not be detectable. For instance, a comparison with some wind-tunnel tests I carried out some time ago (Francis, *Proc. Roy. Soc.* A, **206**, p. 387, 1951) on thin cork floats shows that the cards Mr. Hughes has analysed were travelling about 50 per cent faster than mine, that is about 5 km/day faster. A semi-permanent ocean current of this magnitude might have been present, but it also might not have been detected by the usual oceanographic methods.

Mr. E. Gold : Nearly 50 years ago, in a review of the Netherland Institute's publication of meteorological tables and charts for the Indian Ocean (*Nature*, 17 Sept. 1908) I drew attention to the facts : (1) that, in the SE. Trades and further south in the westerlies where the wind was fairly steady in direction, the ocean currents flowed in a direction about 45° to left of the direction towards which the wind blew, (2) that V. W. Ekman had just previously developed a theory according to which such a result could be expected from the effect of the earth's rotation (left deviation on the S. Hemisphere, right in the North), (3) that Nansen had found a similar result in the drift of the *Fram* in northern latitudes. In view of this and of the tolerances which Mr. Hughes indicated might be expected in his results, I should like to ask what would be the divergence in the final positions of his drifting objects if he assumed that the currents were 45° from the wind direction in the periods for which this was broadly steady for a substantial time.

Dr. J. N. Carruthers (*communicated*) : The plastic envelopes about which Mr. Hughes has spoken, were made up in the light of plenty of past experiences by other people, but with none of the usual care taken to make all the envelopes identical in point of flotation. Experiments carried out in open stretches of the Mediterranean Sea, where tidal streams are negligible, had earlier shown that the travels made good by thin, flat envelopes containing nothing but a questionnaire postcard in the plastic sheath, differed markedly from those accomplished by thicker envelopes released at the same times and places. These latter had enclosed with them a postcard-sized wafer of cellular cardboard which made them as thick as a slice of common ryebread.

The two slices of natural cork sheet and the folded instruction slip sealed inside the envelopes whose ultimate travels Mr. Hughes has dealt with, were enclosed for two reasons : to make the envelopes heavy enough to escape being blown off wavecrests, so becoming airborne for a brief spell at times of gales, and to avoid loss due to sinking if the outer and tougher plastic casing became punctured by bird-peck or from other cause. The amount of air enclosed was not by any means constant and the flotation was consequently likewise. The envelopes were designedly made just as they were made, so that if inferences as to possible oil-patch drift were based upon the travels which the envelopes ultimately made good, one would paint the gloomiest picture of the possibilities in respect of beach pollution. Mr. Hughes's study amounts therefore to associating the overall chordal travel of such envelopes (not necessarily uniform) with barometrically-inferred wind. To what extent surface current comes into the question will depend upon what that expression is taken to mean in view of the fact that thinner envelopes might well (as bottles certainly would), have performed different overall journeys under the same conditions. In some quarters the easily-transported plastic envelopes which are so convenient for widespread sowing from aircraft have gone out of favour – as at one important fisheries laboratory for instance. They are nevertheless being regularly liberated well off the Atlantic coast of France, and large-scale use of them is planned in the western Indian Ocean during the International Geophysical Year. A form which simulates the Portuguese Man-o'-War by virtue of a long pendant ' concertina ' of thin plastic strip fixed below the envelopes, is claimed to be a great improvement so far as the avoidance of direct windage is concerned, but it can hardly be such unless the tails are always fixed so carefully as not to cant the envelope and thereby provide a ' sail ' for the wind to press underneath.

The general pattern of surface-water movement off our Atlantic seaboard, and a good deal about its dependence on varying wind conditions, is known from innumerable strandings of drift bottles spread over a very long term of years.

Individual listeners to the account given of the stimulating and painstaking study made by Mr. Hughes will make different appraisals of its outcome according to their individual conceptions of what is meant by surface current.

Mr. H. Charnock (*communicated*) : To me the most interesting conclusion of Mr. Hughes's paper is that the surface drift is in almost the same direction as the gradient wind. I can see no reason to doubt the observations in this connection : his result is clearly in line with our observations of the Westerlies over the sea.

His assumption that there is a constant ratio between wind speed and drift velocity has often been made before, but deserves further consideration. If we assume that the variation of wind speed with height is given by the usual logarithmic expression and that, as seems likely, the roughness length (drag coefficient) varies with wind speed, then it follows that the surface drift cannot be linearly proportional to wind speed at an arbitrary height.

This argument does not only apply to surface drift; in the case of mean-square-slope, for example, it implies that the recent paper of Munk (*Q.J.*, **81**, p. 320, 1955) is mildly paradoxical.

The point is that results such as Hughes's should, whenever possible, be analysed in relation to the friction velocity. To a first approximation this is linear with wind-speed and to this extent the argument above is formal only.

Mr. P. Hughes (*in reply*) : I am glad to have this opportunity of thanking Dr. J. N. Carruthers, who was responsible for much of the original Oil Pollution Investigation, for his advice. His wide knowledge of drift methods is evident from his contribution.

As he says, it is difficult to devise an adequate theory for the drift of any surface floating object; research like that of Miss Yeo will be very useful. Her observations seem to confirm my assumption that the windage of drift cards is relatively small at the wind speeds encountered in the open sea during the experiments.

In my paper, I stated that any movement of water, not due to the local wind, appears as an error in the wind factor, k. There is insufficient evidence on which to base a correction for this type of flow. When one considers that for two periods of different wind conditions the values of k were substantially the same, it seems likely that this effect was small.

The use of the assumption that the drift cards move at an angle of 45° to the right of the wind, as Mr. Gold suggests, would result in a divergence of several hundred miles from the actual recovery positions.

Proceedings at meetings of the Society

Ordinary Meeting, 16 January 1957

The meeting took the form of a discussion on ' New methods in the ozone problem.' Si Charles Normand, who was in the chair, gave an introductory survey and was followed by :

Dr. R. M. Goody (Imperial College) on ' The use of infra-red methods '; Dr. H. K Paetzold (Max Planck Institute, Weissenau) on ' Temperature measurements from the Huggin bands '; Dr. C. D. Walshaw (Oxford), on behalf of Dr. H. A. Gebbie (Liège University), o ' The possibility of microwave measurements '; Dr. H. K. Paetzold on ' A filter radiosonde ' Dr. E. Gluckauf (Atomic Energy Research Establishment) on ' A review of chemical methods ' Dr. A. W. Brewer (Oxford) on ' A chemical radiosonde '; Dr. H. K. Paetzold on ' Measure ments at lunar eclipses'.

Ordinary Meeting, 20 February 1957

The following candidates were declared to have been elected by the Council at their meetin on 23 January 1957 :

Fellows

Caröe, Charles Frederick, ' West Hey,' Dawstone Road, Heswall, Wirral, Cheshire.
Fleming, Alan Preston, 43 Hiliary Gardens, Stanmore, Middlesex.
Gillespie, S/Ldr. John Warren, R.Aux.A.F., Leyfield, Worcester Park, Surrey.
Harrison, Paul, High Cross, Constantine, Falmouth, Cornwall.
Hay, James Sutherland, 118 Westwood Road, Bemerton Heath, Salisbury, Wilts.
Ho, Tong Yuen, Malayan Meteorological Service, Kuala Lumpur, Malaya.
Jarvis, Charles Harvey, 69 Penrose Avenue, Carpenders Park, Watford, Herts.
McHutchen, Capt. John Guthrie Scott, ' Latimer,' Arthurlie Drive, Newton Mearns Renfrewshire.
Ng, Thye Er, Malayan Meteorological Service, Kuala Lumpur, Malaya.
Peel, William, B.Sc., A.R.I.C., 3 The Crescent, Thirsk, Yorks.
Saunders, Peter Michael, M.Sc., 7 Rushout Avenue, Kenton, Harrow, Middlesex, (*transfe from Student Membership*).
Stephenson, Peter Maurice, M.Sc., 58 Larkfield Avenue, Kenton, Harrow, Middlesex.
Tan, Beng Keat, c/o Meteorological Office, Kuala Lumpur Airport, Kuala Lumpur, Malaya
Tandoh, Samuel Edwin, c/o Meteorological Dept., Airport, Accra, Gold Coast, Britis West Africa.
Tebbitt, Leslie Henry, 18 Norbury Cross, London, S.W.16.
West, Michael Anthony, 120 Lexham Gardens, London, W.8.

Foreign Members

Court, Arnold, Ph.D., 1524 Arch Street, Berkeley, 8, California, U.S.A.
Schmidt, Franz Heinrich, Ph.D., Scientific Research in Forecasting Division, Royal Netherland Meteorological Institute, De Bilt, Holland.

Student Members

Rudkin, John, ' Eureka,' 307 Pennygate, Spalding, Lincs.
Saiedy, Fuad, Department of Meteorology, Imperial College, Exhibition Road, London, S.W.7
Sein, Shwe U, Department of Meteorology, Imperial College, Exhibition Road, London, S.W.7
Spiro, Stanley, c/o Meteorological Office, H.Q. Bomber Command, Royal Air Force, High Wycombe, Bucks.

Canadian Branch

Fellows

Austin, Harold Arron, B.A., 472 Meredith Road, Calgary, Alberta, Canada.
Coulcher, Blane Anthony, B.A., 608 Broughton Street, Victoria, B.C., Canada.

ASSOCIATES

BLAKE, Michael, M.A., Apt. 2, 42 Cloverdale Avenue, Dorval, P.Q., Canada.
FRASER, Hugh McKay, M.A., 356 Linwood Street, St. James, Winnipeg 12, Manitoba, Canada.
HARVEST, Eric, B.A., 315 Bloor Street West, Toronto 5, Ontario, Canada.
HUNTER, Harry Issac, B.A., P.O. Box 142, R.C.A.F. Station, Fort Nelson, B.C., Canada.
MORGAN, J. C., P.O. Box 648, Montreal 3, Canada.
MOODY, George David, B.Sc., Ste. 3, 746 Osborne Street, Winnipeg 13, Manitoba, Canada.
RIPLEY, Earl Allison, M.A., 3 Isner Avenue, Halifax, N.S., Canada.
STRACHAN, Robert A., M.A., Main Meteorological Office, Trans-Atlantic Administration Building, Montreal Airport, Dorval, P.Q., Canada.

The following candidates were then declared to have been elected that day by the Council:

FELLOWS

AJASHI-NZERIBE, Ferdinand Uwadiegwe, Department of Statistics, Jos, Nigeria.
BLACKBURN, Joseph J. W., 326 Ayer Itam Road, Penang, Malaya.
DILLON, Robert William, 4 Woodward Road, Pershore, Worcs.
FIRTH, Allan William Owen, B.Sc., 16 Wye Road, Brockworth, Glos.
GRANT, Rev. Dr. John Peter, D.D., Uplands Burley, Nr. Ringwood, Hants.
GRAY-HUTCHERSON, Sidney James Barnard, Box 30030, Nairobi, Kenya.
JESSOP, Edgar E., 14 Murrayfield Gardens, Edinburgh 12, Scotland.
MCKELLAR, Henry Archibald, 28 Ferguslie, Paisley, Scotland.
ROBERTS, Robert Owen, 'Tryfan,' Kinmel Avenue, Abergele, N. Wales.
TAYLOR, Deryck Francis Henry, 9 Morland Road, Kenton, Harrow, Middx.

FOREIGN MEMBERS

LARSEN, Søren Hagerup Holck, c/o Dr. G. M. B. Dobson, C.B.E., F.R.S., Watch Hill, The Ridings, Shotover, Oxford.
ROSENAN, Naftali, c/o Meteorological Service, P.O. Box 7036, Tel-Aviv, Israel.
ZIMMERSCHIED, Dr. Wilhelm F., c/o Resident Representative, Quito U.N.T.A.B., P.O. Box 2951, Ecuador.

The following papers were read and discussed:

1. 'Fog precipitation on Table Mountain' by J. F. Nagel (*Q.J.*, **82**, p. 452); presented by Dr. H. L. Penman.
2. 'Precipitation by direct interception of cloud water,' by S. Twomey (C.S.I.R.O., Australia), to be published in *Weather*; presented by Mr. J. H. Hallett.
3. 'The use of a stream function in a two-parameter model of the atmosphere,' by F. H. Bushby and V. M. Huckle (*Q.J.*, **82**, p. 409).
4. 'The representation of the annual temperature variation over central and northern Europe by a two-term harmonic form,' by J. M. Craddock (*Q.J.*, **82**, p. 275).

Ordinary Meeting, 20 March 1957

The following candidates were declared elected that day by the Council:

FELLOWS

APPERLEY, Wilhelmina Grace, Brooklyn, 27 Stuart Avenue, Bare, Morecambe, Lancs.
CORNFORD, Stanley George, B.Sc., Meteorological Office, R.A.F., Syerston, Newark, Notts.
ELLETT, David James, 109 Wellesey Road, Gt. Yarmouth, Norfolk.
GROVE PARK BOYS' GRAMMAR SCHOOL, Wrexham, Denbighshire, (nominee: David Thomas Morgan, M.A.).
MACIVER, William, 'St. Annes,' Sassafras, Victoria, Australia.
MCINNES, Bennet, B.Sc., 3 Cornwallis Place, Edinburgh, 3, Scotland.
O'CONNOR, Thomas C., M.Sc., St. Philomenas, Munster Avenue, Galway, Ireland.
PHEAR, Henry John, M.A., P.O. Box 8066, Salisbury, S. Rhodesia.
SOOD, Bharat Bhushan, 41 Rockstone Lane, Southampton, Hants.
STANHILL, Gerald, Ph.D., The National Vegetable Research Station, Wellesbourne, Warwicks.
WOOD, Kenneth William John, Senior Civil Service Mess, R.A.F., Habbaniya, B.F.P.O. 61.

Foreign Members

Angell, Dr. James Kennedy, 1106 Valley Drive, Alexandria, Virginia, U.S.A.
Borvick, Einar, Meteorologisk Institutt, Blindern, Norway.

Student Member

Evans, James Barrie, 8 Rossett Way, Little Acton, Wrexham, Denbighshire.

Canadian Branch

Associates

Crowe, Ronald Bertrand, 315 Bloor Street West, Toronto, Ontario, Canada.
Hubbert, L. W., 315 Bloor Street West, Toronto, Ontario, Canada.
Mukammal, E. I., 315 Bloor Street West, Toronto, Ontario, Canada.
Wingfield, John Malcolm, 315 Bloor Street West, Toronto, Ontario, Canada.

The following papers were read and discussed :

1. ' Theoretical estimates of the collection efficiencies of small droplets ' by T. Pearcey and G. W. Hill (*Q.J.*, **83**, p. 77); presented by Mr. J. S. Turner.
2. ' Inherent precipitation mechanism in cumulus clouds ' by T. W. R. East (*Q.J.*, **83**, p. 61).
3. ' Radar observations of showers suggesting a coalescence mechanism ' by P. J. Feteris and B. J. Mason (*Q.J.*, **82**, p. 446).

Popular Lectures

To meet the demand for the Society's Popular Lecture to sixth-form pupils, Mr. N. Bradbury repeated his lecture on ' Aviation meteorology ' on the following occasions :

17 January 1957 at Trinity School, Wood Green, by kind invitation of the Education Officer of the Middlesex County Council. Mr. D. Chilton was in the chair.

13 February 1957 at Ealing County School, by kind invitation of the Chief Education Officer of the Middlesex County Council. Instr. Capt. C. R. Darlington, R.N. was in the chair.

14 March 1957 at the Manchester Training College by arrangement with the Chief Education Officer of the City of Manchester. Miss S. M. Valentine, Inspector of Schools, Manchester, was in the chair.

28 March 1957 in the Department of Natural Philosophy, University of Glasgow, by arrangement with the Education Officer of the Corporation of Glasgow. Mr. J. R. Atkinson (Vice-President for Scotland) was in the chair.

29 March 1957 in the Department of Natural Philosophy, University of Edinburgh, by arrangement with the Education Officer of the City of Edinburgh. Mr. J. R. Atkinson was in the chair.

The total attendance at these five lectures was about 1,100.

Reviews

Physics in Meteorology. By A. C. Best. London (Pitman), 1957. Pp. viii, 159; 26 Figs., 13 Tables. 18s.

Dr. Best's object, of writing a book to interest the physics student in meteorological problems, is wholly admirable. Progress in our science, which may be defined as the physics of the atmosphere, will depend largely upon the recruitment of able young physicists in the face of ever-increasing competition. Failure to attract sufficient high-quality graduates in the past may be partly attributed to the scant attention which meteorology receives in university physics courses, but not least to the lack of suitable texts. This book is therefore a step in the right direction.

In it, Dr. Best selects certain topics, e.g., meteorological instruments, cloud physics, radiation, atmospheric electricity, meteorological optics and radio-meteorology, which rest upon the kind of classical physics which should be familiar to the undergraduate, and aims to show how the physical principles of the laboratory find expression in the free atmosphere. He will, no doubt, be criticized for not discussing dynamical processes and the behaviour of weather systems; for standing on the sidelines rather than plunging into the heart of the subject. But, of course, it is difficult to say anything worth while about atmospheric motions in all their complexity to a student having no meteorological background and probably little or no knowledge of hydrodynamics. In the circumstances, the author is probably wise to concentrate on those aspects which can be discussed (although, of course, not fully) in terms of concepts and techniques which the physics student can appreciate.

The disappointing feature of the book is not its scope, but that it curiously fails to bring to life topics which are developing quite rapidly at the present time, and which should whet the appetite of any real student of physics. Dr. Best's treatment which, apart from an occasional lapse, is quite sound, lacks colour. It may not persuade the young physicist of the wide scope for his talents in meteorology; of the enormous range of interesting problems which can be and are being tackled by a wide variety of experimental, observational and theoretical techniques, and of the challenge which research in our subject presents. While it is right and proper to emphasize basic concepts and relationships, there is much to be said for underlining the central problems and for hinting at some of the difficulties. To devote ten of twenty-two pages on cloud physics to the equations of droplet growth by condensation, and only about one page of the chapter on atmospheric electricity to the central problem of charge generation in thunderstorms, to ignore completely developments in radiation since about 1940, and to treat radio-meteorology almost entirely in terms of formulae with hardly a mention of the use of radar in the study of clouds and atmospheric motions, is hardly to capture the present spirit of the science. Such a treatment appears academic and rather dull; the subject is certainly neither.

In discussing clouds, ice crystals, optical phenomena, radar and lightning, photographs are almost essential; the inclusion of a few would have provided a little more value for money in a book which seems somewhat highly priced at 18 shillings.

B.J.M.

Mathematics in Action. By O. G. Sutton. London (G. Bell and Sons), 2nd Edition, 1957. Pp. viii, 236; 54 Figs. 16s. net.

The first edition of Sir Graham Sutton's book was reviewed in this *Journal* in October 1954. The fact that a new edition has appeared only three years after the first indicates how well the public has appreciated the vigour of the different essays on the aims and fields of work in Applied Mathematics which comprise the book. Apart from the correction of errors and ambiguities, few changes have been made in most of the text; for example, the author still speaks of travelling from his college at Shrivenham. But a few pages have been added to the last chapter, on numerical forecasting as an operational method; and there is an additional short appendix on probabilities in coin-tossing experiments. The book remains one in which readers will share the enjoyment of the author in writing it.

T.G.C.

Flugmeteorologie. By Walter Georgii. Frankfurt a. M. (Akademische Verlag.), 2nd Edition, 1956. Pp. xi, 332; 217 Figs., 32 Tables. 35 D.M.

The first edition of this book appeared in 1927. This second edition, extensively revised, is intended for the use of pilots of sailplanes and power-driven aircraft.

The chapters on the structure and thermodynamics of the atmosphere, air masses and fronts in extra-tropical latitudes are all very thorough and readable. Numerous examples of actual updrafts and downdrafts in various meteorological situations, deduced from observations made during flights in sailplanes in Europe and South America, are interesting and apposite, and serve to impress upon the reader that the author is dealing with the real atmosphere and not an idealized model. Another interesting technique for detecting vertical motion in the atmosphere depends on weighting pilot balloons so that they are in neutral equilibrium in still air, and then releasing them from aircraft and plotting their subsequent trajectories; several interesting examples are given as illustrations in the book.

Unfortunately, in dealing with post-war developments the author is less successful. Indeed he appears to be unaware of a great deal of important work which has been published in the English language during the last ten years. For example, when discussing precipitation mechanisms, he deals thoroughly with the work of Bergeron and Findeisen but makes no mention of post-war work on rain from tropical cumuli. The section on the intertropical convergence zone suffers from similar shortcomings, and his treatment of West Indian

hurricanes differs in some important respects from current thought as summarized, for instance, by Bergeron in this *Journal* in 1954. The section on jet streams also contains some inaccuracies; in Fig. 187, which purports to show a section through a jet stream, the position of the tropopause is incorrect, although in Fig. 216, which also shows a cross-section through a jet stream, it is correct.

In summary, those parts of the book which deal with principles which were well established before the Second World War are well worth reading, but those which deal with post-war developments should be treated with caution.

Printing and format are good. Photographs are reproduced well and the numerous line drawings are clear, even when reduced to a small scale.

S.E.V.

Lehrbuch der Klimatologie. By B. P. Alissov, O. A. Drosdov and E. S. Rubinstein. Berlin (Deutsche Verlag der Wissenschaften), 1956. Pp. xvi, 536; 160 Figs., 6 Plates, Tables, 45 D.M.

This book is a German translation, apparently without change, of a Russian *Course in climatology* of which Parts I and II appeared in 1952 and Part III in 1954. It is a very complete and detailed work on general climatology, but only deals incidentally with local or regional climates, even of Russia. The first chapters follow stereotyped lines – the radiation factors of climate (including a map of the radiation balance of the northern land masses) and the thermal economy of the atmosphere; the influence of oceans and continents on climate; atmospheric (including 500 mb) and hydrologic circulations, all in very great detail; and the influence of the pressure distribution and atmospheric circulation, air masses and climatic fronts on climate. Chapter 4 deals in great detail with climatic zones and types, including the history of typology, and takes in much little-known Russian work. Chapter 5 is concerned with the influence of land forms, especially mountains, on climate, local winds – föhn, bora, etc. – and vegetation. Much of this is mesoclimatology; in the next chapter we pass to a very thorough treatment, occupying no less than 82 pages, of the microclimatology of the surface layers of the ground and atmosphere, minor land forms, grass and forest, water surfaces, sea coasts and finally towns. Climatic oscillations are then taken up, first from the point of view of natural changes (including a full account of mathematical methods of analysis) followed by a summary of geological, post-glacial and recent changes (as opposed to oscillations). Next comes an interesting chapter on the influence of man on climate, both accidental and planned. The accidental effects are mainly local; the ' Stalin ' plan for transforming nature is on a grand (or grandiose) scale, the object being to change the climate of, and bring under cultivation, huge areas of arid land. In this connection the microclimatic effect of wind-breaks is very thoroughly gone into.

Part II deals with methodology. In statistical investigations the homogeneity of series of observations is of first importance, and tests and causes of inhomogeneity are discussed. Next is the reduction of short series to a longer period, and statistical treatment of the individual elements and their variations. An interesting chapter deals with the analysis of microclimatic observations, including mapping, heat balance and relation to weather types and wind directions. Sections on machine methods of computation and on the evaluation of marine, upper air and synoptic data conclude the work. A flap at the back holds six large-scale folding charts of the world, January and July temperatures and pressures (with fronts), annual rainfall and Köppen's climatic types.

From this brief summary it will be seen that the book is indeed a rich source of material. The Russian bias is very marked, the writings of non-Russian meteorologists being hardly recognized – of the 157 references (up to and including 1952) 128 are to Russian authors – but from the Western point of view this is not entirely a disadvantage, opening a whole continent of little-known work. To one reader at least the development of climatology in Russia came as a surprise. The book is abundantly illustrated with maps and diagrams in the text and numerous tables, and the standard of production is very high.

C.E.P.B.

Fortschritte in der meteorologischen Forschung seit 1900. By Bernhard Neis. Frankfurt a. M. (Akademische Verlag.), 1956. Pp. xviii, 238; 21 Figs., Tables, 19 photos. 28 D.M.

This book on ' advances in meteorological investigation since 1900 ' is based on a series of lectures at the University of Berlin in 1953/54. The author points out that the twentieth century saw a number of researches begun which made a ' theory of weather ' possible, including Langley's studies of the energy distribution of the solar spectrum and the three-dimensional study of the atmosphere. However, this is neither a formal history nor a textbook, but something in between. The history aspect is maintained by photographs of well-known meteorologists, but the treatment is rather by subjects than by authors, and is often mathematical.

The first section deals with the situation in 1900 in regard to thermodynamics of the atmosphere, classical hydrodynamics and principles of instrumentation, and changes in the course of 50 years. Section 2 covers aerology, aerosol, nuclei, atmospheric electricity, cyclone models, transformation of air masses and aerological analysis, the structure of wind and radiation phenomena. In Section 3 we turn to transformations of energy, ending up with the general circulation. Finally Section 4 deals with ' practical meteorology ' – forecasting and climatology.

The book is well indexed both by author and subject, and should prove useful for reference.

C.E.P.B.

Obituary Notices

Dr. T. OKADA

Dr. Takematsu Okada was born at Fusa, Chiba Prefecture, Japan, on 17 August 1874 and died on 2 September 1956 at the same town. He attended the department of physics in the Imperial University of Tokyo and after graduating there in 1899 he entered the Central Meteorological Observatory, Tokyo, pursuing meteorology and terrestrial magnetism. In 1904 he was appointed superintendent of the forecasting division of the observatory; this position he retained until 1920. He took the degree 'Rigakuhakushi' (Doctor of Science) in 1911. In 1920 he was transferred to directorship of the Imperial Marine Observatory, Kobe, which was established on his initiative. He was elected a member of the Science Research Council in 1920, a member of the International Meteorological Committee in 1921, and a member of the Imperial Academy in 1931. He became acting director of the Central Meteorological Observatory in 1922 and a year later succeeded to the directorship. He held this important post until 1941.

Dr. Okada had been a Fellow of the Meteorological Society of Japan since 1900. He was elected a Fellow of the Royal Meteorological Society in 1921, then an Honorary Member in 1925, and was awarded the Symons Memorial Gold Medal for 1924. He was honoured by the 'Bunkakunsho' (Culture Decoration) from the government of Japan in 1949. His meteorological work covered a wide field. He compiled many books on meteorology in the Japanese language and was the author of *The Climate of Japan* (1931), which is still in use. He also investigated the long-discussed problem of the 'Bai-u' or rainy season in Japan, through which long-range weather forecasting in Japan was so much stimulated. Dr. Okada was a man of high administrative ability as well as a distinguished scientist, and the present status of meteorology and of the Japanese meteorological service owes much to him.

H.A.

Dr. A. H. RICE, D.Sc., M.D., F.R.G.S., F.R.A.S.

Dr. Alexander Hamilton Rice, a Foreign Life Member of the Society since 1931, died at his home in Newport, Rhode Island, on 23 July 1956 in his 81st year. A native of Boston, Mass., he was educated at Harvard University, graduating A.B. in 1898 and M.D. in 1904. Dr. Rice was a man of wide interests and accomplishment. He achieved distinction not only in his chosen profession of medicine and surgery but also as an explorer and geographer and as a generous patron of scientific endeavour. Early in the 1914-18 war he was made a Chevalier of the Legion of Honour for his services to France in the capacities of hospital director and surgeon. From October 1917 to February 1919 he headed the naval school of navigation and nautical astronomy at Newport, R.I. Later for a short while he held a lectureship at the Lowell Institute, but exploration was soon to claim the bulk of his time and energy. His many expeditions included seven to the Columbian Caqueta, Brazilian Amazon and Guiana, during which he surveyed and mapped some half a million square miles of territory. On another expedition led by him in 1924-25 to Rio Branco, Uraricuera and Parima he successfully used a hydroplane for reconnaissance and aerial photography, and gave what is said to have been the first conclusive demonstration of the efficiency of short-wave low-power radio in such work. Dr. Rice established and supported the Harvard University Institute of Geographical Exploration, contributing between $25,000 and $35,000 to its upkeep annually over a quarter of a century. Among his numerous honours were the awards of the patron's gold medal of the Royal Geographical Society in 1914, of the David Livingstone centenary medal of the American Geographic Society, and, in 1939, of a gold medal of the Société de Géographie, Paris. He was at one time a vice-president of the Royal Geographical Society.

E.L.H.

Mr. T. L. A. WAITE, B.Sc., A.K.C.

Thomas Lawrence Arthur Waite, who had held Fellowship in the Society since 1941, died at Nottingham on 22 July 1956 at the age of 39. He received his education at Berwick Grammar School and King's College, London. Having graduated in 1939, he joined the staff of the Meteorological Office and served during the war with the Royal Air Force as meteorological officer in England, France and Germany. After his demobilization, which was preceded by a period at S.H.A.E.F., Mr. Waite spent 2½ years at sea as senior meteorological officer on O.W.S. *Explorer* and O.W.S. *Observer*. Returning to land duties in April 1950, he was posted to R.A.F. Watnall.

E.L.H.

Mr. W. SALMOND, F.S.I., C.E., F.R.I.B.A., F.R.I.C.S.

Intimation has recently reached the Society that Mr. William Salmond died at Dundee on 2 March 1956 in his 78th year, after a rather long period of illness. Mr. Salmond was a partner in the Dundee firm of Maclaren, Soutar and Salmond, chartered architects and surveyors. He became a Life Fellow of the Scottish Meteorological Society in 1914 and was among those transferred to the Royal Meteorological Society at the amalgamation of the two bodies in 1921. During the war of 1914-18 Mr. Salmond held a commission in the Royal Engineers. On the outbreak of hostilities in 1939 he was appointed an area quartering commandant; this post he retained until about 1943.

E.L.H.

Mr. H. G. BUSK

We have to record the death, in 1956, of Henry Gould Busk. Mr. Busk, who resided latterly at Lymington, Hampshire, was elected to Fellowship of the Society on 16 November 1910 while still an undergraduate at King's College, Cambridge. In the same year he published through the Cambridge firm of W. Heffer and Sons a booklet entitled *What will the weather be ? The amateur forecaster's vade mecum.* So successfully did this little work meet popular demand that a second and enlarged edition was required within a few months.

E.L.H.

Mr. A. G. MADDOCK, A.I.Struct.E.

Alfred George Maddock, of Guildford, Surrey, who first held Fellowship in the Society more than 30 years ago and was re-elected on 17 May 1950, died on 3 February 1956. After a period at the Royal Naval College, Greenwich, Mr. Maddock saw much service in observation balloons during the war of 1914-18. Later he was for a time engaged on tidal investigations under the London County Council.

E.L.H.

FOR PUBLICATION JULY–AUGUST

Prepared under the auspices of the Royal Meteorological Society

CLOUD STUDY

A PICTORIAL GUIDE

By F. H. Ludlam and R. S. Scorer
D.I.C., F.R.Met.S. M.A., Ph.D., F.R.Met.S.

Foreword by R. C. SUTCLIFFE, O.B.E., Ph.D., F.R.S.
President of the Royal Meteorological Society

This is a new and authoritative guide, suitable for the novice yet indispensable also to the more expert reader. It is the work of two authors who have taken a leading part in the post-war research which has so greatly improved our understanding of clouds. The illustrations form a unique collection : here are to be found the pick of the magnificent photographic resources of the Royal Meteorological Society and the R.A.F., together with many contributions from private sources. Each of the 75 photographs (several of which are in full colour) is accompanied by a fully descriptive caption; while at the beginning of the book there is an introductory section explaining the principles governing cloud formation.

Size $9\frac{1}{4} \times 6\frac{1}{8}$ *in.* 80 *pages* 12*s.* 6*d. net*

This book will be available to Members of the Royal Meteorological Society at a reduced price. Details will be announced subsequently.

JOHN MURRAY, 50 ALBEMARLE STREET, W.1

PYRHELIOMETER

For the Measurement of SOLAR RADIATION

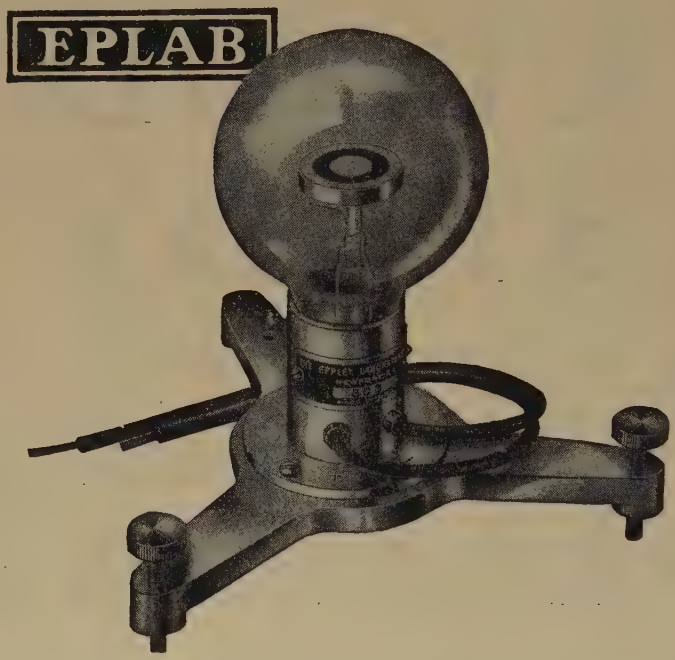

Eppley Pyrheliometers are used for solar radiation measurements at ninety-eight weather stations in the continental United States, Canada, Alaska, Greenland, Iceland, Caribbean Sea, and the Pacific Ocean. Sixty-two of these stations are under the direction of the United States Weather Bureau.

The Eppley Pyrheliometer was adopted as standard equipment by the Weather Bureau after considerable experimentation. It was found to be the best instrument so far tested by the Bureau.

Used in conjunction with a suitable recorder, the Eppley Pyrheliometer will provide an accurate and reliable record of total solar and sky radiation on a horizontal surface.

Bulletin No. 2 on Request

THE EPPLEY LABORATORY INC.

Scientific Instruments

20 Sheffield Avenue Newport, Rhode Island, U.S.A.

COMBINED INTENSITY AND TOTAL RAINFALL RECORDER

as designed and patented by

DEPARTMENT OF SCIENTIFIC AND INDUSTRIAL RESEARCH
ROAD RESEARCH LABORATORY

BRITISH PATENT NO. 722717

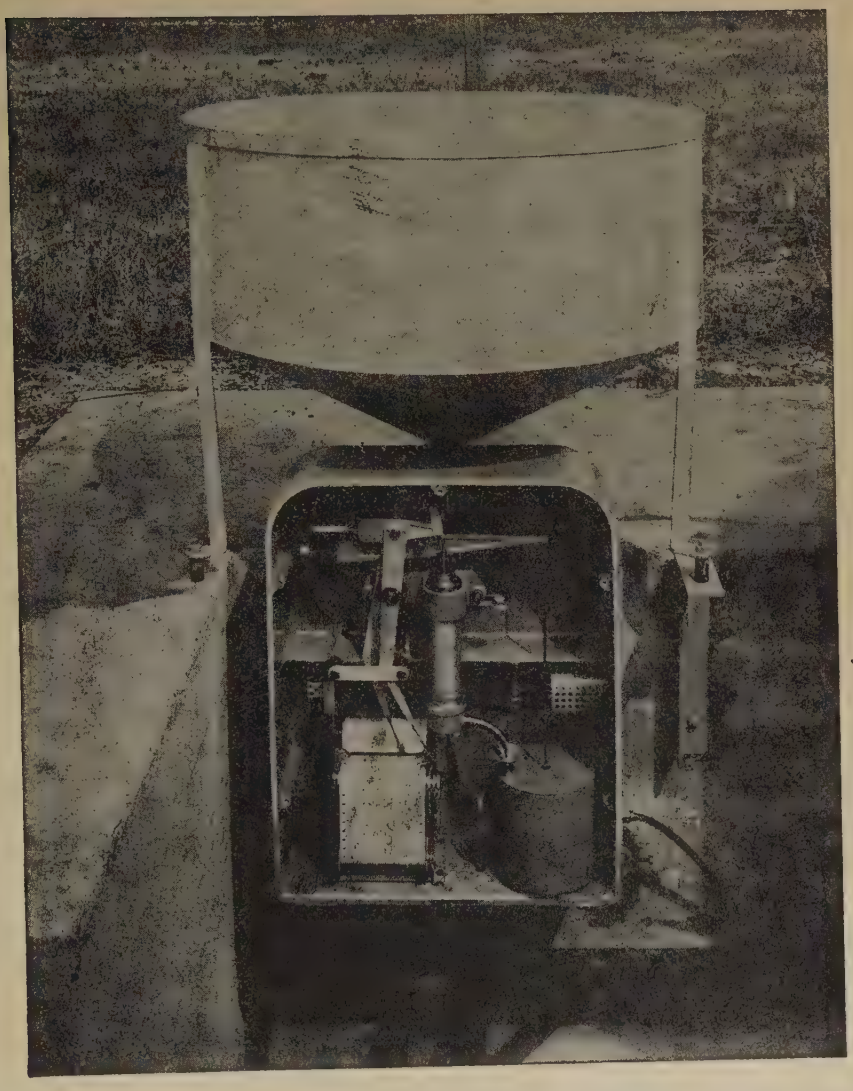

Sole manufacturing and selling rights of this instrument are vested in

TEASELL & BOWLEY (INC) LTD.,
75-79 Hagley Road, Halesowen, England

by

THE NATIONAL RESEARCH DEVELOPMENT CORPORATION,
1 Tilney Street, London, W.1

SIR RICHARD GREGORY

(President of the Royal Meteorological Society, 1928-29)

HIS LIFE AND WORK

W. H. G. Armytage

'It is a story well worth telling, and Professor Armytage has done a useful service in delineating this sympathetic portrait while the memory of his subject is still fresh in many minds.'—*Times Literary Supplement.*

'Professor Armytage has performed a notable and worthwhile task in presenting the varied activities and the wide span of his work.' —*Guardian Journal.*

21s.

MACMILLAN & CO. LTD.

St. Martin's Street, London, W.C.2

Meteorology for Mariners

An invaluable reference manual for the practising meteorologist on board ship. With more than one hundred maps, charts and diagrams. **20s.** (*post* 1s.)

Weather Map

An introduction to weather forecasting. Fully illustrated with a series of 37 typical charts. (4th edition). **10s. 6d.** (*post* 8d.)

Observer's Handbook

Observation and recording of meteorological data explained in detail. Illustrated on a lavish scale including a complete cloud atlas and numerous useful conversion tables. (2nd edition). **15s.** (*post* 1s. 1d.)

from Government Bookshops HMSO *or through any bookseller*

physics in METEOROLOGY

By A. C. Best, O.B.E., D.Sc., Deputy Director of the Meteorological Office. Many of the more common meteorological phenomena can be explained in terms of the laws of the physical laboratory – meteorology is in fact one branch of physics and the purpose of this book is to demonstrate that fact by describing and explaining a selection of meteorological phenomena in terms familiar to the student of physics. The topics dealt with include clouds and rain, wind, radiation, electrical and optical phenomena and the effects of meteorological factors upon radio propagation. The author has been a member of the staff of the Meteorological Office since 1926, during which time he served both in the research branches and on the operational side of the Office at home and overseas. From all booksellers, 18/- net.

PITMAN Parker Street, Kingsway, London, W.C.2

For Your Upper Air Soundings

USE

THE G.I.P. HYDROGEN GENERATOR

Much more economical than aluminium or calcium hydride. Gas production with no sudden increases in pressure. **Used successfully in Adelie Land by the French and in Greenland by the British Expeditions.** Available in different models producing 1, 2 or 3 cubic metres by special patented ready-for-use refills - Excess gas production impossible.

LA G.I.P.

SOCIÉTÉ DES GAZ INDUSTRIELS DE PROVINCE

155, Boulevard Malesherbes, **PARIS.** Téléphone Wagram 22-96

Marconi's 3 cm STORM WARNING RADAR

TYPE SNW 50

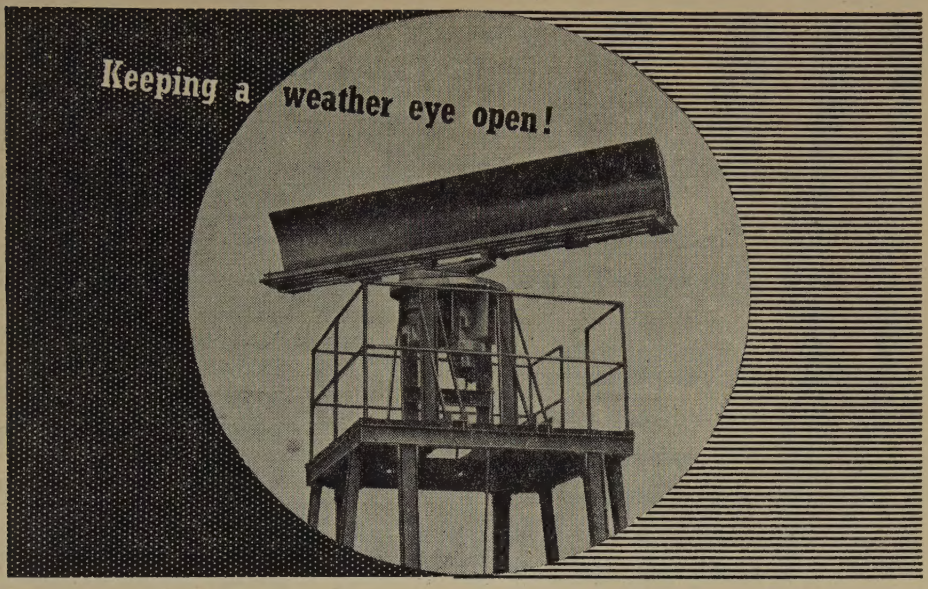

"Radar . . . meteorologists' most important new instrument since they commenced to use aeroplanes"

A. C. BEMIS (Massachusetts Institute of Technology)

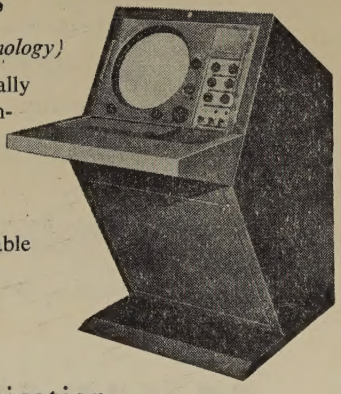

Marconi's Storm Detection Radar, Type SNW 50 is specially designed to present an accurate picture of storms and rain-producing clouds over ranges up to 200 n.m. It can therefore meet the needs of Meteorological Departments and Airport Authorities, particularly where it is required to derive information from inaccessible areas.
Features include :—High Power Working, High-gain Tiltable Aerial (remote-controlled from display unit), Full Off-Centring Facility (enabling any sector to be expanded to cover the whole area of the tube), Remote Displays, Static or Mobile Versions available.

Lifeline of Communication

MARCONI

Planning & Installation of Military & Civil Radar Systems

MARCONI'S WIRELESS TELEGRAPH COMPANY LIMITED, CHELMSFORD, ESSEX

R2

MUFAX Recorders think for themselves

They switch on; make an accurate, visual record of any graphic material transmitted and switch off again—entirely automatically.

They operate for long periods without *any* attention and then only for replenishment of MUFAX recording paper at 30-hour intervals or longer.

For absolute accuracy, dependability and minimum attention—it's MUFAX every time.

Publications 8749, 8691 and 8696 tell you all about it.

MUIRHEAD

PRECISION ELECTRICAL INSTRUMENTS

MUIRHEAD & COMPANY LIMITED, Beckenham, Kent, England
MUIRHEAD INSTRUMENTS INC., 677 Fifth Avenue, New York 22, N.Y., U.S.A.
MUIRHEAD INSTRUMENTS LIMITED, Stratford, Ontario, Canada

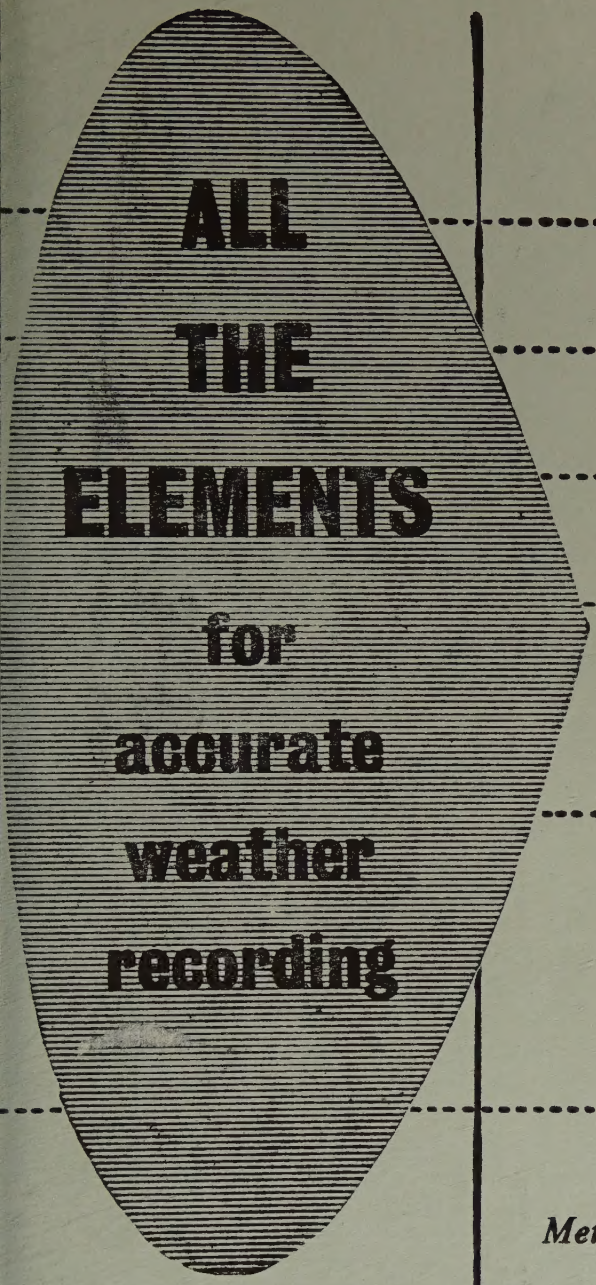

Thermometers

Hygrometers

Barometers

Rain Gauges

Sunshine Recorders

Wind Direction and Velocity Indicators, etc.

Meteorological Instruments by

NEGRETTI & ZAMBRA LTD

Manufacturers of instruments for the indication, recording, controlling of :— Temperature, pressure, liquid level, volume, specific gravity, humidity, etc.

122, REGENT STREET, LONDON, W.1
'Phone: REGent 3406. 'Grams: Negretti, Piccy, London
Branches : Birmingham, Cardiff, Glasgow, Leeds, Manchester, Nottingham.
Agents or Subsidiaries in most countries.

THE DINES
TILTING SYPHON RAIN GAUGE

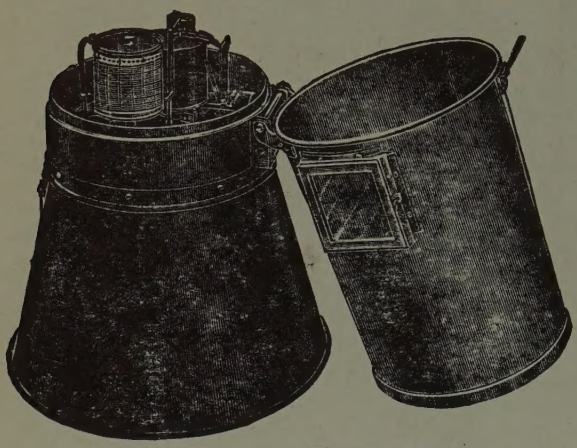

This is the very latest type of Self-recording Rain Gauge, fitted with an tilting arrangement which ensures an complete syphoning when the rainn water has filled the float chamber.

The Instrument Measures
Overall height – 34″
Diameter of base – 20″

Price and further particulars on application

Manufactured and supplied by

HEATH, HICKS & PERKEN (THERMOMETERS) **LTD.**

NEW ELTHAM, LONDON, S.E.9

Phone : ELTham 3836 *Grams* : "Optimus, Souphone," London

F. DARTON & CO. LTD.

Makers of :

THERMOGRAPHS
BAROGRAPHS
HYGROGRAPHS
PRECISION HAIR HYGROMETERS
ALTIMETER CALIBRATORS
KEW PATTERN BAROMETERS
FORTIN'S PRINCIPLE BAROMETERS
GRASS & SOLAR THERMOMETERS
RAIN GAUGES, etc.

All enquiries to : Established 1834

WATFORD FIELDS, WATFORD, HERTS

Tel. : WATFORD 6019 & 6010

Printed in Great Britain by The Salisbury Press Ltd., Publicity House, Wilton Road, Salisbury, Wilts. (2117)